The regulation of Kv4.2 and KChIP1 trafficking to the plasma membrane

Thesis submitted in accordance
with the requirements of the
University of Liverpool

for the degree of

Doctor in Philosophy

by

Sarah Elizabeth Flowerdew

December 2009

DECLARATION

This thesis is the result of my own work. The material contained in the thesis has not been presented, nor is currently being presented, either wholly or in part for any other degree or other qualification.

The research was carried out in the Department of Physiology, Faculty of Medicine. All work presented was performed by the candidate.

Abstract

Neurons carry information via the action potential. As well as travelling down the axon, this can back-propagate into the dendrites, informing them of the firing status of the neuron. This is important for the synaptic plasticity underlying long term potentiation that contributes to learning and memory. The back-propagation of action potentials is regulated by the Kv4 family of voltage-gated potassium channels. To be functional, these channels must be trafficked to the plasma membrane. This requires interactions with accessory proteins, a major family of which are the potassium channel interacting proteins, or KChIPs. Previous work had shown that the trafficking of Kv4.2 and KChIP1 from the endoplasmic reticulum to the plasma membrane occurs via a non-conventional, COPII-independent exocytic pathway. This pathway has, however, not been fully characterised.

The aim of this thesis was to further characterise the traffic of Kv4.2 channels to the plasma membrane. The non-conventional trafficking pathway used by Kv4.2 and KChIP1 was investigated. Confocal fluorescence microscopy using fluorescently tagged proteins or immunofluorescence was used to visualise the localisation of these proteins in transfected HeLa and Neuroblastoma 2A cells under varying conditions. These experiments confirmed that Kv4.2 expressed alone in these cells was localised to the Golgi apparatus, but was trafficked to the plasma membrane in the presence of KChIP1. This trafficking required the Rab GTPase Rab1, and required KChIP1 to have functional EF-hand domains, able to bind Ca^{2+}/Mg^{2+}. In addition, KChIP1-EYFP alone localised to punctate vesicles which were co-localised with the SNAREs VAMP7 and Vti1a. Use of RNAi to knockdown these two SNAREs in cells inhibited Kv4.2 trafficking, but had no effect on the conventionally trafficked protein VSVG. Thus the trafficking of Kv4.2/KChIP1 appears to occur via a non-conventional, Rab1-, VAMP7- and Vti1a-dependent pathway.

Other potential binding partners of the Kv4 channels and the KChIPs were investigated. A possible interaction of KChIP1 with 14-3-3γ, detected in yeast two-hybrid assays, was investigated but it was not possible to confirm this interaction. It was confirmed, however, that SAP97 could promote Kv4.2 channel trafficking to the plasma membrane in HeLa cells, but inhibited the trafficking of the channel to the plasma membrane in the presence of KChIP1. In addition, three isoforms of PSD-93 were found to have this inhibitory effect. One possible explanation for this inhibition of traffic is an interaction between SAP97 or PSD-93 and KChIP1. This was investigated further, and it was shown that KChIP1 could alter the cellular localisation of SAP97, suggesting that they interact. Together, these experiments shed light on the varied ways in which neurons can regulate Kv4 channel trafficking and function. Further studies of these newly characterised pathways and interactions will be important to our understanding of the molecular regulation of neuronal signals.

Table of Contents

Abbreviations

4-AP	4-aminopyridine
Aβ	amyloid beta
ADP	adenosine diphosphate
Ala	alanine
AMPA	α-amino-3-hydroxyl-5-methyl 4-isoxazole-propionate
ARF	ADP-ribosylation factor
Asp	aspartate
ATP	adenosine triphosphate
bAP	backpropagating action potential
Bet1	blocked early in transport 1
BSA	bovine serum albumin
CaCO-2 cells	human colorectal carcinoma cells
CALP	calsenilin-like protein
CaMKII	Ca^{2+}/calmodulin-dependent protein kinase II
cDNA	complementary DNA
CFTR	cystic fibrosis transmembrane conductance regulator
CHO cells	Chinese hamster ovary cells
COPI	coatomer protein complex I
COPII	coatomer protein complex II
COS-1/COS-7 cells	CV-1 in origin, carrying SV40. Immortalised CV-1 cells from African green monkey kidney
C-terminal	carboxy-terminal
CTX	cardiotoxin
DlgA	*Drosophila* disc large tumour suppressor
DNA	deoxyribonucleic acid
dNTPs	deoxyribonucleotides
DPP	dipeptidyl-peptidase
DRE	downstream-regulatory-element in DNA
DREAM	downstream-regulatory-element-antagonist modulator
DTT	dithiothreitol
ECFP	enhanced cyan fluorescent protein
ECL	enhanced chemiluminescence
EF3	EF-hand domain 3
EF2-4	EF-hand domains 2, 3 and 4
EGTA	ethylene glycol-bis(2-aminoethylether)-N,N,N′,N′-tetracetic acid
EGFP	enhanced green fluorescent protein
ER	endoplasmic reticulum
ERGIC	ER-Golgi intermediate compartment
ERK	extracellular signal-regulated kinase
EYFP	enhanced yellow fluorescent protein
FLAG	peptide tag, with sequence N-DYKDDDDK-C
GABA	γ-aminobutyric acid
GAP	GTPase-activating protein
GAT-1	GABA transporter-1
GDP	guanosine diphosphate

GEF	guanine nucleotide-exchange factor
GFP	green fluorescent protein
GK	guanylate kinase
Gly	glycine
GOS28	Golgi SNAP receptor complex member 1 (GOSR1)
GPI	glycosylphosphatidylinositol
GRK	G protein-coupled receptor kinase
GST	glutathione-s-transferase
GTP	guanosine triphosphate
HEK293	Human embryonic kidney 293 cells
HeLa cells	cell line derived from human cervical carcinoma
HEPES	N-(2-hydroxyethyl)piperazine-N′-(2-ethanesulfonic acid)
HRP	horseradish peroxidase
IPTG	isopropyl-1-thio-β-D-galactopyranoside
I_{to}	transient outward current
KChAP	potassium channel associated protein
KChIP	potassium channel interacting protein
KCNK	two-pore domain potassium channel
kDa	kiloDaltons
Kif17	kinesin family member 17
Kir	inward rectifying potassium channel
KIS	potassium channel inactivation suppressor
Kv channel	voltage-gated potassium channel
ml, µl	millilitres, microlitres
LAMP1	lysosomal-associated membrane protein 1
LTD	long-term depression
LTP	long-term potentiation
M, mM, µM, nM	molar, millimolar, micromolar, nanomolar
MAGUK	membrane-associated guanylate kinase
mink	miniature potassium channel
MiRP	minK-related protein
mRNA	messenger ribonucleic acid
Mw	molecular weight
NCS	neuronal calcium sensor
NCS-1	neuronal calcium sensor-1
Neuro2A cells	neuroblastoma2A cells
NIL-16	neuronal interleukin-16
NMDA	N-methyl-D-aspartate
NMR	nuclear magnetic resonance
NO	nitric oxide
NSF	N-ethylmaleimide-sensitive factor
NTA	nitrilotriacetic acid
N-terminal	amino-terminal
PAGE	polyacrylamide gel electrophoresis
PBS	phosphate-buffered saline
PBT	PBS containing 0.1% Triton X-100 and 0.3% BSA
PC12 cells	cell line derived from rat adrenal pheochromocytoma
PCR	polymerase chain reaction
PCTV	prechylomicron transport vesicle

PDZ	post-synaptic density 95, *Drosophila* disc large tumor suppressor, zonula occludens-1 protein
PKA	protein kinase A
PKC	protein kinase C
PMSF	phenylmethylsulfonyl fluoride
PPTX	protein with pentraxin domain
PSD	post-synaptic density
Rab	Ras-related proteins found in the brain
RabGDF	Rab GDI displacement factors
RabGDI	Rab GDP dissociation inhibitors
Ras	gene family named after the rat sarcoma where first discovered
RNAi	RNA interference
RRV	Ross river virus
RT-PCR	reverse transcription PCR
SAP	synapse associated protein
SDS	sodium dodecyl sulphate
SDS-PAGE	sodium dodecyl sulphate – polyacrylamide gel electrophoresis
Sec22	secretion gene 22
S.E.M.	standard error of the mean
SH3	SRC homology domain 3
siRNA	small interfering RNA
SNAP	soluble NSF attachment protein
SNARE	soluble NSF attachment protein receptor
SRP	signal recognition particle
TASK	TWIK-related acid-sensitive K^+ channel
TBC domain	Tre-2, Bub-2, Cdc16 domain
TEA	tetraethylammonium
TGN	*trans*-Golgi network
TRITC	tetramethyl rhodamine iso-thiocyanate
Triton-X-100	t-octylphenoxypolyethoxyethanol
Tween™-20	polysorbate 20
VAMP7	vesicle-associated membrane protein 7
VSVG	vesicular stomatitis viral glycoprotein
VTC	vesicular tubular cluster
Vti1a	vesicle transport through interaction with t-SNAREs homolog 1a
YFP	yellow fluorescent protein
zo-1	zona occludens-1

Chapter 1

Introduction

1.1 An overview of neuronal signalling

Multi-cellular organisms need to be able to both sense their external environment, and respond to it. This requires co-ordination between different parts of the organism's body, its organs and tissues. In less complex organisms, and in slow moving organisms such as plants, this co-ordination can be achieved through the local actions of chemical hormonal messengers. Animals too have these slow hormonal signalling pathways. However, these typically require the hormones to circulate around the organism, taking time to reach their target organs, needing specialist receptors to give specificity to the signal, and lasting until the hormones can be degraded. To co-ordinate movement and rapid responses to changing environmental stimuli, animals have instead developed specialised cells capable of transmitting rapid electrical signals. In addition, with increasing complexity comes a need to fully co-ordinate all aspects of an organism in a central processing area – the brain and central nervous system. The cell type responsible for processing this data is the neuron. These neurons are elongated cells, specialised in the transmission of electrical signals (Figure 1.1) (Alberts et al. 2008). However, these electrical signals are generated by the movement of ions, and at the connection between two neurons, the electrical signal causes chemical release, causing further electrical signals in the next neuron.

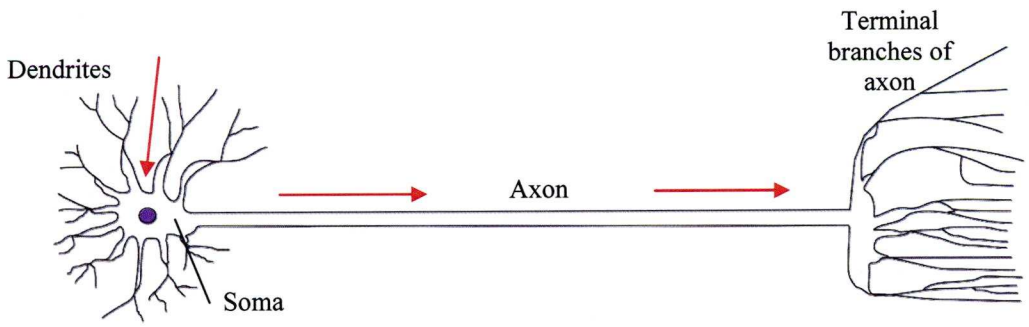

1.1: Diagrammatic representation of a neuron.
Neurons are elongated cells, specialised for the rapid transmission of electrical signals along their length. Inputs are received at the dendrites, before undergoing summation at the soma (cell body). The signal then travels along the axon, which finishes in many terminal branches, forming synapses with other neurons, or other cell types. Red lines indicate this direction of information flow. Adapted from *Alberts et al. 2008.*

Neurons receive a variety of inputs, which can be excitatory or inhibitory, onto highly branched dendrites and the cell body (soma). These then undergo a process of summation. If the incoming signal at a given time is great enough, an action potential is triggered, and the plasma membrane is depolarized sequentially along the length of the axon. This is achieved through the influx of Na^+ ions at a region of the membrane, depolarizing it away from a negative resting potential, and triggering Na^+ influx in neighbouring regions of membrane. This is followed by a delayed efflux of K^+ out of the cell, repolarizing that area of the membrane so that it is ready to fire again. When the action potential reaches the presynaptic nerve terminal, it then triggers an influx of Ca^{2+} ions, causing the fusion of synaptic vesicles with the presynaptic membrane, and the release of neurotransmitter into the synaptic cleft. The binding of neurotransmitters to their receptors on the postsynaptic membrane can then trigger membrane depolarisation in the next neuron, or in a muscle cell (Alberts et al. 2008).

The three ions, Na^+, K^+ and Ca^{2+}, are thus essential for the processes of electrical transmission in neurons. Beyond this, they also play a role in many other vital cellular processes, such as the influx of nutrients, the regulation of cellular volume, and the secretion of electrolytes (Gouaux and MacKinnon 2005). However, these ions are unable to cross the plasma membrane without ion channels, pumps and exchangers, which form an aqueous channel or pocket within a trans-membrane protein allowing passage of an ion (Gouaux and MacKinnon 2005). In neurons, these channels are often voltage-gated, opening in response to the firing state of the cell. This can in turn help shape the electrical properties of the cell, and the processing of signals (Bloodgood and Sabatini 2008; Kim and Hoffman 2008).

One important property of neurons is that they can modulate the strength of their firing in response to previous levels of input. This synaptic plasticity is modulated by long-term potentiation (LTP) and long-term depression (LTD) and is thought to be the molecular mechanism underlying learning and memory

(Alberts et al. 2008). At a basic level, LTP is evoked when a short period of presynaptic firing potentiates a postsynaptic membrane, so that further inputs generate a greater response, whilst LTD is the inverse of this (Alberts et al. 2008). This depends on the interplay between the opening of AMPA receptors in response to the excitatory neurotransmitter glutamate, depolarisation of the membrane, and the opening of glutamate- and depolarisation-sensitive NMDA receptors, which allow an influx of Ca^{2+} (Bloodgood and Sabatini 2008). If this calcium influx is short lived (a few seconds) but the cytosolic Ca^{2+} elevation is of high concentration (the micromolar range), then LTP is induced, whilst longer duration of a lower concentration cytosolic Ca^{2+} signal (a few hundred nanomolar) induces LTD (Yang et al. 1999(2)).

The resting level of intracellular Ca^{2+} in a neuron is in the range of 40-100nM, but this can rise due to influx from outside the cell, or the release of Ca^{2+} from internal stores such as the endoplasmic reticulum (ER) (Burgoyne 2007). As discussed above, this rise can lead to the release of neurotransmitter into the synapse, and to synaptic plasticity. In addition, changes in Ca^{2+} concentration can modulate ion channel activity, induce gene expression, and even regulate apoptosis (Burgoyne 2004). This is not limited to neuronal cells, and Ca^{2+} signals and signalling networks can have a wide range of effects in many cell types, comprehensively reviewed in Berridge et al. (2000). The way in which this elevation in the concentration of a single ion within the cell can have so many varied effects can be due to differences in signal magnitude and duration, as discussed above for LTP and LTD. In addition, the localisation and spatial regulation of the concentration rise may be important (Berridge et al. 2000). However, a major mechanism for the transduction of a calcium response is through the action of calcium sensor proteins (Burgoyne 2007). These can increase the complexity of the calcium signalling network by having different Ca^{2+} affinities, subcellular localisations or tissue expression patterns, by targeting specific downstream effectors, or by having different kinetics of action (Burgoyne 2007). One major family of sensors in the brain are the neuronal calcium sensor (NCS) proteins (Burgoyne 2004).

In addition to calcium, potassium also has a vital role to play in neuronal activity, and influences LTP. Whilst the main nerve impulse travels from dendrite to soma to axon, action potentials from the axonal hillock can also move in a retrograde manner back into dendrites, so called backpropagating action potentials (bAPs) (Jerng et al. 2004a). The bAPs help to inform a neuron of its firing status (Jerng et al. 2004a) and as timing is important in determining whether LTP or LTD is induced, the regulation of bAPs is important in regulating the strength of synapses (Migliore et al. 1999). This regulation is achieved through the action of potassium channels. As the distance from the soma increases, action potentials are attenuated by the action of voltage-gated potassium channels (Hoffman et al. 1997; Ramakers and Storm 2002). Currents through these channels repolarise the membrane, limiting the firing frequency of action potentials (Hoffman et al. 1997), and in fact, the internalisation of these regulating potassium channels has been proposed as a secondary method of altering synaptic strength (Kim and Hoffman 2008).

Alteration of the levels of voltage-gated potassium channels at the plasma membrane, by the regulation of both protein synthesis and trafficking to and from the cell surface, thus gives the neuron a further way to regulate neuronal activity. In addition, a neuron is a highly polarised cell, and trafficking to dendrites must be differentiated from that to axons. This can be achieved through protein motifs specific for trafficking to certain compartments, by the directed trafficking of vesicles containing newly synthesised proteins, or by regulating the endocytosis of proteins out of particular membranes (Arnold 2006). To aid in the regulated synthesis of proteins in an elongated cell, the ER of neurons is distributed throughout the dendrites and soma (Horton and Ehlers 2003). In addition, some dendrites, usually the longest (Horton et al. 2005), have outposts of the Golgi apparatus (Ehlers 2007), used in the trafficking of both secretory and integral membrane proteins (Horton and Ehlers 2003). It should also be noted that proper dendritic growth requires classical ER-Golgi-plasma membrane trafficking (Ehlers 2007; Ye et al. 2007).

The particular voltage-gated potassium channels involved in the regulation of firing frequency and bAPs will be introduced in the next section, followed by a discussion of their interacting partners, and how these influence the trafficking of channels to the plasma membrane.

1.2 Voltage-gated potassium channels

There are four known types of potassium channel: voltage-gated, Ca^{2+}-activated, inward rectifier and potassium leak channels (Kim and Hoffman 2008). In general, these channels have a long aqueous pore through the plasma membrane, connected to a short selectivity filter, to keep the rate of ion flux high (Gouaux and MacKinnon 2005). The crystal structure of the similar bacterial KcsA potassium channel shows acidic residues at the mouth of the channel to promote the entry of cations (Doyle et al. 1998). The selectivity filter contributes oxygen atoms to compensate for the dehydration of the ion as it passes through the channel, and the spacing of these helps differentiate between Na^+ and K^+ (Doyle et al. 1998; Gouaux and MacKinnon 2005). Finally, the presence of multiple K^+ ions in the selectivity filter creates an electrical repulsion to promote the flow of ions (Doyle et al. 1998; Gouaux and MacKinnon 2005).

The voltage-gated potassium channels were first discovered through the *Shaker* mutation of hyperexcitable *Drosophila* (Papazian et al. 1987). The *Shaker* superfamily is now known to contribute to potassium currents in both the brain and heart (Birnbaum et al. 2004). These proteins are encoded by the KCN genes, and in modern nomenclature form 12 families of Kv channels (Gutman et al. 2003). The Kv superfamily are characterised by having 6 transmembrane domains per α subunit, and are sensitive to phrixotoxin and 4-aminopyridine (4-AP). They also inactivate rapidly and recover quickly (Birnbaum et al. 2004). To form an active channel, four α subunits must multimerise. This seems to require a 130 amino acid T1 tetramerisation domain (Birnbaum et al. 2004), with one monomer co-ordinating a Zn^{2+} ion via two cysteines and a histidine, and an adjacent monomer contributing a cysteine residue from its T1 domain (Bixby et al. 1999). Interestingly two of these cysteines may form a disulphide bond in the presence of NO, allowing redox regulation of the potassium channel (Wang et al. 2007(1); Covarrubias et al. 2008). The T1 domain also prevents different members of the Kv family from forming heteromultimers, with a 20 amino acid section of the A and B region of T1 contributing to subfamily specificity (Shen and Pfaffinger 1995; Xu et al. 1995).

K^+ channels in neurons are responsible for the resting potential of the cell, can oppose depolarisation away from this resting potential, and repolarise action potentials (Kim and Hoffman 2008). As such, mutations in these channels have been suggested as a cause of the hyperexcitability found in epilepsy (Birnbaum et al. 2004). In support of this, drug-induced seizure in rats was seen to reduce levels of both Kv1.2 and Kv4.2 in the hippocampus 3-6 hours post trauma (Tsaur et al. 1992). Also, a patient with temporal lobe epilepsy had a premature stop codon in the KCND2 gene for Kv4.2, and when expressed in cells this mutant channel produced a lower current density than the wild-type (Singh et al. 2006). However, it should be noted that a Kv4.2 knockout mouse did not show any innate epilepsy, suggesting other channels or factors may also have a role (Chen et al. 2006(2)).

The large number of Kv channel proteins is reflected in the wide variety of currents they are known to produce. For example, in cardiac myocytes, at least 5 potassium currents with different characteristics are known, mediated by the Kv channels (Patel and Campbell 2005). These may differ in their kinetics. In the rodent cardiac ventricle there are both fast and slow transient outward currents (I_{to}) mediated by Kv4.2/Kv4.3 and Kv1.4 respectively (Patel and Campbell 2005). Alternatively, they may differ in their subcellular localisation. The A-type currents in neurons may be mediated by Kv1.4 or Kv3.4 in the axon, and by the Kv4 family in the somatodendritic compartment (Kim and Hoffman 2008). It is the Kv4 family that are the focus of this thesis.

1.2.1 Kv4 family

The Kv4 family were first characterised in 1971 (Maffie and Rudy 2008), and three members of this family are now known (Gutman et al. 2003). They all have 6 exons of similar size, although their introns differ (Isbrandt et al. 2000). They have a cytoplasmic N-terminus, followed by the T1 tetramerisation domain, and then six transmembrane helices (S1-6). Of these, S4 has positive arginine and

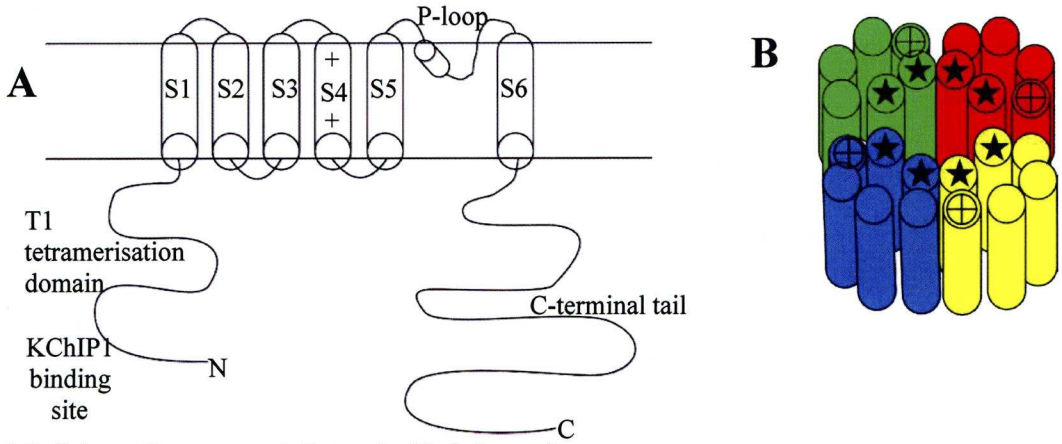

1.2: Schematic representations of a Kv4 channel.
The figures indicate the arrangement of α helices in a Kv4 α subunit.

- **A)** The arrangement of a single α subunit, with six transmembrane domains, and large N- and C-terminal cytoplasmic tails. Helix S4 is thought to be the voltage-sensor, as it is highly charged. Helices S5 and S6, and their connecting P-loop, contribute to the pore through the membrane.
- **B)** The arrangement of helices from four α subunits in a complete tetramer. Each subunit is displayed in a different colour. The N- and C-termini of each subunit, and the connecting loops between helices, have been removed for clarity. Voltage-sensing helix S4 is represented by the + symbol, and helices S5 and S6 from each subunit, contributing to the pore through the membrane, are represented by the star.

Adapted from *Birnbaum et al. 2004.*

lysine residues at every third position, and is therefore thought to be the voltage sensor. Finally, helices S5 and S6 from each α subunit contribute to the pore through the membrane, with their connecting P-loop forming the selectivity pore (Figure 1.2) (Birnbaum et al. 2004). Potassium channels are often glycosylated at their S1-S2 linker, but none of the Kv4 channels have the consensus sequence for this, and do not seem to be glycosylated (Isbrandt et al. 2000; Birnbaum et al. 2004). They can, however, be highly phosphorylated (Misonou and Trimmer 2004). The Kv4 channels also contain a 16 amino acid dileucine motif, which seems to be involved in their targeting to the somatodendritic compartment of neurons (Birnbaum et al. 2004; Arnold 2006).

The Kv4 family of channels are mainly responsible for A-type currents in the brain and fast I_{to} in the heart, and there is much evidence to support this. Firstly, Kv4.2 and Kv4.3 are expressed at high levels in the brain (Misonou and Trimmer 2004) and are present in the heart (Isbrandt et al. 2000). Both the A-type currents and the Kv4 proteins are sensitive to 4-AP, arachidonic acid and heteropodotoxin, but not tetraethylammonium (TEA) (Tkatch et al. 2000; Ramakers and Storm 2002). Both channel and current are activated at

hyperpolarised, subthreshold potentials, are completely inactive at -40mV, and are then rapidly inactivated (Tkatch et al. 2000; Kim and Hoffman 2008). Finally, both recover rapidly from inactivation, in tens to hundreds of milliseconds (Tkatch et al. 2000; Covarrubias et al. 2008). All of this confirms the important role of Kv4 family proteins in generating both I_{to} and A-type currents.

The general role of these currents is to regulate cellular excitability. This is highlighted in the hearts of hypertensive rats, which have lower I_{to} due to fewer Kv4.2 and Kv4.3 channels (Goltz et al. 2007). In the brain, the role of the A-type current is to pace the firing of action potentials during repetitive firing, in particular delaying excitation, and regulating the delay between depolarisation and firing, and the delay between two action potentials (Maffie and Rudy 2008). They also attenuate the amplitude of bAPs with increasing distance from the soma (Hoffman et al. 1997), and so as discussed above, suppressing A-type currents reduces the threshold for LTP induction (Ramakers and Storm 2002).

The different Kv4 proteins are not equivalent, however, and have specific roles and functions. They are, for example, expressed in different brain regions (Birnbaum et al. 2004), and whilst both Kv4.2 and Kv4.3 are affected in hypertensive epicaridal myocytes, it seems only Kv4.2 is affected in the endocardium (Goltz et al. 2007). Also, in a Kv4.2 knockout mouse, levels of Kv4.3 in the brain were completely unaltered (Guo et al. 2005; Menegola and Trimmer 2006). It is the better characterised Kv4.2 that has been studied in this thesis, and is discussed below.

1.2.2 Kv4.2

Kv4.2 mRNA is found in human brain by Northern blot and also in the heart and other tissues by RT-PCR (Isbrandt et al. 2000). In rodent brain, it is found on the plasma membrane of the soma and dendrites, but is not in the axon or

presynaptic membranes (Alonso and Widmer 1997). It is especially found at sites of axonal contact (Alonso and Widmer 1997), and is seen as punctae in the postsynaptic side of some GABAergic synapses (Jinno et al. 2005), whilst being excluded from non-GABAergic synapses (Burkhalter et al. 2006).

There is much evidence to highlight the specific role of Kv4.2 channels in A-type and I_{to} currents, as well as in the regulation of LTP. Firstly, estimates of Kv4.2 mRNA abundance correlate with levels of maximal A-type conductance (Tkatch et al. 2000), reduction in Kv4.2 levels by RNAi reduced hippocampal A-type currents (Lauver et al. 2006), and overexpresion of Kv4.2 decreased cell excitability (Kim et al. 2005). In addition, the knockout of Kv4.2 in mice eliminated the cardiac fast I_{to} (Guo et al. 2005). The role of Kv4.2 may be more important in rodent heart, and Kv4.3 may play a larger role in dogs and humans (Dixon et al. 1996; Niwa et al. 2008). Moreover, Kv4.2 channels regulate neuronal bAPs so that each dendritic compartment can act semi-independently as a signalling unit (Cai et al. 2004). Overexpression of Kv4.2 decreased the propagation of bAPs, whilst a dominant negative mutant had the opposite effect (Kim et al. 2005). Also, in Kv4.2 knockout mice, A-type currents are eliminated in the majority of cortical pyramidal neurons (Nerbonne et al. 2008), the amplitude of bAPs is larger, and the threshold for the induction of LTP is lower (Chen et al. 2006(2)). Kv4.2 channels also seem to be internalised in response to LTP (Kim et al. 2007). It therefore seems clear that Kv4.2 channels have a vital role in the correct functioning of the heart and brain.

The expression of Kv4 channels in heterologous systems however, such as *Xenopus* oocytes, produced channels with kinetics that did not match with those observed in native systems (Maffie and Rudy 2008). Also, neurons with similar expression patterns of Kv4 channels have different A-type currents (Tkatch et al. 2000). It was observed that heterotetramers (e.g. of Kv4.2 and Kv4.3) are more similar to native channels than homotetramers (Guo et al. 2002). A major factor, though, is the regulation of Kv4 channels by accessory proteins.

1.3 KChIPs

The KChIPs (K^+ channel interacting proteins) were discovered in 2000, after a yeast two-hybrid screen for binding partners interacting with the N-terminal 80 amino acids of rat Kv4.3 revealed three new proteins (An et al. 2000). KChIP3 was also separately discovered as calsenilin, a binding partner of the presenilins (Buxbaum et al. 1998), and an N-terminally extended variant is known as the transcriptional repressor DREAM (Carrion et al. 1999; Spreafico et al. 2001). KChIP4 was discovered in 2002, also as a binding partner of the presenilins (Morohashi et al. 2002).

As well as binding to Kv4 proteins in yeast two-hybrid assays, the KChIPs were also seen to co-localise with Kv4 channels at the plasma membrane and alter current density, as will be discussed in more detail below (An et al. 2000). The crystal structure of KChIP1 has been solved, revealing a hydrophilic face and a hydrophobic face important for channel interactions (Scannevin et al. 2004). The importance of the KChIPs in normal channel function is revealed by the fact that Kv4.2 knockout mice show reduced levels of KChIPs 1-3 (Guo et al. 2005; Chen et al. 2006(2); Nerbonne et al. 2008), that the Kv4 channels are only sensitive to arachidonic acid in the presence of a KChIP (Birnbaum et al. 2004), and that the requirement for Zn^{2+} in channel assembly and tetramerisation can be overcome by co-expression with KChIPs (Kunjilwar et al. 2004; Wang et al. 2007(1)).

The four KChIP genes give rise to many splice variants (Misonou and Trimmer 2004). There are three splice variants of KChIP1 (Pruunsild and Timmusk 2005). KChIP2 has 8 isoforms (Decher et al. 2004), expressed mostly in the heart (Kuo et al. 2001). KChIP3 has two predominant isoforms (although more have been described), whilst KChIP4 has 6 isoforms (Pruunsild and Timmusk 2005). Whilst the general effects of the KChIPs seem to be similar, there is much evidence that the different splice isoforms differ in the details of their actions (Bahring et al. 2001; Patel et al. 2002a; Decher et al. 2004). A major example of this is KChIP4a, and the newly discovered KChIPs 2x and 3x, which contain K^+

channel inactivation suppressor (KIS) domains (Holmqvist et al. 2002; Trinkle-Mulcahy et al. 2008). This domain appears to be a putative transmembrane domain (Jerng and Pfaffinger 2008) which may alter the interaction site with the Kv4 channel (Trinkle-Mulcahy et al. 2008), and causes the KChIP to slow Kv4 channel opening and disrupt the channel's rapid inactivation, in contrast to the actions of other KChIPs (Jerng and Pfaffinger 2008).

It seems that different KChIPs may be expressed in different brain areas, or work in conjunction with different Kv4 channels. For example, KChIPs 2, 3 and 4 are expressed with Kv4.2 in excitatory CA1 pyramidal cells, whilst KChIP1 and Kv4.3 are expressed in inhibitory interneurons (Rhodes et al. 2004). The situation *in vivo* is likely more complicated than this, however, as some brain regions express multiple Kv4 proteins (Rhodes et al. 2004). There is also evidence that the same KChIP may have differing effects on different members of the Kv4 family (Nakamura et al. 2001a). Also, it seems that the individual KChIPs may not be essential, as KChIP1, KChIP2 or KChIP3 knockout mice are not embryonic lethal. They do, however, have various phenotypes, that seem to differ depending on the KChIP knocked out, suggesting that the KChIPs are not fully redundant (Kuo et al. 2001; Lilliehook et al. 2003; Xiong et al. 2009).

1.3.1 KChIPs and Kv4 channels

One of the main roles of the KChIPs is to interact with Kv4 channels, to promote their trafficking to the plasma membrane, to alter the kinetics of the channel at the plasma membrane, and thus to regulate the currents produced by these channels. A variety of studies have given insights into each of these aspects of KChIP function.

The major interaction of a KChIP with a Kv4 α subunit is through the N-terminus of the channel (Bahring et al. 2001). Structures of human KChIP1 with rat Kv4.3 (Figure 1.3A) reveal that four KChIPs bind to the four Kv4 α subunits

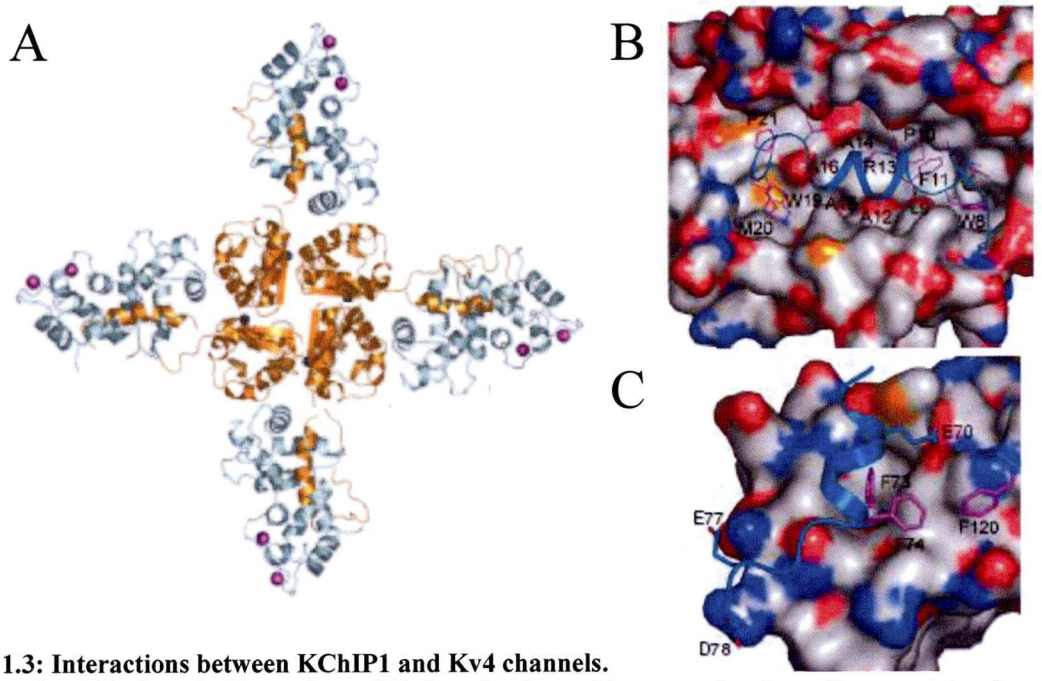

1.3: Interactions between KChIP1 and Kv4 channels.
KChIP1 binds to the N-terminus of Kv4 α subunits, and increases the channel's current density.

- **A)** Crystal structure of KChIP1 and the N-terminus T1 domain of Kv4.3. The view is looking down on the central pore, showing the cross-shaped octamer structure of Kv4 α subunits in orange, and KChIPs in blue. There are Zn^{2+} ions at the interface between Kv4 subunits, shown as grey spheres, and each KChIP is bound to two Ca^{2+} ions, shown as pink spheres. From *Pioletti et al. 2006.*
- **B)** The first interaction site between Kv4.3 and KChIP1. The Kv4.3, shown as a ribbon, binds into a hydrophobic groove on the surface of KChIP1, shown as a surface representation. The residues of Kv4.3 important for the interaction are shown in magenta. From *Wang et al. 2007(2).*
- **C)** The second interaction site between Kv4.3 and KChIP1. Residues 70-78 of Kv4.3 T1 domain are shown as a blue ribbon, whilst the KChIP1 is shown as a surface representation. The interaction is mediated by hydrophobic residues and salt bridges. The residues of Kv4.3 important in this interaction are shown in magenta. From *Wang et al. 2007(2).*

forming an intact channel, in a cross-shaped octamer (Pioletti et al. 2006). Each KChIP is bound to two neighbouring Kv4 subunits. The first interaction is between a helix of hydrophobic residues 6-21 of the N-terminus of human Kv4.3, and a hydrophobic pocket of human KChIP1 formed from a 40° movement of helix H10 (Figure 1.3B) (Wang et al. 2007 (2); Wang 2008). Tryptophan 8 and phenylalanine 11 seem to be particularly important Kv4 residues in this interaction, and this hydrophobic helix appears to kink around a highly conserved proline residue at position 10 (Zhou et al. 2004). This interaction seems to be important for the KChIP's effects on channel trafficking (Pioletti et al. 2006). The second region of binding is due to salt bridges and hydrophobic interactions forming between helix 2 of KChIP1, and amino acids 70-78 in the T1 tetramerisation domain of Kv4, and this helps mediate KChIP's effects on channel gating (Figure 1.3C) (Pioletti et al. 2006; Wang et al. 2007 (2)). It seems

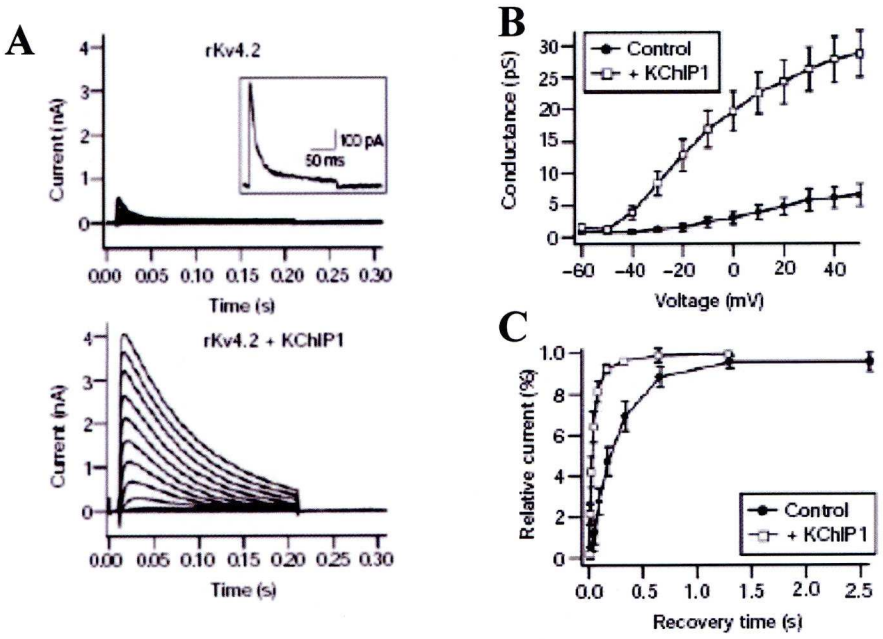

1.4: Effects of KChIPs on Kv4 currents.
Electrophysiology experiments performed using rat Kv4.2 and rat KChIP1 in Chinese hamster ovary (CHO) cells.

- **A)** Current-voltage traces of cells transiently transfected with Kv4.2 alone (top panel), or Kv4.2 with KChIP1 (bottom panel), revealing the increase in current density in cells co-transfected with KChIP1. From *An et al. 2000.*
- **B)** Graph showing peak current conductance at various voltages in cells transfected with Kv4.2 alone (black circles) or with KChIP1 (white squares). This highlights the increased peak conductance in cells co-transfected with KChIP1. From *An et al. 2000.*
- **C)** Graph showing the percentage of peak current recovered over time in cells transfected with Kv4.2 alone (black circles) or with KChIP1 (white squares). This highlights the more rapid recovery from inactivation in cells co-transfected with KChIP1. From *An et al. 2000.*

that both these regions of Kv4 are necessary for the interaction, and the second region is sufficient (Scannevin et al. 2004). The C-terminus of the channel may also be important, as mutations in the C-terminus of the Kv4 channel have effects on the binding of KChIP and its ability to alter channel kinetics (Callsen et al. 2005; Han et al. 2006). Finally, mutations in the inner pore of Kv4.3 had a different response to KChIPs, suggesting this region may also be important (Wang et al. 2002). In addition, three regions around the EF-hand domains of the KChIP are important for forming the hydrophobic crevice that the channel binds – the EF1-EF2 linker, the EF3-EF4 linker, and the C-terminal region of the protein after EF4 (Ren et al. 2003).

In the absence of KChIPs, Kv4.2 channels are retained in the cell, where they are hypophosphorylated, and relatively unstable (Misonou and Trimmer 2004). The

binding of KChIPs (without KIS domains) to a Kv4 channel stimulates its trafficking to the plasma membrane (O'Callaghan et al. 2003; Shibata et al. 2003). This increases current density in the region of 12-fold (Figure 1.4A) (An et al. 2000). Once expressed at the plasma membrane, the KChIP remains bound to the channel, and alters its kinetics (Figure 1.4B-C). This includes hyperpolarising the voltage required for activation, slowing the time constant of inactivation, but accelerating the kinetics of recovery from inactivation (An et al. 2000). In particular, it seems that KChIP1 slows the fast inactivation of Kv4.2 from its open state, whilst promoting inactivation from the closed state by increasing the rate of channel closing (Beck et al. 2002). It should be noted that those KChIP isoforms with a KIS domain do not promote the surface trafficking of Kv4 channels (Covarrubias et al. 2008), and slow the time courses of both activation and inactivation (Figure 1.5) (Morohashi et al. 2002; Jerng and Pfaffinger 2008).

The importance of the KChIPs can be seen from the effects of KChIP knockout mice. KChIP2 knockout mice lack cardiac I_{to}, and are more susceptible to induced arrhythmias (Kuo et al. 2001). This links with the observation that both dogs and humans have an I_{to} gradient across their left ventricular wall. This is not caused by a gradient in Kv4 channel distribution, but rather in KChIP2 (Kuo et al. 2001). KChIP3 knockout mice had reduced fast-inactivating currents in the brain, and this increased LTP (Lilliehook et al. 2003). This reflects the

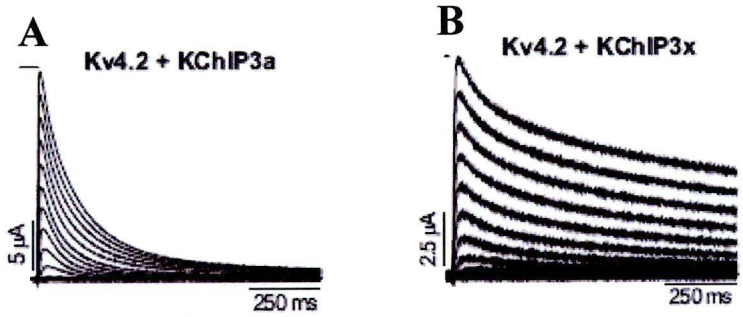

1.5: Graphs showing the inactivation of Kv4.2 channels.
Xenopus oocytes were transfected with Kv4.2 and an isoform of KChIP3. Cells were then depolarised by differing amounts, and the outward currents measured over time.

- **A)** Representative current trace from cell co-transfected with Kv4.2 and KChIP3a.
- **B)** Representative current trace from cell co-transfected with Kv4.2 and the KIS domain-containing KChIP3x.

The graphs reveal the slower inactivation of the Kv4.2 channel when co-expressed with a KIS domain KChIP. From *Jerng and Pfaffinger 2008.*

observation that it is the actions of Kv4.3 and KChIP3 together that control the pacemaker activity of dopaminergic neurons in the substantia nigra, a brain region implicated in Parkinson's disease (Liss et al. 2001). Also in the brain, KChIP1 knockout mice appear to be more susceptible to drug-induced seizures, likely through the reduction in Kv4 trafficking in these animals (Xiong et al. 2009).

1.3.2 Alternative functions of KChIPs

KChIP3 was separately discovered as downstream-regulatory-element-antagonist modulator, or DREAM (Spreafico et al. 2001), a DNA-binding transcriptional repressor. It has since been shown that all 4 KChIPs can bind to DRE (downstream-regulatory-element) motifs in DNA (Link et al. 2004), although KChIPs 1 and 2 are not localised to the nucleus (Venn et al. 2008). KChIP3 appears to bind DNA as a monomer (Osawa et al. 2001), and this represses transcription. However, the KChIPs can bind Ca^{2+} ions, and this causes a conformational change in the KChIP, and possibly dimerisation, causing it to dissociate from DNA (Carrion et al. 1999; Osawa et al. 2001). DREAM has been implicated in the regulation of the genes for prodynorphin, important for pain and emotional memory, the immediate early transcription factor *c-fos* (Carrion et al. 1999), and *NCX3*, involved in neuronal viability and Ca^{2+} homeostasis (Gomez-Villafuertes et al. 2005; Venn et al. 2008). In addition, all four KChIPs may have a role in the regulation of a range of genes involved in circadian day-night oscillations (Link et al. 2004).

KChIP3 was also discovered as calsenilin, and KChIP4 as calsenilin-like protein (CALP) due to their ability to bind to presenilin-1 and presenilin-2 (Buxbaum et al. 1998; Morohashi et al. 2002). This involves residues 421-431 at the C-terminus of presenilin, and the C-terminus of the KChIP (Morohashi et al. 2002). The presenilins are commonly the site of mutations responsible for early-onset familial Alzheimer's disease, and these mutations increase the production of β-amyloid (Aβ), as well as inducing apoptosis (Buxbaum et al. 1998). Binding of

KChIP4 with presenilin-2 changed the localisation of both proteins to a reticular and perinuclear distribution (Morohashi et al. 2002). Also, overexpression of KChIP3 increased levels of Aβ42 and apoptosis, an effect that was potentiated by co-expression with presenilin-2 (Jo et al. 2001), whilst KChIP3 knockout mice showed decreased levels of Aβ40 and Aβ42 in the brain, compared to wild-type mice (Lilliehook et al. 2003). This may be due to the ability of calsenilin to increase the activity of γ-secretase, one of the cleavage enzymes responsible for the production of Aβ, an effect potentiated by presenilin (Jo et al. 2005). Interestingly, though, overexpression of KChIP4 with presenilin-2 seemed to have no effect on the secretion of Aβ (Morohashi et al. 2002), suggesting KChIPs 3 and 4 may have differing activities. The effects of KChIP3 may be physiologically relevant, as Alzheimer's disease patients show increased expression of KChIP3 in the brain (Jo et al. 2004), and calsenilin co-localised with Aβ42 in a mutant mouse Alzheimer's disease model (Jo et al. 2004).

Finally, KChIPs 3 and 4 have been proposed to have several other, seemingly unrelated, roles in cells. Firstly, KChIP3, in its Ca^{2+}-bound form, can bind to hormone-activated vitamin D receptors, so may have a role in vitamin D disorders (Lusin et al. 2008). Secondly, KChIP3 can stimulate the ATP-induced exocytosis of dense core granules in neuroendocrine cells (Venn et al. 2008). Finally, both KChIP3 and KChIP4 can bind Golgi glycosyltransferases, affecting their ER-Golgi trafficking (Quintero et al. 2008). Many of these varied roles may reflect cell type specific activities, or be due to differences in intracellular localisation of proteins. Much further work will be needed to identify their physiological relevance, and the molecular mechanisms of their actions, although many of these roles may reflect the ability of KChIPs to act as calcium sensors.

1.3.3 KChIPs are part of the NCS family and can bind Ca^{2+} ions

The KChIPs form one of five classes of proteins belonging to the neuronal calcium sensor (NCS) family, and were the most recent to evolve, being present during evolution from fish onwards (Burgoyne 2004). Like all NCS proteins,

they can bind Ca^{2+} with micromolar or submicromolar affinities, and this causes a change in their conformation, allowing interaction with other proteins to change and regulate their physiological function (Burgoyne 2004). The KChIPs have an N-terminal basic region, which shows most variability, and a more conserved C-terminal region, containing the Ca^{2+}- binding regions (Figure 1.6A) (Osawa et al. 2001; Burgoyne 2007). The crystal structure of KChIP1 shows similarities to other NCS proteins (Scannevin et al. 2004). This showed 10 α helices with the N-terminal H1 and C-terminal H10 flanking the Ca^{2+} binding sites (Figure 1.6B).

The NCS proteins bind to Ca^{2+} via EF-hand domains, highlighted in Figure 1.6B. These are 29 amino acid helix-loop-helix motifs, named after the helices in parvalbumin, and it is residues 1, 3, 5, 7, 9 and 12 that are involved in actually co-ordinating the Ca^{2+} ion (Burgoyne 2007). Perhaps the best known of calcium binding proteins is calmodulin, and like calmodulin, NCS proteins all have 4 EF-hand domains. However, the most N-terminal EF hand (EF hand 1) is non-

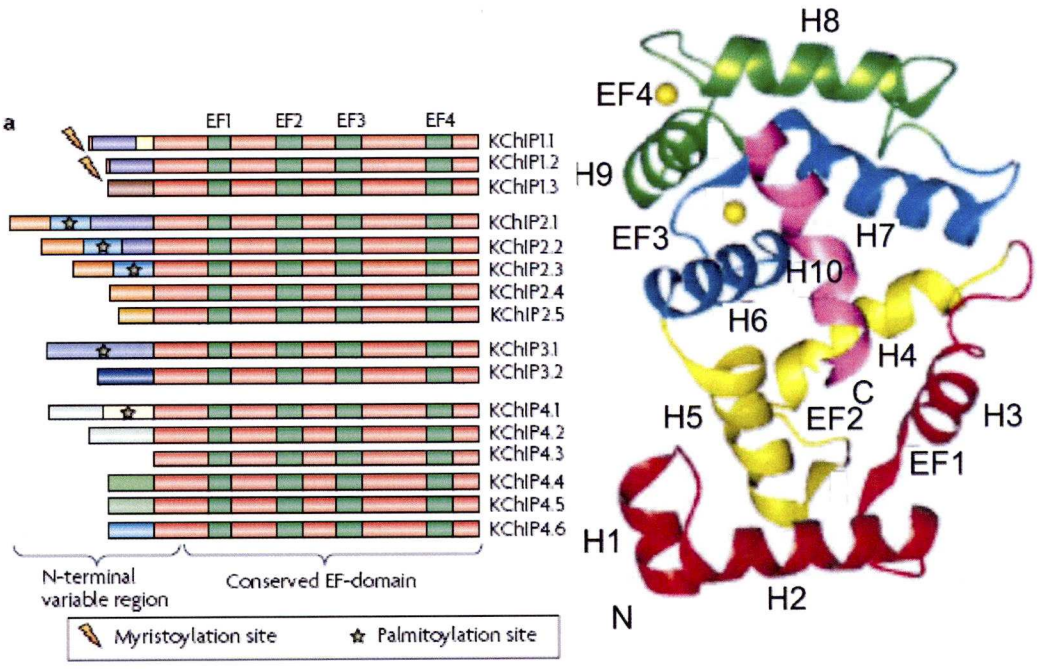

1.6: Structure of the KChIPs, and their EF-hand domains.

A) Schematic of the domain organisation of isoforms of the four KChIPs, showing their EF hands and conserved C-terminus, with more variable N-termini. From *Burgoyne 2007.*

B) The crystal structure of KChIP1 shows its 10 α helices, and four EF-hand domains. In this structure, two of the EF hands, EF3 and EF4, had bound Ca^{2+} ions, represented by yellow spheres. From *Scannevin et al. 2004.*

functional in all NCS proteins, due to a cysteine-proline substiution in the putative Ca^{2+} binding loop (Hwang et al. 2004). Typically, EF-hand proteins are inactive at 10^{-7}-10^{-8}M Ca^{2+}, and active at higher concentrations of 10^{-5}-10^{-6}M, but different EF-hands can have different Ca^{2+} affinities (Ikura 1996). In addition, the levels of Mg^{2+} in cells at rest is much higher than Ca^{2+}, suggesting the possibility of EF-hand domains activating by swapping from a Mg^{2+}- to Ca^{2+}-bound state (Aravind et al. 2008). This in fact seems to be the case with the KChIPs, with EF-hand 2 being a low affinity site with a preference for Mg^{2+} due to a glutamate to aspartate change at position 12 of the EF-hand. EF-hand 2 may even be completely inactive in KChIP1 (Osawa et al. 2005; Chen et al. 2006(1); Schwenk et al. 2008). One of the remaining sites seems to be a high-affinity Ca^{2+} binding site, likely EF4 in KChIP1, with the remaining EF-hand a slightly lower affinity site, but still Ca^{2+} bound in the activated protein (Craig et al. 2002; Chang et al. 2003; Zhou et al. 2004). It therefore seems likely that the KChIPs exist in two physiological states, with $3Mg^{2+}$ bound at resting Ca^{2+} concentrations, and in a $2Ca^{2+}/1Mg^{2+}$ state at higher intracellular Ca^{2+} concentrations (Schwenk et al. 2008).

The binding of Ca^{2+} to the EF-hands of a KChIP changes the arrangement of EF-hands, and its helical content, as shown by circular dichroism (Osawa et al. 2001; Chang et al. 2003), and it has been confirmed that it is only the binding of Ca^{2+}, not Mg^{2+}, that has this effect (Craig et al. 2002). The binding of KChIP3 to DNA, in its role as the transcriptional repressor DREAM, is abolished by binding Ca^{2+}, which leads to its multimerisation (Craig et al. 2002; Osawa et al. 2005), although there is some debate about whether this requires binding of Ca^{2+} to a single EF-hand (Osawa et al. 2005), or at multiple sites (Craig et al. 2002). Interestingly, 3D structures have also revealed that the C-terminus of KChIP3 contains a unique helix which may stabilise it in a dimeric formation, and contribute to its specific functions compared to KChIP1 (Yu et al. 2007; Lusin et al. 2008).

The binding of Ca^{2+} to EF-hands also appears to be important to the role of KChIPs in trafficking and regulating Kv4 channels. When the KChIPs were first discovered, it was shown that a form of KChIP1 mutated in EF-hands 2, 3 and 4 (EF2-4) did not bind Ca^{2+}, but could still bind and co-immunoprecipitate with Kv4 α subunits. However, the mutant KChIP lost its ability to modulate Kv4.2 currents (An et al. 2000). This separation of binding from kinetic modulation is also seen in mutants of the Kv4 channel (Callsen et al. 2005). The distribution of Kv4.2 also changed when co-expressed with mutant EF2-4 KChIP1, although it could no longer traffic to the plasma membrane, and this again suggests binding is not impaired in the mutant protein (Hasdemir et al. 2005). However, an EF2-4 mutant of KChIP4 has been shown not to bind Kv4.2 by co-immunoprecipitation (Morohashi et al. 2002), and mutating the EF-hand of KChIP2d, a shortened isoform with just one EF-hand, did not prevent it from modulating the kinetics of Kv4.3 channels (Patel et al. 2002b). In a major structural paper, Pioletti et al. (2006) agreed that the triple EF2-4 mutant was unable to modulate Kv4.3 channel kinetics. However, they argued that although single and some double EF-hand mutants were able to bind an N-terminal section of Kv4.3, both the EF3/EF4 double mutant, and EF2-4 triple mutant could not. This was suggested to be because of unfolding of the mutant proteins, although this is in contrast to the findings of Hasdemir et al. (2005), where both wild-type and EF2-4 mutant KChIP1 were present in the same intracellular structures. Therefore, the requirements for Ca^{2+}-binding by KChIP1, for both interaction with Kv4 channels, and modulation of their kinetics, still needs to be fully elucidated, especially contrasting single or double EF-hand mutations with the better characterised EF2-4 triple mutant.

1.3.4 Post-translational modifications and localisations of KChIPs

The localisation of isoforms of all 4 KChIPs, expressed alone in cells, has been determined. KChIP1 shows an unusual punctate distribution, in COS-7 cells, HeLa cells, and neurons (O'Callaghan et al. 2003; Hasdemir et al. 2005; Venn et al. 2008). KChIP2 is usually found associated with the plasma membrane (Venn et al. 2008), due to the palmitoylation of larger isoforms. This palmitoylation is

not necessary for interaction with the Kv4 channel, but is required for trafficking of the Kv4 channel, and for the KChIP2 to be localised to the plasma membrane in the absence of channel (Takimoto et al. 2002). KChIPs 3 and 4 are diffusely cytoplasmic in COS-7 cells, and found in both the cytoplasm and nucleus of PC12 cells. KChIP3 can also be isolated from HEK293 cell nuclear extracts, fitting its proposed role in transcriptional regulation. KChIP3 induced cell death in HeLa cells (Jo et al. 2001; Venn et al. 2008). One isoform of each of the four KChIP proteins was seen to co-localise with Kv4.2, stimulate its traffic to the plasma membrane, and then co-localise with the channel at the cell surface (Venn et al. 2008).

The interesting punctate distribution of KChIP1 expressed alone in cells made this an interesting target for further investigation. In order to show this punctate localisation, the KChIP1 has to be myristoylated on glycine 2, but this is always exposed, in contrast to other NCS proteins where the myristoyl tail is exposed only in response to Ca^{2+} binding (O'Callaghan et al. 2003). In fact, KChIP1 does not need to bind Ca^{2+} to access these vesicular structures, and an EF2-4 mutant can redistribute Kv4.2 channels into these vesicles (Hasdemir et al. 2005). These vesicles were shown to be mobile, and to be closely distributed with dendritic Golgi outposts in hippocampal neuron preparations (Hasdemir et al. 2005). In addition, the best co-localisation of these punctate vesicles was seen with ERGIC-53, a marker of the ER-Golgi intermediate compartment, and there was no co-localisation with constituents of the COPII coat, or with endosomal Rab proteins (O'Callaghan et al. 2003). This suggests a role for these vesicles in ER-Golgi trafficking, as discussed in more detail below.

As well as some isoforms being myristoylated or palmitoylated, there is evidence that the KChIPs can be regulated by phosphorylation. KChIP3 can be phosphorylated on serine 95 by the kinases GRK2 and 6, and can be dephosphorylated in a Ca^{2+}-dependent manner. This phosphorylation inhibits the trafficking of Kv4.2 to the plasma membrane (Ruiz-Gomez et al. 2007). This post-translational modification adds another level of regulation to the tightly

controlled expression of Kv4 channels. There are a range of other known modulators of these channels, and these are discussed in more detail below.

1.4 Alternative regulators of Kv4 channels

It is of vital importance to the neuron or cardiac myocyte that it is able to fully regulate Kv4 channels, in order to regulate A-type currents and hence cellular excitability. In addition to the KChIPs, a number of other proteins have been found that can interact with the Kv4 α subunits and alter their properties. Like the KChIPs, these proteins can exert their influence by regulating channel trafficking, by modulating channel kinetics, or by affecting both. In fact, there is growing evidence that multiple regulators may affect Kv4 channels together, forming ternary complexes (Jerng et al. 2005). Those proteins regulating channel function and kinetics will be discussed first, then those with a role in trafficking Kv4 channels, followed by a discussion of the membrane-associated guanylate kinase (MAGUK) family of proteins, and their potential interactions with Kv4 channels.

1.4.1 Regulating channel function and kinetics

A large number of proteins have been discovered that can influence Kv4 channel kinetics. However, it should be noted that many of these make the kinetics less like those seen in native channels (Maffie and Rudy 2008), and it still remains unclear what role these proteins may play. One example comes from the Kvβ subunits, which are known to be important in trafficking and regulating Kv1 channels, and can induce fast inactivation in non-inactivating Kv channels (Pongs et al. 1999). These can bind Kv4 channels, and have effects similar to KChIP2, but so can a Na^+ channel β subunit and the physiological relevance for many of these interacting partners remains unclear (Deschenes and Tomaselli 2002).

Other proteins seem to compete with the KChIPs for binding to the Kv4 α subunit. These include syntaxin 1A, which has been shown to modulate the magnitude of Kv4 currents, and their gating (Yamakawa et al. 2007). It should be noted, however, that syntaxin 1A has been shown to bind sepahrose and agarose beads in biochemical experiments, increasing the chance of false positive results

in interaction studies (Fletcher et al. 2003). Syntaxin 1A also has a clearly defined role in the SNARE fusion machinery of neurotransmitter vesicle release (Schiavo and Stenbeck 1998), so the purpose of, and the mechanism underlying, any interaction with Kv4 channels remains unclear. The *KCNE1-4* genes encode the heart specific minK, and the minK-related proteins, MiRP1-3. These can all bind Kv4.2 and Kv4.3, and slow the time constants of both activation and inactivation (Zhang et al. 2001). MiRP1 has also recently been shown to have a transmembrane domain like the KIS domain in some KChIP isoforms, which may explain how it can have similar kinetic effects to KChIP4a (Jerng and Pfaffinger 2008). Another NCS family member, NCS-1, can also bind to Kv4 channels, slowing their rate of inactivation, and increasing their surface expression, but the physiological significance of this is not clear (Nakamura et al. 2001b; O'Callaghan et al. 2003).The KChIPs are certainly more effective at binding Kv4 (Ren et al. 2003), likely due to a LFxxVM motif in helix H10 of KChIP1, which forms part of the Kv4 binding site (Zhou et al. 2004).

One problem with the role of KChIPs as the major modulators of Kv4 channels is that they slow the kinetics of inactivation, making currents less like fast-inactivating native currents. This led to the discovery of a protein expressed from a brain mRNA that could accelerate inactivation (Nadal et al. 2001), and paved the way for the identification of dipeptidyl-peptidases (DPP) 6 and 10 (Radicke et al. 2005; Clark et al. 2008). These are type II membrane glycoproteins, with a single transmembrane domain, large extracellular C-terminus, and alternately spliced intracellular N-terminus (Clark et al. 2008). They are expressed in both brain and heart (Radicke et al. 2005) with a distribution that matches Kv4.2. It should be noted, however, that DPP6 was also seen in the striatum lucidum of the hippocampal mossy fibre, a brain structure lacking Kv4.2 or Kv4.3 expression, suggesting an alternative function for DPP6 (Clark et al. 2008). The DPPs can be immunoprecipitated by Kv4.2 subunits (Jerng et al. 2004b), and appear to bind to Kv4.2 extracellularly near the channel's first transmembrane domain (Kim and Hoffman 2008). The effect of this interaction is to promote voltage-dependent activation, possibly via interaction with the channel's voltage sensor (Dougherty and Covarrubias 2006). Both DPP6 and DPP10 also increase the trafficking of

Kv4 channels to the plasma membrane (Zagha et al. 2005). However, it should be noted that the two DPP proteins can have subtly different quantitative effects on channel kinetics (Jerng et al. 2004b), and DPP6 may predominate in the heart, with DPP10 in the brain (Zagha et al. 2005). However, it seems that native currents can be most closely matched by a ternary complex of Kv4 channel, DPP protein and KChIP (Radicke et al. 2005). In this complex, channel trafficking is not further enhanced from expression with either accessory protein alone, but the channel kinetics are different from either binary complex (Jerng et al. 2005). Even so, this does not completely match the characteristics of the native neuronal A-type current, suggesting yet another level of regulation (Jerng et al. 2005).

The common cellular process of phosphorylation is also important in Kv4 channel regulation, and the channel α-subunits contain 2 PKA (protein kinase A) sites, 3 C-terminal ERK (extracellular signal-regulated kinase) sites, 2 C-terminal PKC (protein kinase C) sites, and 2 C-terminal CaMKII (Ca^{2+}/calmodulin-dependent kinase) sites (Kim and Hoffman 2008). The kinase c-Src can also interact with Kv4.3 and inhibition of this kinase reduced peak Kv4.3 currents (Gomes et al. 2008). Phosphorylation by either PKA or PKC reduces the probability of channel opening (Birnbaum et al. 2004), and phosphorylation of serine 616 by ERK decreases A-type currents (Hu et al. 2007). Interestingly, PKA phosphorylation seems to require that the channel have bound KChIP (Patel and Campbell 2005).

Finally, a variety of both physiological and exogenous chemicals can affect channel activity. These include some fatty acids and arachidonic acid, which can influence channel currents (Holmqvist et al. 2001). In fact, part of their kinetic effects requires the presence of the KChIP, suggesting that arachidonic acid may bind to both the Kv4 channel and the KChIP (Holmqvist et al. 2001). There are also several Kv4-specific toxins. These include heteropodatoxin, which exerts its effects through modulating channel gating, as well as occluding the channel pore (Zarayskiy et al. 2005), and the Taiwan cobra cardiotoxin CTX3, which binds to KChIP1 and enhances its interaction with Kv4 channels (Lin et al. 2004). The

small molecule CL-888 can also decrease peak and steady state currents, and can bind via KChIP1 to Kv4.3 (Bowlby et al. 2005).

1.4.2 Regulating channel trafficking

Some proteins interact with the Kv4 channels and influence both their kinetics and trafficking. This includes the KChIPs and DPP proteins, as well as MiRP1, which influences channel kinetics as discussed above, and channel progression to the plasma membrane (Chandrasekhar et al. 2006). Alternatively, there are other modulators of the Kv4 channels that exert their functions solely on the trafficking of the channel to the plasma membrane. These include the actin binding protein filamin, which increases channel trafficking (Petrecca et al. 2000) and the microtubule motor Kif17 (kinesin family member 17), which may be important for the trafficking of Kv4 channels to dendrites (Chu et al. 2006). The depolymerisation of actin by cytochalasin D also causes the channel to redistribute to the cell surface (Wang et al. 2004), highlighting the importance of the cytoskeleton in trafficking. Monocultures of cerebellar granule cells also need to make contact with mossy fibre cells in order for Kv4 channels to target to dendrites, and require glutamate signalling for clustering of these channels (which may link with the role of MAGUK proteins discussed below) (Shibasaki et al. 2004).

Whilst phosphorylation on some residues can inhibit Kv4 channels, phosphorylation of serines 438 and 459 by CaMKII promotes surface expression of Kv4.2, and also increases total levels in the cell (Varga et al. 2004). The K^+ channel associated protein (KChAP) can also bind Kv4.3, and increases the plasma membrane localisation of a range of Kv channels (Wible et al. 1998; Kuryshev et al. 2000). Meanwhile, neuronal interleukin-16 (NIL-16) reduces surface expression of Kv4.2 (Fenster et al. 2007), and PPTX (protein with pentraxin domain) binds Kv4.2 and traps it intracellularly (Duzhyy et al. 2005).

1.4.3 MAGUK proteins

The MAGUK family of proteins are characterised by having several PDZ domains, named for the three proteins where they were originally discovered: post-synaptic density 95 (PSD-95), *Drosophila* disc large tumour suppressor (DlgA) and zona occludens-1 (zo-1). Over 400 PDZ-domain containing proteins are known in mammals (Kim and Sheng 2004). These are often expressed in the brain, but also, for example, in the heart (Muller et al. 1995). The PDZ domain has six β strands, forming a partially opened barrel, topped on each side with an α helix (Feng and Zhang 2009).This can bind to the C-terminus of target proteins (Kim and Sheng 2004). In addition, the PDZ-domains are found in tandem arrays, and in conjunction with other protein interaction motifs. For example, one of the best studied families of MAGUK proteins are the PSD-95 family (Figure 1.7), which have 3 PDZ domains, plus an SH3 domain and a guanylate kinase-like domain (although this lacks enzymatic activity) (Kim and Sheng 2004). This allows these proteins to bind to many other proteins, and bind together as multimers, in order to cluster and scaffold other proteins (Kim and Sheng 2004; Feng and Zhang 2009).

There are four members of the PSD-95 family: PSD-95 (also known as SAP90), PSD-93 (also known as chapsyn-110), SAP102 and SAP97 (Kim and Sheng 2004). Of these, PSD-95 and PSD-93 are enriched in the post-synaptic density, where they cluster NMDA receptors, and may be important in synaptic function.

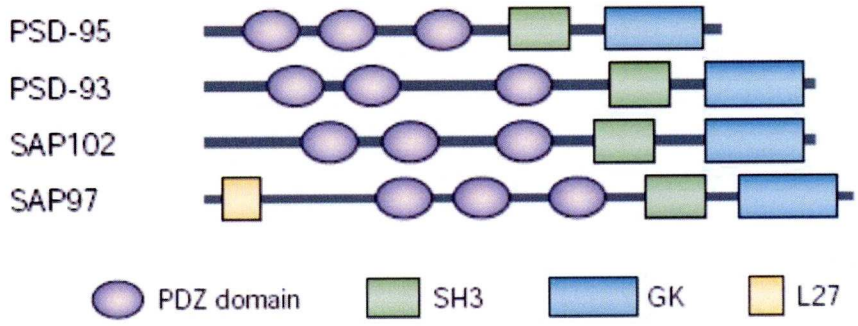

1.7: The PSD-95 family of MAGUK proteins.
Schematic representations of the domains found in four members of the PSD-95 family, PSD-95, PSD-93, SAP102 and SAP97. Each has three PDZ domains, an SH3 domain, and a GK guanylate kinase-like domain. In addition, SAP97 has an L27 domain. These allow for each PSD-95 protein to make interactions with several other proteins and effectors. Adapted from *Kim and Sheng 2004.*

Meanwhile, SAP97 and SAP102 are found in dendrites, axons, the cytoplasm and synapses of neurons, and may be involved in trafficking to the plasma membrane (Kim and Sheng 2004). These different proteins have various isoforms, and these can have a range of post-translational modifications. For example, SAP97 has two known splice isoforms (Muller et al. 1995). PSD-93 has many isoforms, of which PSD-93δ has a cysteine residue for palmitoylation (also seen in PSD-95 for post-synaptic targeting), PSD-93ζ has an L27 domain (also used by PSD-95β to target to synapses via protein-protein interactions), but PSD-93ε has neither (Parker et al. 2004). Thus different isoforms may have different intracellular roles. It has also been shown that PSD-95 and PSD-93α/β can only cluster neuronal ion channels when palmitoylated, whilst SAP97 and SAP102 are unpalmitoylated, and cannot cluster channels (El-Husseini et al. 2000).

PSD-93 and PSD-95 seem to share many functions, and are found in the same synapses by electron microscopy (DeGiorgis et al. 2006). PSD-93 localises to neuronal cholinergic synapses, and might have a role in stabilising nicotinic acetylcholine receptors. However, recent work with PSD93 knockout mice has shown them to be normal, and clustering of nicotinic acetylcholine receptors was unaffected (Parker et al. 2004), suggesting the presence of a compensatory protein, possibly PSD-95. PSD-95 is found at the post-synaptic density, and is found on the plasma membrane when expressed in COS-1 cells (Tiffany et al. 2000). It has well characterised binding to AMPA receptors, preventing their lateral diffusion in the synaptic membrane (Bats et al. 2007), and can cluster NMDA receptors (Kim and Sheng 2004). SAP97 was discovered in the presynaptic terminals of excitatory synapses in the hippocampus, where it exists in both a hydrophilic and membrane-associated form (Muller et al. 1995). In COS-1 cells it was seen to be perinuclear (Tiffany et al. 2000). Electron microscopy work has also identified SAP97 at the edges of post-synaptic densities, near AMPA receptors (DeGiorgis et al. 2006). Recent work has also shown a role for SAP97 in the non-conventional trafficking of NMDA receptors from the ER to dendritic Golgi outposts in neurons (Jeyifous et al. 2009).

Both SAP97 and PSD-95 can bind to potassium channels, including inward rectifier (Kir) channels (Leyland and Dart 2004), increasing the number of them at the cell surface and causing them to cluster (Horio et al. 1997). There is also evidence they can have roles beyond trafficking and clustering, as PSD-95 can reduce Kir2.3 channel conductance (Kim and Sheng 2004). They can also bind to Kv1 channels, where interestingly PSD-95 can cluster Kv1 channels and prevent their internalisation (Jugloff et al. 2000; Tiffany et al. 2000), whilst SAP97 retains the channel within membrane-bound organelles in the cell, preventing its trafficking (Tiffany et al. 2000). More importantly for this study, PSD-95 and SAP97 can also bind to Kv4 channels, as shown by co-immunoprecipitation and co-localisation by immunohistochemistry in brain slices (Gardoni et al. 2007). This interaction requires the PDZ domain of PSD-95 or SAP97, and a valine-serine-alanine-leucine PDZ-binding motif in the C-terminus of Kv4.2 (Wong et al. 2002; Gardoni et al. 2007; El-Haou et al. 2009). This interaction also requires the palmitoylation of PSD-95 (Wong et al. 2002). Both SAP97 and Kv4.2 can be phosphorylated, but this does not affect their interaction (Gardoni et al. 2007). However, phosphorylation of SAP97 by CaMKII (Kim and Sheng 2004) does promote the trafficking of both SAP97 and Kv4.2 to dendritic spines (Gardoni et al. 2007). It seems that SAP97 can promote trafficking of Kv4.3 to the plasma membrane (El-Haou et al. 2009), although this was in cells stably transfected with KChIP2, and the separate contributions of the SAP97 and KChIP2 to channel trafficking were not fully assessed. The SAP97 also increased the channel's current density, although to a lesser extent than the KChIPs (El-Haou et al. 2009). In addition, SAP97 knockdown by RNAi reduced the levels of Kv4.2 in the postsynaptic compartment, suggesting this PDZ-domain protein may be important in Kv4 trafficking (Gardoni et al. 2007). On the other hand, PSD-95 increases the surface expression of Kv4.2 and causes it to cluster, so may be a key anchor at the synapse membrane (Wong et al. 2002; Gardoni et al. 2007). This may have a role physiologically, by bringing the Kv4 channels close to NMDA receptors, thus influencing LTP (Wong et al. 2002). It has also been shown that a mutation in the Kv4.2 channel causing epilepsy is missing the PDZ-domain binding site (Singh et al. 2006). These proteins thus seem to be another important class of Kv4 regulators *in vivo*.

1.5 Traffic through the secretory pathway

It is apparent from the work described above that the trafficking of Kv4 channels to the plasma membrane is vital in regulating their function, and hence neuronal activity. Although association with accessory proteins, especially the KChIPs, can promote this trafficking, many of the molecules and mechanisms facilitating this trafficking are likely to be those used by the standard secretory pathway. Protein synthesis and trafficking via this conventional pathway will be introduced, with sections on two important groups of proteins regulating this pathway, the Rabs and SNAREs. However, there is growing evidence of non-conventional trafficking pathways in cells, and these will be discussed, before focussing on the evidence for the non-conventional trafficking of Kv4 channels.

1.5.1 Protein synthesis and retention at the ER

The first step on the secretory pathway is the endoplasmic reticulum. Proteins with transmembrane domains, for example Kv4 channels, have a signal sequence at the N-terminus of their sequence. This consists of at least one basic residue, followed by a stretch of 6-20 hydrophobic residues. This is recognised by the signal recognition particle (SRP), a cytoplasmic ribonucleoprotein. This binds to the signal sequence as it emerges from the ribosome, temporarily inhibiting elongation. The SRP then binds to the SRP receptor on the ER membrane, causing the displacement of the SRP. The ribosome can then recommence translation, with the newly synthesised protein being inserted across the ER membrane co-translationally. This is more fully reviewed in Wilkinson et al. 1997.

Once translated, multispan transmembrane proteins are often retained within the ER (Trombetta and Parodi 2003). In particular, there are ER quality control checks, designed to degrade proteins that are synthesised but not folded into their native state. This involves chaperones and other folding factors, in a regulated network for protein folding and retention (Trombetta and Parodi 2003). Beyond this, misfolded proteins can exit from the ER if they present a correct ER exit

signal (Kincaid and Cooper 2007), and there is evidence for Golgi quality control, but the mechanisms of this are unclear (Trombetta and Parodi 2003). In fact, proteins can have a range of signals for trafficking to, or retention in, various organelles, but these are not well understood (Rothman and Wieland 1996). One of the best known is the dilysine ER retention motif, first identified in yeast, but shown to also be functional in mammalian cells. Some potassium channels instead have dibasic RXR motifs. These bind to the COPI coat, to allow proteins to recycle back from the Golgi to the ER (Cosson and Letourner 1994; Zerangue et al. 1999). Alternatively, there are three known ER-exit signals, which likely bind to parts of the COPII coat to promote ER-to-Golgi trafficking (Watanabe and Riezman 2004). G-protein coupled receptors have these export signals (Dong et al. 2007) and some ion channels may have them as well, but very little is known about specific signals in Kv4 channels (Misonou and Trimmer 2004).

1.5.2 Conventional ER-to-Golgi trafficking

Early work on the exocytic trafficking of newly synthesised proteins came from pioneering work on characterising intracellular organelles and determining their function. The important contributions of three of the founders of modern cell biology – Albert Claude, Christian de Duve and George E Palade – were acknowledged by the award of the 1974 Nobel Prize for Physiology or Medicine. This was awarded for Claude's development of methods for preparing cells for electron microscopy, which were later refined by Palade. It also acknowledged Claude's development of the technique of cell fractionation by centrifugation to separate different organelles, used by de Duve for characterising lysosomes (Edstrom 1992). Palade combined electron microscopy with cell fractionation to study intracellular trafficking, and developed pulse-chase experiments with radiolabelled amino acids, to follow newly synthesised protein in the cell, with an improved time resolution. This work showed that proteins traffic from the rough ER to the *cis*- and then *trans*-Golgi, and that this process requires ATP. Palade also suggested that proteins were trafficking between organelles in vesicles (Palade 1975). Following on from this work, Rothman and colleagues

started to use vesicular stomatitis viral glycoprotein (VSVG) to study the synthesis and trafficking of transmembrane proteins. This showed that such proteins were being inserted across the membrane of the ER during, or immediately after, protein synthesis. These studies also laid the foundation for *in vitro* reconstitution experiments, studying protein synthesis and trafficking in cell-free systems (Katz et al. 1977a; Katz et al. 1977b). Later work by Rothman also identified different populations of trafficking vesicles, distinguishing between those for ER-Golgi traffic, and those involved in the Golgi-plasma membrane step (Rothman and Fine 1980). VSVG continues to be used to study the dynamics of ER-Golgi trafficking, and temperature sensitive mutants and GFP-tagged versions of the protein have been developed (Presley et al. 1997). These can be trapped in the ER or Golgi at different temperatures, and their onward trafficking visualised using fluorescence microscopy. Finally, much early

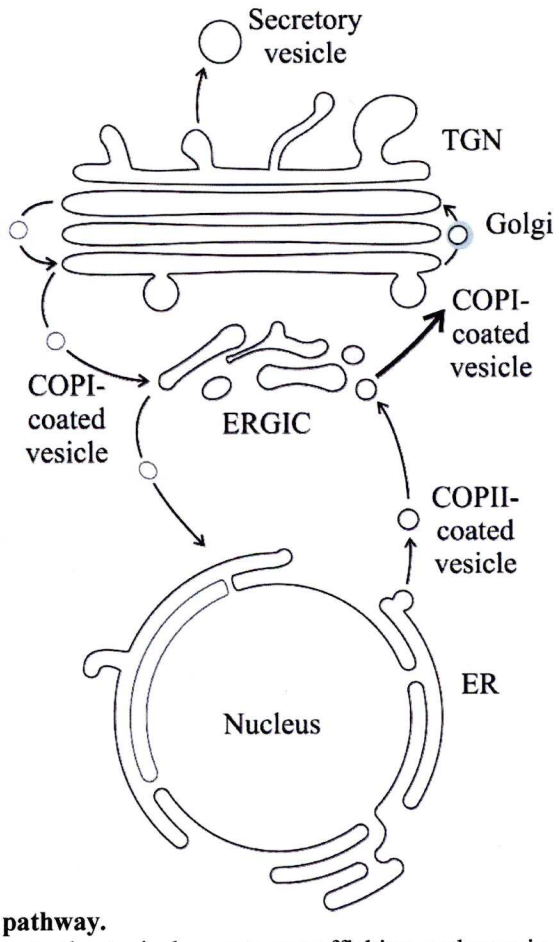

1.8: The secretory pathway.
The diagram represents the typical secretory trafficking pathway in a vertebrate cell. The various organelles on the secretory pathway are shown, with trafficking occurring in the direction of arrows. Traffic between organelles occurs in coated vesicles, with COPII and COPI being important coats for ER-Golgi trafficking.
ER = endoplasmic reticulum, ERGIC = ER Golgi intermediate compartment, TGN = *trans*-Golgi network.

work in identifying the important proteins involved in exocytic trafficking came from Schekman and colleagues using yeast. In a seminal paper from 1980, they identified 23 secretory yeast mutants, with these genes later identified with the Sec proteins (Novick et al. 1980). This work proved to be important, as much of the machinery and number of coats is conserved, although the number of proteins in humans is greatly expanded (Bock et al. 2001; Bonifacino and Glick 2004). The typical vertebrate pathway is shown in Figure 1.8.

The pathway starts at specific, relatively immobile regions of the ER, which are cleared of ribosomes. These are called either ER exit sites, or the transitional ER, and it is here that newly synthesised proteins are packaged into COPII-coated vesicles (Figure 1.9) (Glick 2000; Stephens et al. 2000). This involves some level of cargo sorting, as VSVG is concentrated 5-6-fold on ER exit (Bannykh et al. 1996). The first component of the COPII coat to bind the ER is the GTPase Sar1. Mammals have two isoforms of this, which are largely redundant, but the traffic of some cargoes may be Sar1b specific (Shoulders et al. 2004). Sec12 is needed as a Sar1 GEF (guanine nucleotide exchange factor) converting Sar1 to its GTP bound form (Barlowe et al. 1994). This releases the N-terminal tail of Sar1, which allows it to bind membranes, and allows it to recruit Sec23/Sec24 (Rothman and Wieland 1996; Shoulder et al. 2004). These proteins, especially

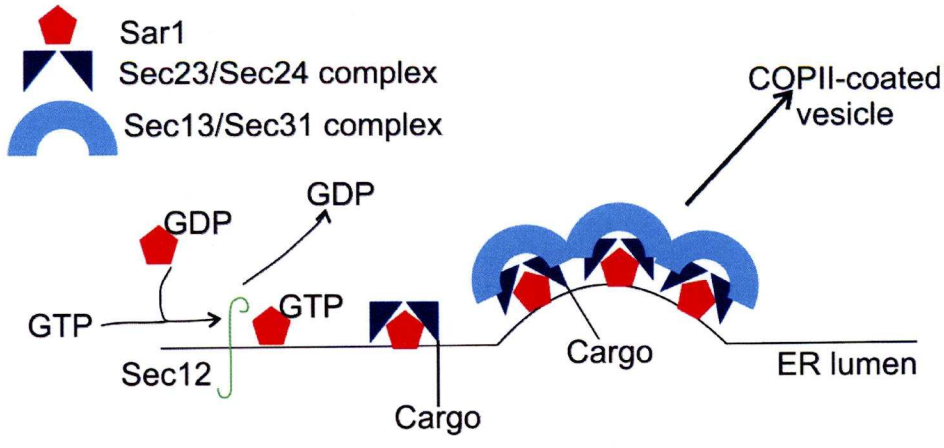

1.9: The assembly of a COPII-coated vesicle.
This shows the conventional model of the assembly of a COPII coat on the membrane of the endoplasmic reticulum (ER). The guanine nucleotide exchange factor Sec12 converts Sar1 from its GDP- to GTP-bound form, allowing it to interact with the ER membrane. Sec23/Sec24 are then recruited, and can interact with cargo molecules. Finally, the Sec13/Sec31 complex binds, and induces membrane curvature, allowing the vesicle to bud from the membrane. Adapted from *Kuehn and Schekman 1997.*

Sec24, are thought to form a complex with cargo and/or ER export signals, and may play a role in sorting and concentrating proteins in COPII-coated vesicles (Kuehn et al. 1998). Next, Sec13 and Sec31 bind. These form the protein scaffold, and can even self-assemble into a lattice *in vitro* (Gurkan et al. 2006; Stagg et al. 2006), deforming the membrane into a bud (Matsuoka et al. 1998). The vesicle then traffics away from the ER, in ~60nm diameter vesicles (Barlowe et al. 1994). This requires microtubules and the motor proteins dynein/dynactin (Presley et al. 1997), and Sec23 interacts with dynactin to facilitate this (Watson et al. 2005). Finally, an arginine finger from Sec23 promotes the GTPase activity of Sar1 (Bonifacino and Glick 2004), and this causes first Sar1 and then the rest of the coat to disassemble from the membrane (Barlowe et al. 1994; Rothman and Wieland 1996). The COPII coat is not required for traffic to or through the Golgi (Kuge et al. 1994; Stephens et al. 2000).

In vertebrates, the next step in the trafficking pathway seems to be the ER-Golgi intermediate compartment (ERGIC), also known as vesicular tubular clusters (VTCs) (Glick 2000). Once uncoated, COPII vesicles may homotypically fuse to form the ERGIC (Glick 2000), and ER exit sites face towards the ERGIC (Bannykh et al. 1996). 3D ultra-rapid freezing electron microscopy reveals branched tubules and flattened sacs, separate from the ER or Golgi, surrounded by uncoated budding and fusing vesicles (Ladinsky et al. 1999). Most tested proteins pass through the ERGIC on route from ER to Golgi (procollagen is an exception, as will be discussed below), and the greater the level of protein production, the larger the ERGIC (Stephens and Pepperkok 2004; Simpson et al. 2006).

There is much debate about the next step in trafficking to the Golgi. Individual ERGIC clusters may move towards the *cis*-Golgi on microtubules and then aggregate to give the first Golgi cisterna (Scales et al. 1997; Glick 2000). Alternatively, COPI coated vesicles, which are required for retrograde trafficking in yeast (Cosson and Letourner 1994), may act as both anterograde and retrograde carriers in vertebrates (Rothman and Wieland 1996; Rowe et al.

1996). There is evidence for two populations of COPI vesicles, one containing anterograde markers, and the other proteins for retrograde traffic (Nickel et al. 1998). Also, antibodies against β-COP, a constituent of the COPI coat, blocked VSVG in the ERGIC (Peter et al. 1993). Knockdown of the GEF for the COPI GTPase ARF1, or locking ARF1 in the GTP-bound form using a Q71L mutation, blocked VSVG in the ERGIC, as well as disrupting the *cis*-Golgi and ERGIC (Dascher and Balch 1994; Szul et al. 2007). Also, COPI vesicles have been observed trafficking from the cell periphery to the Golgi (Stephens et al. 2000), and a variety of tested cargoes require COPI for anterograde trafficking (Stephens and Pepperkok 2004). A big question is how the cell sorts anterograde and retrograde cargoes into different populations of COPI vesicles (Glick 2000), although this may involve the ERGIC53/VIP36 family of proteins (Nickel et al. 1998).

COPI coat assembly shares similarities with the COPII coat. Firstly, the GTPase ARF1 undergoes GDP-GTP exchange, with the assistance of soluble GEFs with Sec7 domains, and with ARF1 bound to membranes via a myristoyl tail (Franco et al. 1996; Goldberg et al. 1998). However, unlike COPII, ARF1 then recruits all other members of the COPI coat together as a single complex (Bonifacino and Glick 2004). This coatomer complex consists of α-COP, β-COP, β′-COP, γ-COP, δ-COP, ε-COP and ζ-COP (Bednarek et al. 1995). Like Sar1, ARF1 is vital both for recruiting the COP coat, and triggering its disassembly by GTP hydrolysis (Rothman and Wieland 1996). This step is sensitive to non-hydrolysable GTPγS (Pepperkok et al. 1998). ARF1 may also be required for COPII/COPI coat exchange (Rowe et al. 1996), and for maintaining Golgi structure (Dascher and Balch 1994). Once delivered to the Golgi, transmembrane proteins then appear to move through it in sequential steps (Balch et al. 1984), with COPI required for traffic between Golgi cisternae (Orci et al. 1997). Proteins then exit in secretory vesicles for traffic to the plasma membrane. The exact organisation and route through the Golgi is controversial, however (Mironov et al. 1998; Patterson et al. 2008), but will not be discussed further here.

1.5.3. Rab GTPases

The process of vesicular secretory trafficking must be highly regulated and compartment specific and one group of vital proteins is the Rab GTPase family. These are Ras-related proteins found in the brain, and around 20-25kDa in size (Schwartz et al. 2007). The family is encoded by about 11 genes in budding yeast, and 60 human genes, reflecting the evolutionary increase in trafficking complexity (Bock et al. 2001; Lee et al. 2009). Even essential Rabs, such as Rab1, may have different isoforms, and there are different expression profiles of these isoforms in different cell types (Gurkan et al. 2005). Rab proteins are GTPases, and as such exist in an inactive, GDP-bound form, and a GTP-bound active form. In this active form they can associate with membranes through (usually) two C20 prenyl groups, attached to C-terminal cysteine residues. This is essential to their function (Lee et al. 2009). They may also be phosphorylated, and thus be downstream of signalling pathways (Schwartz et al. 2007).

The activation of Rabs is tightly regulated. Guanine nucleotide exchange factors (GEFs) allow the exchange of GDP for GTP, at which point the Rab-GTP can associate with a range of protein effectors (Grosshans et al. 2006). This may include recruiting the GEF for another Rab. However, the Rab can catalyse the GTP back to GDP, a process accelerated by the GTPase activating proteins (GAPs). Rab GDP dissociation inhibitors (RabGDI) then promote the removal of Rab-GDP from membranes, and are themselves dissociated from the Rab by Rab GDI displacement factors (RabGDFs) (Lee et al. 2009). Most Rab GAPs have a TBC (Tre-2, Bub-2, Cdc16) domain, of which there are ~51 in the human genome (Bernards 2003). Some of these have been matched to their specific Rabs, including TBC1D20, which was shown to be specific for Rab1 *in vivo* (Haas et al. 2007).

Different Rabs are found throughout the cell (Schwartz et al. 2007), but specific Rabs have specific localisations and functions. In general, this involves organizing membrane domains that control the trafficking of cargoes to different

destinations (Schwartz et al. 2007). Often this involves regulating the fusion of SNARE complexes, and possibly proofreading them, or regulating the tethering of vesicles in the step prior to SNARE fusion (Rothman and Wieland 1996; Bonifacino and Glick 2004). They may also interact with motor proteins, to direct the transport of vesicles (Hammer and Wu 2002). In fact, it has been proposed that they act at the centre of trafficking hubs, regulating SNAREs, tethers and motor proteins (Gurkan et al. 2005). It is Rabs 1a, 1b and 2 that are vital for vesicular trafficking from ER to Golgi (Tisdale et al. 1992). Rab2 may have a role in the formation of COPI-coated vesicles (Buffa et al. 2008), is found in the ERGIC, and may play a role in anterograde/retrograde cargo segregation (Tisdale and Balch 1996). Meanwhile, depletion of Rab1, or using a mutant inactive version of its RabGAP TBC1D20, inhibited the trafficking of VSVG to the plasma membrane, disrupted COPII localisation, and fragmented the Golgi and ERGIC (Haas et al. 2007), highlighting Rab1's importance in ER-Golgi trafficking.

1.5.4 SNARE proteins

There are more than 36 human SNARE (soluble NSF attachment receptor) proteins, each containing a 60-70 amino acid SNARE motif, and typically a C-terminal transmembrane domain to anchor them to membranes (Jahn and Scheller 2006). Three, or more usually four, SNARE proteins come together, and their SNARE motifs form one of four α helices that assemble into a coiled coil, as shown in Figure 1.10. If these SNARE proteins are on two different membranes (a *trans* configuration), then it is thought that formation of this coiled coil produces a mechanical force that drives membrane fusion (Jahn and Scheller 2006). Each fusion machine consists of between 3 and 15 SNARE complexes. Once membrane fusion is complete, the SNARE complex is disassembled by the actions of SNAP proteins and NSF, using energy obtained from the hydrolysis of ATP by NSF (Jahn and Scheller 2006).

The fusion of two membranes needs controlling, in order to keep proteins compartmentalised correctly, and to ensure that secretion of proteins can be controlled. It is therefore important to have specificity and regulation. The central '0' layer of the interacting SNARE complex contains four conserved residues, 3 glutamines and 1 arginine. Each SNARE protein contributes one of these residues, and can therefore be classified as a Q or R SNARE, and the majority of *in vivo* SNARE complexes have a $Q_AQ_BQ_CR$ arrangement (Jahn and Scheller 2006). However, it has been shown *in vitro* that as long as this glutamine and arginine distribution is obeyed, that any SNARE complexes can form (Fasshauer et al. 1999; Yang et al. 1999(1)). Whilst there is certainly evidence that SNARE proteins can drive membrane fusion without requiring other accessory proteins (Hu et al. 2003), it seems that specificity may also depend on tethering factors, Rab proteins, and the localisation of SNAREs in the cell (Yang et al. 1999(1); Hong 2005). Nevertheless, the complement of SNAREs on a membrane or vesicle does help determine which other membranes it can bind with, and hence to some extent defines that compartment (Jahn and Scheller 2006).

The SNAREs for ER-Golgi trafficking seem to be highly conserved from yeast onwards (Kloepper et al. 2007). The conventional trafficking pathway involves a complex of syntaxin 5, membrin and rBet1, which is then bound by Sec22b to form the complete SNARE complex (Xu et al. 2000). Both Sec22b and rBet1 are

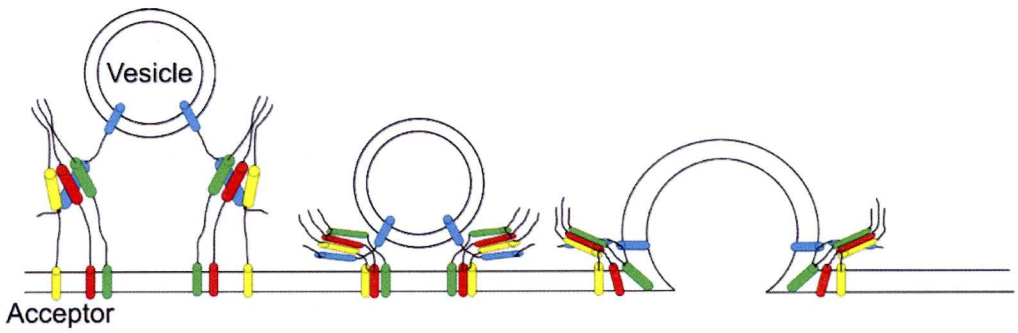

1.10: The formation of a SNARE complex allows fusion of two membranes.
Four SNARE proteins come together to form a complete SNARE complex. In this case, one SNARE is shown on the vesicle and three on the acceptor membrane, each coloured separately. As the SNARE helices interact to form a coiled coil, the SNARE proteins, and the membranes they are bound to, come closer together. Eventually this leads to the formation of a fusion pore, and the joining of the two membranes. Adapted from *Jahn and Scheller 2006.*

enriched at ER exit sites, whilst membrin is seen on small vesicles moving from ER to Golgi (Chao et al. 1999), and syntaxin 5 is required for the fusion of COPII-coated vesicles to form the ERGIC (Bentley et al. 2006). It therefore seems that this SNARE complex is required on COPII- and COPI-coated vesicles, and the ERGIC (Dascher et al. 1994; Hay et al. 1998).

Alternatively, a SNARE complex containing Ykt6, GOS28, syntaxin 5 and rBet1 has been described in the literature in the Golgi (Zhang and Hong 2001). GOS28 shows a steady-state localisation in the Golgi (Hay et al. 1998), where it has a role in the docking and fusion of vesicles with the *cis*-Golgi (Subramaniam et al. 1996). Ykt6 is also an interesting SNARE, as it contains a profilin-like 5 stranded antiparallel sheet surrounded by three α helices, known as a longin domain (Hong 2005). Ykt6 can be prenylated to allow interaction with membranes (Zhang and Hong 2001), but this is masked by the longin domain (Hasegwa et al. 2004), which also inhibits SNARE complex formation (Hong 2005; Wang and Tang 2006). This longin domain also directs Ykt6 to an unusual punctate distribution in PC12 cells, which corresponds to neither the ERGIC nor endosomes (Hasegwa et al. 2003; Hasegwa et al. 2004).

Finally, there is a third SNARE complex implicated in ER-Golgi trafficking, this time in the non-conventional trafficking of prechylomicron transport vesicles (PCTVs) in the intestine. This involves the SNAREs VAMP7, Vti1a, rBet1 and syntaxin 5 (Siddiqi et al. 2006a), and antibodies against VAMP7 prevented the delivery of triacylglycerol from ER to Golgi (Siddiqi et al. 2006b). In these studies, VAMP7 was found in the ER and Golgi of intestinal cells, but not in the ER of the kidney or liver, suggesting this is a tissue-specific pathway (Siddiqi et al. 2006b). It should also be noted that VAMP7 is not expressed in the heart (Advani et al. 1998).

This ER localisation of VAMP7 is surprising, as this SNARE is more commonly associated with lysosomes, and many studies have found it co-localised with

lysosomal markers (Advani et al. 1998; Advani et al. 1999; Martinez-Arca et al. 2003). Both VAMP7 and Vti1a seem to be more typically involved in endosome/lysosome or lysosome/lysosome fusion, in complex with syntaxins 7 and 8 (Bogdanovic et al. 2002; Pryor et al. 2004; Casey et al. 2007). However, immunogold electron microscopy has shown VAMP7 to be most associated with the ERGIC (Coco et al. 1999), and in a proteomic map of the secretory pathway VAMP7 was in COPI-coated vesicles, and Vti1a in the smooth ER, Golgi and COPI-coated vesicles (Gilchrist et al. 2006). VAMP7 was also in small vesicles dispersed throughout the cytoplasm of CaCO-2 cells, which were not associated with Golgi or lysosome markers (Galli et al. 1998). VAMP7 also appears to have an important role in neuronal growth, and is enriched in neurons (Wang and Tang 2006), where it regulates neurite outgrowth (Martinez-Arca et al. 2000). This could explain its localisation to both punctate structures within the cell body of neurons, and to the leading edge of the growth cone (Coco et al. 1999). Like Ykt6, VAMP7 is a longin-domain SNARE and this domain both inhibits SNARE complex formation, and influences the protein's localisation (Martinez-Arca et al. 2003; Uemura et al. 2005).

1.5.5 Non-conventional trafficking pathways

Whilst the bulk of cellular protein traffic goes via the standard pathway described in section 1.5.2, and is under the common regulation of the protein families discussed above, there are examples of other non-conventional routes through the cell, some of which will be discussed below. Although many of the underlying mechanisms of trafficking are conserved from yeast to humans, there are differences in trafficking, not least that both COPII- and COPI-coated vesicles can bud from the ER in yeast (Bednarek et al. 1995). In fact, yeast seem to have three populations of ER-Golgi vesicles, for soluble cargoes, GPI-anchored cargos, and transmembrane and other proteins, regulated by cargo adaptor sorting (Castillon et al. 2009). This segregation of GPI-anchored proteins requires ceramide synthesis, but seems to be due to protein-protein interactions rather than lipid partitioning, possibly by interacting with individual SNARE proteins

(Muniz et al. 2001; Morsomme et al. 2003; Watanabe et al. 2008). This pathway is also still COPI-dependent (Sutterlin et al. 1997).

Mammalian GPI-anchored proteins are also trafficked via a non-conventional route, requiring the cargo adaptor p24 proteins (Takida et al. 2008). However, there is evidence that GPI-anchored proteins still require Sar1 GTP hydrolysis for sorting into COPII-coated ER exit sites, as does another unusual cargo, procollagen (Stephens and Pepperkok 2004). Procollagen is an interesting cargo as it is too large for standard COPII vesicles. Indeed, although it buds at or near to ER exit sites, requiring COPII, it may then traffic in microtubule-dependent spherical structures that are not COPII coated, and do not go via the ERGIC (Stephens and Pepperkok 2002; Stephens and Pepperkok 2004). Alternatively, and more controversially, uncoated tubules and sacs may form from distended regions of the ER, 600-800nm in diameter (Mironov et al. 2003). Onward trafficking may or may not then require COPI (Mironov et al. 2003; Starkuviene and Pepperkok 2007).

In the intestine, triacylglycerol is resynthesised in the ER, and transported to the growing chylomicron by prechylomicron transport vesicles (PCTVs) (Kumar and Mansbach 1997). These are 100-500nm in diameter, and in contrast to procollagen vesicles, can bud from the ER in a COPII-independent manner, whilst requiring COPII for later fusion with the Golgi (Siddiqi et al. 2003). As discussed in section 1.5.4, the trafficking of these vesicles from ER-to-Golgi also requires a novel SNARE complex (Siddiqi et al. 2006a). The PCTVs also appear to lack COPI (Siddiqi et al. 2003). Meanwhile, viral primary membrane proteins can traffic from the ER in a completely COPII-independent manner (Husain and Moss 2003).

The cystic fibrosis transmembrane conductance regulator (CFTR) also seems to have a COPI-independent trafficking route, although it does require COPII. What is interesting about this protein is that it can traffic from the ER to the distal

Golgi, and then back to the *cis*-Golgi, and that this unusual pathway is Rab1 and Rab2-independent (Yoo et al. 2002). The α_{2B}-adrenergic receptor also seems to traffic in a Rab1-independent manner (Wu et al. 2003). Finally, the protein H-Ras can traffic via both the standard pathway and a COPII/COPI-independent, non-vesicular pathway (Zheng et al. 2007), and a mutant GABA transporter-1 (GAT-1) can traffic in a COPII/COPI/ERGIC-independent manner, although this mutation prevents it from sorting to axons correctly (Reiterer et al. 2008). Even more extremely, both the simian rotavirus RRV, and K-Ras can traffic directly from the ER to the plasma membrane, without transiting the Golgi (Jourdan et al. 1997; Apolloni et al. 2000).

1.5.6 ER-retention of K^+ channels

Many ion channels, and particularly K^+ channels, are localised to the ER when expressed alone in non-neuronal cells, as discussed in Section 1.5.1. One mechanism for this is through RXR ER retention motifs. These direct the recycling of the protein from the Golgi back to the ER, by allowing the protein to interact with the COPI coat (Cosson and Letourner 1994; Zerangue et al. 1999). An important family of proteins in regulating this are the 14-3-3 proteins. Humans have seven isoforms of 14-3-3 proteins (β, γ, ε, ζ, η, τ, σ), which form homo- or heterodimers, in order to bind to phosphorylated target proteins (Shikano et al. 2006). This binding can be to specific sequences as Mode I binding (R(S/Aromatic)(Basic)(pS/T)XP) or Mode II binding (RX(Aromatic)(Basic)(pS/T)XP) (Aitken et al. 2002). Alternatively, there is growing evidence for Mode III binding to a C-terminal SWpTY motif, using the same 14-3-3 binding groove (Coblitz et al. 2005). There is also evidence *in vitro* of binding to non-phosphorylated substrates, again via the same binding pocket, but it is not clear if this is significant *in vivo* (Tzivion and Avruch 2001; Aitken et al. 2002).

The 14-3-3 proteins do not have an enzymatic function. Rather, it is thought that they exert their effects through scaffolding proteins together, clamping enzymes

to their targets, or masking retention signals. They may in fact have multiple roles with one substrate (Shikano et al. 2006; Tzivion et al. 2001). 14-3-3 proteins have been shown to have many roles associated with ion channels, and in particular regulating their trafficking. This includes promoting the surface expression of 2-pore-domain TASK channels, KCNK leak channels, and, in plants, outward rectifying K^+ channels (O'Kelly et al. 2002; Rajan et al. 2002; Berg et al. 2003). One mechanism suggested for this, and shown to be active for ATP-sensitive K^+ channels, is that binding of 14-3-3 proteins to phosphorylated residues near to RXR ER-retention motifs competes with binding to the COPI coat for retrieval of the channel back to the ER (Trombetta and Parodi 2003; Heusser et al. 2006). It is not clear if the different isoforms have differing roles in this (Tzivion and Avruch 2001). In fact, the high level of sequence conservation in the protein binding pocket argues either against isoform specificity, or for the importance of other regions in the dimer (Aitken et al. 2002). It does seem that 14-3-3γ is the major isoform in the Golgi, with a role in protein trafficking and the secretory pathway (Roth et al. 1994; Aitken et al. 2002). A 14-3-3γ knockout mouse did show changes to some protein expression, however it had no phenotype, and general exocytosis seemed not to be impaired (Steinacker et al. 2005), suggesting some redundancy of action.

When expressed alone in cells, Kv4.2 shows a perinuclear pattern of localisation. As many other K^+ channels are retained in the ER when expressed alone in non-neuronal cells, it has been argued that this is also the case for Kv4.2. In support of this, studies have shown co-localisation with the ER-resident marker calnexin (Shibata et al. 2003). However, this paper also showed that mutation of the only RXR ER-retention motif in Kv4.2 had no effect, implying it is non-functional. Furthermore, other studies have shown that ECFP-Kv4.2 does not co-localise with the ER markers calnexin or protein disulphide isomerase, but shows clearer co-localisation with the *cis*-Golgi marker β-COP and Golgi-targeted EYFP (O'Callaghan et al. 2003; Hasdemir et al. 2005). These data would therefore argue that usually the Kv4.2 channel is localised to the Golgi when expressed alone in non-neuronal cells.

1.5.7 Trafficking of Kv4.2 channels

Many of the proteins in section 1.5.6 that use non-conventional trafficking pathways are unusual, because of their viral origins, large size, or specific membrane anchor. In contrast, the Kv4.2 channel would be expected to follow a conventional trafficking route, but there is evidence to suggest that this is not the case.

As discussed above, the Kv4.2 channel is localised to the Golgi when expressed alone in cells. Co-expression with KChIP1 causes trafficking of both the KChIP and Kv4.2 channel to the plasma membrane (O'Callaghan et al. 2003). The requirement for COPI in this trafficking was shown using a dominant negative mutant of ARF1. This blocked Kv4.2/KChIP1 trafficking, as well as VSVG, used as a control for conventional trafficking. However, although a dominant negative form of Sar1 blocked VSVG trafficking, and inhibited Kv4.2 from reaching the Golgi when expressed alone, it did not completely block Kv4.2/KChIP1 trafficking to the plasma membrane (Hasdemir et al. 2005). This suggests that Kv4.2/KChIP1 traffic via a different pathway to the bulk COPII-dependent route. However, this has not been further characterised. In neurons, Kv4.2 trafficking is polarised to the dendrites, due to a 16 residue dileucine motif (Rivera et al. 2003). The channels then cluster on the neuronal membrane, at sites distinct from synapses or gap junctions, in a way that is not mechanistically understood (Kollo et al. 2006). However, it seems likely that this will require further protein interactions that have yet to be characterised.

1.6 Aims and Objectives

The focus of this study was on the trafficking of Kv4.2 channels, with their accessory protein KChIP1, to the plasma membrane. Several questions were to be addressed. Firstly, the KChIPs can bind to Ca^{2+} ions, and this appears to be important for promoting the trafficking of Kv4 channels to the plasma membrane. There is debate in the literature, however, about whether EF-hand mutant proteins can still bind to the Kv4 channel α-subunits, and how many EF-hand domains are required for this. One aim was therefore to compare the effects on Kv4.2 of a single EF-hand mutant of KChIP1 to the better characterised triple EF-hand mutant. Secondly, previous work had suggested that Kv4.2 and KChIP1 were trafficking to the plasma membrane via a non-conventional, COPII-independent pathway. However, this had not been further characterised. One area of particular interest was in the proteins that could regulate this intracellular trafficking, and in particular Rab1 and ER-Golgi SNAREs. This led to several aims: to investigate whether Rab1 is required for Kv4.2/KChIP1 trafficking; to identify SNARE proteins associated with KChIP1-positive punctae in cells; to use RNAi to look for the functional effects of such SNAREs on Kv4.2/KChIP1 trafficking. Thirdly, many other proteins are known to be able to regulate Kv4.2 trafficking and function. Two families of proteins were of interest. The 14-3-3 proteins have been implicated in the regulation of ion channel trafficking, but there are no studies in the literature focussed on possible interactions with Kv4 channels. One aim was to see whether 14-3-3 isoforms could bind to Kv4 channels. Meanwhile, the PSD-95 family of MAGUKs, especially SAP97, are known to interact with Kv4 channels, and promote their trafficking and clustering. However, little is known about the effects of SAP97 in a ternary complex with KChIP1 and Kv4.2, and how these two accessory proteins might jointly affect the channel. A final aim was therefore to compare the effects of KChIP1 and PSD-95 family proteins on Kv4.2, when expressed separately, or together.

Chapter 2

Materials and Methods

2.1 Plasmids

The **KChIP1-EYFP** plasmid is of KChIP1a (GenBank® accession number AF199597) in an enhanced yellow fluorescence protein vector (EYFP) (O'Callaghan et al. 2003).

The **pcDNA-KChIP1** vector encoded the same KChIP1 sequence as above, but inserted into a pcDNA3.1(-) vector (O'Callaghan et al. 2003).

The **KChIP1-pHcRed** plasmid took the KChIP1 sequence from above, and inserted it into the pHcRed-Tandem-N1 vector (Hasdemir et al. 2005).

The **KChIP1-EF3-EYFP** plasmid had mutations at positions D135A and G140A, corresponding to positions 1 and 6 of EF hand 3. This was a kind gift of Dr B. Hasdemir.

The **KChIP1-EF2-4-EYFP** plasmid had Ala substitution mutations for the Asp at position 1 and Gly at position 6 in EF hands 2, 3 and 4. This corresponded to KChIP1 (D99A, G104A, D135A, G140A, D183A, G188A)-EYFP (Hasdemir et al. 2005).

The **KChIP1-EF2-4-pHcRed** plasmid took the same KChIP1-EF2-4 mutant sequence as described above, and inserted this into the pHcRed-Tandem-N1 vector. This was a kind gift of Dr B. Hasdemir.

The **KChIP2-ECFP** encodes human KChIP2.3 (Gen Bank®accession number DQ148481) in the pECFP-N1 enhanced cyan fluorescence protein vector (Venn et al. 2008).

The **FLAG-KChIP2** plasmid took the same KChIP2 sequence as discussed above, and inserted it into a pFLAG-CMV-4 vector (Venn et al. 2008).

The **KChIP3-EYFP** plasmid encodes human KChIP3.1 (Gen Bank®accession number DQ148485) in an EYFP vector (Venn et al. 2008).

The **KChIP4-ECFP** plasmid contains the sequence for human KChIP4.1 (Gen Bank®accession number DQ148487) in an ECFP vector (Venn et al. 2008).

The **pcDNA-Kv4.2** plasmid has human Kv4.2 (NM_012281) in the pcDNA3.1(+) vector (Hasdemir et al. 2005).

The **mCherry-Kv4.2** plasmid was made by cutting out the Kv4.2 sequence from the pcDNA-Kv4.2 sequence, and inserting it into an mCherry-C1vector (Clontech, CA, USA), using the endonucleases EcoRI and KpnI.

The construct of **ARF1-EYFP** was previously described in Handley et al. 2007.

The **EYFP-Golgi** plasmid consists of the EYFP fluorescence tag attached to the N-terminus of β1,4-galactosyltransferase. This gives targeting to the *trans-* and *medial*-Golgi. This was obtained from Clontech.

The **VSVG-GFP** plasmid encoded a temperature sensitive ts045 version of vesicular stomatitis viral glycoprotein in a green fluorescent protein vector and was a gift from Dr J. Presley (Presley et al. 1997).

The plasmid of **TBC1D20** [TBC (Tre-2/Bub2/Cdc16) domain family, member 20] was a gift from Prof F. Barr. This was shown to be a Rab1 GAP (GTPase-activating protein) in Haas et al. 2007.

The **VAMP7-GFP** plasmid was a kind gift from Prof T. Galli, and encodes the SNARE protein VAMP7 in a GFP plasmid (Martinez-Arca et al. 2003).

A plasmid was also obtained encoding the **longin domain** of VAMP7 fused to GFP, a kind gift of Prof T. Galli (Proux-Gillardeaux et al. 2007).

The **EGFP-SAP97** plasmid encodes SAP97 in a pEGFP-C1 construct, and was a kind gift of Prof L-Y. Lian, University of Liverpool.

The plasmids encoding **PSD-93δ-GFP**, **PSD-93ε-GFP** and **PSD-93ζ-GFP** were all in pEGFP-N1 vectors, and were all kind gifts from Prof L-Y. Lian.

An **mCherry-PSD-95** plasmid, encoding human PSD-95 in an mCherry vector, was a kind gift from Dr L. Haynes.

2.2 Antibodies

The antibodies used in this thesis are shown in Table 1. This includes their source, and the dilution used for immunofluorescence and Western blotting as appropriate.

Table 1: List of antibodies and their dilutions.

Antibody	Description	Supplier	Immuno-fluorescence Dilution	Western blotting Dilution
14-3-3β	Rabbit polyclonal	Prof A. Aitken (University of Edinburgh, UK)	N/A	1:3000
14-3-3γ	Rabbit polyclonal	Prof A. Aitken (University of Edinburgh, UK)	1:500	1:5000
β-Actin (A-5441)	Mouse monoclonal	Sigma Aldrich (MO, USA)	N/A	1:5000
GFP (JL8)	Mouse monoclonal	Clontech (CA, USA)	N/A	1:1000
GOSR1 (GOS28)	Mouse monoclonal	Abcam (Cambridge, UK)	1:500	N/A
Kv4.2	Rabbit polyclonal	Exalpha Biologicals (MA, USA)	1:500	N/A
LAMP1	Rabbit polyclonal	Affinity Bioreagents (CO, USA)	1:500	N/A
Membrin	Mouse monoclonal	Abcam (Cambridge, UK)	1:500	N/A
Sec22L1 (Sec22b)	Mouse monoclonal	Abnova (Taipei, Taiwan)	1:500	N/A
Syntaxin 7	Rabbit polyclonal	Synaptic Systems (Goettingen, Germany)	1:750	N/A
Syntaxin 8	Rabbit polyclonal	Synaptic Systems (Goettingen, Germany)	1:750	N/A

VAMP7	Mouse monoclonal	Abcam (Cambridge, UK)	1:500	N/A
VAMP7	Rabbit polyclonal	Prof T. Galli (Institut Jacques Monod, France)	1:500	N/A
Vti1a	Mouse monoclonal	BD Biosciences (CA, USA)	1:500	1:2000
Ykt6	Chicken	Dr J. Hay (University of Montana, USA) *Hasegwa et al. 2003*	1:500	N/A

For immunofluorescence, five secondary antibodies were used in this thesis. Anti-mouse and anti-rabbit IgG conjugated to TRITC (tetramethylrhodamine β-isothiocyanate) were obtained from Sigma-Aldrich (MO, USA). These were used at a 1:80 dilution, in PBS (phosphate buffered saline) with 3% BSA (bovine serum albumin). A goat anti-chicken Texas Red conjugated antibody (Abcam, Cambridge, UK) was used at a 1:80 dilution for experiments with the anti-Ykt6 antibody. Alexa® Fluor-488-conjugated anti-mouse antibody and Alexa® Fluor-594-conjugated anti-rabbit antibody were obtained from Molecular Probes/Invitrogen (CA, USA), and used at a 1:250 dilution. For Western blotting, the secondary antibody was an HRP- (horse radish peroxidase) conjugated anti-mouse or anti-rabbit antibody from Sigma. This was diluted 1:400 in PBS with 3% skimmed milk powder.

2.3 HeLa cell culture

HeLa cells were cultured in 75cm^2 flasks, in 20ml Dulbecco's modified Eagle's medium (Gibco/Invitrogen, CA, USA), with 5% foetal bovine serum (Gibco), 1% non-essential amino acids (Gibco), and 1% penicillin-streptomycin (10000 units/ml penicillin, 10000μg/ml streptomycin, Gibco). Cells were kept at 37°C, in a 5% CO_2 atmosphere. For immunocytochemistry, cells were grown in 24-well plates, with glass coverslips. Cells were plated at ~4x10^5 per well, in 1ml supplemented media, and incubated 5-24 hours before transfection. To obtain

samples for SDS-PAGE gels, HeLa cells were grown in 6-well plates, with ~$1.2x10^6$ cells per well, in 3ml supplemented media. Again, cells were left 5-24 hours before transfection.

For the transfection reaction mixture, 3µl per µg DNA of GeneJuice (Novagen/Merck, Darmstadt, Germany) was incubated for 5 minutes at room temperature with OptiMEM serum-free media (Gibco) to give a total reaction volume of 100µl for immunocytochemistry experiments, and 300µl for larger wells for SDS-PAGE samples. Either 1µg (for immunocytochemistry) or 3µg (for SDS-PAGE samples) of each plasmid DNA was then added, and the mixture incubated for a further 15 minutes, before being added dropwise to the cells. Cells were then left for 24-72 hours post-transfection.

2.4 PC12 cell culture

PC12 cells were cultured in suspension in 20ml RPMI1640 media (Gibco), containing 10% horse serum (Gibco), 5% foetal bovine serum, and 1% penicillin/streptomycin. Cells were incubated at 37°C in a 5% CO_2 atmosphere. For transfection, cells were trypsinized the day before transfection, and added to poly-D-lysine coated coverslips (BD Biosciences, CA, USA) in 24-well plates.

Cells were transfected using 3µl Lipofectamine2000 (Invitrogen, CA, USA) per µg plasmid in 100µl OptiMEM media (Gibco), following the manufacturer's instructions. After addition of DNA, the final reaction mixture was incubated for 20 minutes at room temperature. Growth media was removed from the cells, and the transfection mixture added to each well, with 400µl serum-free RPMI. After 4-6 hours, this was removed, and replaced with 1ml RPMI media supplemented with serum. Cells were left for 24-48 hours post-transfection.

2.5 Neuro2A cell culture

Neuroblastoma 2A (Neuro2A) cells were cultured in $75cm^2$ flasks, in 20ml Dulbecco's modified Eagle's medium, with 10% foetal bovine serum, and 1% penicillin-streptomycin. Cells were kept at 37°C, in a 5% CO_2 atmosphere. For immunocytochemistry, cells were plated on glass coverslips in wells of a 24-well plate, in 1ml media, at a density of ~$4x10^5$cells per well. For SDS-PAGE samples, cells were grown in 3ml supplemented media, in wells of a 6-well plate, at a density of ~$1.2x10^6$ cells per well. Cells were transfected with a GeneJuice reaction mix, as outlined for HeLa cells above, 24 hours after plating, and then left for a further 24-72 hours.

2.6 Immunocytochemistry

After transfection, cells on coverslips were gently washed three times in phosphate buffered saline (PBS): 137mM NaCl, 2.7mM KCl, 10mM Na_2HPO_4, 2mM NaH_2PO_4, pH 7.4. Cells were then fixed in PBS with 4% formaldehyde at 4°C overnight. For coverslips of cells only transfected with colour-tagged constructs, the coverslips were then washed in PBS again, before being air dried, and mounted on ProLong Gold Antifade (Invitrogen).

For immunofluorescence, cells were washed in PBS after fixation, and then permeabilised in PBT (PBS, 0.1% Triton X-100, 0.3% bovine serum albumin) for 30 minutes at room temperature. Cells were then incubated with the primary antibody overnight at 4°C. Antibodies were diluted as listed in Table 1 in PBS with 0.3% BSA. The primary antibody was then removed, cells washed three times in PBT, and the secondary antibody added for one hour at room temperature. The secondary antibodies were diluted as discussed above. Cells were washed again in PBT, and then dried, before mounting on ProLong Antifade Gold.

2.7 Confocal Microscopy

Transfected cells were viewed using a Leica TCS-SP2-AOBS confocal microscope (Leica Microsystems, Heidelberg, Germany), using a 63x water immersion objective with a 1.2 numerical aperture. The pinhole was set to Airy, to be optimal for each fluorescence setting used. The wavelengths used for excitation, and the emission ranges recorded, are shown for different combinations of fluorophores in Table 2.

Images were viewed using LCSLite software (Leica), and this software was used to draw regions of interest to obtain data for further analysis. The first region of interest was drawn around the perimeter of the cell, visible from background fluorescence. The second was drawn ~1μm within this, to give the region of the plasma membrane. The total fluorescence from the fluorophore of interest in each region was recorded. Data from these experiments was plotted and statistically analysed in Excel 2007 (Microsoft, WA, USA). The percentage of total cellular fluorescence found in the plasma membrane region was calculated for each cell, and the mean and standard error of the mean (S.E.M) for all cells under a given condition were calculated. To normalise the data, any background samples were subtracted, for example the percentage of Kv4.2 fluorescence at the plasma membrane in cells expressing Kv4.2 alone. Data was then normalised to one of the conditions, often to cells expressing Kv4.2 with KChIP1, as discussed in the figure legend. The normalised data is always shown as the left-most column on graphs. Data sets were statistically compared using Student's unpaired *t* test. Images were manipulated in CorelDraw Graphics Suite X4 (Corel Corporation, Ottawa, Canada). All fluorescence quantitation combines data from 2 or more experimental repeats.

Table 2: Fluorophores used in confocal microscopy, and the excitation and emission spectra used.

Fluorophore	Exciting wavelength, nm	Emission spectra, nm
ECFP alone	405	448-510
EYFP alone	488	500-550
EGFP alone	488	505-615
TRITC alone	543	570-680
mCherry alone	594	620-700
ECFP & TRITC	405 543	450-510 570-680
EYFP/EGFP & TRITC	488 543	500-540 570-680
ECFP & mCherry	405 594	450-510 620-700
EYFP/EGFP & mCherry	488 594	500-540 620-700
GFP & HcRed	488 594	515-585 610-700
EYFP & Texas Red	488 594	500-535 600-720
Alexa® Fluor 488 & Alexa® Fluor 594	488 594	500-550 605-670
ECFP & EYFP	405 488	440-485 505-550
EGFP & EYFP	476 514	480-510 565-590
ECFP & EGFP & mCherry	405 488 594	440-485 505-550 620-660
EGFP & EYFP & TRITC	476 514 543	480-510 530-560 570-680
EGFP & EYFP & mCherry	476 514 594	480-510 530-560 620-700

2.8 siRNA knockdown

Expression of SNARE proteins was inhibited using siRNA constructs. These were obtained from Ambion/Appelera Europe (Ambion, TX, USA), as pre-designed siRNAs from their *Silencer* range. These were designed against the human genes of interest. The name of each construct as used in this thesis, is given with their Ambion siRNA ID# and their 5'-3' sense sequence in Table 3. In addition, *Silencer* negative control siRNA #1 was used for negative controls in this thesis. All constructs were resuspended in nuclease free water, to give a final concentration of 100nM when used for transfection.

Table 3: List of siRNA constructs used in this thesis.
* Sec22 construct 2 was not effective in this study (see Chapter 3)

Gene name	Thesis name	Ambion siRNA ID#	5'-3' Sense sequence
SYBL1 (VAMP7)	Construct 1	241467	UGAGAGAACAAGGAGUUAAtt
	Construct 2	241468	CGGUUCAAGAGCACAGACAtt
	Construct 3	241469	GACAAAGUGAUGGAGACUCtt
Vti1a	Construct 1	37855	GGGAUGUACAGCAACAGAAtt
	Construct 2	37946	GGGCACAUCUGCUCGAUAAtt
	Construct 3	38033	GGAGGAAUUUAAAUGAGCUtt
GOSR1 (GOS28)	Construct 1	111531	GCGGCAUAGAGACAUAUUGtt
	Construct 2	111532	GCAAACUUUAUGGCAAUACtt
Sec22	Construct 1	15641	GGCUAACAAUUUGUCCAGUtt
	Construct 2*	15549	GGAGCCAUGACUUUUCACUtt

Cells were transfected (as described above) with the siRNA constructs of interest, along with untagged-Kv4.2 and KChIP1-EYFP, VSVG-GFP, or Kv4.2 and SAP97-GFP, as described in the text. Coverslips were then processed for immunocytochemistry 72 hours post-transfection and images obtained, as discussed above. The percentage of fluorescence at the plasma membrane was also calculated and normalised as discussed above.

Several methods were used to confirm the efficacy and specificity of the siRNA constructs. Firstly, cells were transfected with KChIP1-EYFP, and VAMP7 visualised using anti-VAMP7 immunostaining, in cells both in the absence and presence of RNAi. For this experiment, all microscope settings, in particular gain and offset levels, were kept identical between cells. A region of interest was drawn around the perimeter of the cell, and the mean cellular fluorescence for the VAMP7 immunostaining was recorded for cells from both conditions. Secondly, real-time PCR was performed to look for changes in the expression levels of the mRNA for the protein being knocked down. The method for this is described in section 2.9 below. Finally, Western blots were performed to look for changes in protein expression levels in lysates from cells in the absence or presence of siRNA. These were performed as described in section 2.10 below, using anti-Vti1a antibodies.

2.9 Real-time PCR

HeLa cells were left for 72 hours post-transfection. mRNA was extracted using TRIzol reagent (Invitrogen) according to the manufacturer's instructions. Briefly, 1ml TRIzol was added per 9.5cm^2 well of cells, and passed several times through a pipette before being transferred to an eppendorf. This was left for five minutes before 0.2ml chloroform was added, vigorously mixed, and left for a further 2 minutes. This was then centrifuged at 12000g for 15 minutes at 4°C. The aqueous phase was mixed with 0.5ml isopropanol, and incubated at room temperature for 10 minutes, before centrifugation at 12000g for 10 minutes at 4°C. The supernatant was then discarded, and the pellet washed in 1ml 75% ethanol. This was then centrifuged at 7500g for 5 minutes at 4°C, the supernatant discarded and the pellet air-dried. mRNA was resuspended in 30µl RNase free water (Sigma) by heating at 60°C for 10 minutes, and stored at -80°C.

cDNA was produced using ImProm-II reverse transcriptase (Promega, WI, USA) following manufacturer's instructions. For each reaction, 1µl of mRNA was

mixed with 20pmol/0.5µg Oligo (dT)15 primers (Promega) and 3µl nuclease free water (Sigma). This was incubated at 70°C for 5 minutes, then quick chilled to 4°C for 5 minutes, and held on ice. To this was added 4µl ImPromII 5X buffer (Promega), 2.4µl $MgCl_2$ (Promega, to give a final reaction concentration of 3mM), 1µl dNTPs (Promega, to give a final concentration of 0.5mM of each dNTP), along with 1µl ImPromII reverse transcriptase (Promega), and water added to bring the final volume to 20µl per reaction. The reaction proceeded with 5 minutes annealing at 25°C, 60 minutes at 42°C to extend the first strand, and 15 minutes of heat inactivation at 70°C.

For real-time PCR, cDNA was diluted 1:10, and 2µl used per well. In a total volume of 15µl, 7.5µl SYBR Green PCR master mix (Applied Biosystems, Warrington, UK) was used with 1µl primer mix (50mM each of forward and reverse primers). Each primer and cDNA combination was repeated in triplicate. Experiments were run on a Bio-Rad iQ5 thermal cycler (Bio-Rad, CA, USA). Cycles were performed as follows: 95°C for 15 minutes, then 55 cycles of 95°C for 10 seconds and 60°C for 30 seconds, 1 cycle of 95°C for 30 seconds and 55°C for 30 seconds, finally followed by 81 cycles of 30 seconds at increasing temperatures, starting at 55°C, to obtain a melt curve. After checking each run had completed correctly, the threshold cycle (Ct) was recorded, and averaged for each primer and cDNA set. The relative levels of mRNA for each primer and for each cDNA were calculated by comparison to results with primers for β-actin, using the $2^{-\Delta\Delta Ct}$ method ($\Delta Ct = Ct_{target\ mRNA} - Ct_{\beta\text{-}actin}$, $\Delta\Delta Ct = \Delta Ct_{RNAi\ or\ control} - \Delta Ct_{control}$). The mean $2^{-\Delta\Delta Ct}$ value for each siRNA treatment over 5 runs was then calculated and plotted, along with the standard error of the mean.

2.10 SDS-PAGE and Western blotting

Transfected cells grown in a 6-well plate were lysed in 200µl of 2xSDS Laemmli buffer (Sigma). Samples were boiled for 5 minutes, and then loaded onto a 10% SDS-PAGE gel. Gels were also loaded with See Blue® Plus 2 Prestained Standard molecular weight markers (Invitrogen). The separated proteins were

then transferred from the gel to a nitrocellulose membrane. This was stained with Ponceau-S solution (Sigma) to confirm successful protein transfer. All incubations were carried out at room temperature, with agitation. Membranes were washed in distilled H_2O, and then twice in PBS. Following this, they were incubated in blocking solution (PBS with 3% skimmed milk powder) for 1 hour. Membranes were then incubated in a primary antibody solution for 1 hour. This consisted of PBS with 3% skimmed milk powder, and antibodies diluted as shown in Table 1. Membranes were then washed three times in PBS with 0.05% Tween^{TM}-20 (Sigma), and then with PBS alone. After this, the membrane was incubated for 1 hour in a solution of the appropriate secondary antibody conjugated to horseradish peroxidise (Sigma), diluted 1:400 in PBS with 3% milk. Following this, the membranes were washed a further three times in PBS with 0.05% Tween^{TM}-20, and once with PBS alone, then incubated with PBS containing 0.5M NaCl for 30 minutes. Finally, the membranes were washed twice in distilled H_2O, before being dried. Signals were detected using the ECL Plus Western Blotting Detection System (Amersham Biosciences, Buckinghamshire, UK), and imaged using a Bio-Rad ChemiDoc XRS system. Images were processed with Bio-Rad Quantity One software.

2.11 Production of GST and GST-KChIP1 protein

BL-21 cells transformed with plasmids to express either GST protein, or GST-KChIP1 protein, were a gift from Dr B Hasdemir. These were streaked on agar plates with 100μg/ml ampicillin, and a colony picked and grown overnight in 100ml superbroth (0.5% w/v NaCl, 1.5% w/v tryptone, 2.5% w/v yeast extract) with antibiotics. The next day, this was added to 900ml superbroth with antibiotics. Protein production was induced at OD_{600} with 1mM isopropyl-l-thio-β-D-galactopyranoside (IPTG, Sigma). After 3-4 hours, cells were pelleted by centrifugation for 20 minutes at 4000rpm and 4°C, and then lysed in breaking buffer (500mM KCl, 100mM HEPES, 5mM ATP, 5mM $MgCl_2$, 2mM 2-mercaptoethanol, pH 7.0). Protease inhibitor cocktail (Sigma) was also added. The samples were kept at -80°C until further use. Thawed samples were then passed through a Constant Systems Ltd cell disruptor (Constant Systems,

Northamptonshire, UK). Samples were then spun in an ultracentrifuge for 1 hour at 33000rpm (100000g) at 4°C. The supernatant was added to washed Glutathione-Sepharose 4B beads (GE Healthcare Europe, Uppsala, Sweden), and incubated for 1 hour at 4°C, with agitation. The unbound fraction was removed by centrifugation at 1000rpm for 30 seconds. The beads were washed three times in ice-cold PBS. The protein of interest was eluted in three 1ml samples of GST-elution buffer (65mM Trizma® base (Sigma) and 10mM reduced glutathione (Sigma), pH 8.0). In each case, 1ml of elution buffer was added to the beads, and incubated for 10 minutes at 4°C with agitation, then spun at 1000rpm for 30 seconds. The protein from each elution step was removed and stored at -80°C until needed. The concentration of protein in each elution was determined by comparison to standard concentrations of bovine serum albumin run on an SDS-PAGE gel.

2.12 Pull down assays

Around 7.5mg of each protein (GST alone as a control, and GST-tagged KChIP1, both prepared as above) were diluted 1:10 in 0.5M Tris-HCl (pH8.0) and bound to washed Glutathione-Sepharose 4B beads (GE Healthcare Europe) for one hour at 4°C. The beads were again washed in 0.5M Tris-HCl, before ~20mg bovine brain sample (a kind gift of Dr M. Graham and Dr L. Haynes) was added. Initially, dialysed whole brain lysate was used. This was incubated with the beads overnight at 4°C. Otherwise, the experiment was performed as described below, but without ATP or $MgCl_2$ in the buffer solutions. Bovine brain cytosol was used in a second experiment. This was dialysed against cytosol buffer containing Na_2ATP (Sigma) and $MgCl_2$, in the presence of 1μM free Ca^{2+} (25mM Tris-HCl, 50mM KCl, 5mM EGTA, 5mM NTA, 1mM DTT, 2.67mM $MgCl_2$, 1mM ATP, 5.07mM $CaCl_2$, pH7.8). The bovine brain cytosol was incubated with the beads for 30 minutes at room temperature, to allow the phosphorylation of proteins by the endogenous kinases in the cytosol. In both cases, the beads were then packed into a Sigma 1.5cm diameter gravity flow column, and washed in ~100ml cytosol buffer with 1μM free Ca^{2+} to remove any unbound proteins. Proteins which were bound in a Ca^{2+}-dependent manner were

then eluted using 6ml cytosol buffer with no Ca^{2+}, in the presence of EGTA, using a flow rate of ~0.2ml/minute. The column was then washed with another 6ml of this solution, before any proteins bound in a Ca^{2+}-independent manner were eluted using a high salt cytosol buffer, with 1M NaCl, at a flow rate of ~0.2ml/minute. To concentrate the eluted proteins, they were methanol precipitated. Briefly, 600µl aliquots of eluted protein and 600µl methanol (pre-chilled to -20°C) were mixed, and 25µl of 2.5mg/ml soybean trypsin inhibitor (Sigma) was added. Samples were incubated at -20°C for 30 minutes, and then centrifuged for 4 minutes at 4°C, at 13000rpm. The supernatant was removed, and the pellet left to air dry at room temperature. Each pellet was resuspended in 15µl SDS Laemmli sample buffer (Sigma), and boiled for 5 minutes, before samples for each protein and elution step were pooled. These were then run on SDS-PAGE gels, and either transferred to nitrocellulose membrane for Western blotting, or stained with Coomassie blue stain to visualise the proteins present.

Chapter 3

Characterising the non-conventional trafficking pathway used by KChIP1 and Kv4.2

3.1 Introduction

The Kv4 family of voltage-gated potassium channels is responsible for the rapidly-inactivating outward potassium currents in a variety of neurons (Hoffman et al. 1997; Lauver et al. 2006), as well as in cardiac myocytes (Dixon et al. 1996). By allowing a flow of potassium ions out of a cell, they regulate the frequency with which action potentials can fire (Hoffman et al. 1997). Also, the localisation of these channels to the somatodendritic compartment of neurons (Birnbaum et al. 2004) means that such effects are limited to certain cellular compartments, giving these channels a specific role in regulating post-synaptic membrane excitability, confining action potentials to specific regions of the dendritic arbour (Ramakers and Storm 2002; Cai et al. 2004), and influencing the plasticity underlying long-term potentiation, learning and memory at a molecular level (Ramakers and Storm 2002; Chen et al. 2006(2)). Mutations in these channels have also been implicated in some forms of temporal lobe epilepsy (Singh et al. 2006).

To have its effects, a channel must be correctly trafficked to the plasma membrane of a cell. Understanding the process by which this occurs, and how it is regulated, could therefore be very important for understanding brain function in both health and disease. The trafficking of Kv4 channels to the plasma membrane is influenced by a variety of accessory proteins (Birnbaum et al. 2004). In particular, the KChIPs were the first family of proteins identified with this role (An et al. 2000). It is now known that four KChIPs bind to the four α-subunits of a complete Kv4 channel, in a cross-shaped octameric structure (Pioletti et al. 2006). This promotes channel trafficking (Shibata et al. 2003), as well as altering channel kinetics (Birnbaum et al. 2004). Much previous work has concentrated on the trafficking of Kv4.2 with KChIP1, and has revealed that they use a non-conventional pathway (Hasdemir et al. 2005).

Most channels and transmembrane proteins, when unfolded or unable to fully traffic to the plasma membrane, will be retained within the ER (Misonou and Trimmer 2004). It is known that Kv4.2 expressed alone in non-neuronal cells has

a perinuclear localisation, and some papers have argued that this corresponds to the ER (Bahring et al. 2001; Shibata et al. 2003). However, other work has shown overlap between the channel and markers for the Golgi (O'Callaghan et al. 2003), suggesting that the channel is able to exit the ER when expressed alone, but is trapped at a later stage in the exocytic pathway. The localisation of fluorescently-tagged KChIP1 expressed alone is also unusual, being associated with punctate, mobile vesicles (O'Callaghan et al. 2003; Hasdemir et al. 2005). The identity of these vesicles is not clear, although they partially overlap with markers of the ERGIC (O'Callaghan et al. 2003). Finally, when both the Kv4.2 channel and KChIP1 are expressed together, and traffic to the plasma membrane, they do so in a COPII-independent manner, contrasting with the standard marker of ER-Golgi-plasma membrane trafficking, VSVG (Hasdemir et al. 2005). Together, these data suggest that Kv4.2/KChIP1 trafficking is occurring via a non-conventional cellular pathway.

There are several aspects of this non-conventional pathway that are still not characterised. Firstly, the KChIP proteins, as members of the NCS family, are able to bind to Ca^{2+} ions via their EF hand domains (An et al. 2000). However, it is not clear whether this binding has a regulatory role, allowing the protein to respond to changes in calcium levels in the cell, or a structural function, allowing the protein to correctly fold. It seems that Ca^{2+} binding is required for correct trafficking of Kv4.2 to the plasma membrane by KChIP1 (An et al. 2000; Hasdemir et al. 2005). However, there is debate in the literature about whether the KChIP needs to have bound Ca^{2+} in order to bind Kv4.2 channel proteins, and how many of the EF-hands must be intact (Pioletti et al. 2006). The effect of such mutant proteins on general cellular trafficking pathways is also unclear. This was investigated by quantifying the percentage of fluorescence from anti-Kv4.2 immunostaining found at the plasma membrane, in the presence of fluorescently-tagged versions of wild-type and EF-hand mutant KChIP1.

The other aspect of this investigation concerned the regulation of the trafficking and fusion of KChIP1/Kv4.2 containing vesicles, in particular in the ER-to-Golgi

step of trafficking, en route to the plasma membrane. Proteins known to regulate VSVG trafficking were investigated, as well as those implicated in other non-conventional pathways. The Rab-GTPases have an important role in regulating trafficking (Rothman and Wieland 1996; Hammer and Wu 2002; Schwartz et al. 2007), and Rab1 is particularly associated with ER-Golgi trafficking (Tisdale et al. 1992). Requirement for this protein in the trafficking of both VSVG-GFP and fluorescently-visualised Kv4.2/KChIP1 was investigated by over-expression of a Rab-GAP specific for Rab1 (Haas et al. 2007), to convert the Rab into its inactive GDP-bound form. The SNARE proteins are more directly involved in the fusion of vesicles with their target membranes, forming the fusion machinery (Jahn and Scheller 2006). These need to come together in the correct combination in order for fusion to occur. Therefore, the complement of SNARE proteins present on a membrane helps to define a given compartment (Jahn and Scheller 2006). Antibodies against various SNAREs implicated in ER-Golgi trafficking were used to visualise these proteins in cells, and look for co-localisation between them and KChIP1-EYFP containing vesicles. SNAREs of interest were then assessed for functional activity, using RNAi to reduce their levels in cells, and to look for effects on the trafficking of both the marker VSVG-GFP, and the Kv4.2 channel with KChIP1. Finally, the trafficking of Kv4.2 by KChIP1 was also compared to that of the related protein KChIP2. This work reveals some similarities between the trafficking of the well-characterised marker VSVG and that of Kv4.2/KChIP1, but also characterises several novel aspects of this non-conventional pathway.

3.2 Results

3.2.1 Characterising KChIP1 and Kv4.2

To begin this study, it was necessary to characterise the localisation of KChIP1 and Kv4.2 when expressed both alone and together in cells, to confirm that previous findings could be replicated.

Previous work had shown KChIP1 to have an unusual punctate distribution in a variety of cell lines, and primary hippocampal neuron preparations (O'Callaghan et al. 2003; Hasdemir et al. 2005; Venn et al. 2008). An EYFP-tagged version of KChIP1 was available in the lab (O'Callaghan et al. 2003), and could be

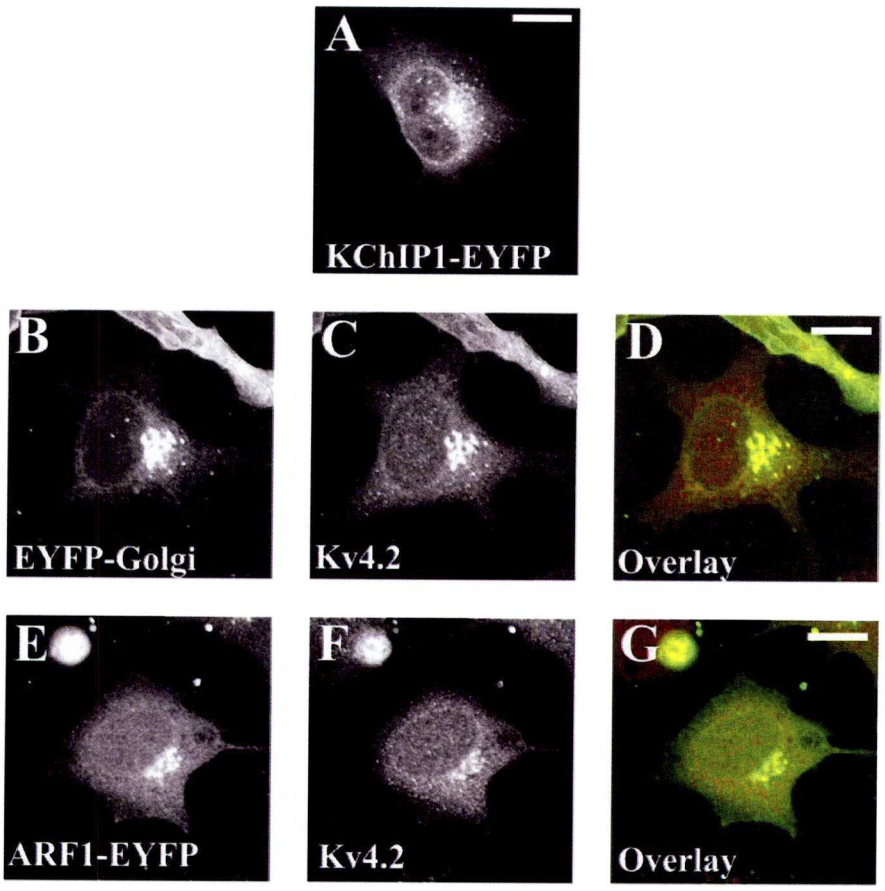

3.1: Localisation of Kv4.2 and KChIP1 in HeLa cells.
HeLa cells were transfected with KChIP1-EYFP or Kv4.2, and the localisation of Kv4.2 assessed using Golgi markers.

A) HeLa cell transfected with KChIP1-EYFP.

B-D) HeLa cell transfected with EYFP-Golgi (Green) and Kv4.2 (Red), with co-localisation shown as yellow in the overlay.

E-G) HeLa cell transfected with ARF1-EYFP (Green) and Kv4.2 (Red), with co-localisation shown as yellow in the overlay.

In all cases, Kv4.2 localisation was determined using anti-Kv4.2 immunostaining with a TRITC-conjugated secondary antibody, and scale bars represent 10μm.

visualised in fixed cells using confocal fluorescence microscopy. Figure 3.1A shows a representative HeLa cell expressing only KChIP1-EYFP. The KChIP showed a punctate distribution throughout the cell, but was especially clustered in the perinuclear region.

The localisation of Kv4.2 has been suggested in some papers to be conventional ER retention of an un-trafficked channel (Shibata et al. 2003). However, the ER retention signal in Kv4.2 is inactive (Shibata et al. 2003), and the localisation seen in previous work is more perinuclear than reticulate. This suggested that the channel is trapped in the Golgi when unable to traffic to the plasma membrane (O'Callaghan et al. 2003; Hasdemir et al 2005). To further confirm this, untagged Kv4.2 was expressed in cells, which were then fixed, and immunostained with an anti-Kv4.2 primary antibody, and TRITC-conjugated secondary. Experiments were performed to look for co-localisation between Kv4.2 and EYFP-Golgi, a fluorescently-tagged Golgi-targeting sequence from Clontech, or ARF1-EYFP, a Golgi-resident protein (Handley et al. 2007). Figures 3.1B-G show the results of this in HeLa cells. There was clear co-localisation between the channel and both of the Golgi markers, shown in yellow in the colour overlays. Neither channel nor KChIP were localised to the plasma membrane when expressed alone.

Whilst HeLa cells are amenable for transfection and microscopy, the Kv4 channels are normally expressed in neurons or cardiac myoctyes (Hoffman et al. 1997; Dixon et al. 1996), and it is conceivable that the localisation seen above might be cell-type specific. To address this, mouse neuroblastoma Neuro2A cells were obtained. This neuronal cell-line should be more representative of the cells where the channel is natively expressed. The co-localisation experiment was therefore repeated in this cell type, and representative images are shown in Figures 3.2A and B. Again, the Kv4.2 localised to the perinuclear region, with high levels of co-localisation with both of the Golgi markers. Together these images confirm that Kv4.2 is indeed unusual in being localised to the Golgi when not trafficked to the plasma membrane.

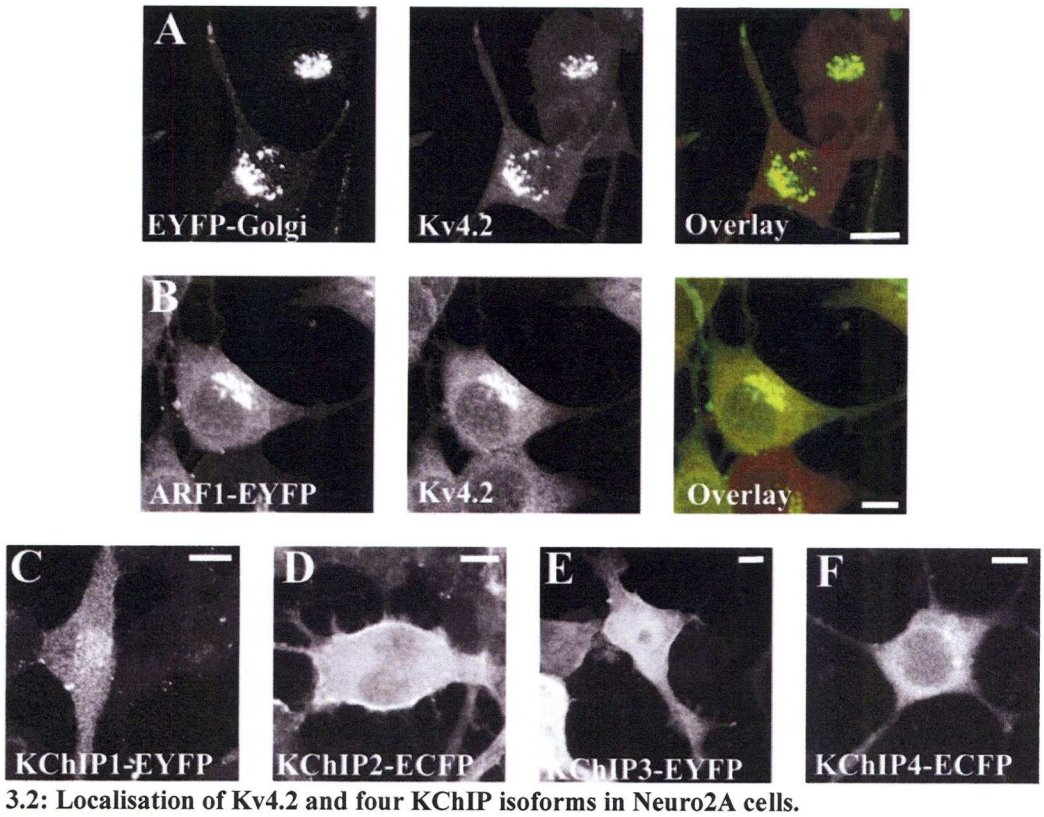

3.2: Localisation of Kv4.2 and four KChIP isoforms in Neuro2A cells.
Neuro2A cells were transfected with Kv4.2 or fluorescently-tagged KChIP isoforms to determine their localisations.

A) Neuro2A cell expressing EYFP-Golgi (Green) and Kv4.2 (Red), with co-localisation shown as yellow in the overlay.

B) Neuro2A cell expressing ARF1-EYFP (Green) and Kv4.2 (Red), with co-localisation shown as yellow in the overlay.

In both cases, Kv4.2 localisation was determined using anti-Kv4.2 immunostaining, with a TRITC-conjugated secondary antibody.

C-F) Neuro2A cells were transfected with **C)** KChIP1-EYFP, **D)** KChIP2-ECFP, **E)** KChIP3-EYFP or **F)** KChIP4-ECFP.

In all cases, the scale bar represents 10μm.

The localisation of one isoform of each of the four KChIPs was also assessed in this cell type. As shown in Figure 3.2C, KChIP1-EYFP was punctate in Neuro2A cells. These punctae were predominantly in the perinuclear region, although they could also be seen further from the nucleus. They generally seemed less widely distributed than in HeLa cells, however. The distribution of the other KChIPs also replicated that seen previously in other cell types (Takimoto et al. 2002). In Figure 3.2D, KChIP2-ECFP was localised to the plasma membrane, whilst in Figure 3.2E KChIP3-EYFP showed some plasma membrane localisation, whilst some was more diffusely cytoplasmic. This likely reflects the post-translational palmitoylation of KChIPs 2 and 3, allowing their plasma membrane association. Finally, Figure 3.2E shows KChIP4-ECFP is also diffusely cytoplasmic, although there is perhaps some brighter labelling in the perinuclear region. The

ability to replicate the findings of previous studies in these cells helps to validate their use for further work with the KChIPs.

Having characterised the intracellular localisation of Kv4.2 and KChIP1 when expressed alone in cells, it was next necessary to confirm the effects of

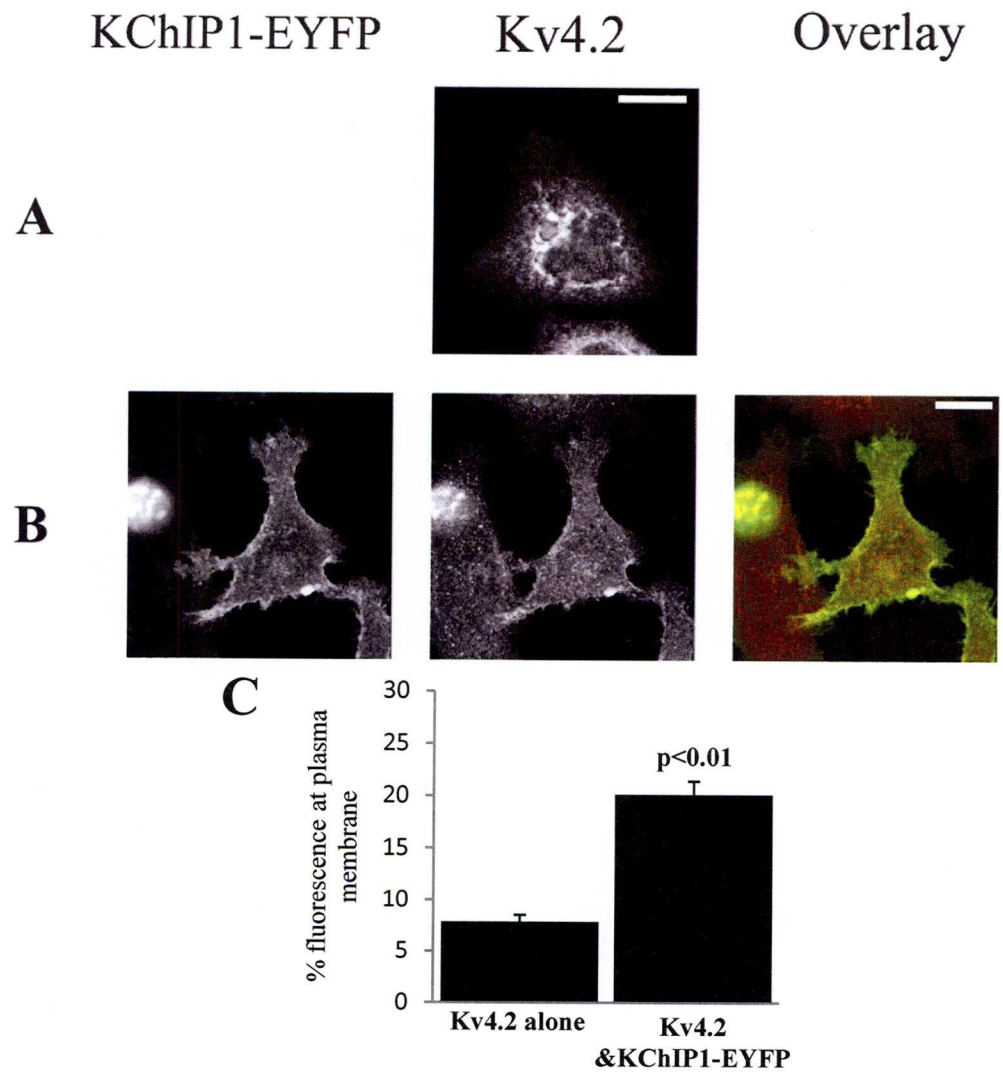

3.3: Co-expression of KChIP1-EYFP promotes the trafficking of Kv4.2 to the plasma membrane, in HeLa cells.

HeLa cells were transfected with Kv4.2, alone or with KChIP1-EYFP, and trafficking of Kv4.2 to the plasma membrane was quantified.

A) HeLa cell expressing Kv4.2.

B) HeLa cell expressing KChIP1-EYFP (Green) and Kv4.2 (Red) with co-localisation shown as yellow in the overlay.

Kv4.2 localisation was determined using anti-Kv4.2 immunostaining with a TRITC-conjugated secondary antibody. In all cases, scale bars represent 10μm.

C) The trafficking of Kv4.2 to the plasma membrane was quantified in terms of the percentage of Kv4.2 fluorescence at the plasma membrane in the presence or absence of KChIP1-EYFP. Data shown as the means for 20 cells for each condition, ±S.E.M.

expressing both together. There is much evidence to support the ability of KChIPs to traffic Kv4 channels to the plasma membrane, using both electrophysiology to measure increases in current density due to channel trafficking (An et al. 2000), and fluorescence to observe the localisation of channel and KChIP at the plasma membrane (Shibata et al. 2003; Hasdemir et al. 2005). Using the constructs described above in HeLa cells, Kv4.2 was detected

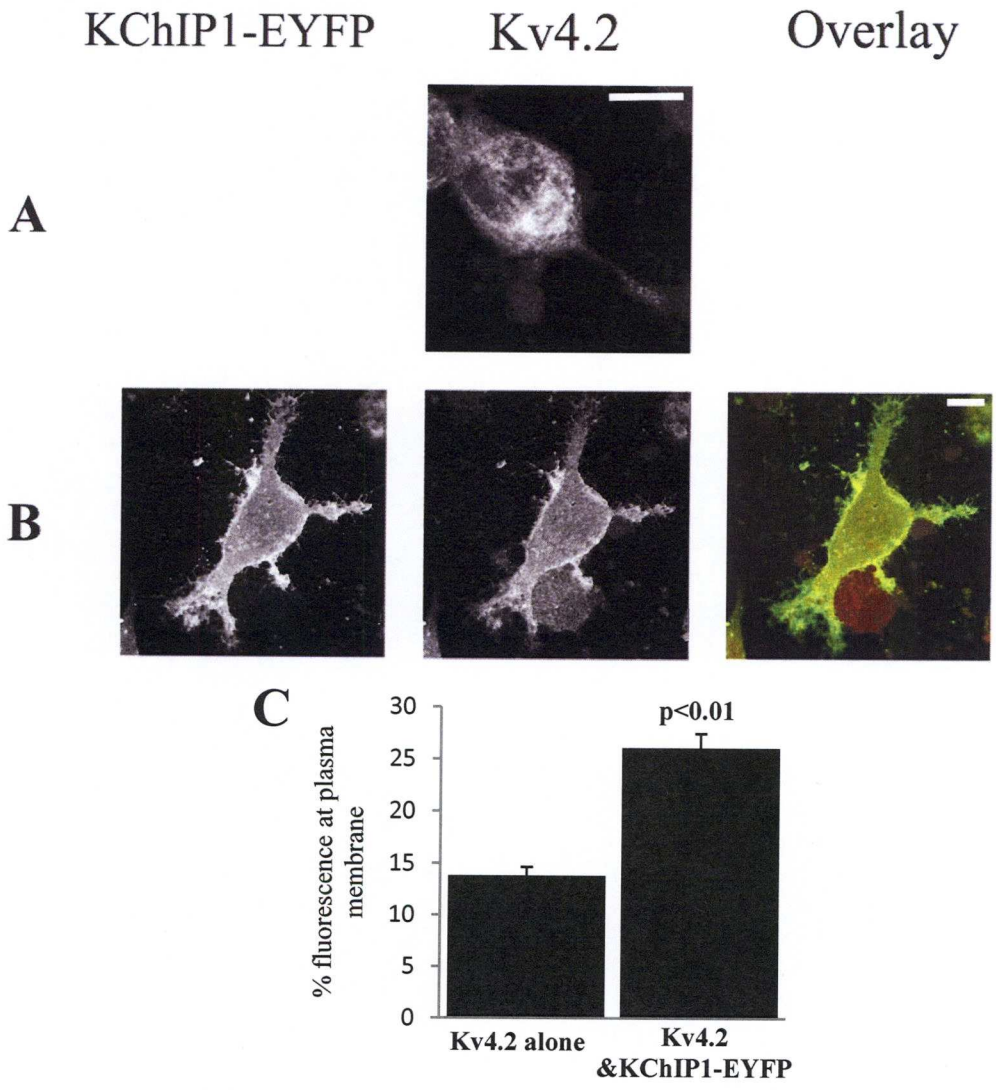

3.4: Co-expression of KChIP1-EYFP promotes the trafficking of Kv4.2 to the plasma membrane, in Neuro2A cells.

Neuro2A cells were transfected with Kv4.2, alone or with KChIP1-EYFP, and trafficking of Kv4.2 to the plasma membrane was quantified.

A) Neuro2A cell expressing Kv4.2.

B) Neuro2A cell expressing KChIP1-EYFP (Green) and Kv4.2 (Red) with co-localisation shown as yellow in the overlay.

Kv4.2 localisation was determined using anti-Kv4.2 immunostaining with a TRITC-conjugated secondary antibody. In all cases, scale bars represent 10μm.

C) The trafficking of Kv4.2 to the plasma membrane was quantified in terms of the percentage of Kv4.2 fluorescence at the plasma membrane in the presence or absence of KChIP1-EYFP. Data shown as the means for 20 cells for each condition, ±S.E.M.

by immunostaining, either alone (Figure 3.3A; red in the colour overlays), or with KChIP1-EYFP (Figure 3.3B; green in the colour overlay). It is clear from these images that KChIP1 is able to redistribute Kv4.2 to the plasma membrane. KChIP1 also alters its localisation, and is seen at the plasma membrane in these cells, reflecting its continued binding to the channel after trafficking, in order to modulate the channel's functions and kinetics (An et al. 2000). Kv4.2 trafficking was quantified, using measurements of the percentage of TRITC cellular fluorescence at the plasma membrane, as described in Chapter 2.7. In the absence of KChIP1, approximately 7.5% of TRITC fluorescence was at the plasma membrane (Figure 3.3C). This background is likely due to both background fluorescence due to the antibody approach used, and low level trafficking of the channel in the absence of accessory proteins, and is in line with previous studies using this method (Hasdemir et al. 2005). However, there was a significant increase in plasma membrane fluorescence in the presence of KChIP1-EYFP, to around 20%. As expected from Figure 3.3B, the levels of KChIP1-EYFP at the plasma membrane also increased significantly in the presence of Kv4.2 (data not shown).

These experiments were repeated in Neuro2A cells (Figure 3.4). Again, Kv4.2 alone was perinuclear (Figure 3.4A), but trafficked to the plasma membrane in the presence of KChIP1-EYFP (Figure 3.4B). The similarities in the localisations of these proteins between HeLa and Neuro2A cells are reflected in the quantified data in Figure 3.4C. There is a background level of plasma membrane fluorescence of around 14% in Neuro2A cells, and a significant increase in the presence of KChIP1-EYFP to about 26% of total cellular fluorescence at the plasma membrane.

3.2.2 KChIP1 requires intact EF-hand domains to traffic Kv4.2, but not to access punctate vesicular structures

Having characterised the localisation of the Kv4.2 channel and wild-type KChIP1 in two cell types, it was then possible to compare the effects on trafficking of mutant versions of KChIP1 lacking active EF-hand domains. Two constructs available in the lab were used (Hasdemir et al. 2005). One, designated the EF3 mutant, had a mutation in just EF hand domain 3, one of the high Ca^{2+} affinity sites in KChIP1 (Craig et al. 2002). The other, designated the EF2-4 mutant, had mutations in all three of the potentially active EF hand domains. Each of the mutant KChIP1 proteins was expressed in an EYFP-tagged form, and visualised in HeLa cells. Figures 3.5 A and B shows a typical cell expressing each protein. Both mutants of KChIP1 were punctate in HeLa cells, with a similar distribution to wild-type KChIP1 (compare with Figure 3.1A).

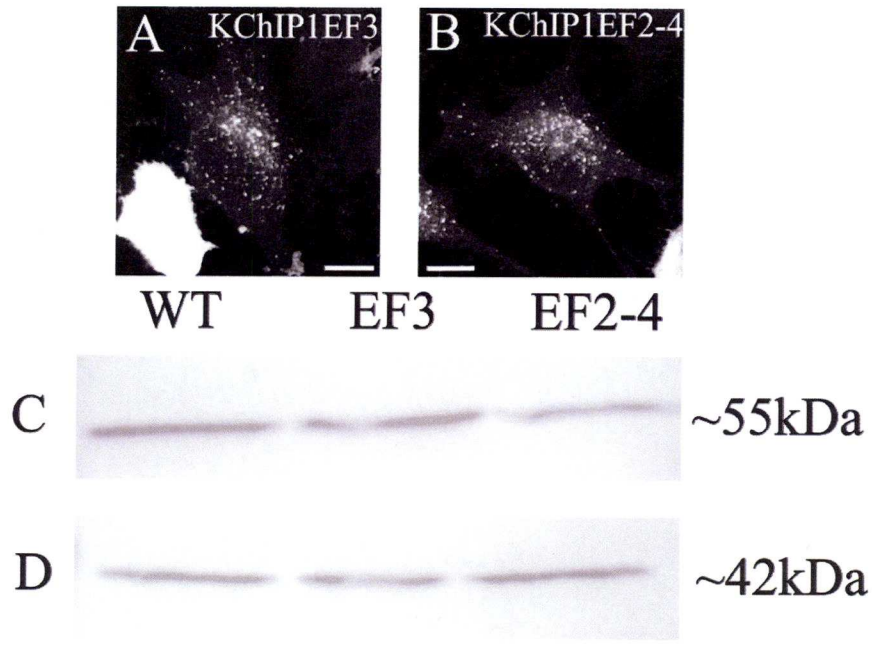

3.5: EF-hand mutants of KChIP1-EYFP show a punctate localisation in HeLa cells, and are expressed at a level similar to wild-type.
HeLa cells were transfected with EF-hand mutations of KChIP1-EYFP to investigate their localisation, and their expression levels were compared to wild-type KChIP1.

- **A)** HeLa cell transfected with KChIP1EF3-EYFP.
- **B)** HeLa cell transfected with KChIP1EF2-4-EYFP.
  Scale bars represent 10μm.
- **C)** Western blot of HeLa cells transfected with either EYFP-tagged wild-type KChIP1 (WT), KChIP1EF3 (EF3) or KChIP1EF2-4 (EF2-4) mutants. Tagged KChIP protein was detected using an anti-GFP antibody, showing similar expression of all three proteins.
- **D)** Western blot of β-actin expression in HeLa cells transfected as described for C), showing equal loading of each lane.

As a further control it was necessary to confirm that these proteins were being expressed at the same level in cells. HeLa cells were therefore transfected with wild-type or mutant EYFP-tagged KChIP1, and lysed 72 hours post-transfection for use in Western blotting. An anti-GFP antibody was used to detect the EYFP tag. As seen in Figure 3.5C, KChIP1-EYFP was detected in all cases at the expected molecular weight of ~55kDa. Expression levels of all three proteins were similar. A blot for β-actin (Figure 3.5D) confirmed the lanes were equally loaded.

Previous work had shown that KChIP1EF2-4 was unable to traffic Kv4.2 to the plasma membrane as effectively as wild-type KChIP1 (Hasdemir et al. 2005). However, the effect of mutating just a single EF-hand had not been fully characterised. HeLa cells were transfected with either Kv4.2 pcDNA alone, or with one of the three KChIP1-EYFP constructs (wild-type, EF3 mutant, or EF2-4 mutant). Cells were fixed after 72 hours, and Kv4.2 visualised with antibodies. Example cells are shown in Figures 3.6A to C. It can be seen from these figures that whilst wild-type KChIP1 traffics Kv4.2 to the plasma membrane, in the presence of either mutant the channel is not at the plasma membrane, but rather has an intracellular punctate distribution. This is different from the normal perinuclear distribution of Kv4.2 alone, but similar to the localisation of KChIP1 expressed alone. However, these effects could be due to a non-specific effect of the mutant KChIP1 on general exocytic trafficking pathways. To investigate this, the trafficking of the marker protein VSVG-GFP was analysed. Cells transfected with VSVG-GFP alone showed trafficking of this marker protein to the plasma membrane, as can be seen in Figure 3.6D. This plasma membrane localisation of VSVG-GFP fluorescence was also seen in the presence of HcRed-tagged wild-type KChIP1 (Figure 3.6E), and HcRed-tagged KChIP1EF2-4 (Figure 3.6F).

The trafficking in both cases was also quantified. The percentage of Kv4.2 fluorescence found at the plasma membrane was determined, the background level of trafficking with Kv4.2 alone was subtracted, and results normalised to those with wild-type KChIP1, as shown in Figure 3.6G. As expected from the figures, trafficking of the channel with either mutant is significantly lower than with wild-type KChIP1, and in fact not significantly different from background

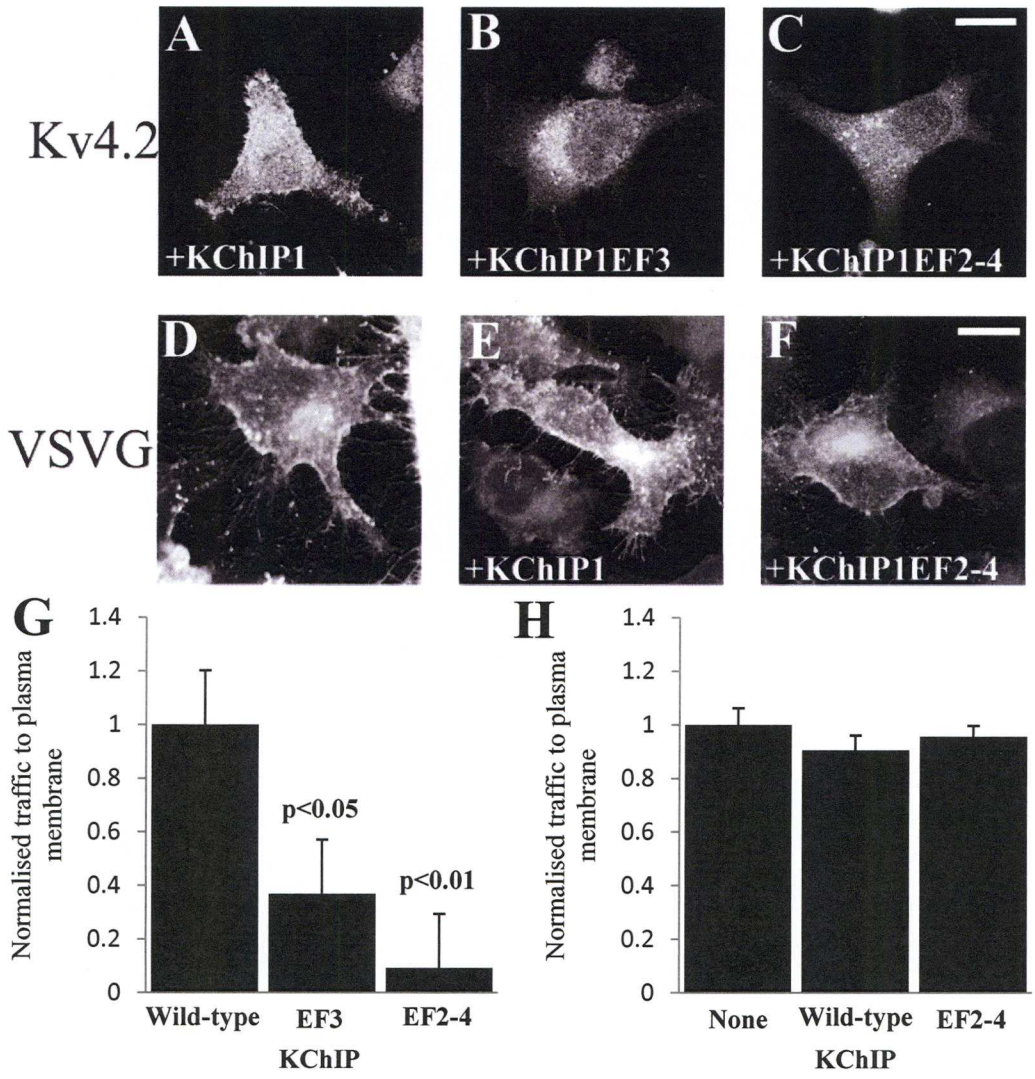

3.6: Effects of KChIP1 with EF-hand mutations on traffic of Kv4.2 and VSVG to the plasma membrane.

HeLa cells were transfected with either Kv4.2 or VSVG-GFP, and the effects of co-transfecting with EF-hand mutants of KChIP1 were observed and quantified.

A-C) HeLa cells were co-transfected with Kv4.2 (detected using anti-Kv4.2 immunostaining) and either **A)** wild-type KChIP1-EYFP, **B)** the single EF-hand mutant KChIP1EF3-EYFP or **C)** the triple EF-hand mutant KChIP1EF2-4-EYFP.

D-F) HeLa cells were co-transfected with VSVG-GFP (detected by confocal imaging), either **D)** alone, **E)** with wild-type KChIP1-HcRed, or **F)** with the mutant KChIP1EF2-4-HcRed.

Scale bars represent 10μm.

G-H) Normalised traffic of **G)** Kv4.2 or **H)** VSVG-GFP in the presence of various KChIP proteins was quantified. Results are shown as means for 20 cells for each condition, ±S.E.M.

levels of Kv4.2 trafficking. Levels of mutant KChIP1 at the plasma membrane were also significantly lower (data not shown). This suggests that disruption of even a single Ca^{2+}-binding site is enough to prevent KChIP1 trafficking Kv4.2 correctly to the plasma membrane. This can be contrasted with the trafficking of VSVG-GFP, quantified in Figure 3.6H, with results adjusted relative to the percentage of fluorescence at the plasma membrane with VSVG-GFP alone. There is no significant difference in plasma membrane fluorescence between cells expressing VSVG-GFP alone, and those co-expressing KChIP1. This confirms that KChIP1EF2-4 does not disrupt the general trafficking pathways of the cell, but rather has a specific effect on Kv4.2 trafficking due to its inability to bind Ca^{2+}/Mg^{2+}.

3.2.3 Rab1 is required for trafficking of both VSVG-GFP and Kv4.2/KChIP1 to the plasma membrane

The above work on EF-hand mutants shows an effect on the trafficking of Kv4.2/KChIP1, but not VSVG-GFP. Combined with previous findings that COPII is required for VSVG trafficking, but not for Kv4.2/KChIP1 (Hasdemir et al. 2005), this suggested two separate exocytic trafficking pathways. This also led to the question of whether proteins regulating the exocytic pathway of VSVG-GFP would have a role in Kv4.2/KChIP1 trafficking as well. One key regulatory protein in ER-Golgi trafficking is the Rab-GTPase Rab1 (Tisdale et al. 1992). However, Rab1-independent trafficking has been shown (Yoo et al. 2002; Wu et al. 2003). The role of this Rab in exocytic trafficking was therefore investigated, by overexpression of the Rab1-specific GAP TBC1D20 (Haas et al. 2007). As a Rab1-GAP, this should promote the hydrolysis of the active Rab1-GTP into inactive Rab1-GDP.

Previous work using TBC1D20 had confirmed its ability to inhibit VSVG-GFP trafficking to the plasma membrane (Haas et al. 2007). As a control, these experiments were repeated in HeLa cells, and fixed cells were visualised using confocal microscopy. In HeLa cells expressing VSVG-GFP alone (Figure 3.7A), it was trafficked to the plasma membrane, whereas in cells co-transfected with TBC1D20 (Figure 3.7B), the VSVG-GFP was trapped intracellularly, in the perinuclear region. Quantification of this data (Figure 3.7E) revealed a significant inhibition of trafficking in the presence of the Rab1-GAP, confirming previous work on the role of Rab1 in VSVG-GFP exocytosis (Haas et al. 2007). Experiments were then performed in HeLa cells co-transfected with KChIP1-EYFP and Kv4.2, in the absence (Figure 3.7C) or presence (Figure 3.7D) of TBC1D20. Whilst both KChIP and channel trafficked to the plasma membrane in control cells, this was inhibited by the Rab1-GAP. In these cells, both KChIP1 and Kv4.2 were trapped in the perinuclear region of the cell, which could be the ER. Quantification of these results, shown in Figure 3.7F, showed that TBC1D20 significantly reduced the percentage of Kv4.2 at the plasma membrane in the presence of KChIP1. This confirms that the trafficking pathways used by VSVG-GFP and Kv4.2/KChIP1 to reach the plasma membrane are both Rab1-dependent.

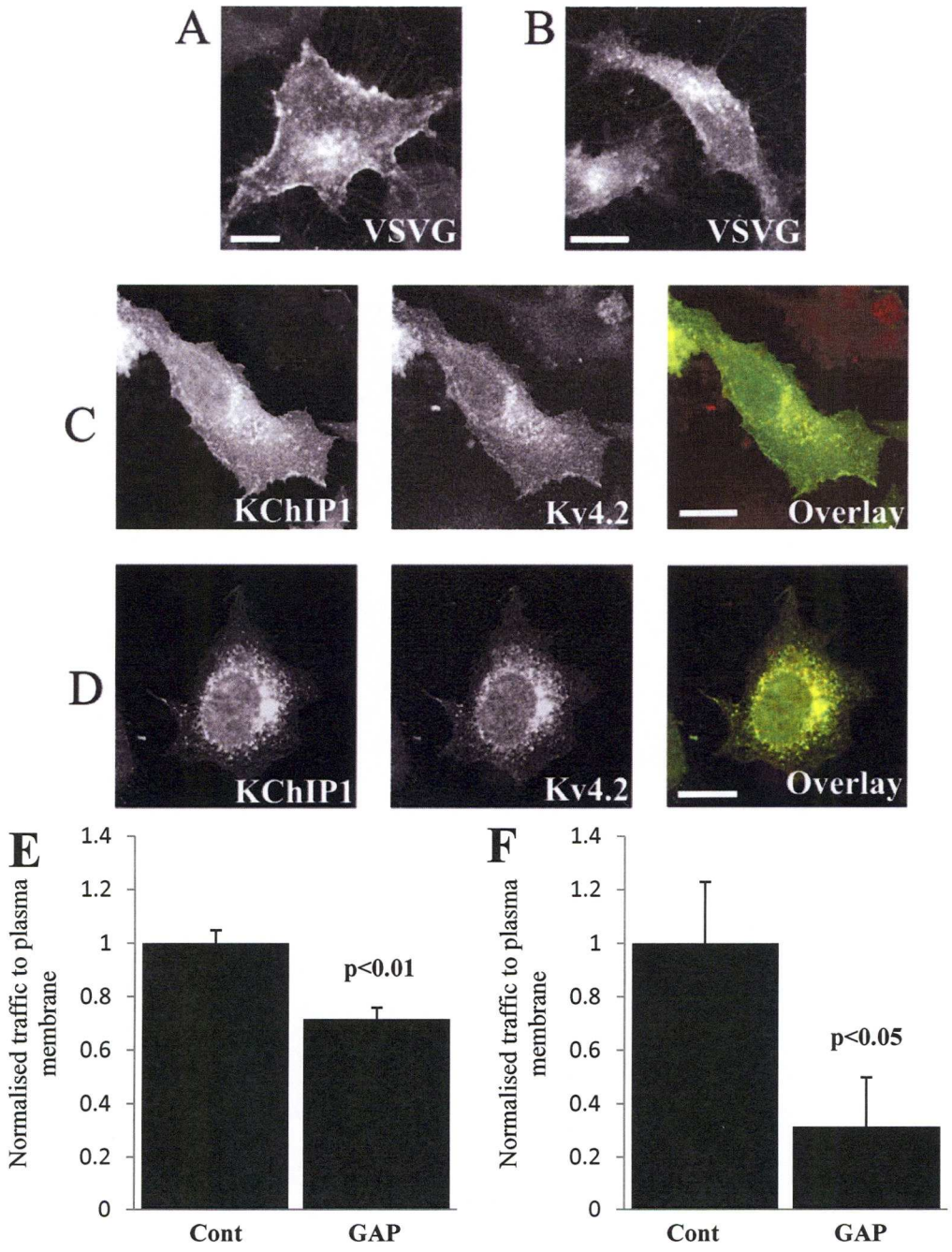

3.7: Inhibition of Rab1 function prevents traffic of VSVG and Kv4.2/KChIP1 to the plasma membrane.

HeLa cells were transfected with either VSVG-GFP or Kv4.2/KChIP1-EYFP and the effects of co-transfecting with the Rab1-GAP TBC1D20 were observed and quantified.

- **A)** HeLa cell transfected with VSVG-GFP, and its localisation visualised.
- **B)** HeLa cell co-transfected with VSVG-GFP and the Rab1-GAP TBC1D20.
- **C)** HeLa cell co-transfected with KChIP1-EYFP (Green) and Kv4.2 (Red), detected by immunostaining.
- **D)** HeLa cell co-transfected with KChIP1-EYFP (Green), Kv4.2 (Red, detected by immunostaining) and the Rab1-GAP TBC1D20.
- **E)** Normalised traffic of VSVG-GFP in the absence (Cont) or presence (GAP) of TBC1D20 was quantified.
- **F)** Normalised traffic of Kv4.2 in the presence of KChIP1-EYFP, and either the absence (Cont) or presence (GAP) of TBC1D20 was quantified.

In the colour overlays, co-localisation is shown in yellow. In all cases, the scale bar represents 10μm. For the quantification, data is shown as the mean of 20 cells for each condition, ±S.E.M.

3.2.4 KChIP1-EYFP-positive vesicles co-localise with the SNAREs VAMP7 and Vti1a

Another important set of proteins in membrane trafficking are the SNARE proteins. These are thought to form part of the machinery that allows vesicles to dock and bind with their target membranes (Jahn and Scheller 2006). The complement of SNAREs on a vesicle or membrane therefore determines which other membranes it can bind to, and hence defines a cellular compartment (Jahn and Scheller 2006). It was therefore interesting to determine which SNAREs were co-localised with the vesicles seen in cells expressing KChIP1-EYFP alone.

HeLa cells were transfected with KChIP1-EYFP, and then fixed and immunostained with antibodies against endogenous SNAREs of interest, visualised using a TRITC-conjugated secondary antibody. Firstly, those SNAREs implicated in the conventional ER-Golgi trafficking route used by VSVG-GFP were investigated (Zhang et al. 1999; Xu et al. 2000). Whilst KChIP1-EYFP was punctate in these cells, there was little to no punctate staining with an anti-membrin antibody (Figure 3.8A) or an anti-Sec22b antibody (Figure 3.8B), and no obvious co-localisation in the colour overlays, or enlarged regions of the cell. Nor was there co-localisation between KChIP1-EYFP and members of a second ER-Golgi SNARE complex implicated in the fusion of vesicles with the *cis*-Golgi (Zhang and Hong 2001), GOS28 (Figure 3.8C) and Ykt6 (Figure 3.8D). Indeed, both of these were found with a pronounced perinuclear, Golgi-like, localisation fitting their proposed role in the *cis*-Golgi.

A third ER-Golgi SNARE complex, implicated in the trafficking of PCTVs in the intestine (Siddiqi et al. 2006a), was then investigated in a similar manner. Again, KChIP1-EYFP was punctate in fixed HeLa cells. However, immunostaining with a mouse monoclonal antibody against VAMP7 (Figure 3.9A), also revealed a punctate distribution, clustered in the perinuclear region. These two sets of punctae clearly overlapped, as shown in yellow in the colour overlay, and in the enlarged inserts. To further confirm this, an alternative rabbit polyclonal antibody against VAMP7 was obtained from Thierry Galli, Institut

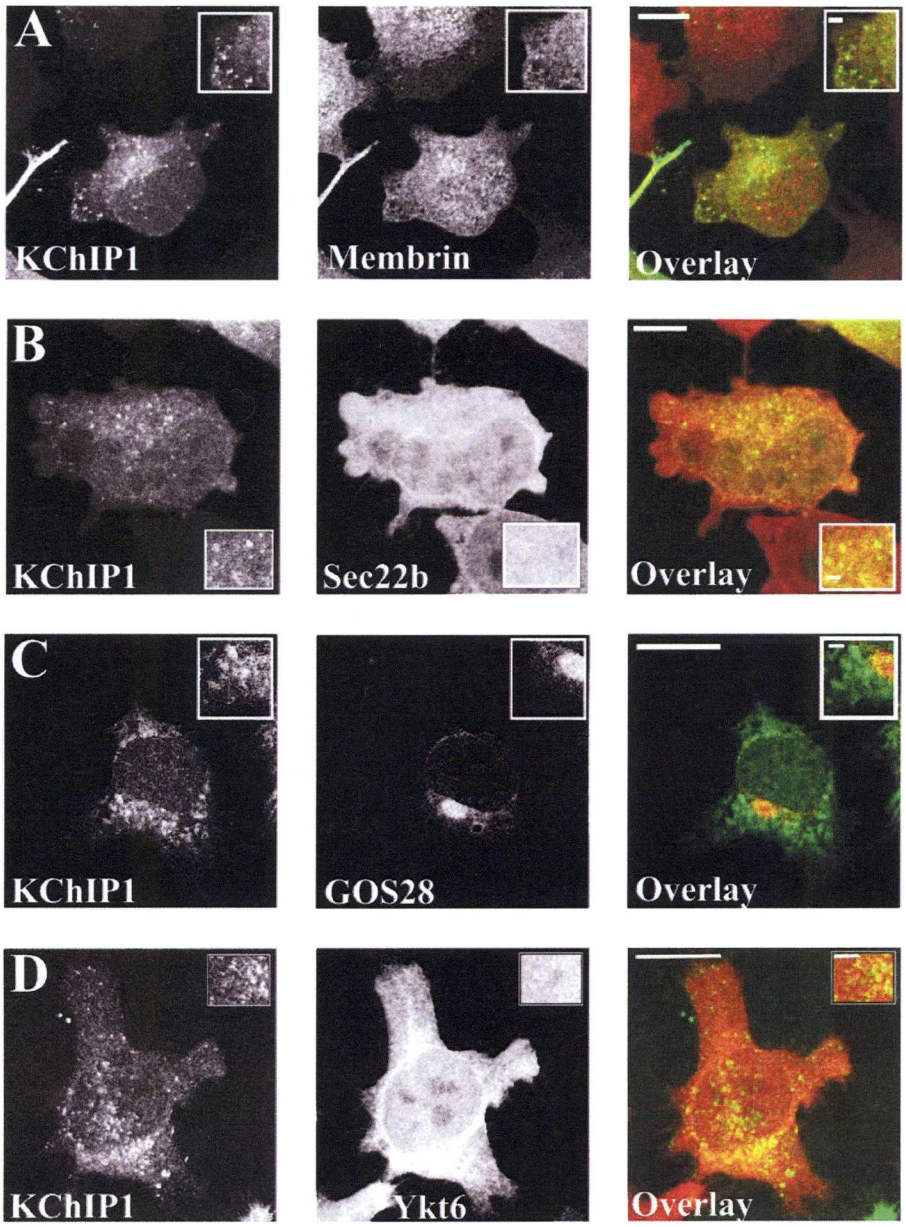

3.8: Lack of co-localisation of KChIP1-EYFP with membrin, Sec22b, GOS28 or Ykt6.
HeLa cells were transfected with KChIP1-EYFP, then fixed and immunostained with mouse monoclonal antibodies specific for:
A) Membrin
B) Sec22b
C) GOS28
D) Ykt6
The images show the localisation of KChIP1, and the indicated SNARE proteins, visualised using a TRITC-conjugated secondary antibody, except for anti-Ykt6 which was visualised using a Texas Red-conjugated anti-chicken secondary. The colour overlays show KChIP1-EYFP in green, the SNARE in red, and co-localisation in yellow. The scale bars represent 10μm in the main images, and 2μm in the enlarged inserts.

Jacques Monod, Paris, and used for immunostaining (Figure 3.9B). This antibody appeared to be less effective, and not all punctae visible in the KChIP1 image had a corresponding VAMP7 puncta. It was therefore not used further. However, all the VAMP7 visualised did co-localise with KChIP1, supporting the idea that VAMP7 is localised to the same vesicles as KChIP1-EYFP. To further confirm this, immunostaining was performed with a mouse monoclonal antibody against Vti1a, the second unique member of this ER-Golgi SNARE complex (Figure 3.9C). This also revealed a punctate distribution, with co-localisation between Vti1a and KChIP1-EYFP.

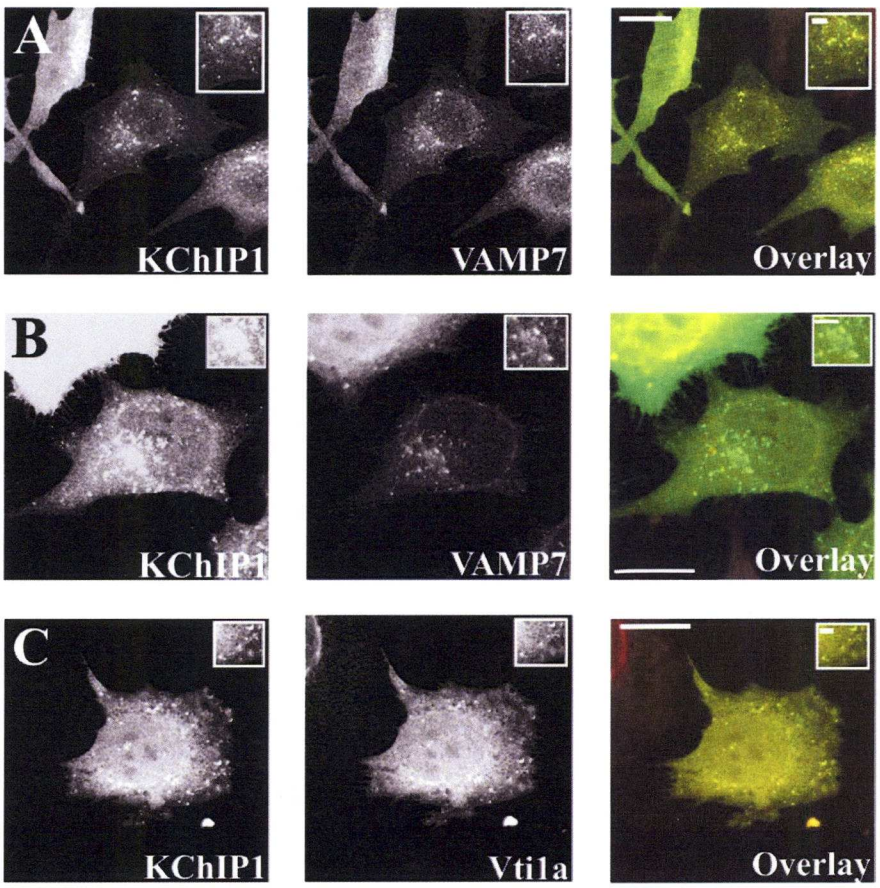

3.9: Co-localisation of KChIP1-EYFP with VAMP7 and Vti1a.
HeLa cells were transfected with KChIP1-EYFP and immunostained against the SNAREs VAMP7 and Vti1a.

- **A)** HeLa cells were transfected with KChIP1-EYFP (Green) and immunostained with a mouse monoclonal antibody against VAMP7 (Red).
- **B)** HeLa cell transfected with KChIP1-EYFP (Green), and immunostained with a rabbit polyclonal against VAMP7 (Red).
- **C)** HeLa cell transfected with KChIP1-EYFP (Green), and immunostained with a mouse monoclonal against Vti1a (Red).

Co-localisation is shown as yellow in the colour overlays. Scale bars represent 10μm in main image, and 2μm in enlarged insert.

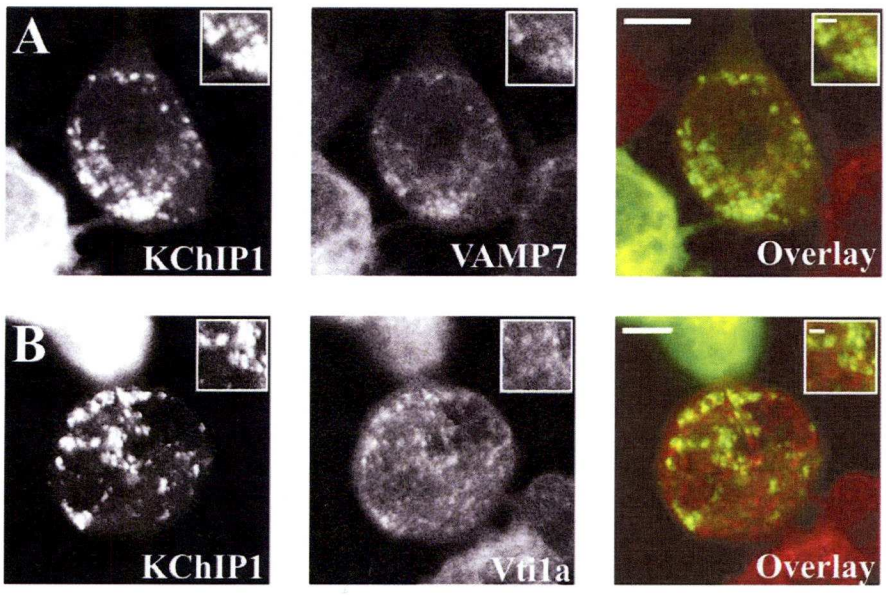

3.10: Co-localisation of KChIP1-EYFP with VAMP7 and Vti1a in PC12 cells.
PC12 cells were transfected with KChIP1-EYFP and immunostained against the SNAREs VAMP7 and Vti1a.

- **A)** PC12 cell transfected with KChIP1-EYFP (Green), and immunostained with a mouse monoclonal against VAMP7 (Red).
- **B)** PC12 cell transfected with KChIP1-EYFP (Green), and immunostained with a mouse monoclonal against Vti1a (Red).

Co-localisation is shown as yellow in the colour overlays. Scale bars represent 5μm in main image, and 1μm in the enlarged insert.

This co-localisation between KChIP1-EYFP and the SNAREs VAMP7 and Vti1a was surprising, as the PCTV SNARE complex was originally described as being specific to the intestine (Siddiqi et al. 2006b). Further control experiments were therefore performed. PC12 cells are often used as a model neuronal cell line (Handley et al. 2007), and are therefore more representative of the endogenous location of KChIP1 and Kv4.2. As seen in Figure 3.10, KChIP1-EYFP was punctate in these cells. There was also co-localisation between KChIP1-EYFP and immunostaining against VAMP7 (Figure 3.10A) and Vti1a (Figure 3.10B). These cells are thicker and more rounded than HeLa cells, making the confocal images less clear. They were therefore not used in further experiments. Also, the KChIP1-EYFP-positive vesicles appear larger in this cell type – this could be due to differences in cell type, aggregation of vesicles, or simply due to the lack of clarity in the confocal images. However, these results are supportive of an association between KChIP1-EYFP and VAMP7 and Vti1a. In addition, in experiments described above EF-hand mutants of KChIP1 had a punctate distribution when expressed alone in HeLa cells (Figure 3.5), similar to that seen for the wild-type protein. It was therefore decided to investigate whether these

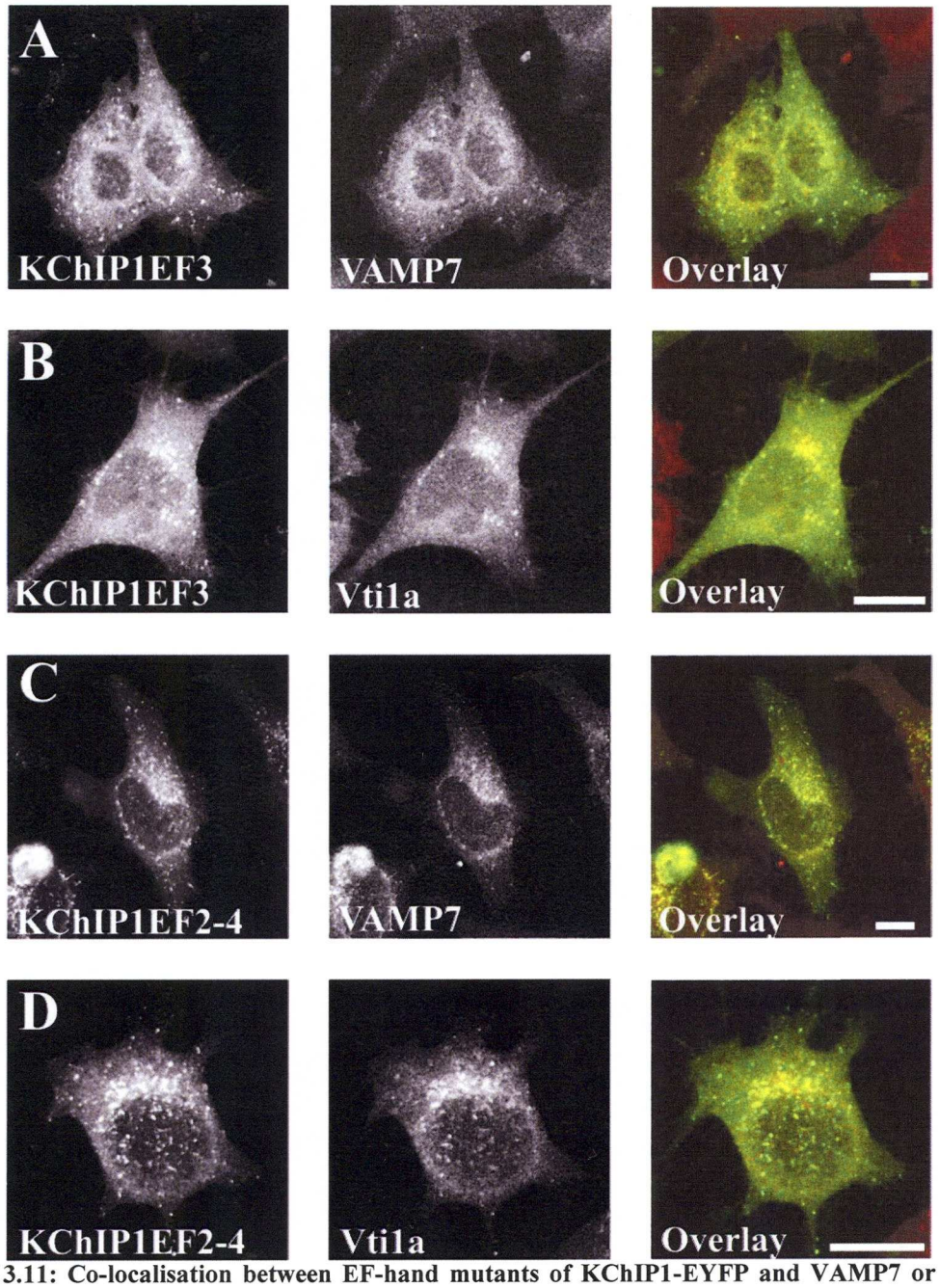

3.11: Co-localisation between EF-hand mutants of KChIP1-EYFP and VAMP7 or Vti1a.

HeLa cells were transfected with EF-hand mutants of KChIP1 and immunostained for VAMP7 or Vti1a.

- **A)** HeLa cell transfected with KChIP1EF3-EYFP (Green), and immunostained against VAMP7 (Red).
- **B)** HeLa cell transfected with KChIP1EF3-EYFP (Green), and immunostained against Vti1a (Red).
- **C)** HeLa cell transfected with KChIP1EF2-4-EYFP (Green), and immunostained against VAMP7 (Red).
- **D)** HeLa cell transfected with KChIP1EF2-4-EYFP (Green), and immunostained against Vti1a (Red).

Antibodies were visualised using a TRITC-conjugated secondary antibody. Co-localisation is shown as yellow in the colour overlays. Scale bars represent 10μm.

mutant proteins could also co-localise with VAMP7 and Vti1a. HeLa cells were transfected with KChIP1EF3-EYFP, fixed and immunostained with antibodies against VAMP7 (Figure 3.11A) or Vti1a (Figure 3.11B). In both cases, KChIP1 was punctate in cells, and showed clear co-localisation with the two SNAREs of interest. These experiments were also repeated with KChIP1EF2-4-EYFP and VAMP7 (Figure 3.11C) or Vti1a (Figure 3.11D), and again, there was co-localisation. This further supports an association between these SNAREs and KChIP1, and also confirms that the EF-hand mutant proteins are able to access the same cellular compartment as the wild-type protein (Hasdemir et al. 2005).

Next, it proved possible to obtain a GFP-tagged construct of VAMP7, and look for co-localisation in HeLa cells between this overexpressed SNARE, and KChIP1-HcRed (Figure3.12A) or KChIP1EF2-4-HcRed (Figure 3.12B). Overexpression of VAMP7-GFP gave a much brighter signal than when endogenous protein was detected with antibodies. Unfortunately, this made it harder to visualise punctate structures in these cells. However, a small number of punctae were observed in the very perinuclear region of the cells in the KChIP1 images, and there was co-localisation with VAMP7. There was also no

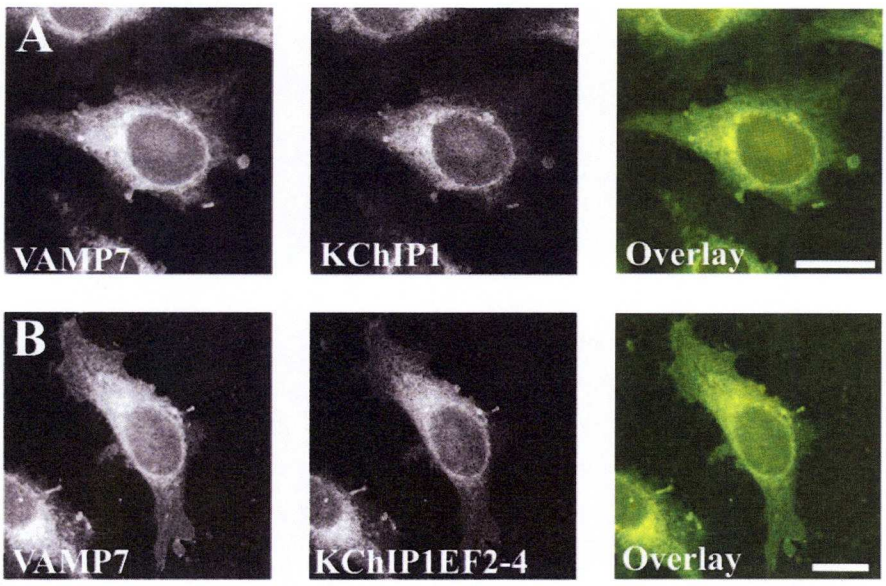

3.12: Co-localisation between VAMP7-GFP and KChIP1.
HeLa cells were transfected with VAMP7-GFP and wild-type or mutant KChIP1-HcRed.

- **A)** HeLa cell transfected with VAMP7-GFP (Green), and KChIP1-HcRed (Red).
- **B)** HeLa cell transfected with VAMP7-GFP (Green), and KChIP1EF2-4-HcRed (Red).

Co-localisation is shown as yellow in the colour overlays. Scale bars represent 10μm.

difference between wild-type and EF2-4 mutant KChIP1, as would be expected from the results in Figure 3.11. However, immunostaining against VAMP7 gave clearer images, and looking at endogenous protein should be more representative of the situation *in vivo* than with overexpressed protein, so for further work the antibody approach was preferred.

For further confirmation of an association between KChIP1 and VAMP7/Vti1a, co-localisation studies were repeated in fixed Neuro2A cells. These were transfected with either wild-type KChIP1-EYFP, or KChIP1EF2-4-EYFP, and then immunostained for SNAREs (Figure 3.13). There was clear co-localisation between wild-type KChIP1 and either VAMP7 (Figure 3.13A) or Vti1a (Figure 3.13B). These images were very similar to those with HeLa cells in Figure 3.9, although the KChIP1 punctae were more confined to the perinuclear region as had been seen previously (Figure 3.2). There was also no difference between the wild-type and mutant proteins, with KChIP1EF2-4-EYFP also showing co-localisation with VAMP7 (Figure 3.13C) and Vti1a (Figure 3.13D).

These data further confirmed an association between KChIP1 and VAMP7/Vti1a. However, as well as forming a complex with rBet1 and syntaxin 5 for the trafficking of intestinal PCTVs (Siddiqi et al. 2006a), these SNAREs are better known for their role in late endocytic endosomal/lysosomal trafficking, with syntaxins 7 and 8 (Bogdanovic et al. 2002). To investigate the possibility of KChIP1 being associated with endosomes or lysosomes, or utilising this better known SNARE complex for trafficking, co-localisation studies were performed in fixed HeLa cells transfected with wild-type KChIP1, and immunostained with rabbit antiserum against syntaxin 7 (Figure 3.14A) or a rabbit antiserum against syntaxin 8 (Figure 3.14B). Whilst there was some overlapping localisation with both SNAREs in the perinuclear region, there were clearly two populations of punctae, with those labelled with KChIP1 distinct from those labelled with anti-syntaxin 7 or anti-syntaxin 8. This was especially clear in the enlarged regions of each cell shown in Figure 3.14. Also, previous work with overexpressed VAMP7

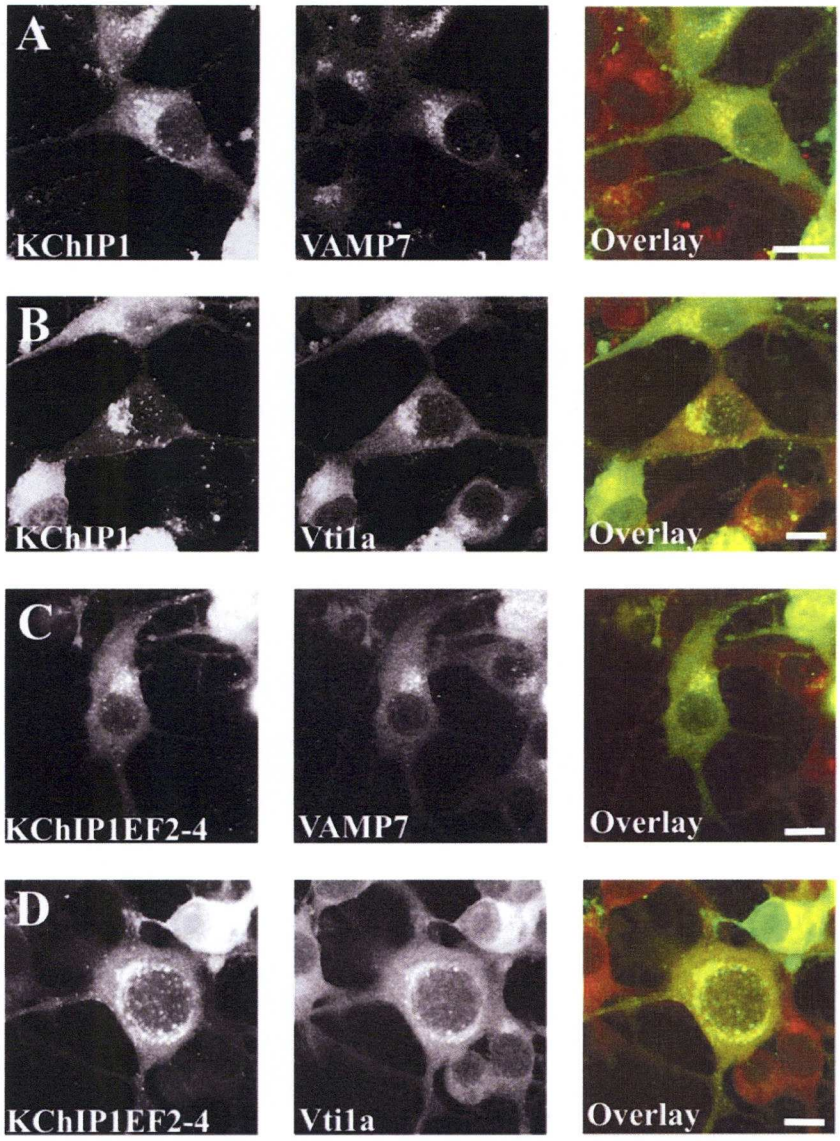

3.13: Co-localisation of KChIP1-EYFP with VAMP7 and Vti1a in Neuro2A cells.

Neuro2A cells were transfected with wild-type or mutant KChIP1 and immunostained for VAMP7 or Vti1a.

- **A)** Neuro2A cell transfected with KChIP1-EYFP (Green), and immunostained against VAMP7 (Red).
- **B)** Neuro2A cell transfected with KChIP1-EYFP (Green), and immunostained against Vti1a (Red).
- **C)** Neuro2A cell transfected with KChIP1EF2-4-EYFP (Green), and immunostained against VAMP7 (Red).
- **D)** Neuro2A cell transfected with KChIP1EF2-4-EYFP (Green), and immunostained against Vti1a (Red).

Antibodies were visualised using a TRITC-conjugated secondary antibody. Co-localisation is shown as yellow in the colour overlays. Scale bars represent 10μm.

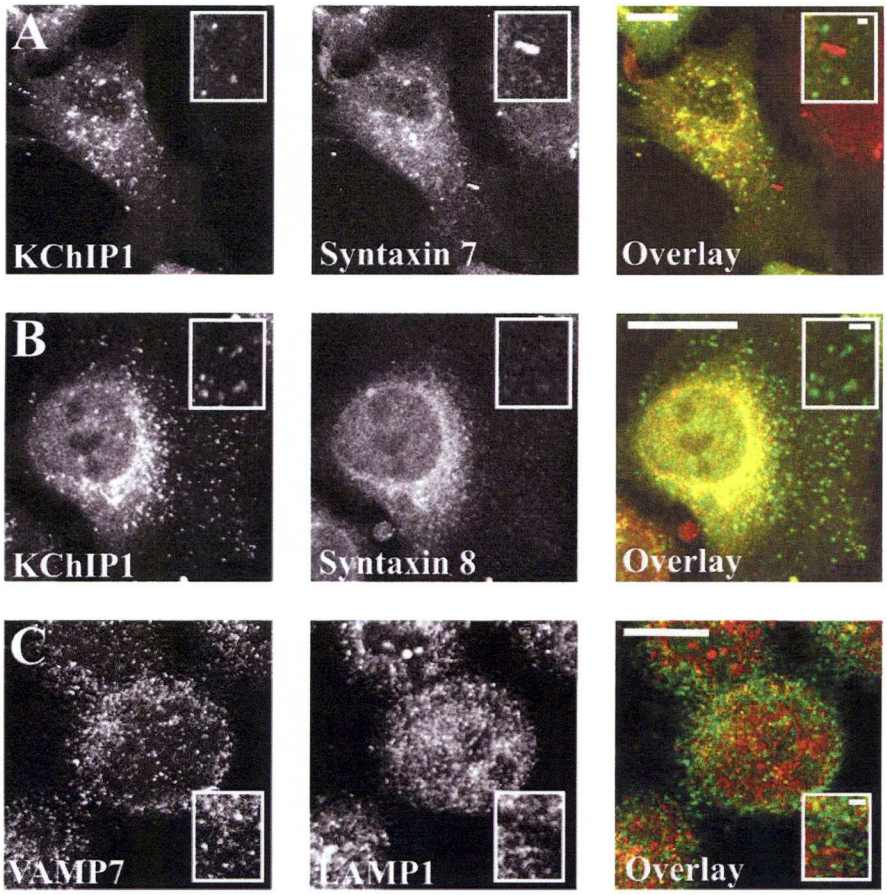

3.14: Lack of co-localisation between KChIP1 and syntaxins 7 or 8, or between VAMP7 and LAMP1.

HeLa cells were transfected with KChIP1 and immunostained for syntaxin 7 or 8, or immunostained against VAMP7 and the lysosomal marker LAMP1.

A) HeLa cell transfected with KChIP1-EYFP (Green), and immunostained with rabbit antiserum against syntaxin 7 (Red), detected with a TRITC-conjugated secondary antibody.

B) HeLa cell transfected with KChIP1-EYFP (Green), and immunostained with a rabbit polyclonal antibody against syntaxin 8 (Red), detected with a TRITC-conjugated secondary antibody.

C) HeLa cell immunostained against VAMP7 (Green), detected using an Alexa Fluor® 488-linked secondary antibody, and against the lysosomal marker LAMP1 (Red), detected using an Alexa Fluor® 594-linked secondary antibody.

Co-localisation is shown as yellow in the colour overlays. Scale bars represent 10μm in the main images, and 2μm in the enlarged inserts.

had shown it associated with markers of lysosomes (Advani et al. 1998; Advani et al. 1999). However, in HeLa cells immunostained against endogenous VAMP7, and against the lysosomal marker LAMP1 (Figure 3.14C) (Advani et al. 1999), there was very little co-localisation, with the majority of staining being distinct VAMP7 and LAMP1 punctae. This work argues against KChIP1 being localised to lysosomes, or requiring the better characterised VAMP7/Vti1a/syntaxin 7/syntaxin 8 SNARE complex for trafficking.

Previous work on VAMP7 has shown it to belong to the longin subfamily of the VAMP/synaptobrevin SNAREs, and suggested this N-terminal longin domain may inhibit SNARE complex formation (Martinez-Arca et al. 2003), and neurite outgrowth in neurons (Wang and Tang 2006). Comparisons were therefore made between the trafficking of Kv4.2 with KChIP1-EYFP in control HeLa cells, and those co-transfected with either full-length VAMP7-GFP (as used in Figure 3.12) or a GFP-tagged version of the longin domain of VAMP7. Images of a TRITC-conjugated secondary antibody against an anti-Kv4.2 primary antibody were obtained for a control cell (Figure 3.15A), and cells co-transfected with VAMP7-GFP (Figure 3.15B) or its longin domain (Figure 3.15C). These showed the channel at the plasma membrane in all cases. The percentage of Kv4.2 localised to the plasma membrane was quantified for 20 cells from each condition, and normalised to the control cells, as shown in Figure 3.15D. This shows that the longin domain did not have an inhibitory effect on Kv4.2 trafficking in this system. Neither did overexpression of full-length VAMP7 potentiate Kv4.2 trafficking. Together these results suggest that availability of VAMP7 is not a limiting factor in Kv4.2/KChIP1 trafficking, and that whilst such trafficking may require VAMP7, this pathway is not regulated by the longin domain of VAMP7 itself.

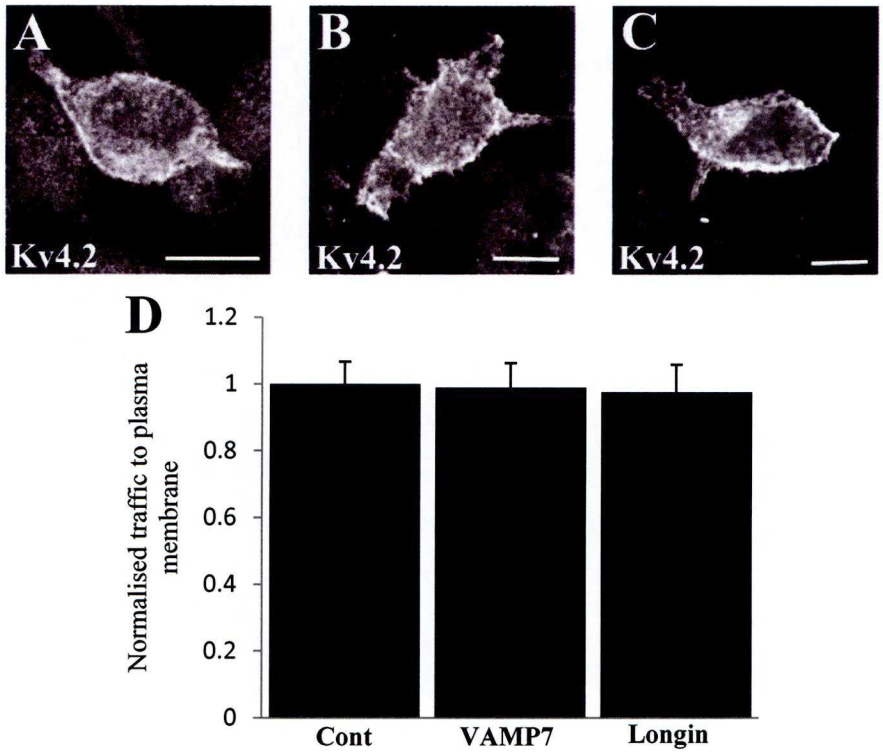

3.15: The longin domain of VAMP7 does not inhibit Kv4.2/KChIP1 trafficking to the plasma membrane.

HeLa cells were co-transfected with Kv4.2, detected with anti-Kv4.2 immunostaining, and a TRITC-conjugated secondary antibody. All cells were also transfected with KChIP1-EYFP.

A) Control cell

B) Cell co-transfected with VAMP7-GFP

C) Cell co-transfected with VAMP7 longin domain-GFP.

Scale bars represent 10μm.

D) Quantification of the normalised trafficking of Kv4.2 to the plasma membrane in the presence of KChIP1-EYFP alone (Cont), co-transfected with VAMP7-GFP (VAMP7), or co-transfected with GFP-tagged longin domain from VAMP7 (Longin). Data is shown as the means of 20 cells for each condition, ± S.E.M.

3.2.5 siRNA knockdown of VAMP7 or Vti1a inhibits trafficking of Kv4.2/KChIP1-EYFP

Work in section 3.2.4 highlighted the co-localisation between KChIP1-labelled punctae and the SNARE proteins VAMP7 and Vti1a. This suggested that these SNAREs might play a functional role in the non-conventional trafficking of Kv4.2 and KChIP1 to the plasma membrane. To investigate this, an RNA silencing approach was used to knock down the levels of various SNAREs, and look at the effects of this on trafficking.

Initially, HeLa cells were transfected with Kv4.2 and KChIP1-EYFP, and then fixed and immunostained with anti-Kv4.2. A control cell is shown in Figure 3.16A, with both channel and KChIP co-localised to the plasma membrane. As a further control, a silent RNAi construct was obtained, to rule out non-specific effects of RNAi (Figure 3.16B), and this also showed Kv4.2/KChIP1-EYFP trafficking to the plasma membrane. Three RNAi constructs were obtained against Vti1a, and three against VAMP7. In all cases, cells were left 72 hours post-transfection. A typical cell transfected with the first of these constructs against Vti1a is shown in Figure 3.16C, whilst a cell co-transfected with VAMP7 RNAi construct 1 is shown in Figure 3.16D. In both cases the channel and KChIP1 were intracellular, and in fact appeared to be in perinuclear punctate structures. The proportion of Kv4.2 present at the plasma membrane for cells from each condition was quantified, and normalised relative to control cells, for both Vti1a RNAi (Figure 3.16E) and VAMP7 RNAi (Figure 3.16F). In each case, the silent RNAi had no effect on Kv4.2 trafficking, whilst all three siRNAs against each SNARE significantly inhibited trafficking, often down to background levels. This supports a functional role for VAMP7 and Vti1a in Kv4.2/KChIP1 trafficking.

In addition, RNAi experiments were repeated in the mouse neuronal Neuro2A cell line. As can be seen from the cells in Figure 3.17A, Kv4.2 was present on the plasma membrane in the presence of KChIP1-EYFP, in both a control cell, and one treated with silent RNAi. One RNAi construct (construct 1) against Vti1a or

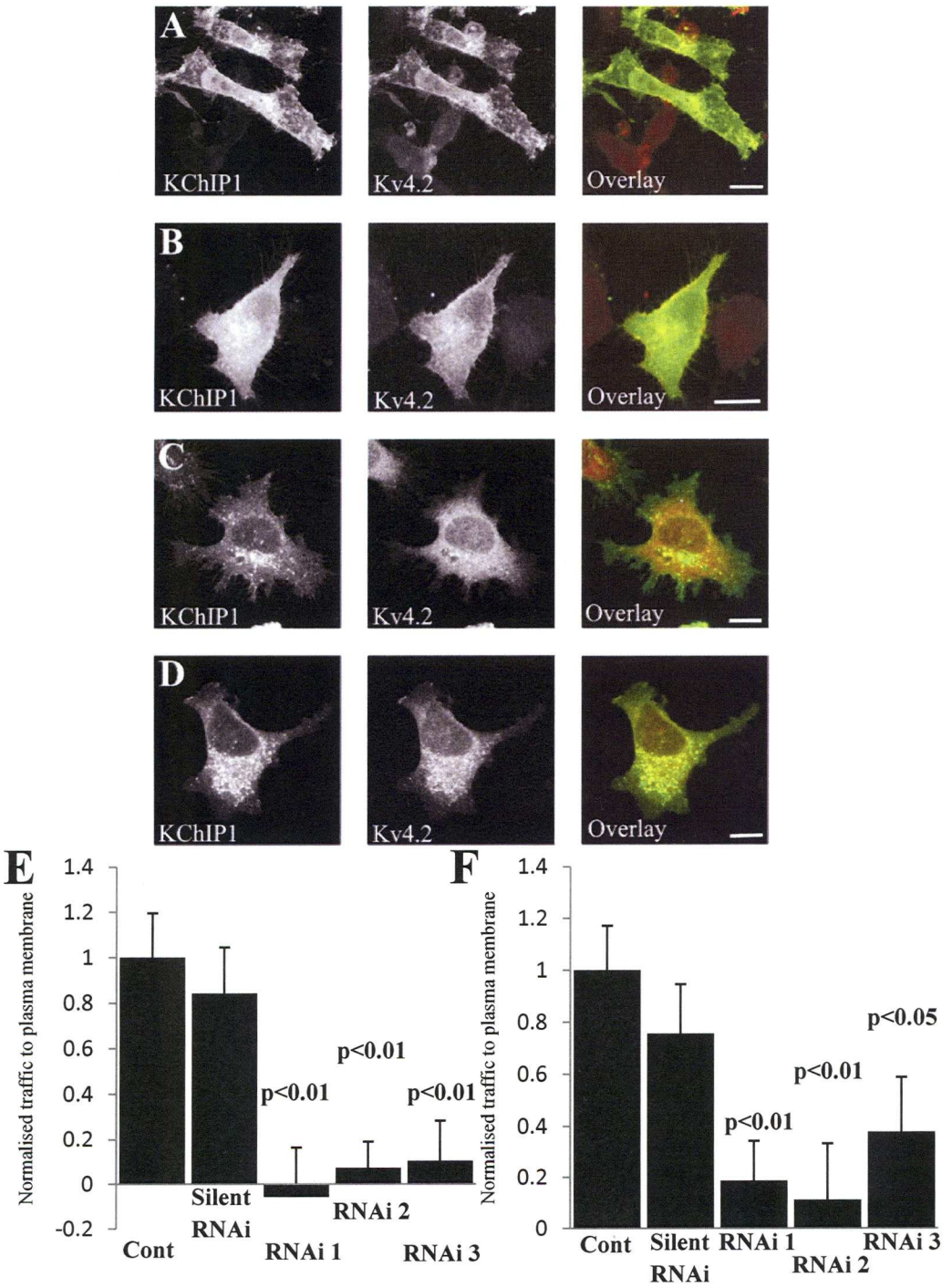

3.16: VAMP7 and Vti1a siRNA inhibits traffic of Kv4.2/KChIP1 to the plasma membrane in HeLa cells.

HeLa cells were co-transfected with to express KChIP1-EYFP (Green) and Kv4.2 (Red) and immunostained with anti-Kv4.2 and a TRITC-conjugated secondary so that localisation of KChIP1 and Kv4.2 could be visualised. Cells were left 72 hours post-transfection

A) Control cell, expressing KChIP1-EYFP and Kv4.2.

B) Cell co-transfected with a silent RNAi as a control.

C) Cell co-transfected with Vti1a RNAi 1.

D) Cell co-transfected with VAMP7 RNAi 1.

Co-localisation is shown as yellow in the colour overlays. Scale bars represent 10μm.

E) Normalised traffic of Kv4.2 in control cells, and cells transfected with either silent RNAi, or three different siRNAs against Vti1a, shown as means ± S.E.M for 20 cells.

F) Normalised traffic of Kv4.2 in control cells, and cells transfected with either silent RNAi, or three different siRNAs against VAMP7, shown as means ± S.E.M. for 25 cells.

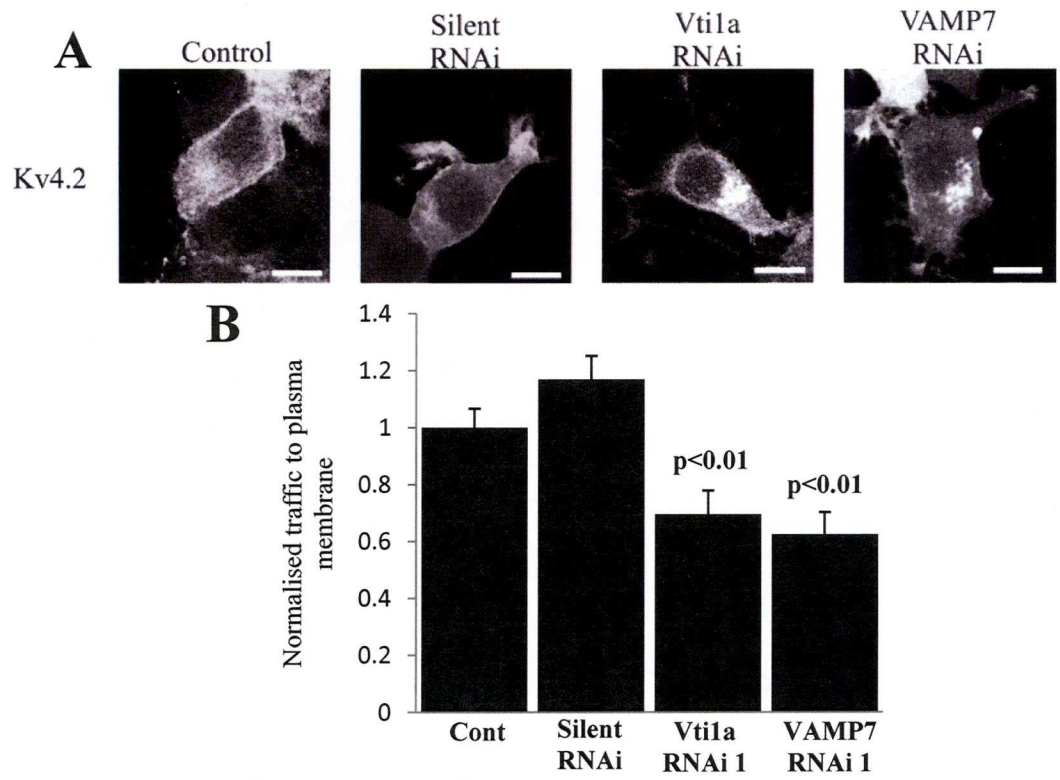

3.17: VAMP7 and Vti1a siRNA inhibit traffic of Kv4.2/KChIP1 to the plasma membrane in Neuro2A cells.

Neuro2A cells were transfected with Kv4.2 and KChIP1-EYFP in the absence or presence of RNAi, and channel trafficking was quantified 72 hours post-transfection.

A) Neuro2A cells were transfected to express Kv4.2 and immunostained with anti-Kv4.2, visualised with a TRITC-conjugated secondary antibody, in the presence of KChIP1-EYFP. A control cell is shown, as well as one co-transfected with silent RNAi, Vti1a RNAi 1, or VAMP7 RNAi1 as indicated. Scale bars represent 10μm.

B) Normalised traffic of Kv4.2 to the plasma membrane in the presence of KChIP1-EYFP was quantified for control (cont) cells, and for those co-transfected with siRNAs. Results are shown as the means of 30 cells for each condition, ± S.E.M. RNAi = RNA interference.

VAMP7 was picked for these studies. In general, the VAMP7 and Vti1a genes share 85 to 90% overall identity with the human equivalents. Of the 19 nucleotides targeted by the RNAi constructs, 16 nucleotides were identical between the mouse and human sequences for each RNAi used. Cells co-transfected with these showed an intracellular localisation for the Kv4.2 channel. The normalised proportion of Kv4.2 trafficked to the plasma membrane under each condition was quantified, as shown in Figure 3.17B. As in HeLa cells, the silent RNAi had no significant effect on channel trafficking, whilst RNAi knockdown of either Vti1a or VAMP7 significantly reduced the proportion of channel fluorescence at the plasma membrane. It should be noted that the effects of the RNAi in Neuro2A cells were quantitatively not as great as in HeLa cells, which could reflect cell-type specific differences in transfection efficiency, or in

the lifetime of Vti1a and VAMP7. Also, the lack of total conservation between the mouse and human sequences targeted by the RNAi would make it less likely to work in this cell type, and the activity of the RNAi in this cell type was not explicitly shown. However, the significant difference in trafficking in the presence of RNAi again points to a role for these SNAREs in this non-conventional trafficking route.

To confirm that the RNAi was knocking down levels of each SNARE as expected, and that this was not having adverse effects on the cell, a number of control experiments were performed. In all cases, experiments were performed with cells left for 72 hours post-transfection with RNAi. Firstly, HeLa cells were transfected with KChIP1, and immunostained for VAMP7 either in the absence (Figure 3.18A) or presence (Figure 3.18B) of VAMP7 RNAi construct 1. Images were obtained with identical microscope settings, and all images had their brightness and contrast adjusted equally. In the presence of RNAi the VAMP7 image appeared much fainter. However, the KChIP1 remained constant as expected, and the morphology and localisation of the KChIP1-labelled punctae was unaffected by the RNAi. Also, the low levels of remaining VAMP7 were still co-localised with KChIP1. The mean fluorescence of the anti-VAMP7 TRITC signal was calculated for both sets of cells and normalised to control cells (Figure 3.18C). This confirms the significant reduction in VAMP7 fluorescence due to RNAi. Also, real-time PCR was used to show a significant reduction in the relative level of VAMP7 mRNA in VAMP7 RNAi-treated cells compared to those treated with the silent RNAi construct (Figure 3.18D). Finally, HeLa cells were transfected with Kv4.2 pcDNA and KChIP1-EYFP either alone, or in the presence of VAMP7 or Vti1a RNAi. Cells were then lysed for Western blotting with an anti-Vti1a antibody (Figure 3.18E). This showed a lower level of Vti1a in cells treated with Vti1a-specific RNAi, whilst RNAi against VAMP7 had no effect on Vti1a levels, as expected. A blot for β-actin (Figure 3.18F) confirmed equal loading of protein in each lane. These results confirm the effective and specific nature of the RNAi used, and show that this RNAi is not disrupting the localisation of KChIP1 in cells.

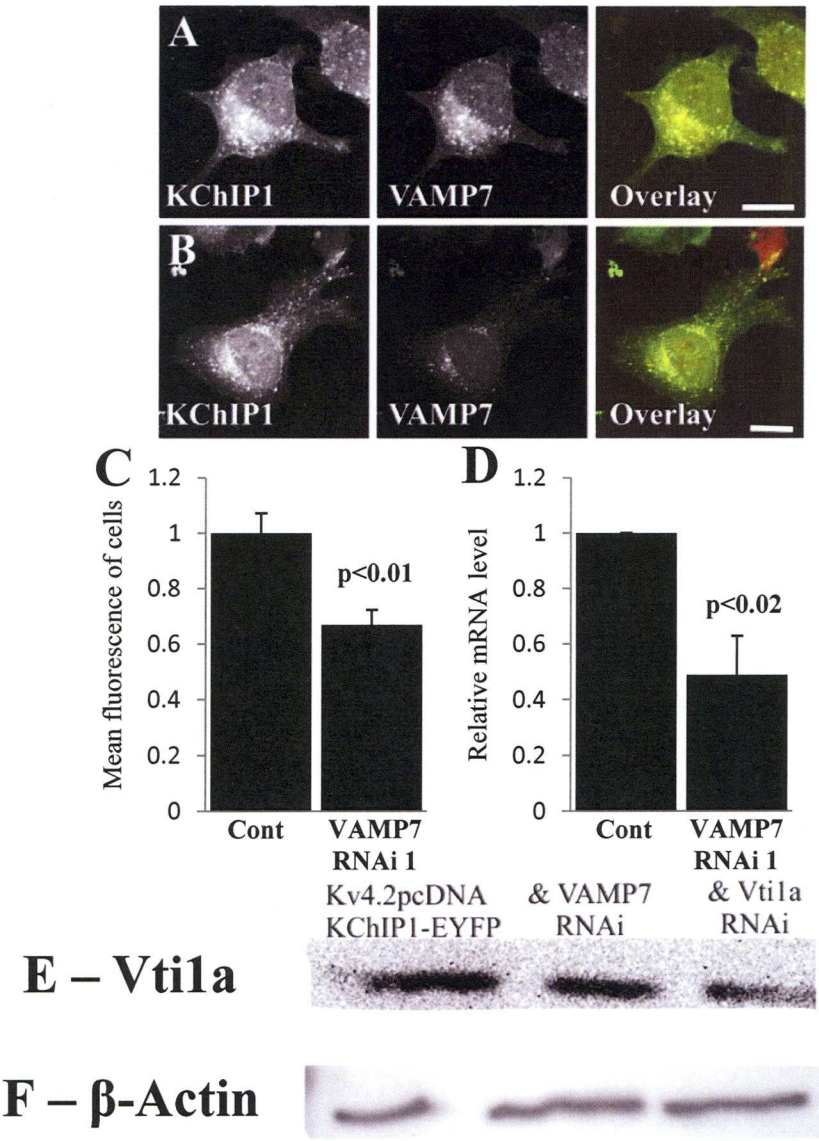

3.18: Confirming the specific effects of VAMP7 and Vti1a RNAi in HeLa cells.
The effect of RNAi against VAMP7 or Vti1a in HeLa cells was assessed by fluorescence measurements, real-time PCR and Western blotting.

- **A)** HeLa cell transfected with KChIP1-EYFP (Green), and immunostained with a mouse monoclonal antibody against VAMP7, visualised using a TRITC-conjugated secondary antibody (Red).
- **B)** HeLa cell transfected with KChIP1-EYFP (Green), and immunostained with a mouse monoclonal antibody against VAMP7, visualised using a TRITC-conjugated secondary antibody (Red), in the presence of VAMP7 RNAi construct 1. The VAMP7 signal appears fainter than in A. Microscope settings, brightness and contrast adjustments were identical for images in A) and B).

Co-localisation is shown as yellow in the colour overlays. Scale bars represent 10μm.

- **C)** Quantification of the mean anti-VAMP7 TRITC fluorescence of cells in the absence (Cont) or presence of VAMP7 RNAi construct 1. Data shown is the mean of 20 cells for each condition, ±S.E.M.
- **D)** Quantification of the relative mRNA levels of VAMP7 in HeLa cells transfected with silent or VAMP7 siRNA, as determined using real-time PCR.
- **E)** Western blot of Vti1a expression in HeLa cells transfected with Kv4.2 and KChIP1-EYFP alone, or in the presence of VAMP7 or Vti1a siRNA.
- **F)** Western blot of β-actin expression in HeLa cells transfected with Kv4.2 and KChIP1-EYFP alone, or in the presence of VAMP7 or Vti1a siRNA.

RNAi = RNA interference.

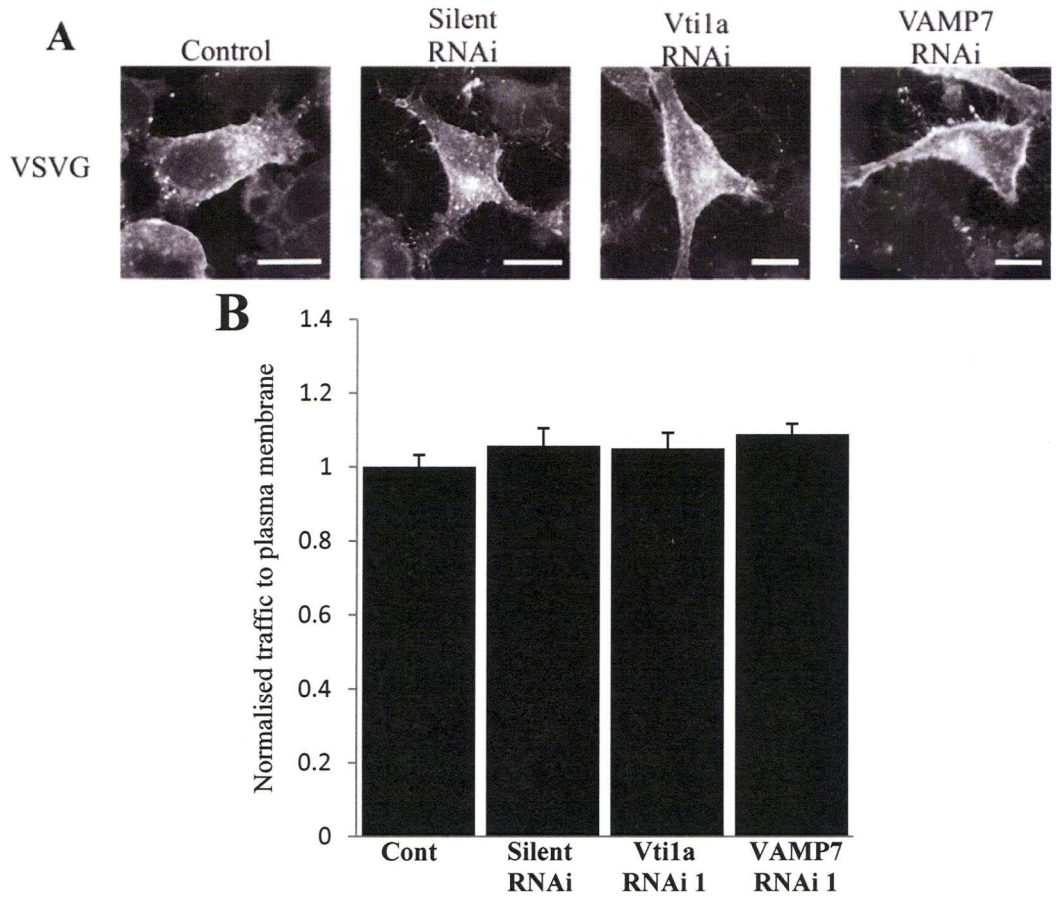

3.19: VSVG trafficking to the plasma membrane is unaffected by Vti1a or VAMP7 RNAi. HeLa cells were transfected with VSVG-GFP in the absence or presence of RNAi and channel trafficking was quantified 72 hours post-transfection.

A) HeLa cells were transfected to express VSVG-GFP and imaged. A control cell is shown, as well as cells co-transfected with silent RNAi, Vti1a RNAi 1, or VAMP7 RNAi 1, as indicated. Scale bars represent 10μm.

B) Normalised trafficking of VSVG-GFP to the plasma membrane was quantified for control (Cont) cells, and cells co-transfected with silent RNAi, Vti1a RNAi, or VAMP7RNAi 1.

Data shown is the mean of 20 cells for each condition, ± S.E.M. RNAi = RNA interference.

As a further control, the effects of Vti1a and VAMP7 RNAi on the trafficking of VSVG-GFP in HeLa cells were tested. The images in Figure 3.19A show HeLa cells fixed 72 hours after transfection with VSVG-GFP either alone (Control) or with silent, Vti1a or VAMP7 RNAi. In all cases, VSVG-GFP was localised to the plasma membrane. This showed that these siRNAs were not generally disrupting trafficking in cells. The proportion of VSVG-GFP at the plasma membrane was quantified for 20 cells from each condition, and normalised to control cells (Figure 3.19B). This confirmed that the trafficking of VSVG was unaffected by knockdown of VAMP7 or Vti1a, as would be expected, as VSVG is known to traffic via a SNARE complex containing Sec22 and membrin (Zhang et al. 1999; Xu et al. 2000).

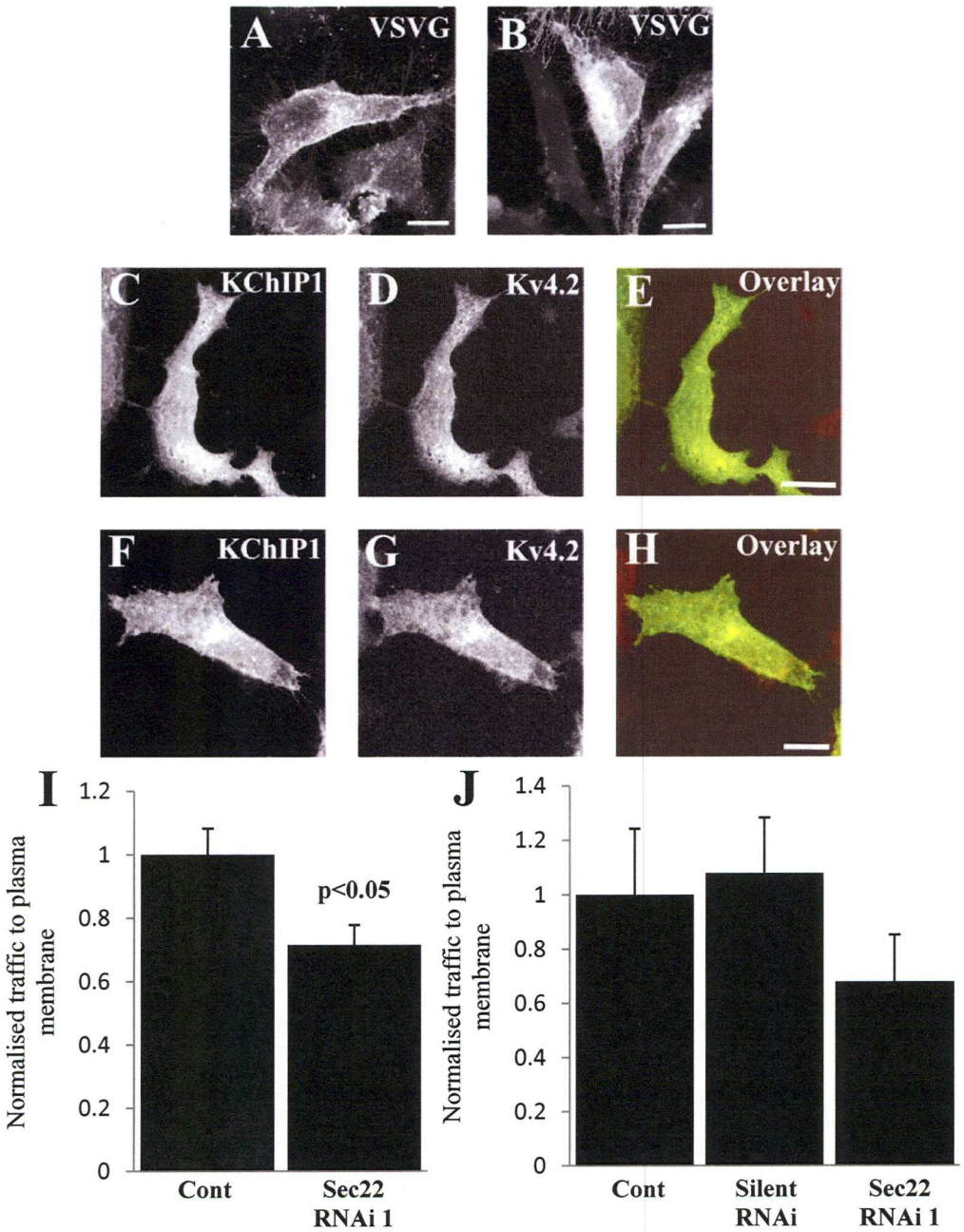

3.20: The effects of Sec22 RNAi on VSVG and Kv4.2/KChIP1 trafficking to the plasma membrane.

HeLa cells were transfected with VSVG-GFP or Kv4.2/KChIP1 in the absence or presence of Sec22 RNAi, and channel trafficking was quantified. Scale bars represent 10μm.

A) HeLa cell transfected VSVG-GFP, detected by confocal microscopy.

B) HeLa cell transfected with VSVG-GFP, in the presence of Sec22 RNAi construct 1.

C-E) HeLa cell transfected with KChIP1-EYFP (**C**, Green) and Kv4.2 (visualised using anti-Kv4.2 immunostaining, with a TRITC-conjugated secondary antibody, **D**, Red), and with co-localisation shown as yellow in the colour overlay (**E**).

F-H) HeLa cell transfected with KChIP1-EYFP (**F**, Green) and Kv4.2 (visualised using anti-Kv4.2 immunostaining, with a TRITC-conjugated secondary antibody, **G**, Red), and with co-localisation shown as yellow in the colour overlay (**H**), in the presence of Sec22 RNAi construct 1.

I) Normalised traffic of VSVG-GFP in the absence (Cont) or presence of Sec22 RNAi construct 1 was quantified. Data shown is the mean of 20 cells for each condition, ± S.E.M.

J) Normalised traffic of Kv4.2, with KChIP1-EYFP, in the absence (Cont) or presence of a silent RNAi construct or Sec22 RNAi construct 1 was quantified. Data shown is the mean of 20 cells for each condition, ± S.E.M. RNAi = RNA interference.

Whilst Sec22 is known to be important in VSVG-GFP trafficking (Xu et al. 2000), the above work suggests it does not play a role in Kv4.2/KChIP1 trafficking. To confirm this, Sec22 was knocked down by RNAi, and its effects on both VSVG-GFP and Kv4.2/KChIP1 were investigated 72 hours post-transfection. Initially, two RNAi constructs were tested, but one of these failed to have an effect on VSVG-GFP trafficking as expected and so was not considered further. In contrast, whilst VSVG-GFP was clearly at the plasma membrane in a control cell (Figure 3.20A), in a cell co-transfected with Sec22 RNAi construct 1 the majority of VSVG was intracellular, in the perinuclear region. The level of plasma membrane fluorescence was quantified and normalised (Figure 3.20I) revealing a significant inhibition of trafficking in the presence of Sec22 RNAi. A control cell transfected with KChIP1 and Kv4.2 (Figure 3.20C-E), showed their typical co-localisation at the plasma membrane, whilst a cell co-transfected with Sec22 RNAi (Figure 3.20F-H) also had both proteins localised at the plasma membrane. The proportion of Kv4.2 at the plasma membrane was quantified and normalised for control cells, and those transfected with either the silent RNAi construct, or Sec22 RNAi construct 1 (Figure 3.20J). Whilst the level of Kv4.2 at the plasma membrane appeared slightly lower in Sec22 RNAi-treated cells, this was not significant, confirming that VSVG-GFP and Kv4.2/KChIP1 are trafficking via different exocytic pathways, dependent on Sec22 and VAMP7/Vti1a respectively.

As a further control, the effect of knocking down GOS28 on VSVG and Kv4.2/KChIP1 trafficking was investigated using two RNAi constructs in HeLa cells. Again, experiments were performed with cells transfected for 72 hours. This SNARE has been implicated in ER-Golgi trafficking (Zhang and Hong 2001), but has not been shown to have a role in VSVG trafficking, and does not co-localise with KChIP1 (Figure 3.8C). As expected, VSVG-GFP was localised to the plasma membrane in both control cells (Figure 3.21A), and those transfected with either GOS28 RNAi construct 1 (Figure 3.21B) or 2 (Figure 3.21C). Quantification of this data (Figure 3.21M) revealed no significant difference on VSVG-GFP trafficking in the three conditions tested. In addition, Kv4.2 and KChIP1 were co-localised at the plasma membrane in control cells

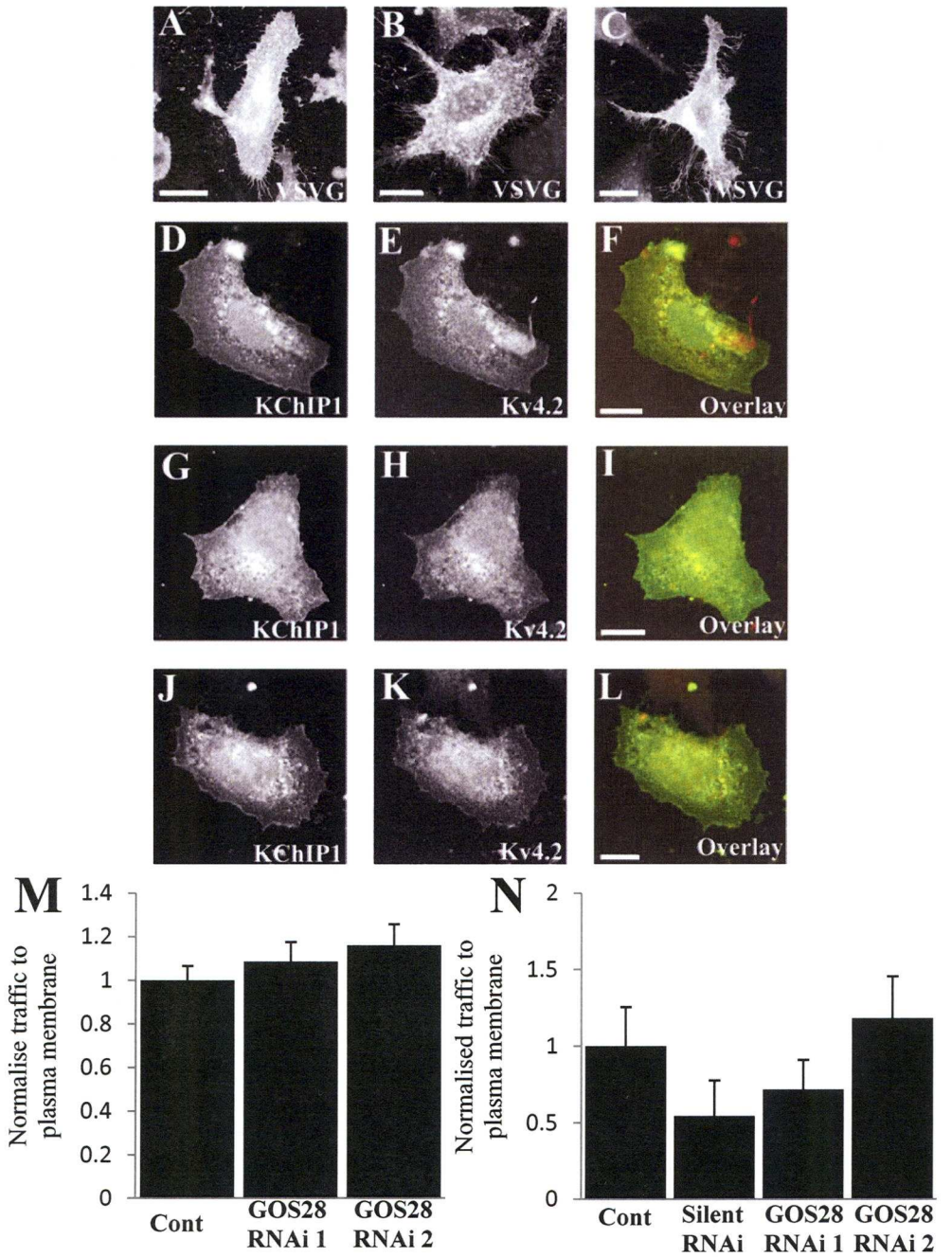

3.21: Effects of GOS28 RNAi on VSVG and Kv4.2/KChIP1 trafficking to the plasma membrane.

HeLa cells were transfected with VSVG-GFP or Kv4.2/KChIP1 in the absence or presence of GOS28 RNAi, and channel trafficking was quantified. Scale bars represent 10μm.

A-C) HeLa cells were transfected to express VSVG-GFP either alone (**A**), or in the presence of GOS28 RNAi construct 1 (**B**) or 2 (**C**).

HeLa cells were transfected to express KChIP1-EYFP (Green, **D**, **G**, **J**) and Kv4.2 (visualised using anti-Kv4.2 immunostaining with a TRITC-conjugated secondary antibody, Red, **E**, **H**, **K**), and co-localisation is shown as yellow in the colour overlays (**F**, **I**, **L**).

D-F) Control HeLa cell expressing KChIP1-EYFP and Kv4.2 only.

G-I) HeLa cell also expressing GOS28 RNAi construct 1.

J-L) HeLa cell also expressing GOS28 RNAi construct 2.

M) Normalised traffic of VSVG-GFP in the absence (Cont) or presence of GOS28 RNAi constructs 1 or 2 was quantified.

N) Normalised traffic of Kv4.2, with KChIP1-EYFP, in the absence (Cont) or presence of a silent RNAi construct or GOS28 RNAi constructs 1 or 2 was quantified.

Data shown is the mean of 30 cells for each condition, ± S.E.M. RNAi = RNA interference.

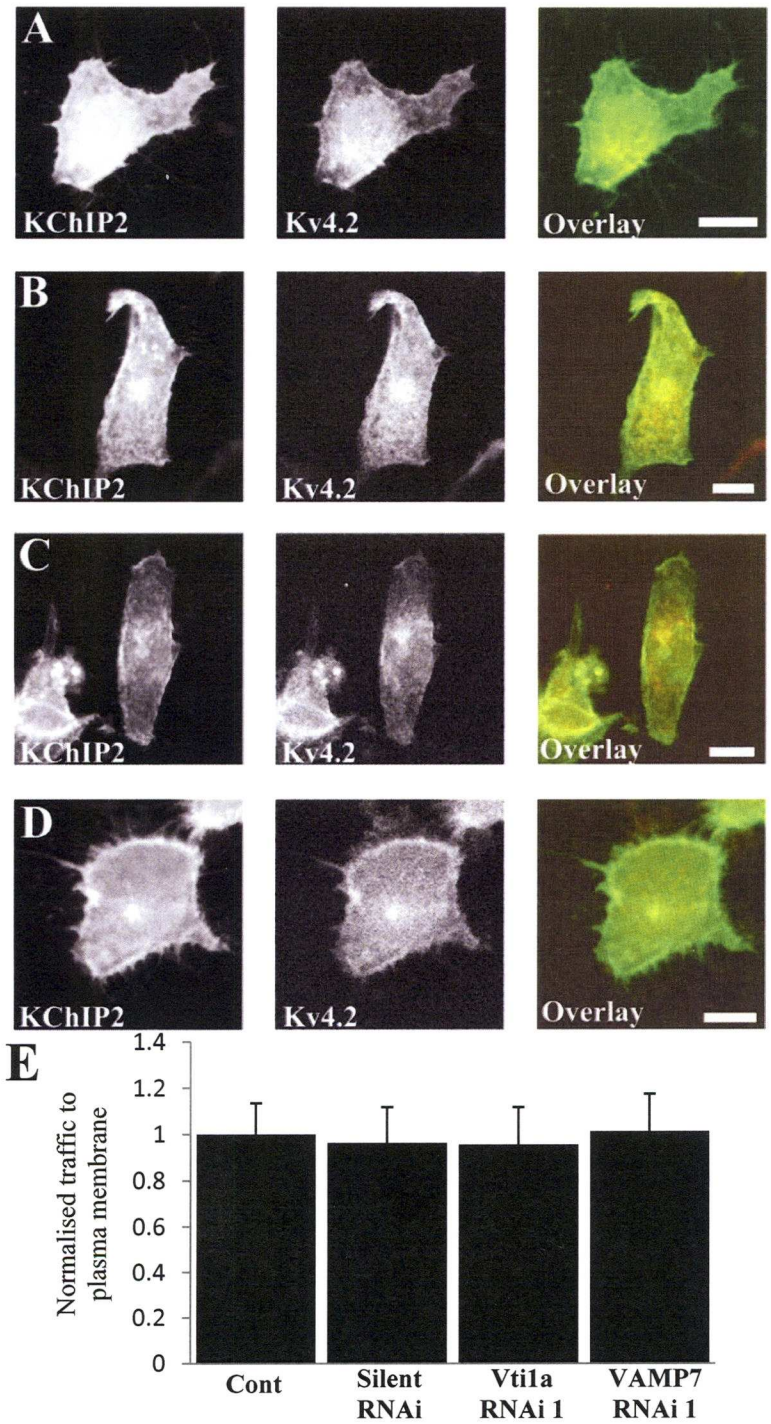

3.22: VAMP7 and Vti1a siRNA does not inhibit the traffic of Kv4.2/KChIP2 to the plasma membrane in HeLa cells.

HeLa cells were transfected with Kv4.2 and KChIP2-ECFP, and the effects of VAMP7 or Vti1a RNAi were observed and quantified.

A) HeLa cell co-transfected with KChIP2-ECFP and Kv4.2.

B) HeLa cell co-transfected with KChIP2-ECFP, Kv4.2 and a silent RNAi construct.

C) HeLa cell co-transfected with KChIP2-ECFP, Kv4.2 and Vti1a RNAi construct 1.

D) HeLa cell co-transfected with KChIP2-ECFP, Kv4.2 and VAMP7 RNAi construct 1.

Cells were visualised by confocal microscopy, with KChIP2-ECFP shown as green in the colour overlays. Kv4.2 was detected by anti-Kv4.2 immunostaining, with a TRITC-conjugated secondary antibody, and is shown as red in the colour overlay. Co-localisation is shown as yellow in the colour overlay. Scale bars represent 10μm.

E) Normalised trafficking of Kv4.2 in the presence of KChIP2 alone (Cont), or with silent RNAi, or with Vti1a RNAi construct 1 or VAMP7 RNAi construct 1. Data shown is the mean of 30 cells for each condition, ± S.E.M. RNAi = RNA interference.

(Figures 3.21D-F), and those co-transfected with either GOS28 RNAi construct 1 (Figures 3.21G-I) or 2 (Figures 3.21 J-L). Quantification of the proportion of anti-Kv4.2 TRITC fluorescence at the plasma membrane (Figure 3.21N) confirmed that whilst there were some differences between cells from the different conditions tested, these were not significant. This supports the idea that neither VSVG nor Kv4.2/KChIP1 requires a GOS28-containing SNARE complex for their trafficking to the plasma membrane.

Having shown that KChIP1 and Kv4.2 were trafficking via a non-conventional, VAMP7 and Vti1a-dependent pathway different from that used by VSVG-GFP, it was interesting to ask if all stimulated traffic of Kv4.2 channels was via this pathway. Other members of the KChIP family are also able to traffic Kv4 potassium channels to the plasma membrane (An et al. 2000). However, only KChIP1 is myristoylated and shows localisation to intracellular vesicles (O'Callaghan et al. 2003), whilst KChIP2 is palmitoylated and localised to the plasma membrane when expressed alone (Takimoto et al. 2002; Venn et al. 2008). It was therefore not clear if the stimulation of Kv4 trafficking by these KChIPs would occur via the same non-conventional pathway, or whether interaction with the channel would occur in distinct cellular compartments. This was investigated by co-transfecting HeLa cells with Kv4.2, KChIP2-ECFP and either VAMP7 or Vti1a RNAi. Cells were left for 72 hours post-transfection before fixation. In a control cell (Figure 3.22A), both KChIP2-ECFP and Kv4.2 were co-localised at the plasma membrane, highlighting the ability of KChIP2 to promote channel trafficking. Co-transfection with silent RNAi (Figure 3.22B) had no effect. However, both the channel and KChIP2 were also co-localised to the plasma membrane in cells co-transfected with either Vti1a RNAi (Figure 3.22C) or VAMP7 RNAi (Figure 3.22D). The normalised trafficking of Kv4.2 was quantified for 20 cells from each condition, as shown in Figure 3.22E. This confirms that there was no change in the plasma membrane localisation of Kv4.2 in response to RNAi when co-transfected with KChIP2. This again confirms that these siRNA are not disrupting general trafficking pathways. It also suggests that distinct pathways are utilised by KChIPs 1 and 2 to traffic Kv4 potassium channels to the plasma membrane.

3.3 Discussion

The functional kinetics of ion channels, and their trafficking to the plasma membrane, are key aspects where regulatory proteins can exert their effects. Many previous papers have studied a range of regulatory proteins associated with the Kv4 family of voltage-gated potassium channels (Birnbaum et al. 2004), perhaps the best characterised of which are the KChIPs. In continuing this work, it was important to first confirm that previous findings could be replicated. As expected, KChIP1 showed a typical punctate distribution, both in previously studied HeLa cells, and an alternative neuronal cell type, Neuro2A cells. KChIP1 was also able to increase trafficking of Kv4.2 to the plasma membrane, in line with previous findings (Hasdemir et al. 2005). Previous work, however, left several unanswered questions.

Firstly, there has been some debate about the localisation of Kv4.2 when expressed alone in cells. Many transmembrane proteins are retained in the ER until association with an escort or accessory protein masks their ER retention signal to allow onward exocytic trafficking (Misonou and Trimmer. 2004). KChIP1 was initially proposed to act in this way, as an accessory protein to Kv4.2 to allow its ER exit (Bahring et al. 2001). The localisation of Kv4.2 is clearly perinuclear in all cell types tested, and Shibata et al. (2003) claimed co-localisation between Kv4.2 and the ER marker calnexin. However, other papers have shown that Kv4.2 co-localises not with calnexin, but with markers of the Golgi, including the *cis*-Golgi protein β-COP and the trans-Golgi network protein γ-adaptin (O'Callaghan et al. 2003; Hasdemir et al. 2005). The work presented in Figures 3.1 and 3.2 argues in favour of Kv4.2 being localised to the Golgi, showing co-localisation with Golgi-localised EYFP, and the Golgi resident protein ARF1. This would be in keeping with the finding that the proposed RXR ER retention motif in Kv4.2 is non-functional (Shibata et al. 2003). It remains unclear how this localisation is achieved or maintained by Kv4.2. It suggests, however, that interaction between Kv4.2 and the KChIPs, allowing the channel's onward traffic to the plasma membrane, occurs at or before the Golgi.

Another question raised by previous work centred on the Ca^{2+}-binding EF-hand domains of the KChIPs. One possibility is that these domains act as calcium sensors in the protein, and the binding of Ca^{2+} ions alters the conformation of the KChIP, allowing it to bind to target proteins and mediate an effect. However, it could be that these domains are simply required for the structural integrity of the protein. When the KChIPs were originally discovered (An et al. 2000), it was shown that mutant KChIP1EF2-4 did not bind radioactive Ca^{2+}, and could not modulate channel kinetics or increase current density. However, this triple EF-hand mutant was able to co-localise with Kv4, and was efficiently co-immunoprecipitated with Kv4 α-subunits. Also, it was shown by confocal microscopy that whilst KChIP1EF2-4 could not traffic Kv4.2 to the plasma membrane, the channel changed from a perinuclear localisation to be co-localised with KChIP1EF2-4 punctae (Hasdemir et al. 2005). This argues that trafficking of the channel is Ca^{2+}-dependent, whilst interaction between the channel and KChIP is not. In further support of this, experiments have been performed with KChIP2d, an isoform with only one EF-hand domain. When this domain was mutated, the usual slowing of Kv4.3 inactivation caused by the KChIP was abolished. However, the KChIP retained its ability to accelerate the channel's recovery from inactivation (Patel et al. 2002b). This suggests that the KChIP-Kv4 interaction has both Ca^{2+}-dependent and independent functions (Patel et al. 2004). More recently, however, Pioletti et al. (2006) created combinations of mutations in EF-hands 2, 3 and 4 of KChIP1. Whilst the single mutants, and EF2EF3 or EF2EF4 mutants showed normal binding to the N-terminus of Kv4.3, the EF3EF4 double and EF2-4 triple mutant had impaired binding. It was argued that this was due to the proteins unfolding in the absence of Ca^{2+}. It was also shown that these mutants, but not the less severe single and double mutants, were unable to affect the properties of the full-length protein. However, the interaction between these mutants and the full-length protein was not assessed.

The data shown in Figures 3.5 and 3.6 confirm that KChIP1EF2-4 is unable to traffic Kv4.2 to the plasma membrane as effectively as wild-type KChIP1, but also show that the single EF3 mutant has this same effect. Expressing the triple

mutant with VSVG-GFP had no effect on its trafficking, confirming that KChIP1EF2-4-EYFP is not disrupting general trafficking pathways. However, these data also reveal that both the single and triple mutants are punctate like wild-type KChIP1, and when co-expressed with Kv4.2, cause the channel to become punctate in its localisation. This suggests that being unable to bind Ca^{2+} does not prevent the mutant KChIPs from accessing the same cellular compartments as the wild-type protein, and a Western blot confirms that expression of these mutants is not impaired (Figure 3.5C). The redistribution of the channel away from its usual perinuclear Golgi localisation, to a KChIP1-like punctate distribution, also suggests that the mutants are still able to bind the channel, leading to this change in localisation. Finally, in Figures 3.11 and 3.12, it was shown that the vesicles accessed by the EF-hand mutants of KChIP1 are co-localised with the same SNARE proteins as wild-type KChIP1 vesicles.

Overall, these data, combined with previous literature in the field, would argue that whilst mutations in the Ca^{2+}-binding EF-hands of KChIP1 prevent it from trafficking Kv4.2 to the plasma membrane, they do not impair the interaction of the channel and KChIP. The differences seen in Pioletti et al. (2006) could be due to the interaction studies being performed with only a truncated N-terminal portion of the Kv4.3 α-subunit. In fact, it has been shown that the C-terminal of the Kv4.2 channel is also important for interactions with KChIPs (Callsen et al. 2005; Han et al. 2006), which could explain why binding studies with only the N-terminus of the channel were unsuccessful.

It has been shown that Kv4.2/KChIP1 trafficking is different to that of VSVG-GFP because of their differing requirement for COPII (Hasdemir et al. 2005), and the work with EF-hand mutants also differentiates between these pathways. However, the requirement of Kv4.2/KChIP1 for COPI shows there is some overlap with VSVG-GFP traffic, and this was also the case with the requirement for Rab1 (Figure 3.7). Rab1 is known to be critical for general ER-Golgi trafficking, shown by using dominant negative mutants (Tisdale et al. 1992), and altering active Rab1 levels by using its Rab-GAP perturbs the Golgi and ERGIC

(Haas et al. 2007). However, several proteins are known to be able to traffic through the cell in a Rab1-independent manner, including CFTR (Yoo et al. 2002) and the α_{2B}-adrenergic receptor (Wu et al. 2003). Expression of the ER-resident GAP TBC1D20 allowed the specific inhibition of Rab1 (Haas et al. 2007), and this was able to block both VSVG-GFP and Kv4.2/KChIP1 trafficking to the plasma membrane (Figure 3.7). If further Rab-GAPs can be characterised, then the specificity of this approach makes it an ideal way of investigating the role of Rabs elsewhere in cellular trafficking, and could shed light on the post-Golgi trafficking of Kv4.2. It also suggests that Kv4.2/KChIP1 may utilise the conventional, COPI-dependent pathway from ERGIC to *cis*-Golgi, and that this might be the ER-Golgi step requiring active Rab1.

The major finding from this work is that KChIP1 is co-localised in vesicles with the two SNAREs VAMP7 and Vti1a, further differentiating this pathway from that used by VSVG-GFP. Antibodies against Sec22b inhibit the ER-Golgi trafficking of VSVG-GFP (Zhang et al. 1999), and Sec22 is enriched at ER-exit sites and on COPII-coated vesicles (Chao et al. 1999), where it forms a complex with membrin, syntaxin 5 and rBet1 (Xu et al. 2000). There was no co-localisation between KChIP1-EYFP and antibodies against either Sec22b or membrin (Figure 3.8), and whilst RNAi knockdown of Sec22 inhibited VSVG-GFP trafficking, it had no significant effect on KChIP1/Kv4.2 (Figure 3.20). This confirms that these trafficking pathways differ not only in their COP coat requirements, but in their SNARE proteins as well.

Two alternative SNARE complexes found in the literature were also assessed. One, containing Ykt6, GOS28, syntaxin 5 and rBet1, has been argued to be localised to the *cis*-Golgi (Zhang and Hong 2001). This was also of interest as the longin domain of Ykt6 has been shown to direct it into punctate structures in neuronal-like PC12 cells (Hasegwa et al. 2004). However, there was no co-localisation between KChIP1-EYFP and antibodies against GOS28 or Ykt6 (Figure 3.8), and in non-neuronal HeLa cells, Ykt6 was clearly perinuclear rather than punctate. Also, RNAi against GOS28 had no significant effect on either

VSVG-GFP or KChIP1/Kv4.2 trafficking, which would argue that this SNARE is not a significant regulator of either of the trafficking pathways investigated.

In contrast to the above, there was clear co-localisation between KChIP1 and antibodies against endogenous VAMP7 and Vti1a (Figures 3.9-3.13) in a variety of cell types, for both wild-type and mutant KChIP1, and between over-expressed VAMP7 and KChIP1 as well (Figure 3.12). Knockdown of these proteins using RNAi revealed that they also had a functional role in Kv4.2/KChIP1 trafficking, but not in VSVG-GFP trafficking (Figures 3.16, 3.17, 3.19). This was a surprising result, as the role of VAMP7 and Vti1a in ER-Golgi trafficking had only been shown for PCTV trafficking in the intestine (Siddiqi et al. 2006a; Siddiqi et al. 2006b). These papers showed VAMP7 was in the ER of the intestine, but not of the kidney or liver, and hence argued that this VAMP7-dependent pathway was intestine-specific. However, three different cell types were investigated in this thesis, and the same co-localisation between KChIP1 and VAMP7/Vti1a was seen in all. In addition, VAMP7 is more commonly associated with the endosomal/lysosomal pathway, as VAMP7 has been shown to co-localise with lysosomal markers lgp120 (Advani et al. 1998) and LAMP1 (Advani et al. 1999), to be enriched in secretory lysosomes (Casey et al. 2007), and to form a complex with Vti1a, syntaxin 7 and syntaxin 8 on *Dictyostelium* endosomes (Bogdanovic et al. 2002). However, whilst there was clear co-localisation between KChIP1 and VAMP7/Vti1a, there were clearly distinct populations of KChIP1-EYFP vesicles and those labelled with either syntaxin 7 or 8. In addition, whilst some endogenous VAMP7 co-localised with LAMP1, much of the staining was separate (Figure 3.14). Combined with previous work showing that KChIP1 does not co-localise with Rab proteins associated with the endosomal pathway (O'Callaghan et al. 2003), it therefore seems unlikely that the punctate KChIP1 structures are endosomal in origin, and more likely that VAMP7 and Vti1a are also regulating an ER-Golgi trafficking pathway in cells. In support of this, one isoform of Vti1a has been shown to be perinuclear in localisation in neuronal cells (Antonin et al. 2000), and VAMP7 has been found in punctate and tubulovesicular structures around the cell body and in proximal dendrites of neurons, which were not ER, Golgi or lysosomal in origin (Coco et

al. 1999). Also, in HeLa cells, it has been claimed that only over-expressed VAMP7 co-localised with LAMP1, whilst endogenous protein did not, although these data were not presented in the paper (Coco et al. 1999). Finally, a proteomic map of the secretory pathway found Vti1a in the smooth ER, Golgi and COPI-coated vesicles, and VAMP7 in COPI-coated vesicles also (Gilchrist et al. 2006). Together, this data argues that VAMP7 and Vti1a are regulating a non-conventional, Rab1- and COPI-dependent ER-Golgi trafficking pathway for Kv4.2/KChIP1.

Two further points of interest were raised by this characterisation of a novel intracellular pathway. Firstly, VAMP7 belongs to the VAMP/synaptobrevin family of SNAREs, which share a C-terminal coiled-coil SNARE domain, but differ in having either a short (brevin) or long (longin) N-terminal domain. The ~150 amino acid longin domain of VAMP7 has been shown to inhibit SNARE complex formation (Martinez-Arca et al. 2003), and inhibit the outgrowth and morphogenesis of neuronal neurites (Wang and Tang 2006). However, over-expression of just the GFP-tagged longin domain, or over-expression of full-length VAMP7-GFP had no effect on Kv4.2/KChIP1 trafficking (Figure 3.15). This suggests that the longin domain of VAMP7 does not play a regulatory role in this pathway.

Secondly, having shown that this non-conventional pathway is not confined to PCTVs in the intestine, but is also active in neuronal cells expressing Kv4.2 and KChIP1, it was interesting to ask whether other KChIP proteins stimulate Kv4.2 traffic via this route. KChIP2 was an obvious protein to investigate, as it has many similarities to KChIP1, being able to interact with Kv4 channels and traffic them to the plasma membrane (Shibata et al. 2003; Venn et al. 2008), and so could be investigated with the same assays. However, whilst KChIP1 expressed alone is found on punctate vesicular structures (Figure 3.2) due to its myristoylation (O'Callaghan et al. 2003), KChIP2 is palmitoylated and found on the plasma membrane of COS-7 cells (Shibata et al. 2003) and Neuro2A cells (Figure 3.2). It was therefore possible that KChIP2 could traffic Kv4.2 to the

plasma membrane using the same pathway as KChIP1, or that interaction with the channel might occur in a distinct intracellular compartment. The knockdown of VAMP7 or Vti1a by RNAi, which had inhibited Kv4.2 trafficking with KChIP1, had no effect on the channel reaching the plasma membrane in the presence of KChIP2 (Figure 3.22). This suggests that the KChIPs and Kv4 channels are interacting in different compartments of the exocytic pathway, due to their differing intrinsic localisations. One possibility is that KChIP1, localised to punctate trafficking vesicles, interacts with the channel at this pre-Golgi stage, whilst KChIP2 interacts with the channel at the level of the Golgi, where the channel accumulates when expressed alone, and where KChIP2 is post-translationally modified by palmitoyltransferases (Greaves et al. 2008). Interestingly, KChIP2 is most highly expressed in the heart (Pruunsild and Timmusk 2005) and is the predominant KChIP for regulating Kv4 channel cardiac transient outward current (I_{to}) (Kuo et al. 2001), whilst VAMP7 seems not to be found in the heart (Advani et al. 1998). There could, therefore, be tissue-specific differences in trafficking pathways, as well as differences due to cellular compartmentalisation.

In conclusion, KChIP1-EYFP traffics Kv4.2 to the plasma membrane of cells via a non-conventional, VAMP7- and Vti1a-dependent pathway, which is different from that used in the constitutive secretion of the well-characterised marker protein VSVG-GFP. This trafficking, but not the interaction of the KChIP and channel, can be disrupted by mutation of just one of the Ca^{2+}-binding EF-hand domains of KChIP1, or by reducing the levels of active Rab1 in the cell. There is neither full co-localisation between KChIP1 and the endosomal/lysosomal SNAREs syntaxins 7 and 8, nor between VAMP7 and LAMP1 in HeLa cells. Finally, this KChIP1 pathway is distinct from that used by the related protein KChIP2 to traffic Kv4.2 to the plasma membrane.

Chapter 4

Investigating potential interactions between Kv4.2, KChIP1 and scaffolding proteins

4.1 Introduction

The trafficking of Kv4 channels to the plasma membrane, or their retention within the cell, is one of the key ways a neuron can control the size of the functional plasma membrane pool of the rapidly-inactivating, A-type currents (An et al. 2000; Tkatch et al. 2000). The KChIPs, discussed in Chapter 3, are important regulators of this trafficking. However, there are many other proteins described as affecting Kv4.2 trafficking in the literature (Maffie and Rudy 2008). The physiological significance of these is not clear (Deschenes and Tomaselli 2002). Also, little work has been carried out on potential ternary complexes of Kv4.2, KChIP1 and these alternative accessory proteins. The aim of this section of the thesis was to investigate two families of scaffolding proteins – the 14-3-3 proteins and the PSD-95 family of MAGUK proteins – that may interact with Kv4.2 or KChIP1 to influence their trafficking and clustering at the plasma membrane.

The KChIPs have a major role in regulating Kv4 channels (An et al. 2000; Misonou and Trimmer 2004), but may also have several other roles in cells, including regulating transcription of some genes (Spreafico et al. 2001), and interacting with the presenilin proteins implicated in Alzheimer's disease (Buxbaum et al. 1998). Discovering new interacting partners of the KChIPs could thus shed light on how they achieve these different functions *in vivo*, or even reveal possible new roles. A yeast two-hybrid screen was therefore performed in the lab by Dr Lee Haynes, using full-length KChIP1 and a library of mouse foetal brain cDNA. One interesting, and repeated, hit from this study was with 14-3-3γ (Dr L. Haynes, personal communication). This was of interest as the 14-3-3 family of proteins have known roles in ion channel trafficking (O'Kelly et al. 2002; Trombetta and Parodi 2003), making them credible binding partners of the KChIPs, which also have such a function.

The 14-3-3 family of proteins are known for their ability to bind to phosphorylated target proteins. The 14-3-3 proteins are dimers, and act as scaffolding proteins, bringing two target proteins together or masking signalling sequences within proteins (Shikano et al. 2006). This is important for the trafficking of many ion channels, including various forms of potassium channel

(O'Kelly et al. 2002; Trombetta and Parodi 2003). There is as yet no record of an interaction between 14-3-3 proteins and Kv4 channels in the literature. The yeast two-hybrid interaction with KChIP1 thus suggested that regulation of Kv4.2 could occur through the KChIP, as has been documented for several other Kv4 regulators (Holmqvist et al. 2001; Bowlby et al. 2005). The KChIPs can be phosphorylated (Ruiz-Gomez et al. 2007), but do not have a consensus Mode I or II binding site for 14-3-3 proteins. They would thus require non-consensus binding, as has been reported for other proteins in *in vitro* studies (Tzivion and Avruch 2001). A first aim was therefore to confirm whether the yeast two-hybrid interaction could be replicated by alternative methods. To do this, antibodies against 14-3-3γ were used to look for co-localisation of the protein with KChIP1 in transfected cells. Subsequently, pull-down experiments were performed with GST-tagged KChIP1 against bovine brain cytosol, to look for interactions of KChIP1 with 14-3-3γ and β.

Another interesting group of proteins are the PSD-95 family of MAGUKs, and especially SAP97. These proteins are best known for their role in trafficking and clustering neurotransmitter receptors on the plasma membrane of post-synaptic densities (Kim and Sheng 2004; Bats et al. 2007; Jeyifous et al. 2009). Having several protein interaction motifs means they can cluster together a number of related proteins, for example members of a signalling pathway, or bring proteins into association with the cytoskeleton to ensure their intracellular position (Feng and Zhang 2009).

Both SAP97 and PSD-95 have been shown to interact with Kv4 channels, and promote their trafficking to, and clustering at, the plasma membrane (Gardoni et al. 2007; El-Haou et al. 2009). A potential role for the related protein PSD-93 has not been investigated, however. Also, the Kv4 channels are most likely associated with a KChIP *in vivo*, and studies have not looked at the effects of having both KChIPs and SAP97 interacting with the channel. There were several strands to this investigation, all based on expressing Kv4.2 in cells with KChIP1, a PSD-95 family protein or both, and quantifying levels of trafficking to the plasma membrane. Firstly, the effects of SAP97 alone on Kv4.2 were compared to its effects in the presence of KChIP1. Secondly, similar experiments were

performed with three isoforms of PSD-93, to see if this protein could promote channel trafficking, and to investigate any isoform specific effects. Finally, possible interactions between SAP97 and KChIP1 were investigated. This work potentially reveals a novel interaction between SAP97 and KChIP1 that may affect the distribution of Kv4 channels in cells.

4.2 Results

4.2.1 14-3-3 proteins as potential interacting partners of KChIP1

The KChIP proteins have many potential intracellular roles (Buxbaum et al. 1998; An et al. 2000; Spreafico et al. 2001), and identifying their interacting partners is important for understanding these functions. To try and identify novel binding partners, a yeast two-hybrid screen was performed by Dr Lee Haynes, using KChIP1 and a mouse foetal brain cDNA library. This identified 14-3-3γ as a potential binding partner. This was of interest because several hits gave the same protein, and the gamma isoform was the only one detected (Dr L. Haynes, personal communication). Also, the 14-3-3 proteins are known to play important roles in ion channel trafficking (O'Kelly et al. 2002; Rajan et al. 2002; Berg et al. 2003), and so could be linked to KChIP1's role in the trafficking of Kv4 channels. Experiments were therefore performed to try and confirm this interaction.

Firstly, the localisation of 14-3-3γ in cells was compared to KChIP1. HeLa cells were transfected with KChIP1-EYFP, and after fixation, these cells were immunostained with an antibody against endogenous 14-3-3γ. Two typical cells are shown in Figure 4.1. KChIP1-EYFP showed its usual punctate distribution.

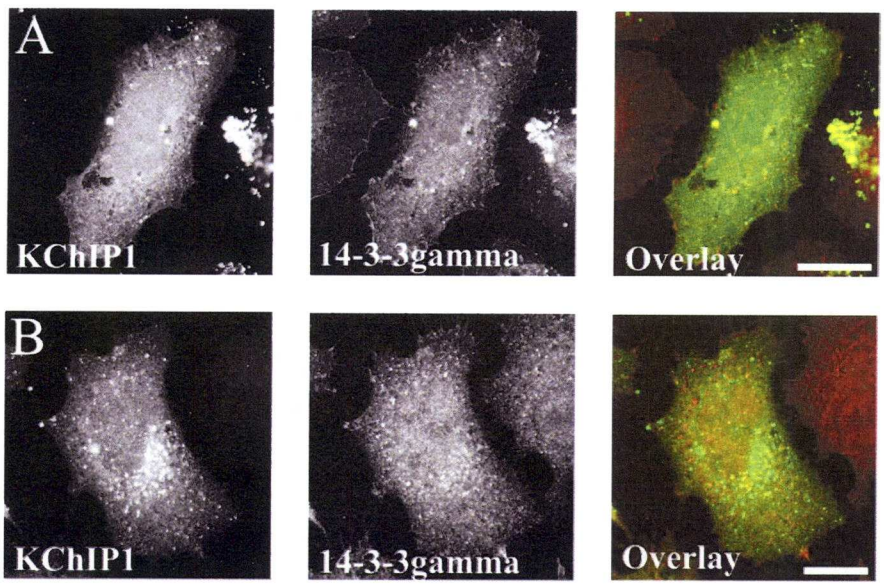

4.1: Co-localisation between KChIP1-EYFP and 14-3-3γ in HeLa cells.
HeLa cells were transfected with KChIP1-EYFP and immunostained for 14-3-3γ.
A) and **B)** show two separate HeLa cells.
In all cells, endogenous 14-3-3γ protein was detected by immunostaining with anti-14-3-3γ antibodies and a TRITC-conjugated secondary. KChIP1-EYFP is shown as green, 14-3-3γ immunostaining in red, and co-localisation in yellow in the colour overlays. The scale bars represent 10μm.

The 14-3-3γ was present at regions of the plasma membrane. However, it also showed a punctate distribution within cells that at least partially co-localised with KChIP1-EYFP (as shown by yellow in the colour overlay) in some punctate structures. This data is therefore supportive of a potential interaction between KChIP1 and 14-3-3γ.

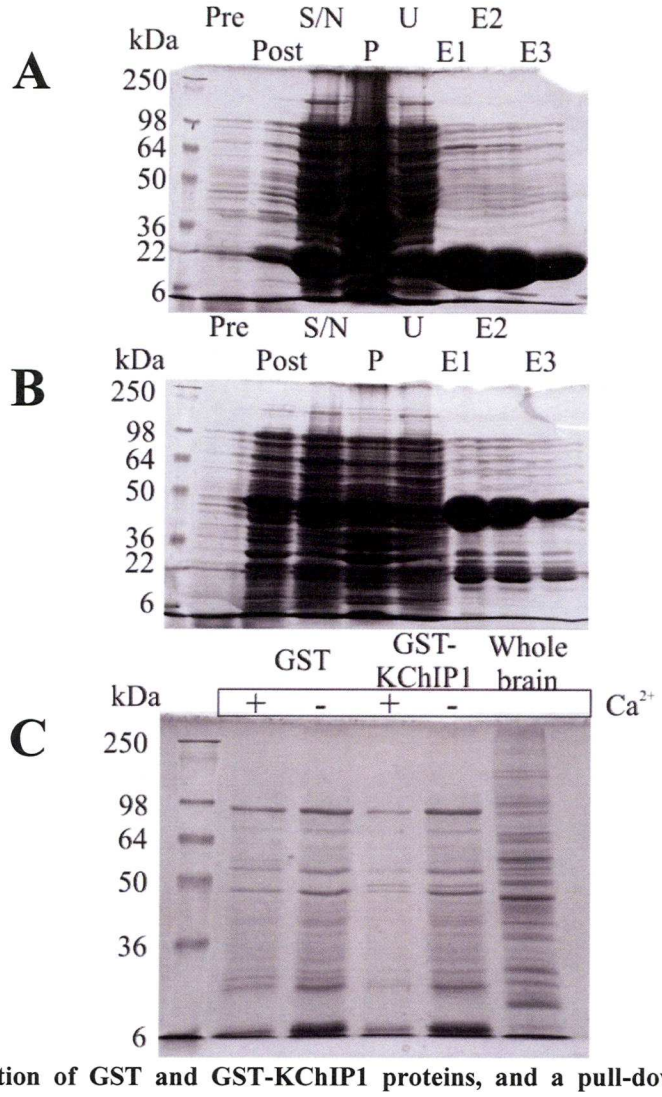

4.2: Production of GST and GST-KChIP1 proteins, and a pull-down assay with these proteins against bovine whole brain lysate.

GST-KChIP1 and GST proteins were produced, and used in a pull-down assay against bovine whole brain lysate in the presence and absence of Ca^{2+}.

A) Production of GST protein, with an expected molecular weight of ~26kDa.

B) Production of GST-KChIP1 protein, with an expected molecular weight of ~51kDa.

kDa = molecular weight markers in kiloDaltons. Pre = pre-induction. Post = post-protein induction. S/N = supernatant. P = pellet. U = unbound fraction. E1/2/3 = elutions.

C) Coomassie-stained gel of a pull-down assay with GST or GST-KChIP1, showing Ca^{2+}-dependent (+) or independent (-) interactions against whole brain lysate. A sample of the whole brain lysate was loaded as a control.

kDa = molecular weight markers in kiloDaltons.

To investigate this interaction further, pull-down assays were used to look for an interaction between GST-tagged KChIP1, immobilised on beads, and 14-3-3 proteins present in bovine brain extracts. In order to perform these experiments, purified GST and GST-KChIP1 proteins were required. BL21 *E. coli* cells transformed with plasmids encoding GST or GST-KChIP1 were available in the laboratory. These were grown up, and protein production induced with IPTG. The protein was then purified using a cell disruptor, and affinity chromatography using Glutathione Sepharose. The results of this purification are shown in Figure 4.2A for GST, and Figure 4.2B for GST-KChIP1. In both cases, there was a large concentration of protein in the three elution fractions, at the expected molecular weight of ~26kDa for GST, and ~51kDa for GST-KChIP1. There was very little contamination in the GST elutions, although the GST-KChIP1 did show some proteins at ~26kDa, which were likely degradation products. A pull-down experiment was then performed, using these proteins attached to Glutathione Sepharose beads to pull out binding partners from bovine whole brain lysate. Bound proteins were eluted in either the absence of Ca^{2+} (Ca^{2+}-dependent interactions) or in high salt (Ca^{2+}-independent interactions) (Figure 4.2C). However, the bands seen in the eluates on this gel were broadly the same for GST as for GST-KChIP1. The only obvious additional band was seen at ~51kDa, so corresponding to the GST-KChIP1 itself.

There were two potential problems with this experimental approach. In order to produce whole brain lysate, detergents are used. It has been observed previously that NCS family proteins are unable to bind their interacting partners in the presence of some detergents (Dr L. Haynes, University of Liverpool, personal communication). To avoid these issues, the experiment was repeated with bovine brain cytosol, which can be produced without such harsh detergents. In addition, 14-3-3 proteins may require their targets to be phosphorylated in order to bind, although KChIP1 is lacking a consensus 14-3-3 binding site. The pull-down experiment was therefore repeated in the presence of Mg^{2+}.ATP, to allow kinases in the bovine brain cytosol to phosphorylate their target proteins. These experiments were also performed to look for Ca^{2+}-dependent and Ca^{2+}-independent interactions, and with immobilised GST as a control. Figure 4.3A shows a Coomassie blue stained gel of the results of this pull-down. This result

was much cleaner than that seen in Figure 4.2C, and there were some bands specific for GST-KChIP1, either as Ca^{2+}-dependent interactions, or in both the Ca^{2+}-dependent and independent interaction lanes. These are highlighted with red dots in the figure. To confirm if there was any binding in this experiment

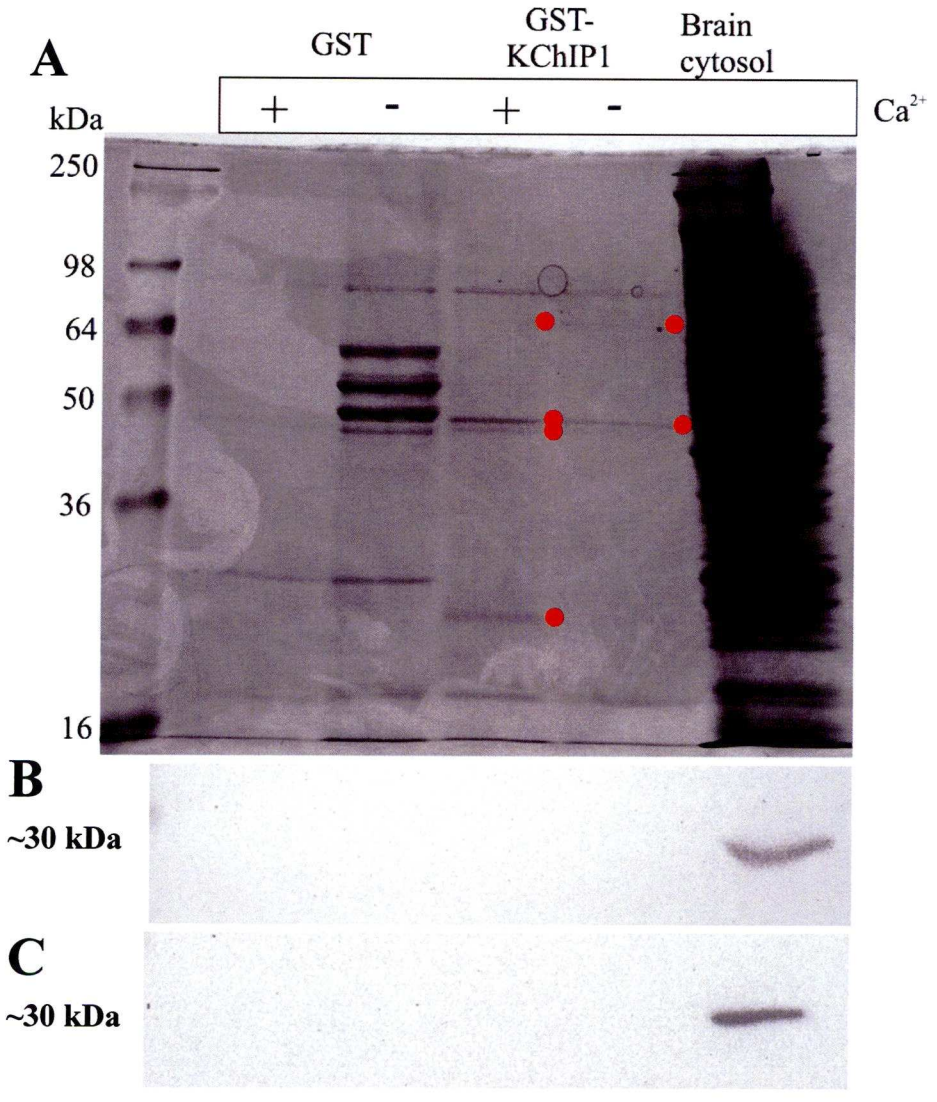

4.3: Pull-down assays with GST and GST-KChIP1 against bovine brain cytosol.
Both GST-KChIP1 and a GST control were used in pull-down assays against bovine brain cytosol, in the presence of Mg^{2+}.ATP, and the presence or absence of Ca^{2+}.

A) Coomassie-stained gel of a pull-down assay using GST and GST-KChIP1 against bovine brain cytosol, showing Ca^{2+}-dependent (+) or independent (-) interactions. A sample of bovine brain cytosol was also loaded as a control. Bands present only in the GST-KChIP1 lanes are highlighted with a red dot.

kDa = molecular weight markers in kiloDaltons.

B) Western blot of samples from the pull-down, using anti-14-3-3γ antibodies. Lanes correspond to those in **A)**. A band was detected at the expected molecular weight of ~30kDa in the bovine cytosol lane.

C) Western blot of samples from the pull-down, using anti 14-3-3β antibodies. Lanes correspond to those in **A)**. A band was detected at the expected molecular weight of ~30kDa in the bovine brain cytosol lane.

between KChIP1 and 14-3-3 proteins, Western blots were performed using samples of the pull-down. Bovine brain cytosol was used a positive control, to confirm the 14-3-3 proteins were present and detectable in the input. The blots were probed with two different antibodies against isoforms of 14-3-3. As the target of the yeast two-hybrid screen, 14-3-3γ was investigated (Figure 4.3B). An alternative protein, 14-3-3β was also investigated, to confirm any isoform specificity (Figure 4.3C). As expected, a band was visible in the brain cytosol lane, at the expected molecular weight of ~30kDa, for both isoforms. However, there were no bands in any of the other lanes, for either 14-3-3γ or 14-3-3β. It was not therefore possible to confirm the interaction seen in the yeast two-hybrid screen, and so the 14-3-3 family of proteins was not considered any further.

4.2.2 Interactions between SAP97 and Kv4.2 in the absence and presence of KChIP1

The PSD-95 family of MAGUK proteins are known to have important roles in trafficking ion channels and receptors to the plasma membrane of neurons and clustering them at particular polarised locations, such as post-synaptic densities (Kim and Sheng 2004). Plasmids encoding tagged versions of these proteins were kindly provided by Prof L-Y. Lian, University of Liverpool. Of this family of proteins, SAP97 was of particular interest as it is thought to have an important role in neuronal trafficking (El-Haou et al. 2009). In work with Kv4 channels, RNAi knockdown of SAP97 reduced levels of Kv4.2 in the post-synaptic compartment (Gardoni et al. 2007). Also, SAP97 was shown to promote Kv4 trafficking to the plasma membrane, and increase current density (El-Haou et al. 2009). This data is difficult to interpret, though, as some experiments were performed in cells stably transfected with KChIP2, and the separate contributions of these proteins were not fully assessed. The aim of this thesis was to compare the effects of SAP97 on Kv4.2 to the effects of KChIP1, and to look at the combined effects of both together.

As a first step, the trafficking of untagged Kv4.2 to the plasma membrane of HeLa cells was investigated in the presence of either KChIP1-EYFP or EGFP-SAP97. A typical cell expressing KChIP1-EYFP and Kv4.2 detected by anti-Kv4.2 immunostaining is shown in Figures 4.4A-C. As expected, both the KChIP1 and the Kv4.2 were localised to the plasma membrane. The experiment was repeated, this time with Kv4.2 and EGFP-SAP97, as shown in Figures 4.4D-F. In this typical cell, the EGFP-SAP97 was visible at the plasma membrane, although it was also present in the intracellular perinuclear region, possibly associated with intracellular membrane-bound compartments such as the ER or Golgi. This cell also showed some Kv4.2 at the plasma membrane, although this appeared less than with KChIP1. The trafficking of Kv4.2 to the plasma membrane was quantified by calculating the percentage of the total fluorescence in a region of interest corresponding to the plasma membrane. Data for 20 cells from each condition are shown in Figure 4.4K, with the background level of Kv4.2 at the plasma membrane subtracted, and then results normalised to cells with Kv4.2 and KChIP1-EYFP. Hence a value of 1 on the y-axis means that the

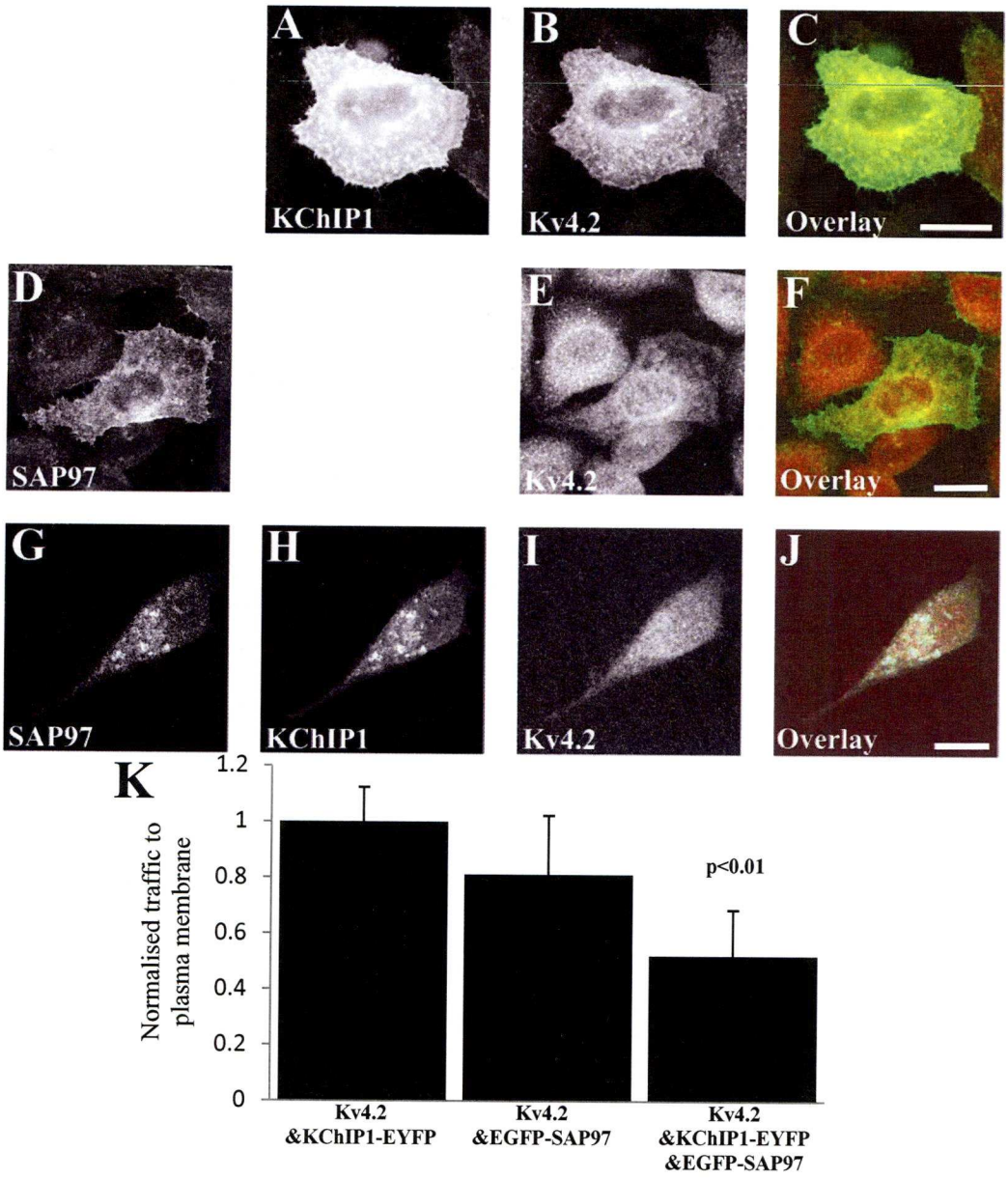

4.4: The trafficking of untagged Kv4.2 to the plasma membrane in the presence of KChIP1-EYFP, EGFP-SAP97 or both.

HeLa cells were transfected to express untagged Kv4.2, in the presence of KChIP1-EYFP, EGFP-SAP97 or both, and the level of channel trafficking to the plasma membrane was assessed.

A-C) HeLa cell expressing KChIP1-EYFP (Green) and Kv4.2 (Red), with co-localisation shown in the overlay in yellow.

D-F) HeLa cell expressing EGFP-SAP97 (Green) and Kv4.2 (Red), with co-localisation shown in the overlay in yellow.

G-J) HeLa cell expressing EGFP-SAP97 (Blue), KChIP1-EYFP (Green) and Kv4.2 (Red).Partial co-localisation is seen as yellow, purple or cyan in the colour overlay, with co-localisation of all three proteins in white.

In all cases, Kv4.2 was detected using anti-Kv4.2 immunostaining with a TRITC-conjugated secondary. The scale bars represent 10μm.

K) Quantification of the percentage of Kv4.2 TRITC fluorescence at the plasma membrane.

Data is shown as the means from 20 cells for each condition, shown ±S.E.M, with a background measurement subtracted, and normalised to the leftmost column of cells co-transfected with KChIP1-EYFP. p-values are given relative to this column.

percentage of Kv4.2 trafficking is equal to that occurring in the presence of KChIP1, whilst a value of 0 means the trafficking matches that seen in control cells expressing the channel alone. The EGFP-SAP97 caused a significant ($p<0.01$) increase in the percentage of Kv4.2 found at the plasma membrane, compared to cells expressing Kv4.2 alone. This increase in trafficking was similar to cells with Kv4.2 and KChIP1-EYFP. This suggests that both KChIP1 and SAP97 may play a role in regulating the trafficking of Kv4 channels to the plasma membrane.

As a continuation of this study, cells were transfected with Kv4.2 pcDNA, KChIP1-EYFP and EGFP-SAP97. Cells were carefully visualised, with measurements of narrow emission ranges, to ensure the GFP and EYFP signals were separate (see Chapter 2). A typical cell is shown in Figures 4.4G-J. Unlike the doubly transfected cells, none of the proteins were present at the plasma membrane, including SAP97. This was confirmed by quantifying the trafficking of Kv4.2, as shown in Figure 4.4K. This showed that trafficking of Kv4.2 to the plasma membrane in triply transfected cells was significantly lower than in cells expressing Kv4.2 with KChIP1-EYFP. It was also lower than in cells expressing Kv4.2 with EGFP-SAP97. Together, these data suggested that EGFP-SAP97 was somehow able to inhibit the stimulation of Kv4.2 trafficking caused by KChIP1-EYFP when the three proteins were expressed together. This led to further experiments to confirm and investigate this observation.

The above work confirmed that EGFP-SAP97 can stimulate the trafficking of Kv4.2 to the plasma membrane (El-Haou et al. 2009). However, the data in Chapter 3 show that the trafficking of Kv4.2 with KChIP1 is via a non-conventional, VAMP7- and Vti1a-dependent pathway. It was therefore interesting to ask whether the trafficking of Kv4.2 with EGFP-SAP97 also required this non-conventional SNARE complex. As a control, HeLa cells were first transfected with Kv4.2 pcDNA and KChIP1-EYFP alone (Figure 4.5A), or with VAMP7 RNAi construct 1 (Figure 4.5B). As expected, when co-expressed, both the Kv4.2 and the KChIP1 were at the plasma membrane (Figure 4.5A), whilst this was inhibited in the presence of the RNAi construct. Then cells were

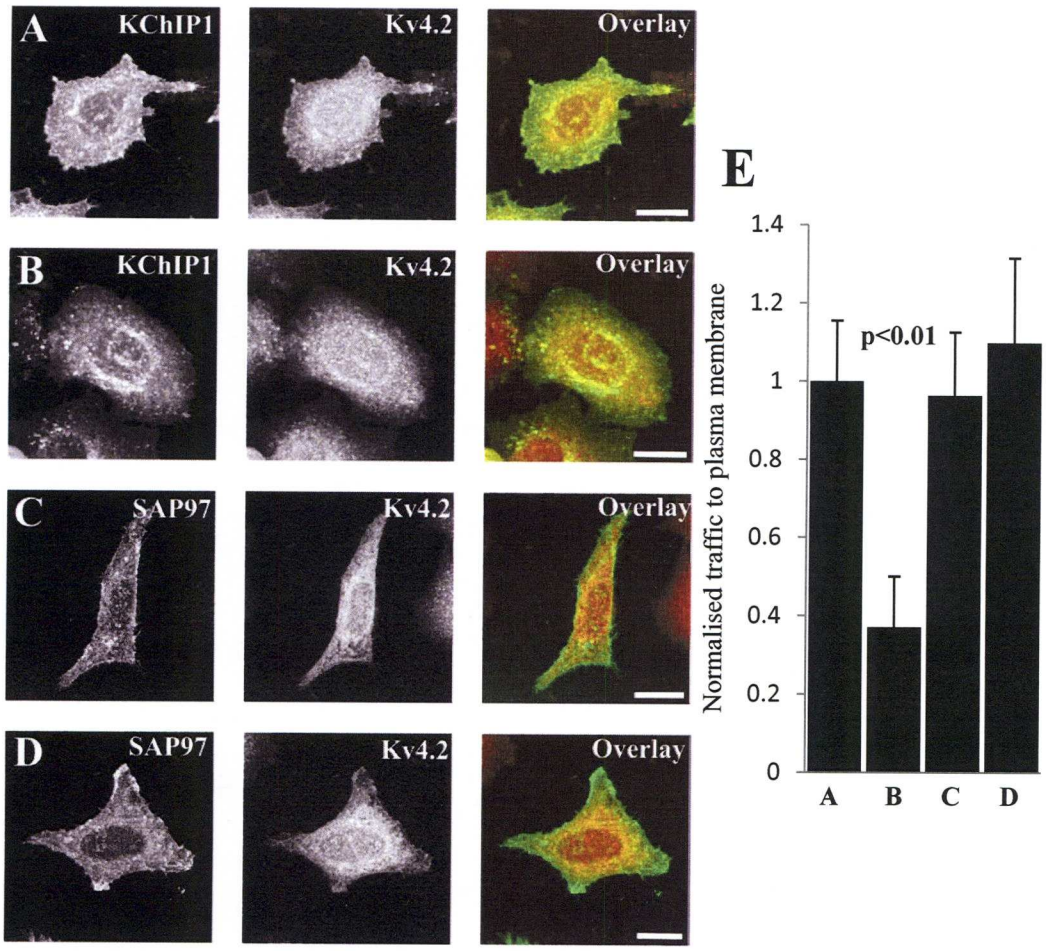

4.5: Trafficking of untagged Kv4.2 to the plasma membrane byKChIP1-EYFP or EGFP-SAP97 in the absence or presence of VAMP7 RNAi.

The importance of VAMP7 in the trafficking of Kv4.2 to the plasma membrane in the presence of either KChIP1-EYFP or EGFP-SAP97 was assessed in HeLa cells.

- **A)** HeLa cell transfected with KChIP1-EYFP (Green) and Kv4.2 pcDNA (Red).
- **B)** HeLa cell transfected with KChIP1-EYFP (Green) and Kv4.2 pcDNA (Red) in the presence of VAMP7 RNAi construst 1.
- **C)** HeLa cell transfected with EGFP-SAP97 (Green) and Kv4.2 pcDNA (Red).
- **D)** HeLa cell transfected with EGFP-SAP97 (Green) and Kv4.2 pcDNA (Red) in the presence of VAMP7 RNAi construct 1.

Kv4.2 localisation was determined using anti-Kv4.2 immunostaining with a TRITC-conjugated secondary. Cells were left 72 hours post-transfection. Co-localisation is shown as yellow in the colour overlays. Scale bars represent 10μm.

- **E)** Quantification of the normalised percentage of Kv4.2 at the plasma membrane under each condition, **A)-D)**, as described above.

Data shown is the means for 20 cells from each condition, ±S.E.M.

transfected with Kv4.2 pcDNA and SAP97 alone (Figure 4.5C), or with VAMP7 RNAi construct 1 (Figure 4.5D). Both the EGFP-SAP97 and Kv4.2 were detectable at the plasma membrane in cells under both conditions. The percentage of Kv4.2 immunostained fluorescence at the plasma membrane was quantified for cells from each condition, and the data normalised, as shown in

Figure 4.5E. This confirms that whilst the VAMP7 RNAi inhibited trafficking of Kv4.2 in the presence of KChIP1-EYFP, it had no effect on the ability of EGFP-SAP97 to stimulate this trafficking. This suggests SAP97/Kv4.2 is not trafficked via the non-conventional pathway characterised in Chapter 3.

The above work used Kv4.2 expressed from a pcDNA construct detected using an anti-Kv4.2 antibody, and TRITC-conjugated secondary. However, an antibody based approach can give high backgrounds in images. To try and improve on this, and to aid in the clarity of images from triply transfected cells, an mCherry-tagged version of Kv4.2 was prepared. As a first test of this construct, HeLa cells were transfected with mCherry-Kv4.2 alone (Figure 4.6A). The Kv4.2 was localised to the perinuclear region, a distribution matching that seen with untagged Kv4.2 (as in Figure 3.1). The percentage of fluorescence in the region of the plasma membrane was quantified for these cells at around 9.7%, similar to the results with untagged Kv4.2 in Figure 3.3. This quantification is shown in Figure 4.6L. Next, HeLa cells were co-transfected with mCherry-Kv4.2 and KChIP1-EYFP (Figures 4.6B-D). As seen previously, the Kv4.2 was localised to the plasma membrane in these cells, as was the KChIP1. Next, cells were transfected with mCherry-Kv4.2 and EGFP-SAP97 (Figures 4.6E-G), and although less clear than the images with KChIP1, it was still possible to see regions of the plasma membrane with both EGFP-SAP97 and mCherry-Kv4.2 fluorescence. Finally, cells were triply transfected with mCherry-Kv4.2, KChIP1-EYFP and EGFP-SAP97 (Figures 4.6H-K). Once again, cells surprisingly showed none of the three proteins at the plasma membrane, with them instead all localised to an intracellular perinuclear region. The percentage of mCherry-Kv4.2 at the plasma membrane was quantified for cells from all of these conditions, as shown in Figure 4.6L. In this case, both the KChIP1 ($p<0.01$) and SAP97 ($p<0.05$) could significantly increase the levels of Kv4.2 at the plasma membrane, although SAP97 was significantly less effective than KChIP1 in this case ($p<0.05$). In contrast there was no significant increase in Kv4.2 at the plasma membrane of triply transfected cells. This supports the finding with untagged Kv4.2 above that co-expression of SAP97 and KChIP1 inhibits the ability of either to promote Kv4.2 trafficking.

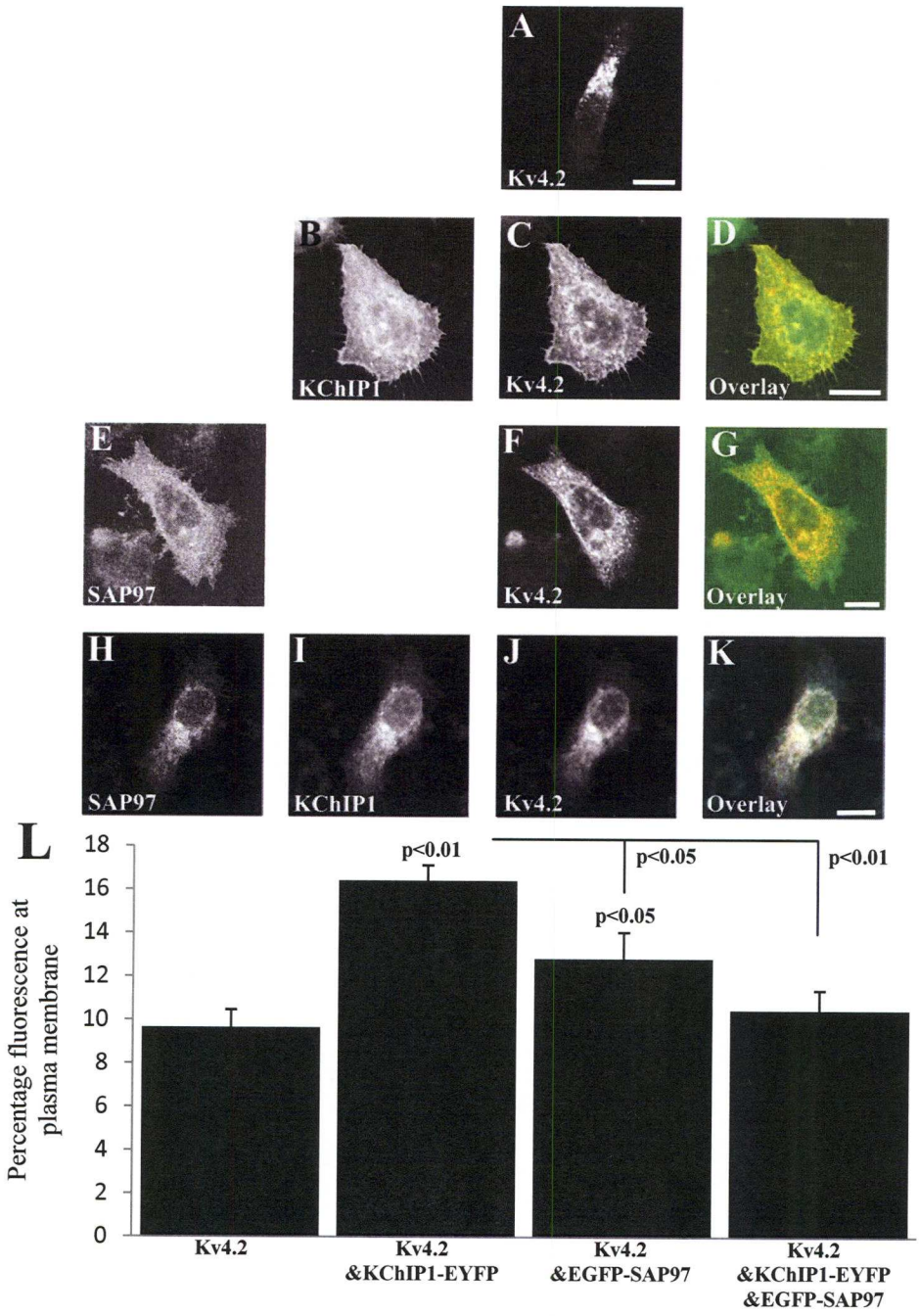

4.6: Trafficking of mCherry-Kv4.2 to the plasma membrane when expressed with KChIP1-EYFP, EGFP-SAP97 or both.

HeLa cells were transfected with mCherry-Kv4.2, and either KChIP1-EYFP, EGFP-SAP97 or both, and the levels of channel trafficking to the plasma membrane were quantified. Scale bars indicate 10μm. Co-localisation is shown as yellow in colour overlays D and G, and white in colour overlay K.

A) HeLa cell transfected with mCherry-Kv4.2.

B-D) HeLa cell transfected with KChIP1-EYFP (Green) and mCherry-Kv4.2 (Red).

E-G) HeLa cell transfected with EGFP-SAP97 (Blue) and mCherry-Kv4.2 (Red).

H-K) HeLa cell transfected with EGFP-SAP97 (Blue), KChIP1-EYFP (Green) and mCherry-Kv4.2 (Red).

L) Quantification of the percentage of mCherry-Kv4.2 at the plasma membrane in cells from each condition. Data is shown as the means from 20 cells for each condition, ±S.E.M. The displayed p-values are relative to cells expressing Kv4.2 alone, or relative to cells expressing Kv4.2 and KChIP1-EYFP (shown by the black line).

All of the proteins investigated are expressed *in vivo* in neurons. So next these experiments were repeated in Neuro2A cells, to investigate any cell-type specific effects. Again, cells were transfected with mCherry-Kv4.2, and either KChIP1-

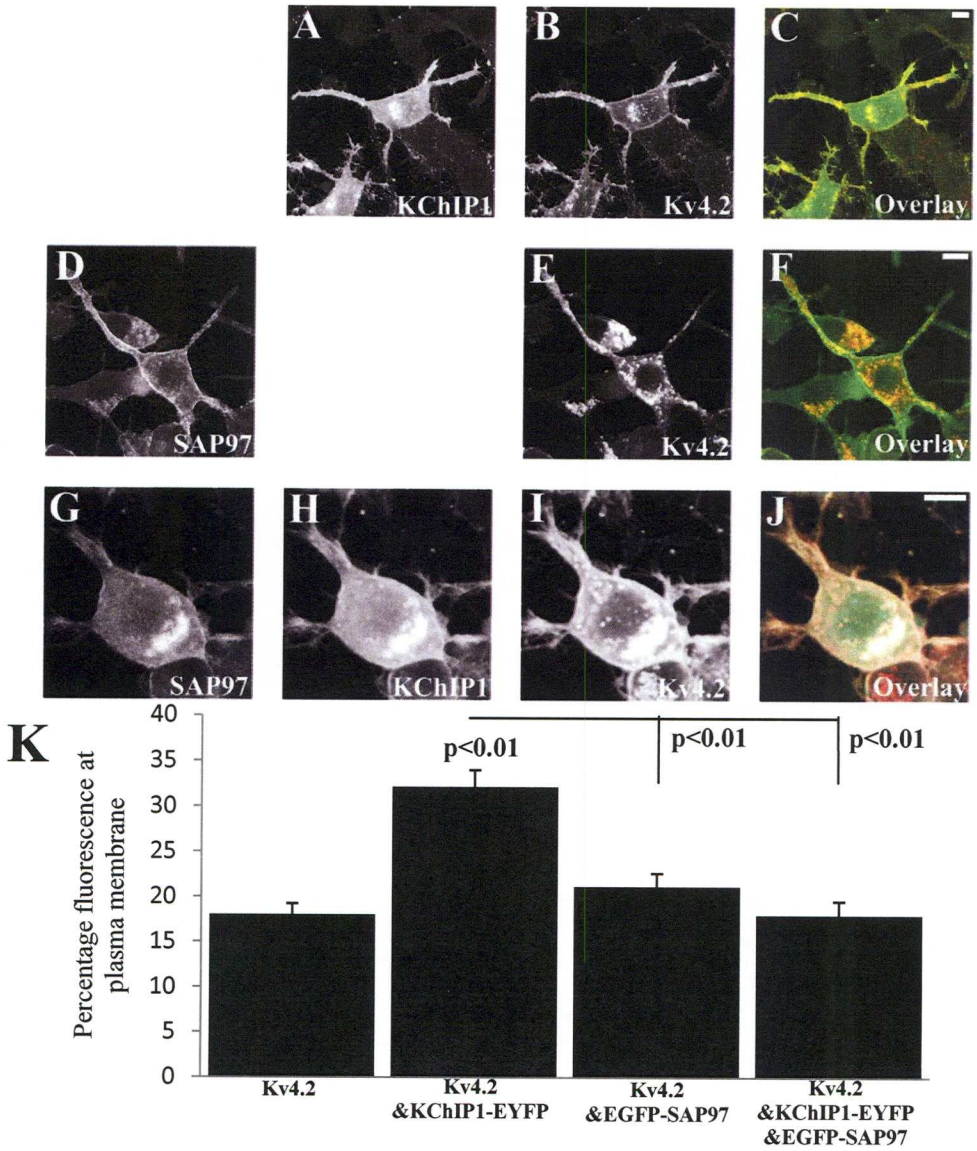

4.7: Trafficking of mCherry-Kv4.2 in Neuro2A cells when expressed with KChIP1-EYFP, EGFP-SAP97 or both.

Neuro2A cells were transfected with mCherry-Kv4.2, and either KChIP1-EYFP, EGFP-SAP97 or both, and the levels of channel trafficking to the plasma membrane were quantified. Scale bars indicate 10μm. Co-localisation is shown as yellow in Figures C and F, and triple co-localisation as white in Figure J.

- **A-C)** Neuro2A cell transfected with KChIP1-EYFP (Green) and mCherry-Kv4.2 (Red)
- **D-F)** Neuro2A cell transfected with EGFP-SAP97 (Green) and mCherry-Kv4.2 (Red).
- **G-J)** Neuro2A cell transfected with EGFP-SAP97 (Blue), KChIP1-EYFP (Green) and mCherry-Kv4.2 (Red).
- **K)** Quantification of the percentage of mCherry-Kv4.2 at the plasma membrane in cells from each condition. Data is shown as the means from 20 cells for each condition, ±S.E.M. The displayed p-values are relative to cells expressing Kv4.2 alone, or relative to cells expressing Kv4.2 and KChIP1-EYFP (shown by the black line).

EYFP (Figures 4.7A-C), EGFP-SAP97 (Figures 4.7D-F) or both (Figures 4.7G-J). mCherry-Kv4.2 was clearly at the plasma membrane with KChIP1-EYFP, but very little was visible at the plasma membrane with EGFP-SAP97. The EGFP-SAP97 did show a clear plasma membrane localisation. Unlike in HeLa cells, all three proteins were visible to some extent at the plasma membrane of triple transfected cells. However, the majority of protein fluorescence was visible in the perinuclear region. This was quantified in terms of the percentage of mCherry-Kv4.2 fluorescence at the plasma membrane (Figure 4.7K). In this cell type, EGFP-SAP97 did not significantly increase the trafficking of Kv4.2 to the plasma membrane. This could indicate a difference in the action of SAP97 between HeLa cells and Neuro2A cells, although the SAP97 was localised to the plasma membrane in both cell types. One possibility is that other proteins or post-translational modifications in this cell type affect the interaction of SAP97 with Kv4.2. However, the inhibition of Kv4.2/KChIP1 trafficking in the presence of SAP97 was seen in this cell type. The quantification revealed that although some Kv4.2 was at the plasma membrane in the triply transfected cells, the majority was intracellular.

To extend upon this observation, it was decided to test the effects of KChIP2-ECFP. This was of interest, because the results of Chapter 3 highlight differences in the mechanisms of trafficking of Kv4.2 between KChIP1 and KChIP2. Although the data in Figure 4.5 confirmed that EGFP-SAP97 did not need the non-conventional SNARE complex required by KChIP1, it was possible that SAP97 was affecting the ability of KChIP1 to traffic Kv4.2 via this pathway. Experiments with KChIP2-ECFP could shed light on how general the SAP97 effect is. Firstly, HeLa cells were transfected with mCherry-Kv4.2 and KChIP2-ECFP (Figure 4.8A), and the Kv4.2 was seen trafficked to the plasma membrane, although not as clearly as with KChIP1. Next, HeLa cells were transfected with mCherry-Kv4.2, KChIP2-ECFP and EGFP-SAP97 (Figure 4.8B), and as seen in the experiments with KChIP1 above, all three proteins were co-localised within the cell, with little to no Kv4.2 at the plasma membrane. However, much more of the KChIP and SAP97 was seen to be retained at the plasma membrane than in the experiments with KChIP1 above. The same two experiments were repeated in Neuro2A cells, with a doubly transfected cell shown in Figure 4.8C, and a triply

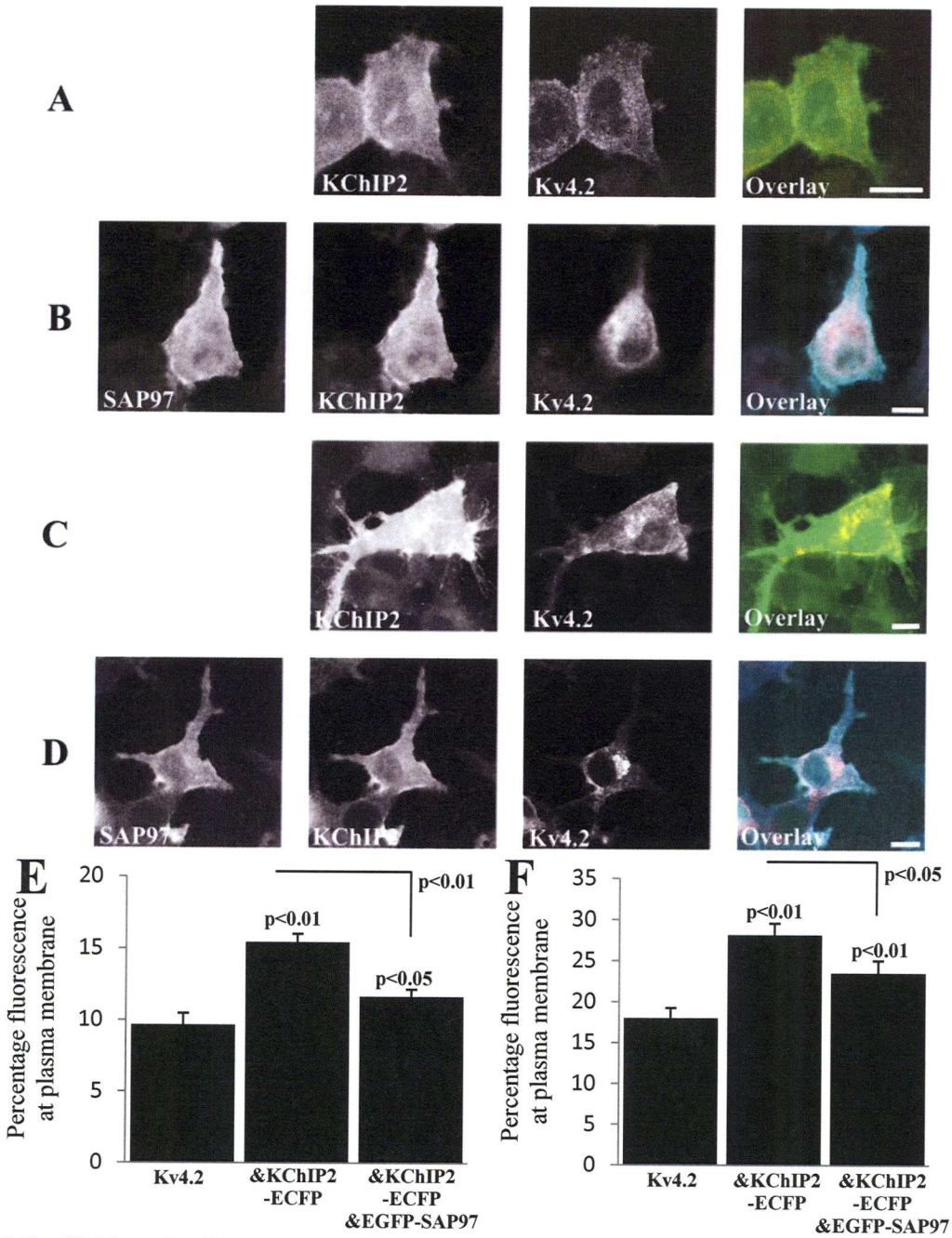

4.8 Trafficking of mCherry-Kv4.2 with KChIP2-ECFP in the absence or presence of EGFP-SAP97.

Both HeLa and Neuro2A cells were co-transfected with mCherry-Kv4.2 and KChIP2-ECFP, with or without EGFP-SAP97. The trafficking of Kv4.2 to the plasma membrane was quantified. Scale bars represent 10μm. Co-localisation is shown in yellow in Figures A and C, and white in Figures B and D.

A) HeLa cell expressing KChIP2-ECFP (Green) and mCherry-Kv4.2(Red).

B) HeLa cell expressing EGFP-SAP97 (Blue), KChIP2-ECFP (Green) and mCherry-Kv4.2 (Red).

C) Neuro2A cell expressing KChIP2-ECFP (Green) and mCherry-Kv4.2 (Red).

D) Neuro2A cell expressing EGFP-SAP97 (Blue), KChIP2-ECFP (Green) and mCherry-Kv4.2 (Red).

The percentage of mCherry-Kv4.2 fluorescence at the plasma membrane was quantified for 20 cells from each condition, shown for HeLa cells in **E)** and Neuro2A cells in **F)**. Data shown is the means ±S.E.M. p-values are shown relative to cells expressing mCherry-Kv4.2 alone, or relative to the doubly transfected cells (shown by the black line).

transfected cell shown in Figure 4.8D. Again, the KChIP2 and Kv4.2 channel were at the plasma membrane in the doubly transfected cells, but all three proteins were mostly perinuclear in the triply transfected cells. The normalised trafficking of mCherry-Kv4.2 to the plasma membrane was quantified for both HeLa cells (Figure 4.8E) and Neuro2A cells (Figure 4.8F). This confirmed the inhibition in Kv4.2 trafficking in the triple transfected cells compared to those expressing Kv4.2 with KChIP2. It also highlighted the independence of this inhibition from the non-conventional trafficking pathway utilised by KChIP1. It may therefore have a potentially wider importance, as it may affect traffic in cells expressing SAP97 along with either KChIP1 or KChIP2.

4.2.3 Interactions between Kv4.2/KChIP1and PSD-93 and PSD-95

The work above had confirmed the ability of EGFP-SAP97 to promote the trafficking of Kv4.2 to the plasma membrane, and suggested a novel inhibitory action when in a ternary complex of Kv4.2, SAP97 and KChIP1/2. However, whilst interactions between Kv4 channels and SAP97 or PSD-95 are known in the literature (Gardoni et al. 2007; El-Haou et al. 2009), there has been less work on the related protein PSD-93. In particular, there are a large number of PSD-93 isoforms (Parker et al. 2004), but little is known about any isoform specific effects they may have, even though they appear to have different intracellular localisation signals (Parker et al. 2004). There were several questions of interest to be addressed. Is PSD-93 able to promote the trafficking of Kv4.2 to the plasma membrane? Does the co-expression of PSD-93 with Kv4.2 and KChIP1 prevent channel trafficking, as was seen with SAP97? Do the different isoforms of PSD-93 give different effects in these experiments? Is the localisation of PSD-93 altered in triply transfected cells, as was seen with SAP97 above? Finally, is there any similarity with the better characterised PSD-95?

To begin with, HeLa cells were transfected with mCherry-Kv4.2, and GFP-tagged versions of PSD-93 in the absence or presence of KChIP1-EYFP. Typical cells from these experiments are shown in Figure 4.9, with cells expressing the δ isoform in Figures 4.9A and B, the ε isoform in 4.9C and D, and the ζ isoform in 4.9E and F. In the doubly transfected cells (Figures 4.9A, C and E), both the GFP-tagged PSD-93 isoforms and the mCherry-Kv4.2 were found intracellularly, with the Kv4.2 showing a perinuclear localisation similar to that seen when it is expressed alone (e.g. Figure 4.6A). This shows that unlike SAP97, these three isoforms of PSD-93 cannot promote the trafficking of Kv4.2 to the plasma membrane. Moreover, in the triply transfected cells (Figures 4.9B, D and F), the PSD-93-GFP, mCherry-Kv4.2 and KChIP1-EYFP are all retained within the cell, in the perinuclear region. The trafficking of mCherry-Kv4.2 to the plasma membrane in 20 cells from each condition was quantified, and is shown in Figure 4.9G. This confirms that the isoforms of PSD-93 are unable to promote the trafficking of mCherry-Kv4.2, as there is no significant difference in plasma membrane fluorescence between cells expressing mCherry-Kv4.2 alone, or with the three isoforms of PSD-93-GFP tested. It also confirms that each of

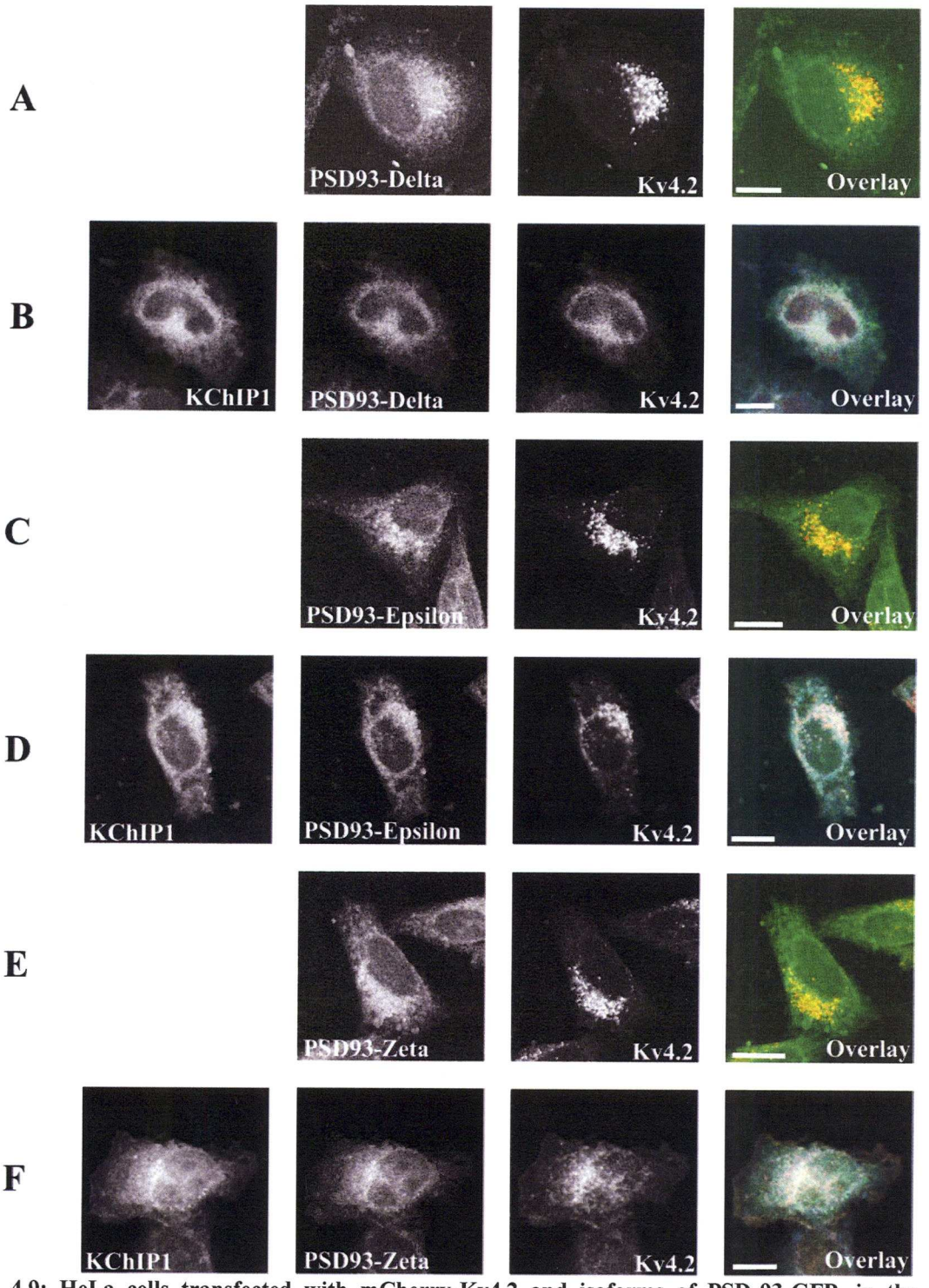

4.9: HeLa cells transfected with mCherry-Kv4.2 and isoforms of PSD-93-GFP, in the absence or presence of KChIP1-EYFP.

Continued overleaf.

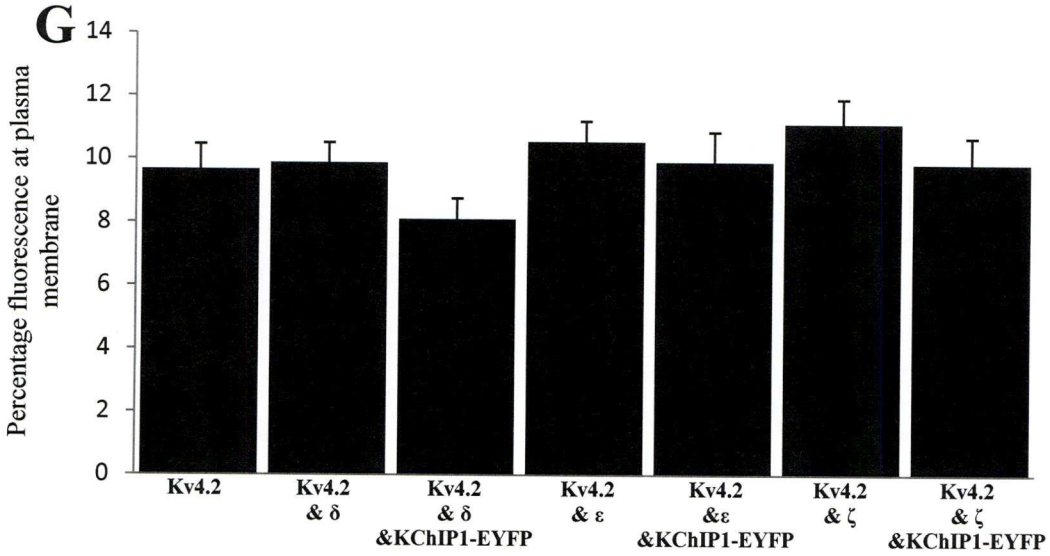

4.9: HeLa cells transfected with mCherry-Kv4.2 and isoforms of PSD-93-GFP, in the absence or presence of KChIP1-EYFP.

HeLa cells were transfected with mCherry-Kv4.2 and isoforms of PSD-93-GFP, but this did not significantly stimulate channel trafficking. Cells were also co-transfected with KChIP1-EYFP and the PSD-93 prevented the stimulation of Kv4.2 trafficking by KChIP1.

A, C, E) HeLa cells co-transfected with an isoform of PSD-93-GFP as shown (Green) and mCherry-Kv4.2 (Red). Co-localisation is shown as yellow in the colour overlays. Scale bars represent 10μm.

B, D, F) HeLa cells co-transfected with KChIP1-EYFP (Green), an isoform of PSD-93-GFP as shown (Blue) and mCherry-Kv4.2 (Red). Triple co-localisation is shown as white in the colour overlays. Scale bars represent 10μm.

G) Quantification of the percentage of mCherry-Kv4.2 at the plasma membrane for cells from each condition shown above. δ,ε,ζ = PSD93-GFP isoform of that name. Data shown is the mean of 20 cells, ±S.E.M.

the tested PSD-93 isoforms is able to inhibit the trafficking of mCherry-Kv4.2 to the plasma membrane when expressed with KChIP1-EYFP. These results are particularly interesting. They confirm that different members of the PSD-95 family of MAGUK proteins have different roles and interacting partners, as SAP97 can bind or influence Kv4.2, whilst these isoforms of PSD-93 cannot. In addition, no isoform specific effects were seen with the three forms of PSD-93 tested, as all three isoforms were able to alter the localisation of mCherry-Kv4.2 and KChIP1-EYFP in triply transfected cells. This may reflect the ability of these proteins to form a ternary complex, or for the PSD-93 to bind the KChIP1. It also supports the findings with SAP97 presented above, and may reflect a more general mechanism of Kv4.2 trafficking inhibition in cells expressing both a KChIP and a PSD-95 family member. As further confirmation, these experiments with PSD-93-GFP, mCherry-Kv4.2 and KChIP1-EYFP were also repeated in Neuro2A cells, which gave similar results (data not shown).

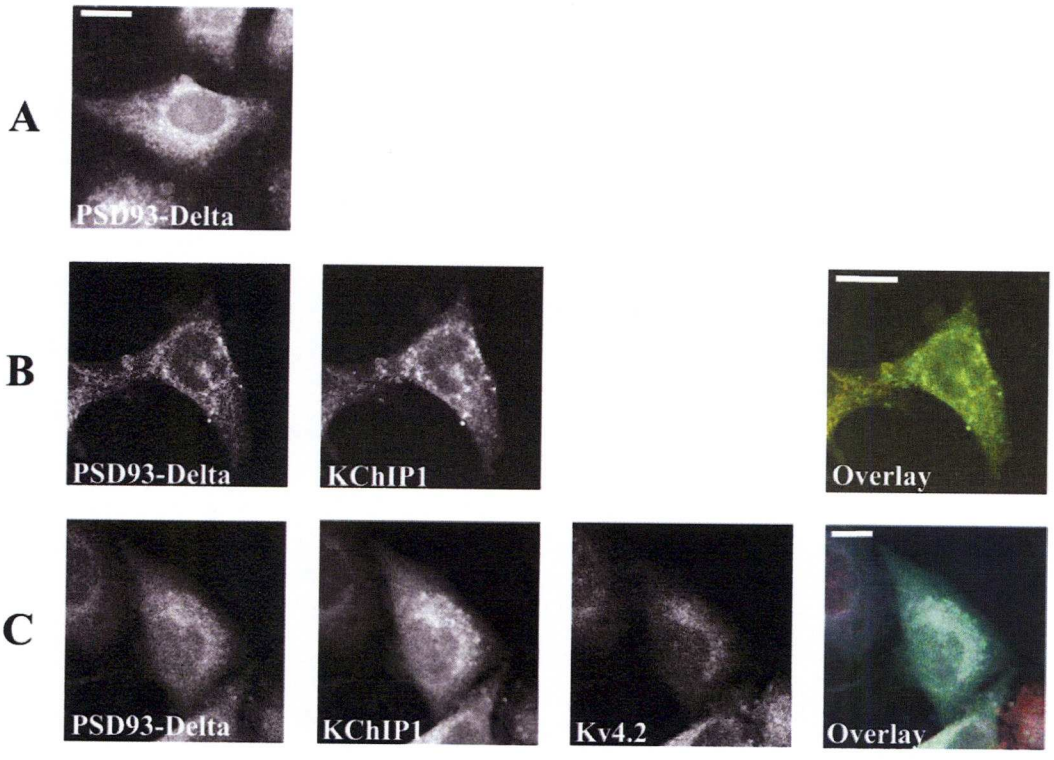

4.10: HeLa cells expressing PSD-93δ-GFP with KChIP1, or KChIP1 and Kv4.2.
The localisation of PSD-93δ-GFP in HeLa cells was investigated when expressed alone, or with KChIP1-EYFP, or with both KChIP1-EYFP and mCherry-Kv4.2.

- **A)** HeLa cell transfected with PSD-93δ-GFP alone.
- **B)** HeLa cell co-transfected with PSD-93δ-GFP (Red) and KChIP1-EYFP (Green). Co-localisation is shown as yellow in the colour overlay.
- **C)** HeLa cell co-transfected with PSD-93δ-GFP (Blue), KChIP1-EYFP (Green), and mCherry-Kv4.2 (Red). Triple co-localisation is shown as white in the colour overlay.

In all images, scale bars represent 10μm.

One interesting aspect of the above work was the observation that although both PSD-93 and Kv4.2 were localised to the perinuclear region when co-expressed, they did not completely co-localise. In addition, co-expression had no functional effect. This suggested that the two proteins did not interact. However, in triply transfected cells, the PSD-93 was able to prevent Kv4.2/KChIP1 trafficking to the plasma membrane, suggesting some kind of interaction. One possibility, therefore, is that the PSD-93 interacts with KChIP1. To investigate this, it was decided to concentrate on just one of the isoforms used above, as all three seemed to have broadly similar effects under these experimental conditions. Therefore, HeLa cells were transfected with either PSD-93δ-GFP alone (Figure 4.10A), with KChIP1-EYFP (Figure 4.10B), or with both KChIP1-EYFP and mCherry-Kv4.2 (Figure 4.10C). The PSD-93δ-GFP alone showed a bright,

diffuse intracellular localisation, particularly around the nucleus. This was perhaps surprising for a protein thought to exert its effects at the plasma membrane of the post-synaptic density (Parker et al. 2004; DeGiorgis et al. 2006). Interestingly, the distribution was altered in the presence of KChIP1-EYFP. The KChIP1-EYFP showed a punctate distribution as expected. However, the PSD-93δ-GFP was also more punctate in these cells, and there was at least partial co-localisation between the KChIP1-EYFP and PSD-93δ-GFP. In the triple transfected cells, all three proteins were intracellular, as seen previously, with none of them associated with the plasma membrane. The change in PSD-93δ localisation when co-expressed with KChIP1, and their co-localisation, suggests an interaction between PSD-93δ and KChIP1-EYFP. This interaction could give rise to the lack of Kv4.2 trafficking in the triply transfected cells. In support of this, both the PSD-93 and KChIP1 also appeared to partially co-

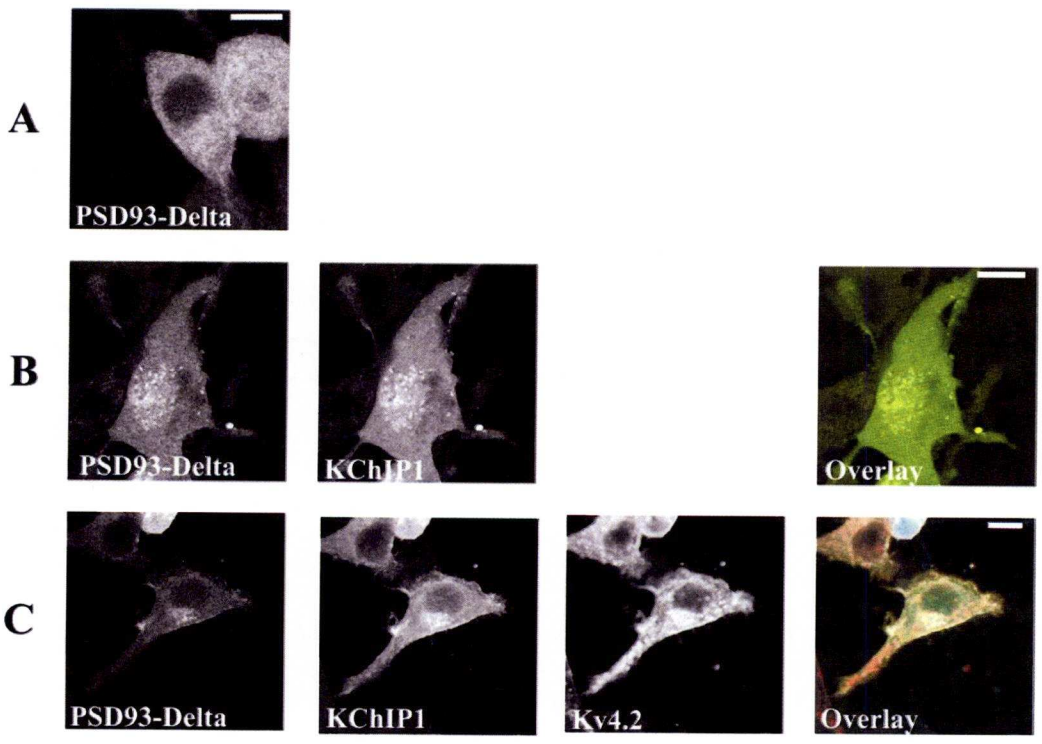

4.11: The localisation of PSD-93δ-GFP in Neuro2A cells.
The localisation of PSD-93δ-GFP in Neuro2A cells was investigated when expressed alone, or with KChIP1-EYFP, or with both KChIP1-EYFP and mCherry-Kv4.2.

- **A)** Neuro2A cell transfected with PSD-93δ-GFP alone.
- **B)** Neuro2A cell co-transfected with PSD-93δ-GFP (Red) and KChIP1-EYFP (Green). Co-localisation is shown as yellow in the colour overlay.
- **C)** Neuro2A cell co-transfected with PSD-93δ-GFP (Blue), KChIP1-EYFP (Green), and mCherry-Kv4.2 (Red). Triple co-localisation is shown as white in the colour overlay.

In all images, scale bars represent 10μm.

localise in punctae in the triply transfected cells. The mechanisms underlying this are unclear however, and the significance of such an interaction *in vivo* will need further investigation.

This experiment was also repeated in Neuro2A cells, and interestingly, some differences were observed. Figure 4.11A shows a cell expressing PSD-93δ-GFP only, with the protein showing a diffuse intracellular localisation, with the brightest signal seen in the perinuclear region. This was less bright and less clustered than in the HeLa cells above, but generally showed a similar distribution. Figure 4.11B shows a cell co-transfected with both PSD-93δ-GFP and KChIP1-EYFP. As with the HeLa cells above, the KChIP1-EYFP was punctate in distribution, and the PSD-93δ-GFP was co-localised with the KChIP1-EYFP in these perinuclear punctae. Figure 4.11C shows a cell triple transfected with PSD-93δ-GFP, KChIP1-EYFP and mCherry-Kv4.2. All three proteins were co-localised in the perinuclear region of these cells. In particular, the PSD-93δ-GFP in the triply transfected cells was mainly in the perinuclear region, clearly co-localised with some of the KChIP1-EYFP, and not diffuse like in Figure 4.11A. This would again suggest an interaction between the KChIP and PSD-93. However, all three proteins were also visible at the plasma membrane. This is similar to the experiments with SAP97 in Neuro2A cells shown above in Figure 4.7. This plasma membrane localisation was especially prominent for KChIP1 and Kv4.2. This suggests that any inhibitory action of members of the PSD-95 family on Kv4.2/KChIP1-EYFP trafficking may be less significant in Neuro2A cells than in HeLa cells.

The above work suggested an interaction between KChIP1 and SAP97 or PSD-93. It is already known in the literature that PSD-95 can interact with Kv4.2 channels (Gardoni et al. 2007). However, as with the other PSD-95 family proteins, potential interactions with the KChIPs have not been investigated. Therefore, HeLa cells were transfected with either mCherry-PSD-95 alone (Figure 4.12A), or with KChIP1-EYFP (Figure 4.12B). However, unlike PSD-93, PSD-95 was at least partially associated with the plasma membrane even when expressed alone. When co-expressed with KChIP1-EYFP, the KChIP1 retained its usual punctate perinuclear distribution. The PSD-95 also showed a

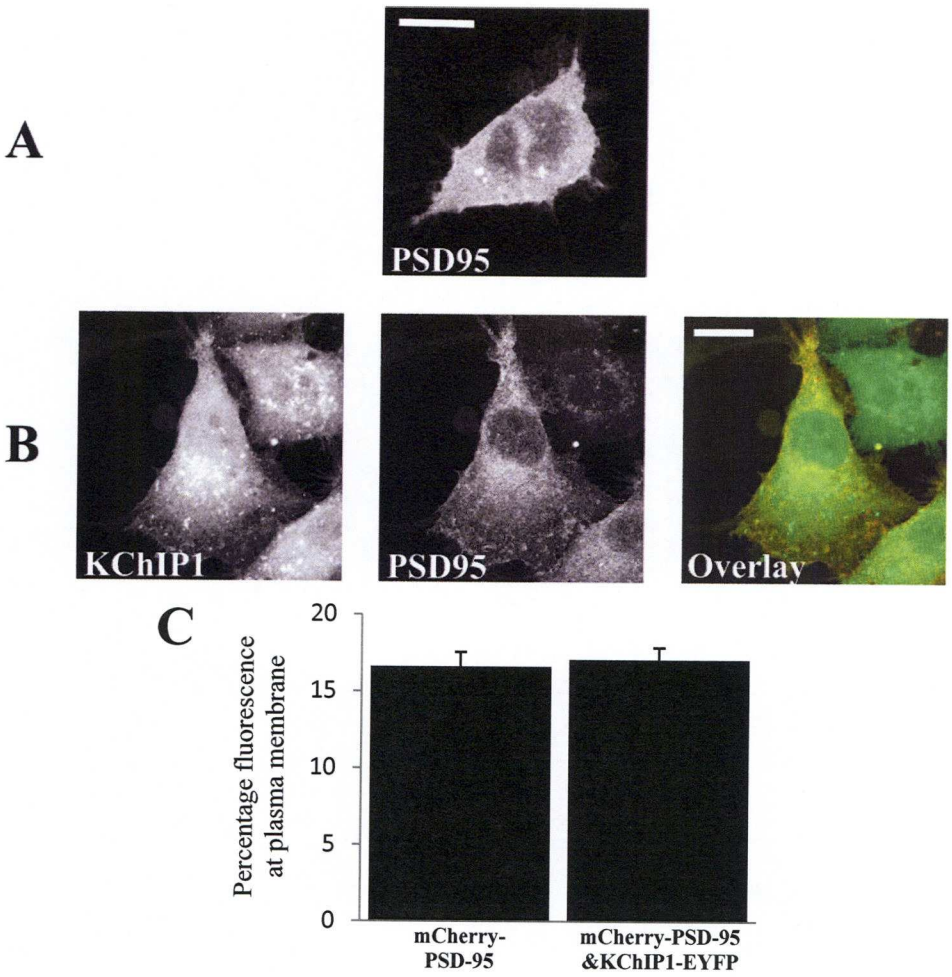

4.12: The localisation of mCherry-PSD-95 in HeLa cells, in the absence and presence of KChIP1-EYFP.

HeLa cells were transfected with mCherry-PSD-95, either alone, or with KChIP1-EYFP. The percentage of mCherry-PSD-95 fluorescence at the plasma membrane was quantified. Scale bars represent 10μm.

- **A)** HeLa cell transfected with mCherry-PSD-95. Some protein was seen localised at the plasma membrane.
- **B)** HeLa cell co-transfected with KChIP1-EYFP (Green) and mCherry-PSD-95 (Red), with co-localisation shown in yellow in the colour overlay. The PSD-95 is seen at the plasma membrane.
- **C)** Quantification of the mean percentage of mCherry-PSD-95 at the plasma membrane in 20 cells from each condition, ±S.E.M. Co-expression with KChIP1-EYFP had no significant effect on PSD-95 localisation.

low level of perinuclear distribution, similar to in the control cell, whilst retaining its plasma membrane localisation. The data from 20 cells for each condition were quantified as shown in Figure 4.12C. This confirms than co-expression with KChIP1 has no effect on PSD-95 localisation. This experiment was also repeated in Neuro2A cells, and gave the same results (data not shown). The fact that PSD-95 and KChIP1 are mostly found in separate compartments of the cell suggests that they may not interact *in vivo*. Nor did KChIP1 promote internalisation of PSD-95, as was seen for SAP97 in triply transfected cells in Figures 4.4G-J. However, these experiments do not preclude a low level of interaction between PSD-95 and KChIP1. More direct investigations would be required to confirm or refute this.

4.2.4 Interactions between SAP97 and KChIP1

When cells were triply transfected with Kv4.2, SAP97-GFP and KChIP1-EYFP, it was noticed that SAP97-GFP was localised to the perinuclear region within the cell, as opposed to a plasma membrane localisation when expressed with just Kv4.2. SAP97-GFP could also promote the trafficking of Kv4.2 to the plasma membrane when they were co-expressed, as could KChIP1, but when all three were co-expressed, this trafficking was inhibited. This suggested that there was an interaction between SAP97 and KChIP1, and it was this that prevented the trafficking of Kv4.2 by either of these accessory proteins. The potential for this interaction with SAP97 to be important in regulating Kv4 trafficking made it of

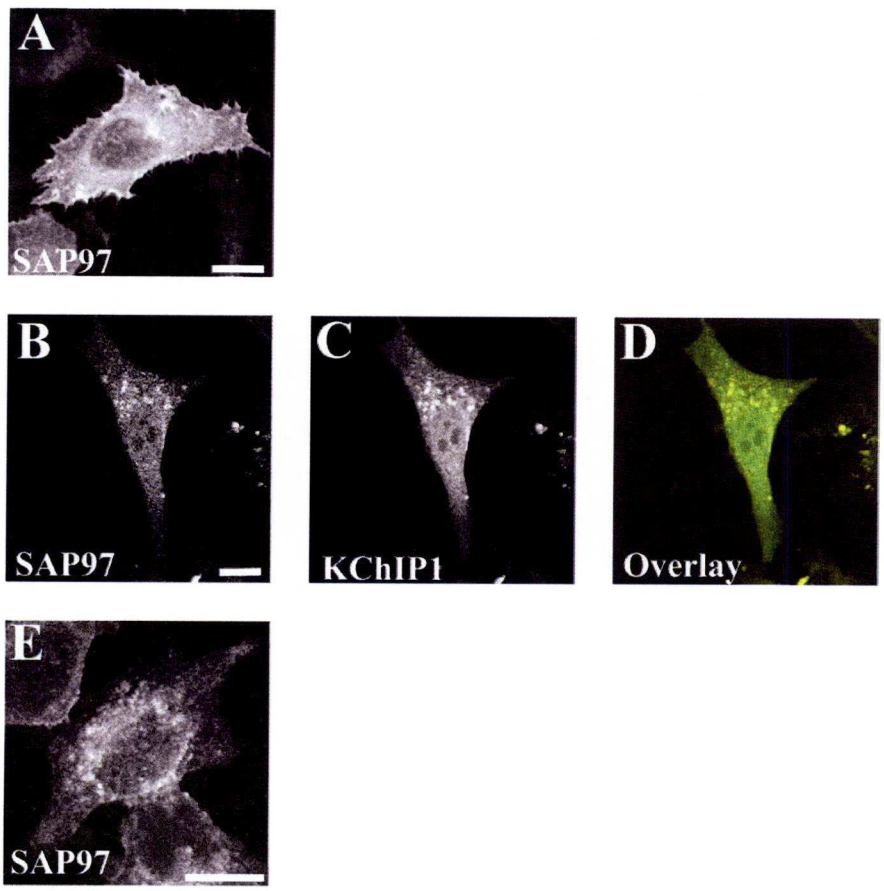

4.13: The localisation of EGFP-SAP97 in HeLa cells in the presence of KChIP1.
HeLa cells were transfected with EGFP-SAP97, either alone, or in the presence of two forms of KChIP1.

- **A)** HeLa cell transfected with EGFP-SAP97 alone, which showed some localisation to the plasma membrane.
- **B-D)** HeLa cell co-transfected with EGFP-SAP97 (Red) and KChIP1-EYFP (Green). Co-localisation is shown as yellow in the colour overlay.
- **E)** HeLa cell co-transfected with EGFP-SAP97 and KChIP1 pcDNA.

In all images, the scale bar represents 10μm.

interest and it was therefore investigated in more detail.

To begin with, HeLa cells were transfected with EGFP-SAP97 alone (Figure 4.13A). This confirmed that EGFP-SAP97 in these cells was at least partially associated with the plasma membrane. This matched the localisation seen in cells co-transfected with Kv4.2, as seen in Figure 4.4 above. This suggests that any interaction between SAP97 and Kv4.2 is not responsible for its internalisation in triply transfected cells. Furthermore, when cells were co-transfected with KChIP1-EYFP (Figures 4.13B-D), the EGFP-SAP97 was no longer seen at the plasma membrane. KChIP1-EYFP showed a typical punctate distribution, and this was now at least partially matched by the distribution of EGFP-SAP97. However, the EYFP and GFP emission spectra are very close. To confirm that the partial co-localisation was not due to bleed through between the KChIP1-EYFP signal and the GFP channel, the experiment was also repeated with untagged KChIP1 (Figure 4.13E). Once again, the SAP97 was no longer at the plasma membrane, and showed a punctate, perinuclear distribution, similar to that seen with the tagged KChIP1. These data suggest an interaction between the two proteins, that may also be responsible for the change in distribution seen in the triply transfected cells in Section 4.2.2.

As this was an unexpected result, these experiments were repeated in Neuro2A cells, to test the effects in a neuronal background. As was seen in HeLa cells, a Neuro2A cell transfected with EGFP-SAP97 alone (Figure 4.14A) showed the protein localised to the plasma membrane. When co-transfected with KChIP1-EYFP (Figures 4.14B-D), much less EGFP-SAP97 was seen at the plasma membrane. Instead, some of the EGFP-SAP97 was visible in perinuclear punctae that co-localised with KChIP1-EYFP. This supports the data from HeLa cells suggesting an interaction between SAP97 and KChIP1. However, some EGFP-SAP97 did remain at the plasma membrane in this cell type. This could reflect a reduced level of interaction between KChIP1 and SAP97 in this cell type, or perhaps a higher level of SAP97 expression compared to KChIP1.

The above experiments suggested an interaction between KChIP1 and SAP97, and it seemed likely that this could be contributing to the inhibition of Kv4.2 and

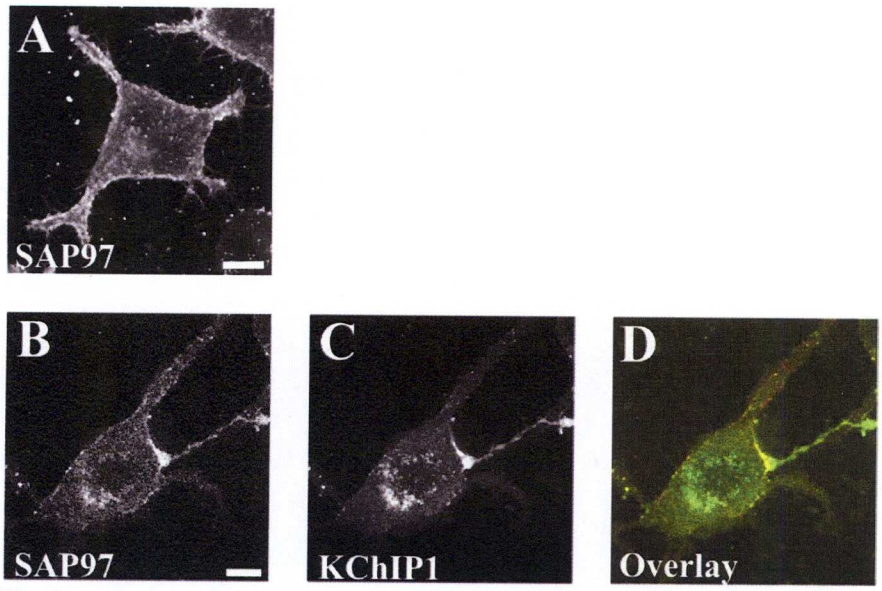

4.14: The localisation of EGFP-SAP97 in Neuro2A cells in the presence of KChIP1-EYFP.

Neuro2A cells were transfected with EGFP-SAP97, either alone, or in the presence of KChIP1-EYFP.

A) Neuro2A cell transfected with EGFP-SAP97 alone, which showed some localisation to the plasma membrane.

B-D) Neuro2A cell co-transfected with EGFP-SAP97 (Red) and KChIP1-EYFP (Green). Co-localisation is shown as yellow in the colour overlay.

In all images, the scale bar represents 10μm.

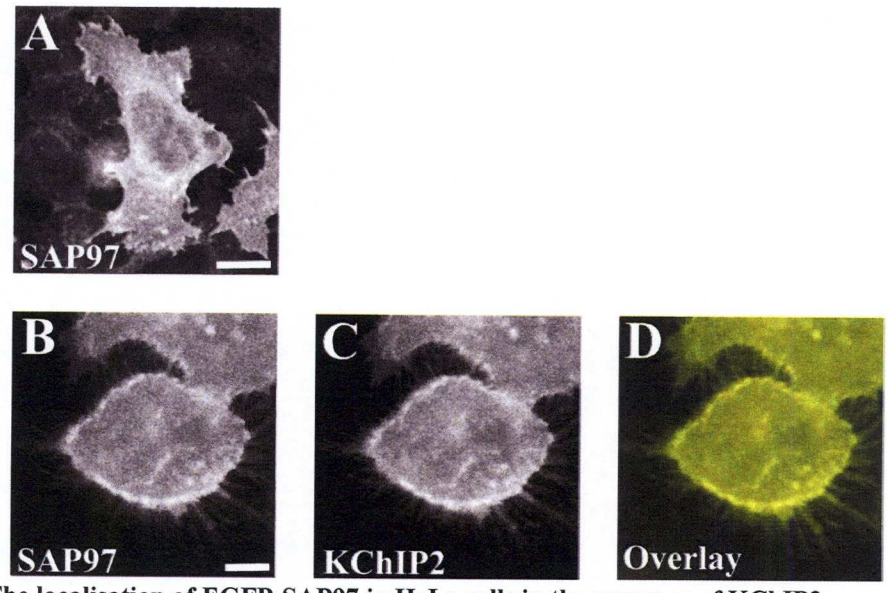

4.15: The localisation of EGFP-SAP97 in HeLa cells in the presence of KChIP2.

HeLa cells were transfected with EGFP-SAP97, either alone, or in the presence of KChIP2-ECFP.

A) HeLa cell transfected with EGFP-SAP97 alone, which showed some localisation to the plasma membrane.

B-D) HeLa cell co-transfected with EGFP-SAP97 (Red) and KChIP2-ECFP (Green). Co-localisation is shown as yellow in the colour overlay.

In all images, the scale bar represents 10μm.

KChIP1 trafficking in the presence of SAP97. In Section 4.2.2 it was shown that cells transfected with EGFP-SAP97, mCherry-Kv4.2 and KChIP2-ECFP also showed this reduction in channel trafficking. It was therefore possible that SAP97 could also be interacting with KChIP2. Experiments were therefore performed in HeLa cells to see what effect co-expression of KChIP2 had on the localisation of EGFP-SAP97. Figure 4.15A shows a control cell expressing EGFP-SAP97 alone, and as expected from the experiments above, this was localised to the plasma membrane. Next, cells were co-transfected with EGFP-SAP97 and KChIP2-ECFP (Figures 4.15B-D) and the EGFP-SAP97 was also localised to the plasma membrane, as was the KChIP2-ECFP. This work was also repeated in Neuro2A cells, with the same results (data not shown). The absence of a change in localisation may well be because KChIP2 is plasma membrane associated in cells (see Figure 3.02D). Therefore, the SAP97 and KChIP2 may in fact be interacting, but remaining at the plasma membrane. This will need confirming by other, more direct biochemical methods. However, if these proteins do interact, it could also explain why SAP97 and KChIP2 remain at the plasma membrane in triple transfected cells, whilst the Kv4.2 is intracellular. This would not be observed with KChIP1, as this appears to interact with SAP97 in KChIP1-positive punctate vesicles in the perinuclear region. These data also suggest that the lack of Kv4.2 trafficking may be due to the interaction of the SAP97 with the KChIP, resulting in both of these proteins being unable to bind the channel, and thus being unable to promote its trafficking.

Having shown this potential interaction, it was interesting to investigate ways in which it might be regulated by the cell. The KChIPs are calcium sensor proteins, as discussed in Chapter 3. One intriguing area for an initial study was whether the calcium binding EF-hand domains of KChIP1 needed to be functional and able to bind to Ca^{2+} in order for the KChIP to interact with SAP97. The two EF-hand mutant versions of KChIP1 used in Chapter 3 were also used here. These experiments were performed in both HeLa (Figures 4.16A and B) and Neuro2A cells (Figures 4.16C and D), to compare the effects of a neuronal background on protein localisation. Figures 4.16A and C show cells transfected with EGFP-

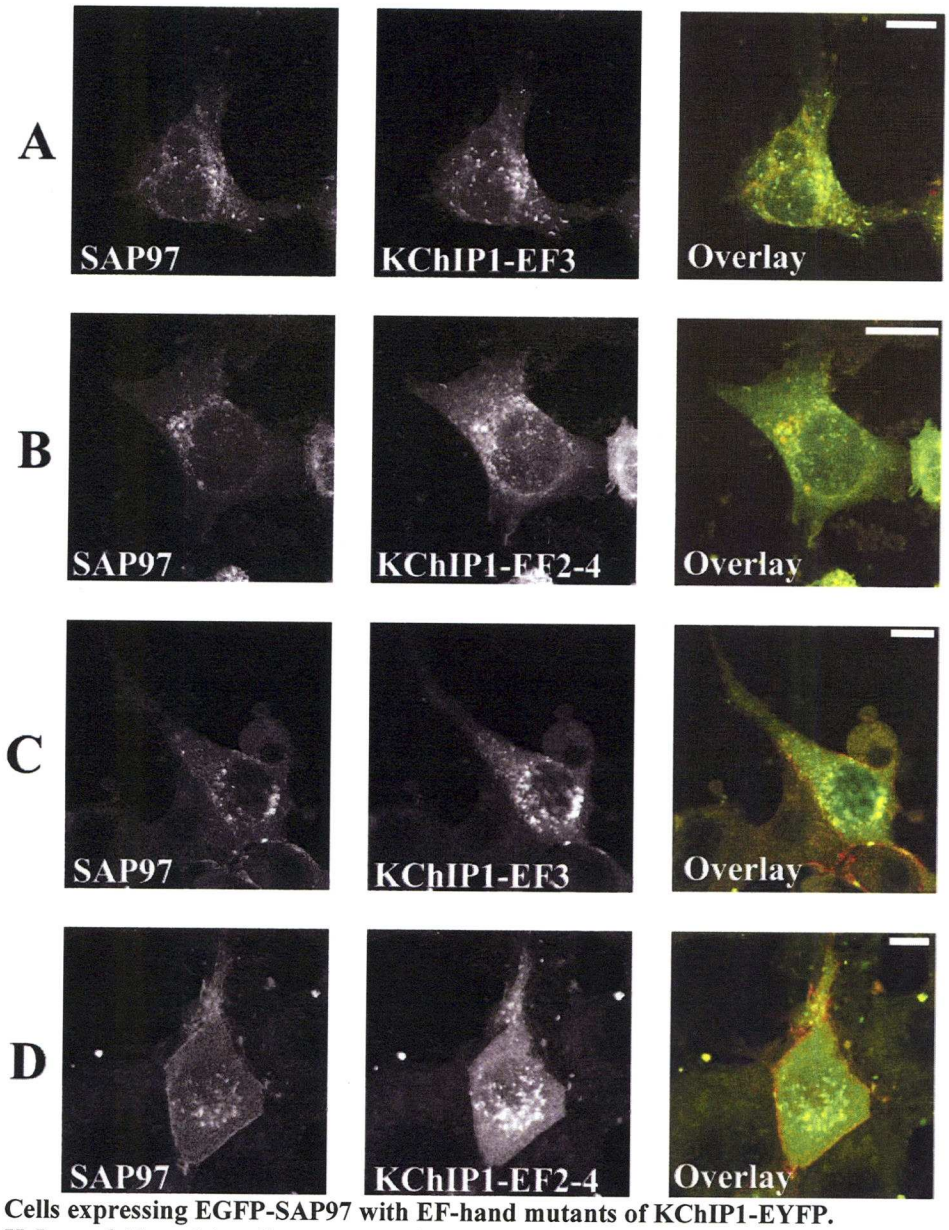

4.16: Cells expressing EGFP-SAP97 with EF-hand mutants of KChIP1-EYFP.
Both HeLa and Neuro2A cells were transfected with EGFP-SAP97 and one of two EF-hand mutants of KChIP1-EYFP to assess the requirement for KChIP1 to have intact EF-hands in order to influence the localisation of EGFP-SAP97.

A) HeLa cell co-transfected with EGFP-SAP97 (Red) and KChIP1-EF3-EYFP (Green).
B) HeLa cell co-transfected with EGFP-SAP97 (Red) and KChIP1-EF2-4-EYFP (Green).
C) Neuro2A cell co-transfected with EGFP-SAP97 (Red) and KChIP1-EF3-EYFP (Green).
D) Neuro2A cell co-transfected with EGFP-SAP97 (Red) and KChIP1-EF2-4-EYFP (Green).

In all images, the scale bar represents 10μm. Co-localisation is shown as yellow in the colour overlays.

SAP97 and KChIP1-EF3-EYFP, and Figures 4.16B and D show cells co-transfected with SAP97-GFP and KChIP1-EF2-4-EYFP. In all cases, the KChIP1-EYFP was localised to perinuclear punctae. This was as expected, as the EF-hand mutants of KChIP1 show the same punctate distribution as the wild-type protein (Figure 3.5). However, the SAP97-GFP also showed a punctate distribution, and the colour overlays showed co-localisation between the SAP97 and KChIP1 mutants. This is different from the plasma membrane localisation of SAP97-GFP when expressed alone (Figure 4.13). This suggests that the EF-hand mutants of KChIP1 are able to bind to SAP97, thus altering its localisation, as does wild-type KChIP1 (see Figures 4.13 and 4.14). It therefore seems that this interaction is not dependent on KChIP1 binding to Ca^{2+}. Generally, the localisation of the two proteins was similar in both the HeLa and Neuro2A cells. One difference, however, was that some SAP97-GFP remained localised to the plasma membrane in the Neuro2A cells in the presence of either KChIP1 mutant. This was also seen with wild-type KChIP1-EYFP (Figure 4.14), supporting the idea that there may be less interaction between KChIP1 and SAP97 in this cell type. The reasons for this remain unclear.

Finally, to try and confirm this potential interaction between SAP97 and KChIP1 a number of biochemical interaction experiments were performed. Samples from the pull-down experiments shown in Figure 4.3 were blotted to see if GST-KChIP1 could bind SAP97 in bovine brain cytosol. In addition, radio-labelled SAP97 was produced by *in vitro* transcription/translation experiments, and interaction studies performed with GST-KChIP1. Finally, immunoprecipitation experiments were performed using lysates from HeLa cells transfected with SAP97-GFP and KChIP1 pcDNA, and antibodies against these two proteins. It was not possible to show a convincing interaction between SAP97 and KChIP1 using any of these methods. Further work will therefore be needed to show whether such a direct or indirect interaction does in fact occur.

4.3 Discussion

There are many proteins that can regulate the trafficking of Kv4 potassium channels to the plasma membrane (see Chapter 1.4.2). This trafficking is a key step for the regulation of neuronal A-type currents, and hence synaptic plasticity, learning and memory (An et al. 2000; Chen et al. 2006(2); Lauver et al. 2006). The discovery of novel regulators of Kv4 trafficking, as well as an understanding of how such regulators can exert their effects, is therefore important for our knowledge of brain function at a cellular and molecular level. In particular, it is becoming increasingly clear that many of these proteins bind to Kv4 channels at the same time and can have their effects modified by binding within such a complex (Jerng et al. 2005). The interactions between KChIP1 and two protein families, the 14-3-3 proteins and the PSD-95 family, were investigated in this thesis.

The technique of yeast two-hybrid screens to look for novel protein interactions has become increasingly popular, particularly because their high-throughput nature allows for the testing of many potential target proteins (Bruckner et al. 2009). However, they can give false-positive results, and so all potential interactions need to be verified by alternative means (Sanderson 2009). The identification of 14-3-3γ as a potential binding partner of KChIP1 in one such screen seemed highly plausible, as both proteins are known to have roles in regulating ion channel trafficking (An et al. 2000; O'Kelly et al. 2002; Rajan et al. 2002). There is no evidence of a direct interaction between 14-3-3 proteins and the Kv4 channels in the literature, and so it was possible that 14-3-3γ could affect Kv4.2 trafficking by binding to its accessory protein KChIP1. In support of this, Figure 4.1 revealed co-localisation between KChIP1-EYFP and endogenous 14-3-3γ detected by antibodies. However, assays with GST-KChIP1 and bovine brain cytosol (Figure 4.3) did not pull down either 14-3-3γ or an alternate isoform 14-3-3β. The yeast two-hybrid interaction could therefore be due to a false positive identification. Alternatively, the interaction could be specific for another 14-3-3 isoform, although this seems unlikely, as all hits seen for 14-3-3 proteins in the yeast two-hybrid screen were for the γ-isoform (Dr L. Haynes, University of Liverpool, personal communication). The use of other biochemical

binding assays, such as co-immunoprecipitation, could also help to investigate this potential interaction further.

The second family of potential KChIP1/Kv4.2 interacting proteins investigated in this thesis was the PSD-95 family of MAGUK proteins. These neuronal proteins contain many protein binding domains, allowing them to scaffold together several binding partners (Kim and Sheng 2004). This could bring downstream regulators nearer to receptors at the plasma membrane, or link proteins to the cytoskeleton (Feng and Zhang 2009). They are perhaps best known for their ability to cluster AMPA and NMDA receptors in the post-synaptic density of neurons (Kim and Sheng 2004; Bats et al. 2007). It is thus likely that they have some role in regulating Kv4 channel trafficking, as these channels also require a specific dendritic localisation (Birnbaum et al. 2004). Indeed, previous work has suggested that both SAP97 and PSD-95 can bind Kv4 channels, and influence their trafficking (Gardoni et al. 2007; El-Haou et al. 2009). It was SAP97 that was particularly interesting for this study, as this seems to be more associated with promoting or inhibiting trafficking, rather than just clustering proteins at the plasma membrane (El-Haou et al. 2009). However, in some experiments the response of Kv4.2 to SAP97 was examined in cells stably transfected with KChIP2 (El-Haou et al. 2009), making it difficult to determine the separate contributions of these two accessory proteins. A first step, therefore, was to confirm that SAP97 could promote the trafficking of Kv4.2 to the plasma membrane. This was indeed the case in HeLa cells, for both untagged Kv4.2 immunostained with anti-Kv4.2 antibodies, and an mCherry-tagged version of the channel (Figures 4.4 and 4.6). These experiments also confirmed that the tagged version of the channel showed the same localisation as untagged Kv4.2, and had the same response to KChIP1-EYFP, validating its use in further experiments. It should be noted that with the mCherry-Kv4.2, the EGFP-SAP97 was less effective at promoting the trafficking of the channel to the plasma membrane than KChIP1 (Figure 4.6), suggesting that the KChIPs may be more important regulators of trafficking in HeLa cells. This would be consistent with the smaller size of electrophysiological effects seen with SAP97 (El-Haou et al. 2009) compared to those seen in other experiments with the KChIPs (An et al. 2000). However, the EGFP-SAP97 still had a significant effect, suggesting that it

should be considered a possible regulator of Kv4 channels, alongside those discussed in Section 1.4.

In Chapter 3 it was shown that the trafficking of Kv4.2 by KChIP1 was via a non-conventional pathway, requiring the SNARE proteins VAMP7 and Vti1a. Having confirmed that SAP97 could also promote Kv4.2 trafficking, it was of interest to determine whether it also occurred via this non-conventional route. Figure 4.5 shows the effects of VAMP7 RNAi on the trafficking of untagged Kv4.2 with either KChIP1-EYFP or EGFP-SAP97. Whilst the VAMP7 RNAi could inhibit trafficking with KChIP1 as seen previously, it had no effect on trafficking of the channel with EGFP-SAP97. This confirms that EGFP-SAP97 does not promote the trafficking of the Kv4.2 channel to the plasma membrane via the same non-conventional pathway as KChIP1. It is, therefore, likely to utilise the conventional COPII-coated vesicle pathway (Glick 2000), and this could be confirmed by experiments with either Sec22 RNAi (Xu et al. 2000), or a Sar1 dominant negative mutant (Hasdemir et al. 2005). Whichever exocytic pathway is used, it is clear that EGFP-SAP97 can abolish the Golgi localisation seen when the channel is expressed alone (O'Callaghan et al. 2003; Hasdemir et al. 2005). This suggests that an interaction between SAP97 and Kv4.2 may be occurring somewhere at or before the Golgi apparatus, even though the SAP97 is generally localised to the plasma membrane (Figure 4.13). This highlights an important intracellular and trafficking role for SAP97, as has been discussed elsewhere in the literature (Horio et al. 1997; Tiffany et al. 2000; El-Haou et al. 2009), in addition to its role of clustering and scaffolding at the plasma membrane (Horio et al. 1997).

A surprising finding was the inability of SAP97 to significantly promote Kv4.2 trafficking to the plasma membrane in Neuro2A cells, even though these should be a better model cell type for neurons where these proteins are expressed *in vivo*. These experiments (Figure 4.7) were performed with mCherry-tagged Kv4.2, and this was less efficiently trafficked to the plasma membrane by SAP97 in HeLa cells than the untagged form of the channel. It may be that this difference is simply more marked in Neuro2A cells. Alternatively, it is possible that the results reflect real differences between the cell types used. This could

include different post-translational modifications of the proteins, affecting their ability to interact. In particular, phosphorylation of target proteins is known to be a general mechanism for the regulation of MAGUK interactions (Kim and Sheng 2004; Gardoni et al. 2007). Other proteins expressed by this cell type could also possibly influence the interactions. It would, therefore, be interesting to carry out further experiments to confirm this cell-specific difference. For example, does SAP97 interact with Kv4.2 in co-immunoprecipitation experiments using Neuro2A cell lysates? Also, could a non-phosphorylatable mutant of either protein restore their interaction and trafficking?

Perhaps the most surprising and intriguing result of this chapter was the observation that whilst either SAP97 or KChIP1 alone promoted Kv4.2 trafficking to the plasma membrane, when expressed together, all proteins appeared trapped within intracellular compartments. That is, the co-expression of SAP97 with KChIP1 seemed to antagonise the trafficking ability that either protein has when expressed alone with Kv4.2. This occurred for both tagged and untagged Kv4.2, and in both HeLa and Neuro2A cells (Figures 4.4, 4.6 and 4.7). In addition, the trafficking of Kv4.2 by KChIP2 was also suppressed by co-expression with SAP97 in both cell types used. These experiments were important for several reasons. Firstly, KChIP2 does not require the same non-conventional pathway as KChIP1, so it is clear SAP97 is not having a specific effect on that pathway. In addition, the SAP97 does not traffic Kv4.2 via a VAMP7-dependent pathway, and yet its ability to traffic the channel is also lost in the triply transfected cells. Moreover, whilst KChIP1 and SAP97 are localised intracellularly with Kv4.2 in the triple transfected cells (e.g. Figures 4.4G-J), much of the KChIP2 and SAP97 are still localised to the plasma membrane in triply transfected cells (e.g. Figure 4.8B). The most plausible explanation for this is that the SAP97 and KChIPs interact, and this prevents their interaction with the Kv4.2 channel. In the case of KChIP1, this could occur in the intracellular punctate vesicles where KChIP1 localises when expressed alone. KChIP2, on the other hand, is associated with the plasma membrane, as is SAP97, and so their interaction could occur there. An interesting area for further study would be to investigate KChIPs 3 and 4, to see if SAP97 also prevented them from stimulating traffic of Kv4 channels to the plasma membrane, and also where the

three proteins localise. It seems, however, that further studies into the trafficking of Kv4 channels need to investigate the combined effects of several regulatory proteins to determine their full effects in cells. This is potentially of importance, as the expression of SAP97 is widespread throughout the brain and myocardium (Muller et al. 1995; El-Haou et al. 2009), so it is likely that it will be expressed in cells that are also expressing Kv4.2 and a KChIP. The findings also raise many questions. If this co-expression of SAP97 prevents Kv4.2 trafficking to the plasma membrane, there may be some regulation of this when neurons require trafficking of the channel. This could for example be via phosphorylation, altering the binding of SAP97, by changing calcium levels sensed by the KChIP, or by some other signalling mechanism. Understanding this will be vital to fully comprehending any role for this interaction *in vivo*.

As well as SAP97 having effects on both KChIP1 and 2, there are effects with other members of the PSD-95 family. Unlike SAP97, the three isoforms of PSD-93 that were tested could not promote the trafficking of Kv4.2 to the plasma membrane in HeLa cells. They could, however, all prevent the trafficking of KChIP1/Kv4.2 to the plasma membrane in triply transfected HeLa cells (Figure 4.9). It seems likely, therefore, that this inhibitory interaction is a general feature of all KChIPs and all PSD-95 family members although more experiments would be required to fully confirm this. It does at least seem likely that there is a shared mechanism for this inhibitory action. Again, the most likely seems to be a direct interaction between certain PSD-95 family members and KChIP1 that prevents the KChIP from interacting with the channel. In support of this, experiments with the δ-isoform of PSD-93 revealed that when it was expressed alone it was diffusely intracellular in localisation, but when co-expressed with KChIP1-EYFP, became punctate and co-localised with the KChIP1, in both HeLa and Neuro2A cells (Figures 4.10 and 4.11). This would suggest that the expression of KChIP1 in these cells was able to alter the localisation of the PSD-93, through some kind of interaction. The related protein PSD-95 was also investigated. This showed a plasma membrane localisation both in the presence and absence of KChIP1 (Figure 4.11), and the two proteins showed a very low level of co-localisation. This could indicate that binding to the KChIPs is specific to some members of the PSD95-family. Alternatively, interactions could be occurring,

that have little effect on the distribution of PSD-95. An important first step in any future work would therefore be to confirm if there are any interactions between KChIP1 and PSD-93 or PSD-95. This would best be achieved through direct binding assays.

PSD-93δ co-localised with KChIP1 in doubly transfected Neuro2A cells (Figure 4.11), as it did in HeLa cells (Figure 4.10). However, there were differences in the localisation of proteins in the triply transfected cells. Whilst all three proteins were co-localised and intracellular in HeLa cells (Figure 4.10), in Neuro2A cells, some of each protein was present at the plasma membrane (Figure 4.11). This was particularly noticeable for KChIP1 and Kv4.2, but was also the case for PSD-93δ. This is similar to the experiments with SAP97 in triply transfected Neuro2A cells (Figure 4.7), where more protein was plasma membrane associated than in triply transfected HeLa cells. There are several possibilities for why these two cell types should show differing effects. One is that the relative expression level of proteins in the two cell types may not be the same. For example, KChIP1 may be expressed at a higher level than PSD-93δ. Whilst much of the KChIP1 would therefore be bound to the PSD-93δ and unable to bind the Kv4 channel, the higher expression level would mean some would be free to bind the Kv4.2 channel and traffic it to the plasma membrane. Another possibility is that the other proteins or signalling cascades in Neuro2A cells may inhibit the interaction of the SAP97/PSD-93 with KChIP1, thus explaining why some KChIP1 is able to traffic Kv4.2 to the membrane. It will obviously be important to characterise such differences in future work, for example, by comparing results using primary neurons, as the Neuro2A cells should be more representative of neuronal cells where these proteins would be expressed together.

The work discussed suggested that some members of the PSD-95 family of proteins might be able to interact directly with the KChIPs. The clearest effects had been seen with SAP97, and so this was investigated more fully. Firstly, EGFP-SAP97 under these experimental conditions was associated with the plasma membrane in both HeLa and Neuro2A cells (Figures 4.13A and 4.14A). This was also the localisation seen in cells expressing SAP97 with Kv4.2 (e.g.

Figures 4.4D-F). It was therefore interesting to ask whether the co-expression of EGFP-SAP97 with KChIP1 would lead to an interaction, and a change in the localisation of SAP97 away from the plasma membrane, as seen in triply transfected cells. This was indeed the case, in both HeLa and Neuro2A cells (Figures 4.13 and 4.14). The punctate distribution of SAP97 in these cells, co-localised with KChIP1-EYFP, is highly suggestive of a SAP97/KChIP1 interaction. An untagged version of KChIP1 was also used in HeLa cells (Figure 4.13E), to ensure that there were no effects due to bleed through of the fluorescence between EYFP and GFP signals. However, the localisation of SAP97 was also changed to intracellular punctae in this experiment. In Neuro2A cells, some SAP97 remained at the plasma membrane in the presence of KChIP1. As discussed above, there do seem to be differences in the behaviour of these proteins between the two cell types investigated. It will require further investigation to discover the underlying mechanisms and significance of this.

The ability of KChIP1 to alter the localisation of EGFP-SAP97 suggested the hypothesis that they could directly interact. In Figure 4.6, it was also shown that SAP97 could reduce the level of Kv4.2 trafficking in the presence of KChIP2-ECFP. It was therefore interesting to see what happened in cells co-transfected with EGFP-SAP97 and KChIP2-ECFP. As shown in Figure 4.15, both the SAP97 and KChIP2 were localised to the plasma membrane in these cells. As discussed previously, one possibility is that the SAP97 is binding to the KChIP2 at the plasma membrane, preventing its interaction with the Kv4 channel, and hence preventing the channel trafficking. To fully confirm this, it would be necessary to directly show a KChIP2-SAP97 interaction.

If SAP97 can interact with the KChIPs, as suggested from this work, then it may be necessary for the cell to have some mechanism to regulate this. One possibility for this is that changes in the level of free Ca^{2+} ions could be sensed by the KChIP through its EF-hand domains, and this could alter its ability to interact with SAP97. To investigate this, the effects of EF-hand mutants of KChIP1 on the localisation of EGFP-SAP97 were investigated (Figure 4.16). As shown in Figure 4.16, both the single (EF3) and triple (EF2-4) mutants of KChIP1-EYFP caused a change in the localisation of SAP97 from the plasma

membrane to intracellular punctae that co-localised with the mutant KChIPs. This would argue that the binding of Ca^{2+} by KChIP1 has no effect its ability to interact with SAP97, and hence that it is not a mechanism for *in vivo* regulation.

A final set of experiments were performed, using biochemical techniques to look for an interaction between KChIP1 and SAP97. This included blotting pull-downs from bovine brain cytosol, performing binding assays with *in vitro* transcribed and translated SAP97 protein, and trying immunoprecipitations with lysates from transfected HeLa cells. None of these experiments produced convincing evidence of an interaction between KChIP1 and SAP97. The change in localisation of SAP97 when co-expressed with KChIP1 would certainly suggest some kind of interaction, and hence further work will be needed to see if this can be replicated biochemically. It will also be important to show whether such an interaction is direct, or requires other proteins to mediate it. The potential importance of such an interaction in regulating Kv4 channel trafficking make this area highly interesting for future study.

The major findings from this chapter included the demonstration that EGFP-SAP97 could promote the trafficking of Kv4.2 to the plasma membrane via a VAMP7-independent pathway. Surprisingly, when EGFP-SAP97, KChIP1-EYFP and Kv4.2 were all co-expressed, none of the proteins were localised to the plasma membrane. In fact, co-expression of EGFP-SAP97 with KChIP1 was also able to re-localise the SAP97 away from the plasma membrane, to a punctate distribution co-localised with KChIP1. This suggests an interaction between SAP97 and KChIP1, which prevents either protein from binding and trafficking Kv4 channels. Finally, it appears that SAP97 can also bind KChIP2, and that KChIP1 can also bind to at least some isoforms of PSD-93. Together, the data presented here suggest a novel mechanism for the regulation of Kv4.2 trafficking, whereby either the SAP97 or the KChIP alone can promote channel trafficking, but expression together leads to them binding each other rather than the channel.

Chapter 5

Discussion

5. Discussion

The work presented in this thesis has focussed on the trafficking of Kv4.2 potassium channels from the ER to the plasma membrane. As members of the Kv4 family of channels, these proteins are responsible for rapidly inactivating, A-type potassium currents in both neurons (Hoffman et al. 1997; Tkatch et al. 2000; Birnbaum et al. 2004) and cardiac myocytes (Isbrandt et al. 2000; Rosati et al. 2001). Such currents have a role in regulating the excitability of the cell (Maffie and Rudy 2008), and, in neurons, contribute to the modulation of synaptic strength needed for learning and memory (Ramakers and Storm 2002). The expression level of Kv4 channels at the plasma membrane determines A-type current density (An et al. 2000), and hence regulation of channel trafficking to the plasma membrane is a key way that the cell can control such currents. To facilitate this regulation, there are several accessory proteins that can bind to the Kv4 channels to promote or retard their trafficking (see section 1.4). The work presented in this thesis has concentrated on a few groups of these proteins, particularly the KChIPs, the 14-3-3 proteins, and the PSD-95 family of MAGUK proteins.

One of the most intriguing previous findings in the literature was that Kv4.2 and KChIP1 traffic via a pathway that requires COPI but not COPII (Hasdemir et al. 2005). The work in this thesis has now also shown that the SNAREs involved in this trafficking are different from the standard complex. This confirms the theory that Kv4.2/KChIP1 trafficking is via a non-conventional pathway. The features of this pathway do not fully fit with those of other known non-conventional ER-Golgi routes (see section 1.5.6). However, the mechanisms used in these alternate pathways suggest some possibilities for Kv4.2/KChIP1 trafficking. One possibility is that vesicles bud directly from the ER with a COPI coat, as seen in yeast (Bednarek et al. 1995). This would then be the coat used for both the ER-ERGIC and ERGIC-Golgi steps in trafficking. Another is that COPII may not be required for trafficking, but may still play a role in ER budding, as is the case for procollagen (Stephens and Pepperkok 2002; Stephens and Pepperkok 2004). This could explain why the experiments in Hasdemir et al. (2005) show a partial

inhibition of trafficking with the COPII mutant. Finally, COPII-independent budding from sites away from ER exit sites has been shown for mis-folded luminal glycoproteins. These vesicles have no discernable coat proteins (Zuber et al. 2007). Immuno-electron microscopy has been used to show that KChIP1-labelled vesicles are not COPII coated (Hasdemir et al. 2005), but this work could be extended to look for alternative coat complexes, and to visualise vesicles budding from the ER, to shed further light on this pathway.

Many of the proteins associated with non-conventional trafficking routes are in some way unusual, for example because of their size (e.g. procollagen) or post-translational modifications (e.g. GPI-anchored proteins) (Stephens and Pepperkok 2002; Castillon et al. 2009). It is unclear why cells would have two ER-Golgi pathways for transmembrane proteins on route to the plasma membrane. It certainly seems that Kv4.2 and KChIP1 pass through the ERGIC, and go to the Golgi (O'Callaghan et al. 2003), as well as going through a COPI-coated vesicle stage (Hasdemir et al. 2005). In support of this, the work in this thesis has shown a requirement for Rab1 in trafficking, a protein known to be important in ER-Golgi trafficking (Tisdale et al. 1992). Also, the original identification of the VAMP7/Vti1a/rBet1/syntaxin 5 SNARE complex was in an ER-Golgi pathway (Siddiqi et al. 2006a). Therefore the non-conventional pathway is not just used by proteins bypassing the Golgi. One possible answer is that the cell uses alternative pathways to allow an early level of cargo sorting before the Golgi. This certainly seems to be the case for some cargoes in yeast (Castillon et al. 2009), and in mammalian cells (Takida et al. 2008), although there is no evidence in the literature of two vesicle populations for transmembrane proteins. The non-conventional pathway described in Chapter 3 could therefore represent the trafficking of alternatively sorted cargo.

To determine if this non-conventional pathway does represent a preliminary sorting of cargo from the ER, it will be important to identify other proteins trafficking via this pathway. The ER-Golgi role of VAMP7 and Vti1a was discovered in the intestine for the trafficking of PCTVs (Siddiqi et al. 2006a;

Siddiqi et al. 2006b). However, this represents a very unusual cargo, found only in the intestine, in vesicles lacking COPI, and only needing COPII for fusion with the Golgi, not for ER budding (Siddiqi et al. 2003). These original papers argued that this pathway was specific to the intestine, as they could not find VAMP7 localised to the ER in liver or kidney cells (Siddiqi et al. 2006b). However, the work in this thesis would argue that at least the SNARE complex of this pathway is more widespread, present in HeLa and Neuro2A cells. What remains unclear is the connection between PCTVs and Kv4.2/KChIP1, and what allows them to traffic along a pathway using the same SNAREs. If other proteins can be identified that also require this SNARE complex then common features of cargo on this pathway, or a common signalling motif, could be identified. One issue is that much previous work in the literature has concentrated on the trafficking of VSVG (Katz et al. 1977a; Katz et al. 1977b; Presley et al. 1997) but this is not trafficked via the same pathway as Kv4.2/KChIP1. As more non-conventional trafficking pathways are identified, it becomes increasingly apparent that more work needs to be done to characterise the trafficking of individual proteins, rather than simply relying on VSVG as a characteristic exocytic marker. An intriguing possibility for further study would be the KCNE1 β accessory subunit for Kv7 channels. When expressed alone, this localises to an unidentified compartment (Chandrasekhar et al. 2006), and so could be behaving like KChIP1, and thus utilising the same pathways for exocytic trafficking of potassium channels.

To try and characterise which other proteins could use this non-conventional pathway, experiments were performed to look at the trafficking of Kv4.2 by KChIP2. Surprisingly, this was not inhibited by the siRNA knockdown of VAMP7 or Vti1a. Although similar at their C-termini, KChIP1 and KChIP2 differ at their N-termini, and in the way in which they are post-translationally modified (Burgoyne 2007). In particular KChIP1 is myristoylated (O'Callaghan et al. 2003), whilst KChIP2 is palmitoylated (Shibata et al. 2003). It could be this modification and the difference in intracellular localisation that it causes that underlies the different trafficking pathways used. In future, these trafficking experiments could be repeated using the alternative splice isoform of KChIP2,

KChIP2c, as this is not palmitoylated (Takimoto et al. 2002). This would therefore reveal whether it is in fact the palmitoylation of KChIP2, or some other region of its sequence, that leads to it using a different trafficking pathway from KChIP1. It would seem most likely that if KChIP2 does not use the non-conventional pathway characterised in this study, it uses the standard COPII-COPI-coated vesicle route. An interesting study could therefore be to use the Sec22 RNAi used in this thesis, or the Sar1 COPII dominant negative mutant used in Hasdemir et al. (2005) to confirm any requirement for the standard pathway. In addition, KChIP3 is palmitoylated (Takimoto et al. 2002), whilst the other NCS proteins are predicted to be myristoylated (O'Callaghan et al. 2005) (and NCS-1 has been shown to traffic Kv4.2 to the plasma membrane (Nakamura et al. 2001b)). It would therefore be interesting to perform experiments with these proteins to see if they behave more like KChIP1 or KChIP2.

The KChIPs, as members of the NCS family of proteins, have highly conserved EF-hand domains able to bind to Mg^{2+} and Ca^{2+}, and may act as Ca^{2+}sensors (Burgoyne 2004; Burgoyne 2007). Many NCS proteins are myristoylated, and this myristoyl tail is often only exposed when the protein is Ca^{2+}-bound, allowing the protein to bind to cellular membranes (Ames et al. 1997; O'Callaghan et al. 2003). However, the myristoyl tail is constitutively exposed in KChIP1 (O'Callaghan et al. 2003), and the effects of Ca^{2+} on KChIP structure are debated in the literature. The best studied work is on the dissociation of KChIP3 from DNA in a Ca^{2+}-bound state (Carrion et al. 1999; Osawa et al. 2001). In work on Kv4 channels, it was originally argued that intact EF-hand domains were needed for KChIP1 to have effects on channel kinetics and trafficking, but not for binding to the channel (An et al. 2000). More recently this has been disputed, with experiments claiming that a triple EF-hand mutant could not bind Kv4.3 (Pioletti et al. 2006). In this thesis it was shown that either a single or triple EF-hand mutant of KChIP1 prevented Kv4.2 trafficking to the plasma membrane, but both caused a redistribution of the channel to punctae co-localised with the mutant KChIP1.This supports the idea of Ca^{2+} dependent and independent roles proposed by Patel et al. (2004). Intriguingly, the reason why the channel does not traffic with the mutant KChIP1 is not known. It may be that the KChIP can only

bind to an additional protein, for example a coat protein, trafficking regulator, or cytoskeleton binding protein, when in a Ca^{2+}-bound state. Performing pull down assays with both the wild-type and mutant proteins, and determining differences between their interactions, could help identify proteins important in channel trafficking.

Two groups of proteins important in regulating intracellular trafficking were also investigated for their role in Kv4.2/KChIP1 trafficking. These were the SNAREs and the Rabs. As discussed above, the non-conventional trafficking pathway characterised in Chapter 3 was shown to require the SNAREs VAMP7 and Vti1a. However, this was quite surprising, as both SNAREs are more commonly associated with trafficking between the endosomes and lysosomes (Bogdanovic et al. 2002; Pryor et al. 2004; Casey et al. 2007). It was possible to show that VAMP7 only partially co-localised with the lysosomal marker LAMP1. Still, it should be noted that *in vitro* SNARE complex formation is promiscuous, as long as the general $Q_AQ_BQ_CR$ formula is observed (Fasshauer et al. 1999; Yang et al. 1999(1)). It has been argued that it is the localisation of the SNAREs that gives them their specificity, and hence that the complement of SNAREs on a compartment defines it (Jahn and Scheller 2006). However, the work by Siddiqi et al. (2006b) showed that VAMP7 can be present in the ER of intestinal cells, in addition to its better characterised location on the lysosomes in many other cell types (Advani et al. 1998; Advani et al. 1999; Martinez-Arca et al. 2003). By showing a requirement for VAMP7 in ER-plasma membrane trafficking, at least in HeLa and Neuro2A cells, the work presented here suggests this SNARE is present on at least two cellular compartments, fulfilling two separate roles. This may suggest that the SNAREs are more multifunctional in the cell than has been previously assumed. It may be that the SNAREs, whilst providing the machinery for membrane fusion, are less important in determining specificity than tethers and other proteins such as the Rabs.

In this study, the Rab1-GAP TBC1D20 was used to reduce Rab1 activity in cells (Haas et al. 2007). This Rab is known to be important in ER-Golgi trafficking

(Tisdale et al. 1992), but some Rab1-independent pathways are known in the literature (Yoo et al. 2002; Wu et al. 2003). However, in this study, Rab1 was required for KChIP1/Kv4.2 trafficking, and for the trafficking of VSVG. This Rab does not therefore distinguish between the two pathways. This may highlight the action of Rab1 at the later trafficking step from ERGIC to Golgi, involving COPI coated vesicles, which may be shared by both pathways. Alternatively, by reducing the level of active Rab1 in these cells, the Golgi may be more generally disrupted (Haas et al. 2007). Another interesting protein for further study would be Rab2. This is also associated with ER-Golgi trafficking (Tisdale et al. 1992), and may be specific for one of the two pathways discussed in this thesis. Discovering specific regulators of this non-conventional pathway would be very useful for future studies.

Two other families of proteins that might regulate Kv4 trafficking were also investigated in this thesis. These were the 14-3-3 proteins and the PSD-95 family of MAGUKs. Importantly, it was not just the potential interaction of these proteins with the Kv4 channel α subunits themselves that was of interest, but potential interactions between these proteins and the KChIPs. There are several examples of regulators in the literature that only appear to have their effects on Kv4 channels in the presence of KChIP1 (see section 1.4), and others that have differing effects on the channel when a KChIP is also present, forming ternary complexes (for example the DPP proteins (Jerng et al. 2005; Radicke et al. 2005)). Whilst studying the effects of these proteins individually is important for understanding their actions on the channel, *in vivo* the cell may well be expressing a range of potential channel regulators. It is also therefore important to study the effects of these proteins in combination. One of the best studied complexes in the literature is of Kv4 channels with a KChIP and DPP family protein (Jerng et al. 2005; Radicke et al. 2005). From the work in Chapter 3 it would certainly be interesting to ask whether, when this complex contains Kv4.2 and KChIP1, it is trafficked via the non-conventional pathway characterised in this thesis.

To identify proteins that interact with KChIP1, and thus might be important for its intracellular functions, a yeast two-hybrid screen was performed by Dr L. Haynes. This suggested that 14-3-3γ could interact with KChIP1 (Dr L. Haynes, personal communication), and so this was investigated further in this thesis. In support of this, there was partial co-localisation between KChIP1-EYFP expressed in HeLa cells, and endogenous 14-3-3γ detected by immunostaining. However, pull-down assays using GST-KChIP1 and bovine brain samples did not show an interaction with 14-3-3γ, or the related isoform 14-3-3β. An interaction between KChIP1 and 14-3-3γ could not therefore be confirmed. It would be interesting to revisit the results of this yeast-two hybrid screen, or perform a new screen, in the quest for novel KChIP1 binding proteins. A larger scale study to compare the interactomes of the 4 different KChIPs would also be interesting, to determine which interactions are important for the various functions of different KChIP isoforms. Also, the work in Chapter 4 suggests an interaction between the KChIPs and PSD-95 family of proteins, and it would be interesting to see if such interactions could also be shown using the yeast two-hybrid method.

The PSD-95 family of MAGUKs are known for their functions in the post-synaptic densities of neurons, where they have documented roles in clustering transmembrane proteins (Kim and Sheng 2004; Bats et al. 2007), and regulating their trafficking to the plasma membrane (Jeyifous et al. 2009). There is evidence that SAP97 can promote the trafficking of Kv4 channels to the plasma membrane (Gardoni et al. 2007; El-Haou et al. 2009), and this was confirmed in this study, at least in HeLa cells. It was also shown, using VAMP7 RNAi, that it does not use the same non-conventional trafficking pathway as KChIP1. However, little work has been done on the combined effects of the KChIPs and PSD-95 family of proteins on Kv4.2 trafficking and function (El-Haou et al. 2009). The work in Chapter 4 suggests that in fact, there is an interaction between at least some members of both protein families. The possible interaction is potentially interesting and important to the *in vivo* regulation of Kv4 channel trafficking. The expression of both these families of proteins is widespread in the brain, and SAP97 is also found in the heart (Muller et al. 1995; Rhodes et al. 2004), so it is

likely that both will be expressed in the same cells. However, the above work shows that when KChIP1 or 2 and SAP97 or PSD-93δ/ε/ζ are expressed together, they inhibit the ability of Kv4.2 to traffic to the plasma membrane. Both SAP97 and KChIP1 can, individually, promote channel trafficking, so when expressed together, it could be assumed that there would be an additive effect of their expression on channel trafficking. This was not seen in either HeLa or Neuro2A cells, using either tagged or untagged Kv4.2. Interestingly, this same inhibitory effect was also seen for SAP97 with KChIP2, arguing that such effects are not dependent on the non-conventional trafficking of KChIP1. This effect was also seen with the three tested isoforms of PSD-93, even though these were unable to promote the trafficking of the channel to the plasma membrane on their own. One likely possibility, then, is that SAP97 or PSD-93 binds to the KChIPs, and that this interaction prevents either protein from interacting with the Kv4 channel. In support of this, co-expression with KChIP1 alters the localisation of SAP97 from the plasma membrane to intracellular punctae, and PSD-93δ from a diffuse distribution in the cytoplasm to distinct punctae. In both cases, the KChIP and the MAGUK are at least partially co-localised when co-expressed. This interaction does not appear to require the KChIP to have bound Ca^{2+}, as this change in localisation was also seen with EF-hand mutants of KChIP1. Attempts to demonstrate an interaction between KChIP1 and SAP97 by use of immunoprecipitation were not convincingly successful and further work will be required to establish if these proteins do indeed interact directly or indirectly.

If an interaction between SAP97 and KChIP1, or a more general interaction between members of these protein families, can be confirmed, it will raise many questions about how this is regulated *in vivo*. This observed inhibition of Kv4 channel traffic would need to be overcome for the cell to express the channel at the plasma membrane and this could be further investigated. Some cell type specific differences were observed in the experiments in this thesis which would also warrant further investigation.

Interestingly, the induction of long-term potentiation (LTP) in neurons is associated with the insertion of AMPA receptors into the post-synaptic membrane, and the internalisation of Kv4 channels (Kim et al. 2007). The MAGUK proteins are known to have trafficking and clustering roles associated with AMPA receptors (DeGiorgis et al. 2006; Bats et al. 2007). It could be that the inhibition of Kv4 trafficking seen in this thesis is also important *in vivo* for regulating synaptic plasticity. The changes in signalling associated with LTP induction could lead to the interaction of SAP97 with the KChIPs, and hence prevent further trafficking of Kv4 channels to the plasma membrane. Again, an understanding of the mechanisms for regulating this would be important for future work. In addition, many cytoskeleton binding proteins have been implicated in regulating Kv4 channel trafficking and function (Petrecca et al. 2000; Wang et al. 2004; Chu et al. 2006). SAP97 also interacts with the actin motor myosin VI (Wu et al. 2002), and so could be important for associating the Kv4 channels with the cytoskeleton. This could play a role in regulating either exocytic trafficking, or channel internalisation away from the plasma membrane.

One well known mechanism of regulating MAGUK protein interactions is through phosphorylation of the target protein, or MAGUK itself (Kim and Sheng 2004; Gardoni et al. 2007). Interaction experiments could thus be repeated with mutant proteins to see if this is the case. These could have serine, threonine or tyrosine residues that are potentially phosphorylated, mutated to residues such as alanine, which are not. Alternatively, such residues could be replaced with amino acids with bulkier, phosphomimetic side chains, to see if this prevented an interaction. These studies could also reveal whether the sites of interaction between SAP97 and KChIP1 are the same as those used for interaction with the channel, which could explain why such an interaction prevents channel trafficking.

In conclusion, the trafficking of Kv4.2 channels by KChIP1 to the plasma membrane is via a non-conventional pathway, requiring Rab1 and the SNAREs VAMP7 and Vti1a. Discovering other proteins that use this pathway will be

important in further characterising it, and in determining how wide-spread and conserved it is in cellular function. In addition, there is evidence to suggest an interaction between SAP97 and KChIP1, that inhibits Kv4 channel trafficking. This could play a role in the regulation of neuronal activity. Future work will need to characterise this interaction, to determine if other members of these protein families can also interact, and to establish the ways in which such interactions are regulated within the cell.

Publications

Some of the work presented in this thesis has been previously published:

Flowerdew, S.E., and R.D. Burgoyne. 2009. A VAMP7/Vti1a SNARE complex distinguishes a non-conventional traffic route to the cell surface used by KChIP1 and Kv4 potassium channels. *Biochemical Journal.* 418:529-540.

Acknowledgments

I would like to thank my superb supervisor, Bob Burgoyne, for his help and support throughout my PhD, and for showing me how to turn a collection of experiments into a cohesive story. I would also like to thank everyone in Red Block - you have helped to make my PhD such an enjoyable experience. To Alan Morgan and Jeff Barclay for their useful suggestions in lab talks, to Lee Haynes for teaching me about cell culture and the magic of Western blotting, to Margaret Graham for teaching me the dark arts of pull downs and immunoprecipitation, as well as listening to my moans when things weren't working, and to Mark Handley for the strangely indescribable conversations about science (and Private Eye). To Ciara and Hannah, for distracting me with the stick insects, to Michele for explaining Switzerland, and to James, who made sure I didn't become radioactive. I also couldn't have done this without Helen and Geoff, who keep the lab running. Lunch wouldn't have been the same without Brian and his crosswords. I'd also like to thank the many past members of the lab – especially Neil, who introduced me to the ways of Red Block, Dan, for finding time to teach me neuronal preparation whilst writing a thesis, and Mark E for providing some competition to get the writing done! Finally, much of this work came out of the PhD project of Burcu Hasdemir, whose preparation of plasmids saved me months of hardship at the start of my PhD. I am forever grateful to her, and all those who provided me with plasmids and reagents, and the Wellcome Trust for funding this work.

I'd also like to thank Carol and Islay, for introducing me to pottery just when I needed a distraction from it all. Thanks for listening to the moans and the panic on a Tuesday. I'd like to thank everyone in my MRes year - Seb, Stu, Abdulwahab, Chris, Helen, Michele and Hannah – for getting me through that first year. I'd also like to thank my undergraduate tutor, Louis Mahadevan, for showing me that research wasn't just undergraduate practical labs, and for sitting me with Carol and Tim that night – it is their fault I ended up in Liverpool at all. I'd like to thank my grandparents – they always insisted that I got my brains from them. I'd like to thank my parents, for always being supportive, even if it wasn't a proper job, even if it meant looking up mitochondria on the internet in the middle of the night, and even if it meant turning the kitchen into a lab to extract the DNA from a tomato. Finally, I'd like to thank Mike. He has been an unfailing support throughout all of this, and always believes me to be a better scientist than I know I am. Thank you.

References

Advani, R.J., H-R. Bae, J.B. Bock, D.S. Chao, Y-C. Doung, R. Prekeris, J-S. Yoo, and R.H. Scheller. 1998. Seven novel mammalian SNARE proteins localize to distinct membrane compartments. *Journal of Biological Chemistry.* 273:10317-10324.

Advani, R.J., B. Yang, R. Prekeris, K.C. Lee, J. Klumperman, and R.H. Scheller. 1999. VAMP-7 mediates vesicular transport from endosomes to lysosomes. *Journal of Cell Biology.* 146:765-775.

Aitken, A., H. Baxter, T. Dubois, S. Clokie, S. Mackie, K. Mitchell, A. Peden, and E. Zemlickova. 2002. Specificity of 14-3-3 isoform dimer interactions and phosphorylation. *Biochemical Society Transactions.* 30:351-360.

Alberts, B., A. Johnson, J. Lewis, M. Raff, K. Roberts, and P. Walter. 2008. "Molecular Biology of the Cell." 5th edition, Garland Science, New York, USA. Chapter 11, pp651-694.

Alonso, G., and H. Widmer. 1997. Clustering of Kv4.2 potassium channels in postsynaptic membrane of rat supraoptic neurons: an ultrastructural study. *Neuroscience.* 77:617-621.

Ames, J.B., R. Ishima, T. Tanaka, J.I. Gordon, L. Stryer, and M. Ikura. 1997. Molecular mechanics of calcium-myristoyl switches. *Nature*. 389:198-202.

An, W.F., M.R. Bowlby, M. Betty, J.Cao, H-P. Ling, G. Mendoza, J.W. Hinson, K.I. Mattsson, B.W. Strassle, J.S. Trimmer, and K.J. Rhodes. 2000. Modulation of A-type potassium channels by a family of calcium sensors. *Nature* 403: 553-556.

Antonin, W., D. Riedel, and G. Fischer von Mollard. 2000. The SNARE Vti1a-β is localized to small synaptic vesicles and participates in a novel SNARE complex. *Journal of Neuroscience.* 20:5724-5732.

Apolloni, A., I.A. Prior, M. Lindsay, R.G. Parton, and J.F. Hancock. 2000. H-ras but not K-ras traffics to the plasma membrane through the exocytic pathway. *Molecular and Cellular Biology.* 20:2475-2487.

Aravind, P., K. Chandra, P.P. Reddy, A. Jeromin, K.V.R. Chary and Y. Sharma. 2008. Regulatory and structural EF-hand motifs of neuronal calcium sensor-1: Mg^{2+} modulates Ca^{2+} binding, Ca^{2+}-induced conformational changes, and equilibrium unfolding transitions. *Journal of Molecular Biology.* 376:1100-1115.

Arnold, D.B. 2006. Polarized targeting of ion channels in neurons. *Pflugers Archiv.* 453:763-769.

Bahring, R., J. Dannenberg, H.C. Peters, T. Leicher, O. Pongs, and D. Isbrandt. 2001. Conserved Kv4 N-terminal domain critical for effects of Kv channel-interacting protein 2.2 on channel expression and gating. *Journal of Biological Chemistry.* 276:23888-23894.

Balch, W.E., W.G. Dunphy, W.A. Braell, and J.E. Rothman. 1984. Reconstitution of the transport of protein between successive compartments of the Golgi measured by the coupled incorporation of N-acetylglucosamine. *Cell.* 39:405-416.

Bannykh, S.I., T. Rowe, and W.E. Balch. 1996. The organization of endoplasmic reticulum export complexes. *Journal of Cell Biology.* 135:19-35.

Barlowe, C., L. Orci, T. Yeung, M. Hosobuchi, S. Hamamoto, N. Salama, M.F. Rexach, M. Ravazzola, M. Amherdt, and R. Schekman. 1994. COPII: a membrane coat formed by Sec proteins that drive vesicle budding from the endoplasmic reticulum. *Cell.* 77:895-907.

Bats, C., L. Groc, and D. Choquet. 2007. The interaction between Stargazin and PSD-95 regulates AMPA receptor surface trafficking. *Neuron.* 53:719-734.

Beck, E.J., M. Bowlby, W.F. An, K.J. Rhodes, and M. Covarrubias. 2002. Remodelling inactivation gating of Kv4 channels by KChIP1, a small-molecular-weight calcium-binding protein. *Journal of Physiology.* 538.3:691-706.

Bednarek, S.Y., M. Ravazzola, M. Hosobuchi, M. Amherdt, A. Perrelet, R. Schekman, and L. Orci. 1995. COPI- and COPII-coated vesicles bud directly from the endoplasmic reticulum in yeast. *Cell.* 83:1183-1196.

Bentley, M., Y. Liang, K. Mullen, D. Xu, E. Sztul, and J.C. Hay. 2006. SNARE status regulates tether recruitment and function in homotypic COPII vesicle fusion. *Journal of Biological Chemistry.* 281:38825-38833.

Berg, D., C. Holzmann, and O. Riess. 2003. 14-3-3 proteins in the nervous system. *Nature Reviews: Neuroscience.* 4:752-762.

Bernards, A. 2003. GAPs galore! A survey of putative Ras superfamily GTPase activating proteins in man and Drosophila. *Biochimica et Biophysica Acta.* 1603:47-82.

Berridge, M.J., P. Lipp, and M.D. Bootman. 2000. The versatility and universality of calcium signalling. *Nature Reviews: Molecular Cell Biology.* 1:11-21.

Birnbaum, S.G., A.W. Varga, L-L. Yuan, A.E. Anderson, J.D. Sweatt, and L.A. Schrader. 2004. Structure and function of Kv4-family transient potassium channels. *Phsyiological Reviews.* 84:803-833.

Bixby, K.A., M.H. Nanao, N.V. Shen, A. Kreusch, H. Bellamy, P.J. Pfaffinger, and S. Choe. 1999. Zn^{2+}-binding and molecular determinants of tetramerization in voltage-gated K^+ channels. *Nature Structural Biology.* 6:38-44.

Bloodgood, B.L., and B.L. Sabatini. 2008. Regulation of synaptic signalling by postsynaptic, non-glutamate receptor ion channels. *Journal of Physiology.* 586:1475-1480.

Bock, J.B., H.T. Matern, A.A. Peden, and R.H. Scheller. 2001. A genomic perspective on membrane compartment organization. *Nature.* 409:839-841.

Bogdanovic, A., N. Bennett, S. Kieffer, M. Louwagie, T. Morio, J. Garin, M. Satre, and F. Brucker. 2002. Syntaxin 7, syntaxin 8, Vti1 and VAMP7 (vesicle-associated membrane protein 7) form an active SNARE complex for early macropinocytic compartment fusion in *Dictyostelium discoideum*. *Biochemical Journal.* 368:29-39.

Bonifacino, J.S., and B.S. Glick. 2004. The mechanisms of vesicle budding and fusion. *Cell.* 116:153-166.

Bowlby, M.R., P. Chanda, W. Edris, J. Hinson, F. Jow, A.H. Katz, J. Kennedy, G. Krishnamurthy, K. Pitts, K. Ryan, H. Zhang, and L. Greenblatt. 2005. Identification and characterization of small molecule modulators of KChIP/Kv4 function. *Bioorganic & Medicinal Chemistry.* 13:6112-6119.

Bruckner, A., C. Polge, N. Lentze, D. Auerbach, and U. Schlatnner. 2009. Yeast two-hybrid, a powerful tool for systems biology. *International Journal of Molecular Sciences.* 10:2763-2788.

Buffa, L., E. Fuchs, M. Pietropaolo, F. Barr, and M. Solimena. 2008. ICA69 is a novel Rab2 effector regulating ER-Golgi trafficking in insulinoma cells. *European Journal of Cell Biology.* 87:197-209.

Burgoyne, R.D. 2004. The neuronal calcium-sensor proteins. *Biochimica et Biophysica Acta.* 1742:59-68.

Burgoyne, R.D. 2007. Neuronal calcium sensor proteins: generating diversity in neuronal calcium signalling. *Nature Reviews: Neuroscience.* 8:182-193.

Burkhalter, A., Y. Gonchar, R.L. Mellor, and J.M. Nerbonne. 2006. Differential expression of I_A channel subunits Kv4.2 and Kv4.3 in mouse visual cortical neurons and synapses. *Journal of Neuroscience.* 26:12274-12282.

Buxbaum, J.D., E-K. Choi, Y. Luo, C. Lilliehook, A.C. Crowley, D.E. Merriam, and W. Wasco. 1998. Calsenilin: A calcium-binding protein that interacts with the presenilins and regulates the levels of a presenilin fragment. *Nature Medicine.* 4:1177-1181.

Cai, X., C.W. Liang, S. Muralidharan, J.P.Y. Kao, C-M. Tang, and S.M. Thompson. 2004. Unique roles of SK and Kv4.2 potassium channels in dendritic integration. *Neuron.* 44:351-364.

Callsen, B., D. Isbrandt, K. Sauter, L.S. Hartmann, O. Pongs, and R. Bahring. 2005. Contribution of N- and C-terminal Kv4.2 channel domains to KChIP interaction. *Journal of Physiology.* 568:397-412.

Carrion, A.M., W.A. Link, F. Ledo, B. Mellstrom, and J.R. Naranjo. 1999. DREAM is a Ca^{2+}-regulated transcriptional repressor. *Nature.* 398:80-84.

Casey, T.M., J.L. Meade, and E.W. Hewitt. 2007. Organelle proteomics: identification of the exocytic machinery associated with the Natural Killer Cell secretory lysosome. *Molecular and Cellular Proteomics.* 6:767-780.

Castillon, G.A., R. Watanabe, M. Taylor, T.M.E. Schwabe, and H. Riezman. 2009. Concentration of GPI-anchored proteins upon ER exit in yeast. *Traffic.* 10:186-200.

Chandrasekhar, K.D., T. Bas, and W.R. Kobertz. 2006. KCNE1 subunits require co-assembly with K^+ channels for efficient trafficking and cell surface expression. *Journal of Biological Chemistry.* 281:40015-40023.

Chang, L-S., C-Y. Chen, and T.T. Wu. 2003. Functional implication with the metal-binding properties of KChIP1. *Biochemical and Biophysical Research Communications.* 311: 258-262.

Chao, D.S., J.C. Hay, S. Winnick, R. Prekeris, J. Klumperman, and R.H. Scheller. 1999. SNARE membrane trafficking dynamics in vivo. *Journal of Cell Biology.* 144:869-881.

Chen, C-P., L. Lee, and L-S. Chang. 2006(1). Effects of metal-binding properties of human Kv channel-interacting proteins on their molecular structure and binding with Kv4.2 channel. *The Protein Journal.* 25: 345-351.

Chen, X., L-L. Yuan, C. Zhao, S.G. Birnbaum, A. Frick, W.E. Jung, T.L. Schwarz, J.D. Sweatt, D. Johnston. 2006(2). Deletion of *Kv4.2* gene eliminates dendritic A-type K^+ current and enhances induction of long-term potentiation in hippocampal CA1 pyramidal neurons. *Journal of Neuroscience.* 26:12143-12151.

Chu, P-J., J.F. Rivera, and D.B. Arnold. 2006. A role for Kif17 in transport of Kv4.2. *Journal of Biological Chemistry.* 281:365-373.

Clark, B.D., E. Kwon, J. Maffie, H-Y. Jeong, M. Nadal, P. Strop, and B. Rudy. 2008. DPP6 localization in brain supports function as a Kv4 channel associated protein. *Frontiers in Molecular Neuroscience.* 1: Article 8.

Coblitz, B., S. Shikano, M. Wu, S.B. Gabelli, L.M. Cockrell, M. Spieker, Y. Hanyu, H. Fu, L.M. Amzel, and M. Li. 2005. C-terminal recognition by 14-3-3 proteins for surface expression of membrane receptors. *Journal of Biological Chemistry.* 280:36263-36272.

Coco, S., G. Raposo, S. Martinez, J-J. Fontaine, S. Takamori, A. Zahraoui, R. Jahn, M. Matteoli, D. Louvard, and T. Galli. 1999. Subcellular localization of tetanus neurotoxin-insensitive vesicle-associated membrane protein (VAMP)/VAMP7 in neuronal cells: evidence for a novel membrane compartment. *Journal of Neuroscience.* 19:9803-9812.

Cosson, P., and F. Letourner. 1994. Coatomer interaction with di-lysine endoplasmic reticulum retention motifs. *Science.* 263:1629-1631.

Covarrubias, M., A. Bhattacharji, J.A. De Santiago-Castillo, K. Dougherty, Y.A. Kaulin, T.R. Na-Phuket, and G. Wang. 2008. The neuronal Kv4 channel complex. *Neurochemical Research.* 33:1558-1567.

Craig, T.A., L.M. Benson, S.Y. Venyaminov, E.S. Klimtchuk, Z. Bajzer, F.G. Prendergast, S. Naylor, and R. Kumar. 2002. The metal-binding properties of DREAM. *Journal of Biological Chemistry.* 277:10955-10966.

Dascher, C., and W.E. Balch. 1994. Dominant inhibitory mutants of ARF1 block endoplasmic reticulum to Golgi transport and trigger disassembly of the Golgi apparatus. *Journal of Biological Chemistry.* 269:1437-1448.

Dascher, C., J. Matteson, and W.E. Balch. 1994. Syntaxin 5 regulates endoplasmic reticulum to Golgi transport. *Journal of Biological Chemistry.* 269:29363-29366.

Decher, N., A.S. Barth, T. Gonzalez, K. Steinmeyer, and M.C. Sanguinetti. 2004. Novel KChIP2 isoforms increase functional diversity of transient outward potassium currents. *Journal of Physiology.* 557.3:761-772.

DeGiorgis, J.A., J.A. Galbraith, A. Dosemeci, X. Chen, and T.S. Reese. 2006. Distribution of the scaffolding proteins PSD-95, PSD-93, and SAP97 in isolated PSDs. *Brain Cell Biology.* 35:239-250.

Deschenes, I., and G.F. Tomaselli. 2002. Modulation of Kv4.3 current by accessory subunits. *FEBS Letters.* 528:183-188.

Dixon, J.E., W. Shi, H-S. Wang, C. McDonald, H. Yu, R.S. Wymore, I.S. Cohen, and D. McKinnon. 1996. Role of the Kv4.3 K^+ channel in ventricular muscle. *Circulation Research.* 79:659-668.

Dong, C., C.M. Filipeanu, M.T. Duvernay, and G. Wu. 2007. Regulation of G protein-coupled receptor export trafficking. *Biochimica et Biophysica Acta.* 1768:853-870.

Dougherty, K., and M. Covarrubias. 2006. A dipeptidyl aminopeptidase-like protein remodels gating charge dynamics in Kv4.2 channels. *Journal of General Physiology.* 128:745-753.

Doyle, D.A., J.M. Cabral, R.A. Pfuetzner, A. Kuo, J.M. Gulbis, S.L. Cohen, B.T. Chait, and R. MacKinnon. 1998. The structure of the potassium channel: molecular basis of K^+ conduction and selectivity. *Science.* 280:69-77.

Duzhyy, D., M. Harvey, and B. Sokolowski. 2005. A secretory-type protein, containing a pentraxin domain, interacts with an A-type K^+ channel. *Journal of Biological Chemistry.* 280:15165-15672.

Edstrom, J-E. 1992. "Nobel Lectures, Physiology or Medicine 1971-1980". Ed. J. Lindsten. World Scientific Publishing Co., Singapore. 'Presentation speech. Nobel Prize for Physiology or Medicine 1974.'

Ehlers, M.D. 2007. Secrets of the secretory pathway in dendrite growth. *Neuron.* 55:686-689.

El-Haou, S., E. Balse, N. Neyroud, G. Dilanian, B. Gavillet, H. Abriel, A. Coulombe, A. Jeromin, and S.N. Hatem. 2009. Kv4 potassium channels form a tripartite complex with the anchoring protein SAP97 and CaMKII in cardiac myocytes. *Circulation Research.* 104:758-769.

El-Husseini, A., J.R. Topinka, J.E. Lehrer-Graiwer, B.L. Firestein, S.E. Craven, C. Aoki, and D.S. Bredt. 2000. Ion channel clustering by membrane-associated guanylate kinases. *Journal of Biological Chemistry*. 275:23904-23910.

Fasshauer, D., W. Antonin, M. Margittai, S. Pabst, and R. Jahn. 1999. Mixed and non-cognate SNARE complexes. *Journal of Biological Chemistry.* 274:15440-15446.

Feng, W., and M. Zhang. 2009. Organization and dynamics of PDZ-domain-related supramodules in the postsynaptic density. *Nature Reviews: Neuroscience.* 10:87-99.

Fenster, C.P., S.D. Fenster, H.P. Leahy, C. Kurschner, and J.A. Blundon. 2007. Modulation of Kv4.2 K^+ currents by neuronal interleukin-16, a PDZ domain-containing protein expressed in the hippocampus and cerebellum. *Brain Research.* 1162:19-31.

Fletcher, S., S.E.H. Bowden, and N.V. Marrion. 2003. False interaction of syntaxin 1A with a Ca^{2+}-activated K^+ channel revealed by co-immunoprecipitation and pull-down assays: implications for identification of protein-protein interactions. *Neuropharmacology*. 44:817-827.

Franco, M., P. Chardin, M. Chabre, and S. Paris. 1996. Myristoylation-facilitated binding of the G protein ARF1GDP to membrane phospholipids is required for its activation by a soluble nucleotide exchange factor. *Journal of Biological Chemistry.* 271:1573-1578.

Galli, T., A. Zahraoui, V.V. Vaidyanathan, G. Raposo, J.M. Tian, M. Karin, H. Niemann, and D. Louvard. 1998. A novel tetanus neurotoxin-insensitive vesicle-associated membrane protein in SNARE complexes of the apical plasma membrane of epithelial cells. *Molecular Biology of the Cell.* 9:1437-1448.

Gardoni, F., D. Mauceri, E. Marcello, C. Sala, M. Di Luca, and A. Jeromin. 2007. SAP97 directs the localization of Kv4.2 to spines in hippocampal neurons. *Journal of Biological Chemistry.* 282:28691-28699.

Gilchrist, A., C.E. Au, J. Hiding, A.W. Bell, J. Fernandez-Rodriguez, S. Lesimple, H. Nagaya, L. Roy, S.J.C. Gosline, M. Hallett, J. Paiement, R.E. Kearney, T. Nilsson, and J.J.M. Bergeron. 2006. Quantitative proteomics analysis of the secretory pathway. *Cell.* 127:1265-1281.

Glick, B.S. 2000. Organization of the Golgi apparatus. *Current Opinion in Cell Biology.* 12:450-456.

Goldberg, J. 1998. Structural basis for activation of ARF GTPase: mechanisms of guanine nucleotide exchange and GTP-myristoyl switching. *Cell.* 95:237-248.

Goltz, D., J-H. Schultz, C. Stucke, M. Wagner, P. Bassalay, A.P. Schowerer, H. Ehmke, and T. Volk. 2007. Diminished Kv4.2/3 but not KChIP2 levels reduce the cardiac transient outward K^+ current in spontaneously hypertensive rats. *Cardiovascular Research.* 74:85-95.

Gomes, P., T. Saito, C. del Corsso, A. Alioua, M. Eghbali, L. Toro, and E. Stefani. 2008. Identification of a functional interaction between Kv4.3 channels and c-Src tyrosine kinase. *Biochimica aet Biophysica Acta.* 1783:1884-1892.

Gomez-Villafuertes, R., B. Torres, J. Barrio, M. Savignac, N. Gabellini, F. Rizzato, B. Pintado, A. Gutierrez-Adan, B. Mellstrom, E. Carafoli, and J.R. Naranjo. 2005. Downstream regulatory element antagonist modulator regulates Ca^{2+} homeostasis and viability in cerebellar neurons. *Journal of Neuroscience.* 25:10822-10830.

Gouaux, E., and R. MacKinnon. 2005. Principles of selective ion transport in channels and pumps. *Science.* 310:1461-1465.

Greaves, J., C. Salaun, Y. Fukata, M. Fukata, and L.H. Chamberlain. 2008. Palmitoylation and membrane interactions of the neuroprotective chaperone cysteine-string protein. *Journal of Biological Chemistry.* 283:25014-25026.

Grosshans, B.L., D. Ortiz, and P. Novick. 2006. Rabs and their effectors: achieving specificity in membrane traffic. *PNAS.* 103:11821-11827.

Guo, W., H. Li, F. Aimond, D.C. Johns, K.J. Rhodes, J.S. Trimmer, and J.M. Nerbonne. 2002. Role of heteromultimers in the generation of myocardial transient outward K^+ currents. *Circulation Research.* 90:586-593.

Guo, W. W.E. Jung, C. Marionneau, F. Aimond, H. Xu, K.A. Yamada, T.L. Schwarz, S. Demolombe, and J.M. Nerbonne. 2005. Targeted deletion of Kv4.2 eliminates $I_{to,f}$ and results in electrical and molecular remodelling, with no evidence of ventricular hypertrophy or myocardial dysfunction. *Circulation Research.* 97:1342-1350.

Gurkan, C., H. Lapp, C. Alory, A.I. Su, J.B. Hogenesch, and W.E. Balch. 2005. Large-scale profiling of Rab GTPase trafficking networks: the membrome. *Molecular Biology of the Cell.* 16:3847-3864.

Gurkan, C., S.M. Stagg, P. LaPointe, and W.E. Balch. 2006. The COPII cage: unifying principles of vesicle coat assembly. *Nature Reviews: Molecular Cell Biology.* 7:727-738.

Gutman, G.A., K.G. Chandy, J.P. Adelman et al. 2003. International Union of Pharmacology. XLI. Compendium of voltage-gated ion channels: potassium channels. *Pharmacological Reviews.* 55:583-586.

Haas, A.K., S-I. Yoshimura, D.J. Stephens, C. Preisinger, E. Fuchs, and F.A. Barr. 2007. Analysis of GTPase-activating proteins: Rab1 and Rab43 are key Rabs required to maintain a functional Golgi complex in human cells. *Journal of Cell Science.* 120:2997-3010.

Hammer, J.A., and X.S. Wu. 2002. Rabs grab motors: defining the connections between Rab GTPases and motor proteins. *Current Opinion in Cell Biology.* 14:69-75.

Han, W., S. Nattel, T. Noguchi, and A. Shrier. 2006. C-terminal domain of Kv4.2 and associated KChIP2 interactions regulate functional expression and gating of Kv4.2. *Journal of Biological Chemistry*. 281:27134-27144.

Handley, M.T.W., L.P. Haynes and R.D. Burgoyne. 2007. Differential dynamics of Rab3A and Rab27A on secretory granules. *Journal of Cell Science.* 120:973-984.

Hasdemir, B., D.J. Fitzgerald, I.A. Prior, A.V. Tepikin, and R.D. Burgoyne. 2005. Traffic of Kv4 K^+ channels mediated by KChIP1 is via a novel post-ER vesicular pathway. *Journal of Cell Biology.* 171:459-469.

Hasegwa, H., S. Zinsser, Y. Rhee, E.O. Vik-Mo, S. Davanger, and J.C. Hay. 2003. Mammalian Ykt6 is a neuronal SNARE targeted to a specialized compartment by its profilin-like amino terminal domain. *Molecular Biology of the Cell.* 14:698-720.

Hasegwa, H., Z. Yang, L. Oltedal, S. Davanger, and J.C. Hay. 2004. Intramolecular protein-protein and protein-lipid interactions control the conformation and subcellular targeting of neuronal Ykt6. *Journal of Cell Science.* 117:4495-4508.

Hay, J.C., J. Klumperman, V. Oorschot, M. Steegmaier, C.S. Kuo, and R.H. Scheller. 1998. Localization, dynamics, and protein interactions reveal distinct roles for ER and Golgi SNAREs. *Journal of Cell Biology.* 141:1489-1502.

Heusser, K., H. Yuan, I. Neagoe, A.I. Tarasov, F.M. Ashcroft, and B. Schwappach. 2006. Scavenging of 14-3-3 proteins reveals their involvement in the cell-surface transport of ATP-sensitive K^+ channels. *Journal of Cell Science.* 119:4353-4363.

Hoffman, D.A., J.C. Magee, C.M. Colbert, and D. Johnston. 1997. K^+ channel regulation of signal propagation in dendrites of hippocampal pyramidal neurons. *Nature.* 387:869-875.

Holmqvist, M.H., J. Cao, M.H. Knoppers, M.E. Jurman, P.S. Distefano, K.J. Rhodes, Y. Xie, and W.F. An. 2001. Kinetic modulation of Kv4-mediated A-current by arachidonic acid is dependent on potassium channel interacting proteins. *Journal of Neuroscience.* 21:4154-4161.

Holmqvist, M.H., J. Cao, R. Hernandez-Pineda, M.D. Jacobson, K.I. Carroll, M.A. Sung, M. Betty, P. Ge, K.J. Gilbride, M.E. Brown, M.E. Jurman, D. Lawson, I. Silos-Santiago, Y. Xie, M. Covarrubias, K.J. Rhodes, P.S. Distefano, W.F. An. 2002. Elimination of fast inactivation in Kv4 A-type potassium channels by an auxiliary subunit domain. *PNAS.* 99:1035-1040.

Hong, W. 2005. SNAREs and traffic. *Biochimica et Biophysica Acta.* 1744:465-517.

Horio, Y., H. Hibino, A. Inanobe, M. Yamada, M. Ishii, Y. Tada, E. Satoh, Y. Hata, Y. Takai, and Y. Kurachi. 1997. Clustering and enhanced activity of an inwardly rectifying potassium channel, Kir4.1, by an anchoring protein, PSD-95/SAP90. *Journal of Biological Chemistry.* 272:12885-12888.

Horton, A.C., and M.D. Ehlers. 2003. Dual modes of endoplasmic reticulum-to-Golgi transport in dendrites revealed by live-cell imaging. *Journal of Neuroscience.* 23:6188-6199.

Horton, A.C., B. Racz, E.E. Monson, A.L. Lin, R.J. Weinberg, and M.D. Ehlers. 2005. Polarized secretory trafficking directs cargo for asymmetric dendrite growth and morphogenesis. *Neuron.* 48:757-771.

Hu, C., M. Ahmed, T.J. Melia, T.H. Sollner, T. Mayer, and J.E. Rothman. 2003. Fusion of cells by flipped SNAREs. *Science.* 300:1745-1749.

Hu, H-J., B.J. Alter, Y. Carrasquillo, C-S. Qiu, and R.W. Gereau IV. 2007. Metabotropic glutamate receptor 5 modulates nociceptive plasticity via extracellular signal-regulated kinase-Kv4.2 signaling in spinal cord dorsal horn neurons. *Journal of Neuroscience.* 27:13181-13191.

Husain, M., and B. Moss. 2003. Evidence against an essential role of COPII-mediated cargo transport to the endoplasmic reticulum-Golgi intermediate compartment in the formation of the primary membrane of Vaccinia virus. *Journal of Virology.* 77:11754-11766.

Hwang, J.Y., R. Schlesinger, and K.W. Koch. 2004. Irregular dimerization of guanylate cyclise-activating protein 1 mutants causes loss of target activation. *European Journal of Biochemistry.* 271:3785-3793.

Ikura, M. 1996. Calcium binding and conformational response in EF-hand proteins. *TIBS.* 21:14-17.

Isbrandt, D., T. Leicher, R. Waldschutz, X. Zhu, U. Luhmann, U. Michel, K. Sauter, and O. Pongs. 2000. Gene structures and expression profiles of three human KCND (Kv4) potassium channels mediating A-type currents I_{TO} and I_{SA}. *Genomics.* 64:144-154.

Jahn, R., and R.H. Scheller. 2006. SNAREs – engines for membrane fusion. *Nature Reviews: Molecular Cell Biology.* 7:631-643.

Jerng, H.H., P.J. Pfaffinger, and M. Covarrubias. 2004a. Molecular physiology and modulation of somatodendritic A-type potassium channels. *Molecular and Cellular Neuroscience.* 27:343-369.

Jerng, H.H., Y. Qian, and P.J. Pfaffinger. 2004b. Modulation of Kv4.2 channel expression and gating by dipeptidyl peptidase 10 (DPP10). *Biophysical Journal.* 87:2380-2396.

Jerng, H.H., K. Kunjilwar, and P.J. Pfaffinger. 2005. Multiprotein assembly of Kv4.2, KChIP3 and DPP10 produces ternary channel complexes with I_{SA}-like properties. *Journal of Physiology.* 568:767-788.

Jerng, H.H, and P.J. Pfaffinger. 2008. Multiple Kv channel-interacting proteins contain an N-terminal transmembrane domain that regulates Kv4 channel trafficking and gating. *Journal of Biological Chemistry.* 283:36046-36059.

Jeyifous, O., C.L. Waites, C.G. Specht, S. Fujisawa, M. Schubert, E.I. Lin, J. Marshall, C. Aoki, T. De Silva, J.M. Montgomery, C.C. Garner, and W.N. Green. 2009. SAP97 and CASK mediate sorting of NMDA receptors through a previously unknown secretory pathway. *Nature Neuroscience.* In press DOI: 10.1038/nn.2362.

Jinno, S., A. Jeromin, and T. Kosaka. 2005. Postsynaptic and extrasynaptic localization of Kv4.2 channels in the mouse hippocampal region, with special reference to targeted clustering at GABAergic synapses. *Neuroscience.* 134:483-494.

Jo, D-G., M-J. Kim, Y-H Choi, I-K. Kim, Y-H. Song, H-N. Woo, C-W. Chung, and Y-K. Jung. 2001. Pro-apoptotic function of calsenilin/DREAM/KChIP3. *FASEB Journal.* 15:589-591.

Jo, D-G., J-Y. Lee, Y.M. Hong, S. Song, I. Mook-Jung, J-Y. Koh, and Y-K. Jung. 2004. Induction of pro-apoptotic calsenilin/DREAM/KChIP3 in Alzheimer's disease and cultured neurons after amyloid-β exposure. *Journal of Neurochemistry.* 88:604-611.

Jo, D-G., J. Jang, B-J. Kim, J. Lundkvist, and Y-K. Jung. 2005. Overexpression of calsenilin enhances γ-secretase activity. *Neuroscience Letters.* 378:59-64.

Jugloff, D.G.M., R. Khanna, L.C. Schlichter, and O.T. Jones. 2000. Internalization of the Kv1.4 potassium channel is suppressed by clustering interactions with PSD-95. *Journal of Biological Chemistry.* 275:1357-1364.

Jourdan, N., M. Maurice, D. Delautier, A.M. Quero, A.L. Servin, and G. Trugnan. 1997. Rotavirus is released from the apical surface of cultured human intestinal cells through nonconventional vesicular transport that bypasses the Golgi apparatus. *Journal of Virology.* 71:8268-8278.

Katz, F.N., J.E. Rothman, D.M. Knipe, and H.F. Lodish. 1977a. Membrane assembly: synthesis and intracellular processing of the vesicular stomatitis viral glycoprotein. *Journal of Supramolecular Structure.* 7: 353-370.

Katz, F.N., J.E. Rothman, V.R. Lingappa, G. Blobel, and H.F. Lodish. 1977b. Membrane assembly in vitro: synthesis, glycosylation, and asymmetric insertion of a transmembrane protein. *PNAS.* 74:3278-3282.

Kim, E., and M. Sheng. 2004. PDZ domain proteins of synapses. *Nature Reviews: Neuroscience.* 5:771-781.

Kim, J., D-S. Wei, and D.A. Hoffman. 2005. Kv4 potassium channel subunits control action potential repolarization and frequency-dependent broadening in rat hippocampal CA1 pyramidal neurones. *Journal of Physiology.* 569:41-57.

Kim, J., S-C. Jung, A.M. Clemens, R.S. Petralia, and D.A. Hoffman. 2007. Regulation of dendritic excitability by activity-dependent trafficking of the A-type K^+ channel subunit Kv4.2 in hippocampal neurons. *Neuron.* 54:933-947.

Kim, J., and D.A. Hoffman. 2008. Potassium channels: newly found players in synaptic plasticity. *Neuroscientist.* 14:276-286.

Kincaid, M.M., and A.A. Cooper. 2007. Misfolded proteins traffic from the endoplasmic reticulum (ER) due to ER export signals. *Molecular Biology of the Cell.* 18:455-463.

Kloepper, T.H., C.N. Kienle, and D. Fasshauer. 2007. An elaborate classification of SNARE proteins sheds light on the conservation of the eukaryotic endomembrane system. *Molecular Biology of the Cell.* 18:3463-3471.

Kollo, M., N.B. Holderith, and Z. Nusser. 2006. Novel subcellular distribution pattern of A-type K^+ channels on neuronal surface. *Journal of Neuroscience.* 26:2684-2691.

Kuehn, M.J., and R. Schekman. 1997. COPII and secretory cargo capture into transport vesicles. *Current Opinion in Cell Biology.* 9:477-483.

Kuehn, M.J., J.M. Herrmann, and R. Schekman. 1998. COPII-cargo interactions direct protein sorting into ER-derived transport vesicles. *Nature*. 391:187-190.

Kuge, O., C. Dascher, L. Orci, T. Rowe, M. Amherdt, H. Plutner, M. Ravazzola, G. Tanigawa, J.E. Rothman, and W.E. Balch. 1994. Sar1 promotes vesicle budding from the endoplasmic reticulum but not Golgi compartments. *Journal of Cell Biology.* 125:51-65.

Kumar, N.S., and C.M. Mansbach. 1997. Determinants of triacylglycerol transport from the endoplasmic reticulum to the Golgi in intestine. *American Journal of Physiology.* 273:G18-G30.

Kunjilwar, K., C. Strang, D. DeRubeis, and P.J. Pfaffinger. 2004. KChIP3 rescues the functional expression of Shal channel tetramerization mutants. *Journal of Biological Chemistry.* 279:54542-54551.

Kuo, H-C., C-F. Cheng, R.B. Clark, J.J-C. Lin, M. Hoshijima, V.T.B. Nguyen-Tran, Y. Gu, Y. Ikeda, P-H. Chu, J. Ross Jr., W.R. Giles, and K.R. Chien. 2001. A defect in the Kv channel-interacting protein 2 (KChIP2) gene leads to a complete loss of I_{to} and confers susceptibility to ventricular tachycardia. *Cell.* 107: 801-813.

Kuryshev, Y.A., T.I. Gudz, A.M. Brown, and B.A. Wible. 2000. KChAP as a chaperone for specific K^+ channels. *American Journal of Physiology: Cell Physiology.* 278:C931-C941.

Ladinsky, M.S., D.N. Mastronarde, J.R. McIntosh, K.E. Howell, and L.A. Staehelin. 1999. Golgi structure in three dimensions: functional insights from the normal rat kidney cell. *Journal of Cell Biology.* 144:1135-1149.

Lauver, A., L-L. Yuan, A. Jeromin, B.M. Nadin, J.J. Rodriguez, H.A. Davies, M.G. Stewart, G-Y. Wu, and P.J. Pfaffinger. 2006. Manipulating Kv4.2 identifies a specific component of hippocampal pyramidal neuron A-current that depends upon Kv4.2 expression. *Journal of Neurochemistry.* 99:1207-1223.

Lee, M-T.G., A. Mishra, and D.G. Lambright. 2009. Structural mechanisms for regulation of membrane traffic by Rab GTPases. *Traffic.* In press DOI: 10.1111/j.1600-0854.2009.00942.x

Leyland, M.L., and C. Dart. 2004. An alternatively spliced isoform of PSD-93/Chapsyn 110 binds to the inwardly rectifying potassium channel, Kir2.1. *Journal of Biological Chemistry.* 279:43427-43436.

Lilliehook, C., O. Bozdagi, J. Yao, M. Gomez-Ramirez, N.F. Zaidi, W. Wasco, S. Gandy, A.C. Santucci, V. Haroutunian, G.W. Huntley, and J.D. Buxbaum. 2003. Altered Aβ formation and long-term potentiation in a calsenilin knock-out. *Journal of Neuroscience.* 23:9097-9106.

Lin, Y-L., S-R. Lin, T.T. Wu, and L-S. Chang. 2004. Evidence showing an intermolecular interaction between KChIP proteins and Taiwan cobra cardiotoxins. *Biochemical and Biophysical Research Communications.* 319:720-724.

Link, W.A., F. Ledo, B. Torres, M. Palczewska, T.M. Madsen, M. Savignac, J.P. Albar, B. Mellstrom, and J.R. Naranjo. 2004. Day-night changes in downstream regulatory element antagonist modulator/potassium channel interacting protein activity contribute to circadian gene expression in pineal gland. *Journal of Neuroscience.* 24:5346-5355.

Liss, B., O. Franz, S. Sewing, R. Bruns, H. Neuhoff, and J. Roeper. 2001. Tuning packemaker frequency of individual dopaminergic neurons by Kv4.3L and KChip3.1 transcription. *EMBO Journal.* 20:5715-5724.

Lusin, J.D., M. Vanarotti, C. Li, A. Valiveti, and J.B. Ames. 2008. NMR structure of DREAM: implications for Ca^{2+}-dependent DNA binding and protein dimerization. *Biochemistry.* 47:2252-2264.

Maffie, J., and B. Rudy. 2008. Weighing the evidence for a ternary protein complex mediating A-type K^+ currents in neurons. *Journal of Physiology.* 586:5609-5623.

Martinez-Arca, S., P. Alberts, A.Zahraoui, D. Louvard, and T. Galli. 2000. Role of tetanus neurotoxin insensitive vescicle-associated membrane protein (TI-VAMP) in vesicular transport mediating neurite outgrowth. *Journal of Cell Biology.* 149:889-899.

Martinez-Arca, S., R. Rudge, M. Vacca, G. Raposo, J. Camonis, V.Proux-Gillardeaux, L. Daviet, E. Formstecher, A. Hamburger, F. Filippini, M. D'Esposito, and T. Galli. 2003. A dual mechanism controlling the localization and function of exocytic v-SNAREs. *PNAS.* 100:9011-9016.

Matsuoka, K., L. Orci, M. Amherdt, S.Y. Bednarek, S. Hamamoto, R. Schekman, and T. Yeung. 1998. COPII-coated vesicle formation reconstituted with purified coat proteins and chemically defined liposomes. *Cell.* 93:263-275.

Menegola, M., and J.S. Trimmer. 2006. Unanticipated region- and cell-specific downregulation of individual KChIP auxiliary subunit isotypes in Kv4.2 knock-out mouse brain. *Journal of Neuroscience.* 26:12137-12142.

Migliore, M., D.A. Hoffman, J.C. Magee, and D. Johnston. 1999. Role of an A-type K^+ conductance in the back-propagation of action potentials in the dendrites of hippocampal pyramidal neurons. *Journal of Computational Neuroscience.* 7:5-15.

Mironov, Jr., A., A. Luini, and A. Mironov. 1998. A synthetic model of intra-Golgi traffic. *FASEB J.* 12:249-252.

Mironov, A.A., A.A. Mironov Jr, G.V. Beznoussenko, A. Trucco, P. Lupetti, J.D. Smith, W.J.C. Geerts, A.J. Koster, K.N.J. Burger, M.E. Martone, T.J. Deernick, M.H. Ellisman, and A. Luini. 2003. ER-to-Golgi carriers arise through direct en bloc protrusion and multistage maturation of specialized ER exit domains. *Developmental Cell.* 5:583-594.

Misonou, H., and J.S. Trimmer. 2004. Determinants of voltage-gated potassium channel surface expression and localization in mammalian neurons. *Critical Reviews in Biochemistry and Molecular Biology.* 39:125-145.

Morohashi, Y., N. Hatano, S. Ohya, R. Takikawa, T. Watabiki, N. Takasugi, Y. Imaizumi, T. Tomita, and T. Iwatsubo. 2002. Molecular cloning and characterization of CALP/KChIP4, a novel EF-hand protein interacting with presenilin 2 and voltage-gated potassium channel subunit Kv4. *Journal of Biological Chemistry.* 277:14965-14975.

Morsomme, P., C. Prescianotto-Baschong, and H. Riezman. 2003. The ER v-SNAREs are required for GPI-anchored protein sorting from other secretory proteins upon exit from the ER. *Journal of Cell Biology.* 162:403-412.

Muller, B.M., U. Kistner, R.W. Veh, C. Cases-Langhoff, B. Becker, E.D. Gundelfinger, and C.C. Garner. 1995. Molecular characterization and spatial distribution of SAP97, a novel presynaptic protein homologous to SAP90 and the *Drosophila* Discs-large tumor suppressor protein. *Journal of Neuroscience.* 15:2354-2366.

Muniz, M., P. Morsomme, and H. Riezman. 2001. Protein sorting upon exit from the endoplasmic reticulum. *Cell.* 104:313-320.

Nadal, M.S., Y. Amarillo, E. Vega-Saenz de Miera, and B. Rudy. 2001. Evidence for the presence of a novel Kv4-mediated A-type K^+ channel-modifying factor. *Journal of Physiology.* 537:801-809.

Nakamura, T.Y., S. Nandi, D.J. Pountney, M. Artman, B. Rudy, and W.A. Coetzee. 2001a. Different effects of the Ca^{2+}-binding protein, KChIP1, on two Kv4 subfamily members, Kv4.1 and Kv4.2. *FEBS Letters.* 499:205-209.

Nakamura, T.Y., D.J. Pountney, A. Ozaita, S. Nandi, S. Ueda, B. Rudy, and W.A. Coetzee. 2001b. A role for frequenin, a Ca^{2+}-binding protein, as a regulator of Kv4 K^+-currents. *PNAS.* 98:12808-12813.

Nerbonne, J.M., B.R. Gerber, A. Norris, and A. Burkhalter. 2008. Electrical remodelling maintains firing properties in cortical pyramidal neurons lacking *KCND2*-encoded A-type K^+ currents. *Journal of Physiology.* 586:1565-1579.

Nickel, W., B. Brugger, and F.T. Wieland. 1998. Protein and lipid sorting between the endoplasmic reticulum and the Golgi complex. *Seminars in Cell & Developmental Biology.* 9:493-501.

Niwa, N., W. Wang, Q.Sha, C. Marionneau, and J.M. Nerbonne. 2008. Kv4.3 is not required for the generation of functional $I_{to,f}$ channels in adult mouse ventricles. *Journal of Molecular and Cellular Cardiology.* 44:95-104.

Novick, P., C. Field, and R. Schekman. 1980. Identification of 23 complementation groups required for post-translational events in the yeast secretory pathway. *Cell.* 21:205-215.

O'Callaghan, D.W., B. Hasdemir, M. Leighton, and R.D. Burgoyne. 2003. Residues within the myristoylation motif determine intracellular targeting of the neuronal Ca^{2+} sensor protein KChIP1 to post-ER transport vesicles and traffic of Kv4 K^{+} channels. *Journal of Cell Science.* 116:4833-4845.

O'Kelly, I., M.H. Butler, N. Zilberberg, and S.A.N. Goldstein. 2002. Forward transport: 14-3-3 binding overcomes retention in endoplasmic reticulum by dibasic signals. *Cell.* 111:577-588.

Orci, L., M. Stamnes, M. Ravazzola, M. Amherdt, A. Perrelet, T.H. Sollner, and J.E. Rothman. 1997. Bidirectional transport by distinct populations of COPI-coated vesicles. *Cell.* 90:335-349.

Osawa, M., K.I. Tong, C. Lilliehook, W. Wasco, J.D. Buxbaum, H-Y.M. Cheng, J.M. Penninger, M. Ikura, and J.B. Ames. 2001. Calcium-regulated DNA binding and oligomerization of the neuronal calcium-sensing protein, calsenilin/DREAM/KChIP3. *Journal of Biological Chemistry.* 276:41005-41013.

Osawa, M., A. Dace, K.I. Tong, A. Valiveti, M. Ikura, and J.B. Ames. 2005. Mg^{2+} and Ca^{2+} differentially regulate DNA binding and dimerization of DREAM. *Journal of Biological Chemistry.* 280:18008-18014.

Palade, G. 1975. Intracellular aspects of the process of protein synthesis. *Science.* 189:347-358.

Papazian, D.M., T.L. Schwartz, B.L. Tempel, Y.N. Jan, and L.Y. Jan. 1987. Cloning of genomic and complementary DNA from *Shaker*, a putative potassium channel gene from *Drosophila. Science.* 237:749-753.

Parker, M.J., S. Zhao, D.S. Bredt, J.R. Sanes, and G. Feng. 2004. PSD93 regulates synaptic stability at neuronal cholinergic synapses. *Journal of Neuroscience.* 24:378-388.

Patel, S.P., D.L. Campbell, M.J. Morales, and H.C. Strauss. 2002a. Heterogeneous expression of KChIP2 isoforms in the ferret heart. *Journal of Physiology.* 539.3:649-656.

Patel, S.P., D.L. Campbell, and H.C. Strauss. 2002b. Elucidating KChIP effects on Kv4.3 inactivation and recovery kinetics with a minimal KChIP2 isoform. *Journal of Physiology*. 545.1:5-11.

Patel, S.P., R. Parai, R. Parai, and D.L. Campbell. 2004. Regulation of Kv4.3 voltage-dependent gating kinetics by KChIP2 isoforms. *Journal of Physiology.* 557.1:19-41.

Patel, S.P., and D.L. Campbell. 2005. Transient outward potassium current, 'I_{to}', phenotypes in the mammalian left ventricle: underlying molecular, cellular and biophysical mechanisms. *Journal of Physiology.* 569:7-39.

Patterson, G.H., K. Hirschberg, R.S. Polishchuk, D. Gerlich, R.D. Phair, and J. Lippincott-Schwartz. 2008. Transport through the Golgi apparatus by rapid partitioning within a two-phase membrane system. *Cell.* 133:1055-1067.

Pepperkok, R., M. Lowe, B. Burke, and T.E. Kreis. 1998. Three distinct steps in transport of vesicular stomatitis virus glycoprotein from the ER to the cell surface in vivo with differential sensitivities to GTPγS. *Journal of Cell Science.* 111:1877-1888.

Peter, F., H. Plutner, H. Zhu, T.E. Kreis, and W.E. Balch. 1993. β-COP is essential for transport of protein from the endoplasmic reticulum to the Golgi in vitro. *Journal of Cell Biology.* 122:1155-1167.

Petrecca, K., D.M. Miller, and A. Shrier. 2000. Localization and enhanced current density of the Kv4.2 potassium channel by interaction with the actin-binding protein filamin. *Journal of Neuroscience.* 20:8736-8744.

Pioletti, M., F. Findeisen, G.L. Hura, and D.L. Minor, Jr. 2006. Three-dimensional structure of the KChIP1-Kv4.3 T1 complex reveals a cross-shaped octamer. *Nature Structural & Molecular Biology*. 13:987-995.

Pongs, O., T. Leicher, M. Berger, J. Roeper, R. Bahring, D. Wray, K.P. Giese, A.J. Silva, and J.F. Storm. 1999. Functional and molecular aspects of voltage-gated K^+ channel beta subunits. *Annals of the New York Academy of Science.* 868:344-355.

Presley, J.F., N.B. Cole, T.A. Schroer, K. Hirschberg, K.J.M. Zaal, and J. Lippincott-Schwartz. 1997. ER-to-Golgi transport visualized in living cells. *Nature.* 389:81-85.

Proux-Gillardeaux, V., G. Raposo, T. Irinopoulou, and T. Galli. 2007. Expression of the Longin domain of TI-VAMP impairs lysosomal secretion and epithelial cell migration. *Biology of the Cell.* 99:261-271.

Pruunsild, P., and T. Timmusk. 2005. Structure, alternative splicing, and expression of the human and mouse KCNIP gene family. *Genomics.* 86:581-593.

Pryor, P.R., B.M. Mullock, N.A. Bright, M.R. Lindsay, S.R. Gray, S.C.W. Richardson, A. Stewart, D.E. James, R.C. Piper, and J.P. Luzio. 2004. Combinatorial SNARE complexes with VAMP7 or VAMP8 define different late endocytic fusion events. *EMBO Reports.* 5:590-595.

Quintero, C.A., J. Valdez-Taubas, M.L. Ferrari, S.D. Haedo, and H.J.F. Maccioni. 2008. Calsenilin and CALP interact with the cytoplasmic tail of UDP-GAL:GA2/GM2/GD2 β-1,3-galactosyltransferase. *Biochemical Journal.* 412:19-26.

Radicke, S., D. Cotella, E.M. Graf, U. Ravens, and E. Wettwer. 2005. Expression and function of dipeptidyl-aminopeptidase-like protein 6 as a putative β-subunit of human cardiac transient outward current encoded by Kv4.3. *Journal of Physiology.* 565:751-756.

Rajan, S., R. Preisig-Muller, E. Wischmeyer, R. Nehring, P.J. Hanley, V. Renigunta, B. Musset, G. Schlichthorl, C. Derst, A. Karschin, and J. Daut. 2002. Interaction with 14-3-3 proteins promotes functional expression of the potassium channels TASK-1 and TASK-3. *Journal of Physiology.* 545:13-26.

Ramakers, G.M.J., and J.F. Storm. 2002. A postsynaptic transient K^+ current modulated by arachidonic acid regulates synaptic integration and threshold for LTP induction in hippocampal pyramidal cells. *PNAS.* 99:10144-10149.

Reiterer, V., S. Maier, H.H. Sitte, A. Kriz, M.A. Ruegg, H-P. Hauri, M. Freissmuth, and H. Farhan. 2008. Sec24- and ARFGAP1-dependent trafficking of GABA transporter-1 is a prerequisite for correct axonal targeting. *Journal of Neuroscience.* 28:12453-12464.

Ren, X., S.H. Shand, and K. Takimoto. 2003. Effective association of Kv channel-interacting proteins with Kv4 channel is mediated by their unique core peptide. *Journal of Biological Chemistry.* 278:43564-43570.

Rhodes, K.J., K.I. Carroll, M.A. Sung, L.C. Doliveira, M.M. Monaghan, S.L. Burke, B.W. Strassle, L. Buchwalder, M. Menegola, J. Cao, W.F. An, and J.S. Trimmer. 2004. KChIPs and Kv4 α subunits as integral components of A-type potassium channels in mammalian brain. *Journal of Neuroscience.* 24:7903-7915.

Rivera, J.F., S. Ahmad, M.W. Quick, E.R. Liman, and D.B. Arnold. 2003. An evolutionarily conserved dileucine motif in Shal K^+ channels mediates dendritic targeting. *Nature Neuroscience.* 6:243-250.

Rosati, B., Z. Pan, S. Lypen, H-S. Wang, I. Cohen, J.E. Dixon, and D. McKinnon. 2001. Regulation of *KChIP2* potassium channel β subunit gene expression underlies the gradient of transient outward current in canine and human ventricle. *Journal of Physiology.* 533:119-125.

Roth, D., A. Morgan, H. Martin, D. Jones, G.J.M. Martens, A. Aitken, and R.D. Burgoyne. 1994. Characterization of 14-3-3 proteins in adrenal chromaffin cells and demonstration of isoforms-specific phospholipid binding. *Biochemical Journal.* 301:305-310.

Rothman, J.E., and R.E. Fine. 1980. Coated vesicles transport newly synthesized membrane glycoproteins from endoplasmic reticulum to plasma membrane in two successive stages. *PNAS.* 77:780-784.

Rothman, J.E., and F.T. Wieland. 1996. Protein sorting by transport vesicles. *Science.* 272:227-234.

Rowe, T., M. Aridor, J.M. McCaffery, H. Plutner, C. Nuoffer, and W.E. Balch. 1996. COPII vesicles derived from mammalian endoplasmic reticulum microsomes recruit COPI. *Journal of Cell Biology.* 135:895-911.

Ruiz-Gomez, A., B. Mellstrom, D. Torneo, E. Morato, M. Savignac, H. Holguin, K. Aurrekoetxea, P. Gonzalez, C. Gonzalez-Garcia, V. Cena, F. Mayor Jr., and J.R. Naranjo. 2007. GRK2-mediated phosphorylation of DREAM regulates membrane trafficking of Kv4.2 potassium channel. *Journal of Biological Chemistry.* 282:1205-1215.

Sanderson, C.M. 2009. The cartographers toolbox: building bigger and better human protein interaction networks. *Briefings in Functional Genomics and Proteomics.* 8:1-11.

Scales, S.J., R. Pepperkok, and T.E. Kreis. 1997. Visualization of ER-to-Golgi transport in living cells reveals a sequential mode of action for COPII and COPI. *Cell.* 90:1137-1148.

Scannevin, R.H., K. Wang, F. Jow, J. Megules, D.C. Kopsco, W. Edris, K.C. Carroll, Q. Lu, W. Xu, Z. Xu, A.H. Katz, S. Olland, L. Lin, M. Taylor, M. Stahl, K. Malakian, W. Somers, L. Mosyak, M.R. Bowlby, P. Chanda, and K.J. Rhodes. 2004. Two N-terminal domains of Kv4 K^+ channels regulate binding to and modulation by KChIP1. *Neuron.* 41:587-598.

Schiavo, G., and G. Stenbeck. 1998. Molecular analysis of neurotransmitter release. *Essays in Biochemistry.* 33:29-41.

Schwartz, S.L., C. Cao, O. Pylypenko, A. Rak, and A. Wandinger-Ness. 2007. Rab GTPases at a glance. *Journal of Cell Science.* 120:3905-3910.

Schwenk, J., G. Zolles, N.G. Kandias, I. Neubauer, H. Kalbacher, M. Covarrubias, B. Fakler, and D. Bentrop. 2008. NMR analysis of KChIP4a reveals structural basis for control of surface expression of Kv4 channel complexes. *Journal of Biological Chemistry.* 283:18937-18946.

Shen, N.V., and P.J. Pfaffinger. 1995. Molecular recognition and assembly sequences involved in the subfamily-specific assembly of voltage-gated K^+ channel subunit proteins. *Neuron.* 14:625-633.

Shibasaki, K., K. Nakahira, J.S. Trimmer, R. Shibata, M. Akita, S-I. Watanabe, and K. Ikenaka. 2004. Mossy fibre contact triggers the targeting of Kv4.2 potassium channels to dendrites and synapses in developing cerebellar granule neurons. *Journal of Neurochemistry.* 89:897-907.

Shibata, R., H. Misonou, C.R. Campomanes, A.E. Anderson, L.A. Schrader, L.C. Doliveira, K.I. Carroll, J.D. Sweatt, K.J. Rhodes, and J.S. Trimmer. 2003. A fundamental role for KChIPs in determining the molecular properties and trafficking of Kv4.2 potassium channels. *Journal of Biological Chemistry.* 278:36445-36454.

Shikano, S., B. Coblitz, M. Wu, and M. Li. 2006. 14-3-3 proteins: regulation of endoplasmic reticulum localization and surface expression of membrane proteins. *Trends in Cell Biology.* 16:370-375.

Shoulders, C.C., D.J. Stephens, and B. Jones. 2004. The intracellular transport of chylomicrons requires the small GTPase, Sar1b. *Current Opinion in Lipidology.* 15:191-197.

Siddiqi, S.A., F.S. Gorelick, J.T. Mahan, and C.M. Mansbach. 2003. COPII proteins are required for Golgi fusion but not for endoplasmic reticulum budding of the pre-chylomicron transport vesicle. *Journal of Cell Science.* 116:415-427.

Siddiqi, S.A., S. Siddiqi, J. Mahan, K. Peggs, F.S. Gorelick, and C.M. Mansbach. 2006a. The identification of a novel endoplasmic reticulum to Golgi SNARE complex used by the prechylomicron transport vesicle. *Journal of Biological Chemistry.* 281:20974-20982.

Siddiqi, S.A., J. Mahan, S. Siddiqi, F.S. Gorelick, and C.M. Mansbach II. 2006b. Vesicle-associated membrane protein 7 is expressed in intestinal ER. *Journal of Cell Science.* 119. 943-950.

Simpson, J.C., T. Nilsson, and R. Pepperkok. 2006. Biogenesis of tubular ER-to-Golgi transport intermediates. *Molecular Biology of the Cell.* 17:723-737.

Singh, B., I. Ogiwara, M. Kaneda, N. Tokonami, E. Mazaki, K. Baba, K. Matsuda, Y. Inoue, and K. Yamakawa. 2006. A $K_v4.2$ truncation mutation in a patient with temporal lobe epilepsy. *Neurobiology of Disease.* 24:245-253.

Spreafico, F., J.J. Barski, C. Farina, and M. Meyer. 2001. Mouse DREAM/Calsenilin/KChIP3: gene structure, coding potential, and expression. *Molecular and Cellular Neuroscience.* 17:1-16.

Stagg, S.M., C. Gurkan, D.M. Fowler, P. LaPointe, T.R. Foss, C.S. Potter, B. Carragher, and W.E. Balch. 2006. Structure of the Sec13/31 COPII coat cage. *Nature.* 439:234-238.

Starkuviene, V., and R. Pepperkok. 2007. Differential requirements for ts-O45-G and procollagen biosynthetic transport. *Traffic.* 8:1035-1051.

Steinacker, P., P. Schwarz, K. Reim, P. Brechlin, O. Jahn, H. Kratzin, A. Aitken, J. Wiltfang, A. Aguzzi, E. Bahn, H.C. Baxter, N. Brose, and M. Otto. 2005. Unchanged survival rates of 14-3-3γ knockout mice after inoculation with pathological prion protein. *Molecular and Cellular Biology.* 25:1339-1346.

Stephens, D.J., N. Lin-Marq, A. Pagano, R. Pepperkok, and J-P. Paccaud. 2000. COPI-coated ER-to-Golgi transport complexes segregate from COPII in close proximity to ER exit sites. *Journal of Cell Science.* 113:2177-2185.

Stephens, D.J., and R. Pepperkok. 2002. Imaging of procollagen transport reveals COPI-dependent cargo sorting during ER-to-Golgi transport in mammalian cells. *Journal of Cell Science.* 115:1149-1160.

Stephens, D.J., and R. Pepperkok. 2004. Differential effects of a GTP-restricted mutant of Sar1p on segregation of cargo during export from the endoplasmic reticulum. *Journal of Cell Science.* 117:3635-3644.

Subramaniam, V.N., F. Peter, R. Philp, S.H. Wong, and W. Hong. 1996. GS28, a 28-kilodalton Golgi SNARE that participates in ER-Golgi transport. *Science.* 272:1161-1163.

Sutterlin, C., T.L. Doering, F. Schimmoller, S. Schroder, and H. Riezman. 1997. Specific requirements for the ER to Golgi transport of GPI-anchored proteins in yeast. *Journal of Cell Science.* 110:2703-2714.

Szul, T., R. Grabski, S. Lyons, Y. Morohashi, S. Shestopal, M. Lowe, and E. Sztul. 2007. Dissecting the role of the ARF guanine nucleotide exchange factor GBF1 in Golgi biogenesis and protein trafficking. *Journal of Cell Science.* 120:3929-3940.

Takida, S., Y. Maeda, and T. Kinoshita. 2008. Mammalian GPI-anchored proteins require p24 proteins for their efficient transport from the ER to the plasma membrane. *Biochemical Journal.* 409:555-562.

Takimoto, K., E-K. Yang, and L. Conforti. 2002. Palmitoylation of KChIP splicing variants is required for efficient cell surface expression of Kv4.3 channels. *Journal of Biological Chemistry.* 277:26904-26911.

Tiffany, A.M., L.N. Manganas, E. Kim, Y-P. Hsueh, M. Sheng, and J.S. Trimmer. 2000. PSD-95 and SAP97 exhibit distinct mechanisms for regulating K^+ channel surface expression and clustering. *Journal of Cell Biology.* 148:147-157.

Tisdale, E.J., J.R. Bourne, R. Khosravi-Far, C.J. Der, and W.E. Balch. 1992. GTP-binding mutants of Rab1 and Rab2 are potent inhibitors of vesicular transport from the endoplasmic reticulum to the Golgi complex. *Journal of Cell Biology.* 119:749-761.

Tisdale, E.J., and W.E. Balch. 1996. Rab2 is essential for the maturation of pre-Golgi intermediates. *Journal of Biological Chemistry.* 271:29372-29379.

Tkatch, T., G. Baranauskas, and D.J. Surmeier. 2000. Kv4.2 mRNA abundance and A-type K^+ current amplitude are linearly related in basal ganglia and basal forebrain neurons. *Journal of Neuroscience.* 20:579-588.

Trinkle-Mulcahy, L., S. Boulon, Y.W. Lam,R. Urcia, F-M. Boisvert, F. Vandermoere, N.A. Morrice, S. Swift, U. Rothbauer, H. Leonhardt, and A. Lamond. 2008. Identifying specific protein interaction partners using quantitative mass spectrometry and bead proteomes. *Journal of Cell Biology.* 183:223-239.

Trombetta, E.S., and A.J. Parodi. 2003. Quality control and protein folding in the secretory pathway. *Annual Review of Cell and Developmental Biology.* 19:649-676.

Tsaur, M-L., M. Sheng, D.H. Lowenstein, Y.N. Jan, and L.Y. Jan. 1992. Differential expression of K^+ channel mRNAs in the rat brain and down-regulation in the hippocampus following seizures. *Neuron.* 8:1055-1067.

Tzivion, G., and J. Avruch. 2001. 14-3-3 proteins: active cofactors in cellular regulation by serine/threonine phosphorylation. *Journal of Biological Chemistry.* 277:3061-3064.

Tzivion, G., Y.H. Shen, and J. Zhu. 2001. 14-3-3 proteins; bringing new definitions to scaffolding. *Oncogene.* 20:6331-6338.

Uemura, T., M.H. Sato, and K. Takeyasu. 2005. The longin domain regulates subcellular targeting of VAMP7 in *Arabidopsis thaliana. FEBS Letters.* 579:2842-2846.

Varga, A.W., L-L. Yuan, A.E. Anderson, L.A. Schrader, G-Y. Wu, J.R. Gatchel, D. Johnston, and J.D. Sweatt. 2004. Calcium-calmodulin-dependent kinase II modulates Kv4.2 channel expression and upregulates neuronal A-type potassium currents. *Journal of Neuroscience.* 24:3643-3654.

Venn, N., L.P. Haynes, and R.D. Burgoyne. 2008. Specific effects of KChIP3/calsenilin/DREAM, but not KChIPs1, 2 and 4, on calcium signalling and regulated secretion in PC12 cells. *Biochemical Journal.* 413:71-80.

Wang, G., C. Strang, P.J. Pfaffinger, and M. Covarrubias. 2007(1). Zn^{2+}-dependent redox switch in the intracellular T1-T1 interface of a Kv channel. *Journal of Biological Chemistry.* 282:13637-13647.

Wang, H., Y. Yan, Q. Lin, Y. Huang, Y. Shen, L. Chen, Y. Chen, Q. Yang, Q. Hao, K.W. Wang, and J. Chai. 2007(2). Structural basis for modulation of Kv4 K^+ channels by auxiliary KChIP subunits. *Nature Neuroscience.* 10:32-39.

Wang, K. 2008. Modulation of clamping:Kv4 and KChIP interactions. *Neurochemical Research.* 33:1964-1969.

Wang, S., S.P. Patel, Y. Qu, P. Hua, H.C. Strauss, and M.J. Morales. 2002. Kinetic properties of Kv4.3 and their modulation by KChIP2b. *Biochemical and Biophysical Research Communications.* 295:223-229.

Wang, Y., and B.L. Tang. 2006. SNAREs in neurons – beyond synaptic vesicle exocytosis. *Molecular Membrane Biology.* 23:377-384.

Wang, Z., J.R. Eldstrom, J. Jantzi, E.D. Moore, and D. Fedida. 2004. Increased focal Kv4.2 channel expression at the plasma membrane is the result of actin depolymerization. *American Journal of Physiology: Heart and Circulation Physiology.* 286:H749-H759.

Watanabe, R., and H. Riezman. 2004. Differential ER exit in yeast and mammalian cells. *Current Opinion in Cell Biology.* 16:350-355.

Watanabe, R., G.A. Castillon, A. Meury, and H. Riezman. 2008. The presence of an ER exit signal determines the protein sorting upon ER exit in yeast. *Biochemical Journal.* 414:237-245.

Watson, P., R. Forster, K.J. Palmer, R. Pepperkok, and D.J. Stephens. 2005. Coupling of ER exit to microtubules through direct interaction of COPII with dynactin. *Nature Cell Biology.* 7:48-55.

Wible, B.A., Q. Yang, Y.A. Kuryshev, E.A. Accili, and A.M. Brown. 1998. Cloning and expression of a novel K^+ channel regulatory protein, KChAP. *Journal of Biological Chemistry.* 273:11745-11751.

Wilkinson, B.M., M. Regnacq, and C.J. Stirling. 1997. Protein translocation across the membrane of the endoplasmic reticulum. *Journal of Membrane Biology.* 155:189-197.

Wong, W., E.W. Newell, D.G.M. Jugloff, O.T. Jones, and L.C. Schlichter. 2002. Cell surface targeting and clustering interactions between heterologously expressed PSD-95 and the *Shal* voltage-gated potassium channel, Kv4.2. *Journal of Biological Chemistry.* 277:20423-20430.

Wu, H., J.E. Nash, P. Zamorano, and C.C. Garner. 2002. Interaction of SAP97 with minus-end-directed actin motor myosin VI. *Journal of Biological Chemistry.* 277:30928-30934.

Wu, G., G. Zhao, and Y. He. 2003. Distinct pathways for the trafficking of angiotensin II and adrenergic receptors from the endoplasmic reticulum to the cell surface. *Journal of Biological Chemistry.* 278:47062-47069.

Xiong, H., K. Xia, B. Li, G. Zhao, and Z. Zhang. 2009. KChIP1: a potential modulator to GABAergic system. *Acta Biochimica et Biophysica Sinica.* 41:295-300.

Xu, D., A.P. Joglekar, A.L. Williams, and J.C. Hay. 2000. Subunit structure of a mammalian ER/Golgi SNARE complex. *Journal of Biological Chemistry.* 275:39631-39639.

Xu, J., W. Yu, Y.N. Jan, L.Y. Jan, and M. Li. 1995. Assembly of voltage-gated potassium channels – conserved hydrophilic motifs determine subfamily-specific interactions between the α-subunits. *Journal of Biological Chemistry.* 270:24761-24768.

Yamakawa, T., S. Saith, Y. Li, X. Gao, H.Y. Gaisano, and R.G. Tsushima. 2007. Interaction of syntaxin 1A with the N-terminus of Kv4.2 modulates channel surface expression and gating. *Biochemistry.* 46:10942-10949.

Yang, B., L. Gonzalez Jr., R. Prekeris, M. Steegmaier, R.J. Advani, and R.H. Scheller. 1999(1). SNARE interactions are not selective. *Journal of Biological Chemistry.* 274:5649-5653.

Yang, S-N., Y-G. Tang, and R.S. Zucker. 1999(2). Selective induction of LTP and LTD by postsynaptic $[Ca^{2+}]_i$ elevation. *Journal of Neurophysiology.* 81:781-787.

Ye, B., Y. Zhang, W. Song, S.H. Younger, L.Y. Jan, and Y.N. Jan. 2007. Growing dendrites and axons differ in their reliance on the secretory pathway. *Cell.* 130:717-729.

Yoo, J-S., B.D. Moyer, S. Bannykh, H-M. Yoo, J.R. Riordan, and W.E. Balch. 2002. Non-conventional trafficking of the cystic fibrosis transmembrane conductance regulator through the early secretory pathway. *Journal of Biological Chemistry.* 277:11401-11409.

Yu, L., C. Sun, R. Mendoza, J. Wang, E.D. Matayoshi, E. Herbert, A. Pereda-Lopez, P.J. Hajduk, and E.T. Olejniczak. 2007. Solution structure and calcium-binding properties of EF-hands 3 and 4 of calsenilin. *Protein Science.* 16:2502-2509.

Zagha, E., A. Ozaita, S.Y. Chang, M.S. Nadal, U. Lin, M.J. Saganich, T. McCormack, K.O. Akinsanya, S.Y. Qi, and B. Rudy. 2005. DPP10 modulates Kv4-mediated A-type potassium channels. *Journal of Biological Chemistry.* 280:18853-18861.

Zarayskiy, V.V., G. Balasubramanian, V.E. Bondarenko, and M.J. Morales. 2005. Heteropoda toxin 2 is a gating modifier toxin specific for voltage-gated K+ channels of the Kv4 family. *Toxicon.* 45:431-442.

Zerangue, N. B. Swappach, Y.N. Jan, and L.Y. Jan. 1999. A new ER trafficking signal regulates the subunit stoichiometry of plasma membrane K(ATP) channels. *Neuron.* 22:537-548.

Zhang, T., S.H. Wong, B.L. Tang, Y. Xu, and W. Hong. 1999. Morphological and functional association of Sec22b/ERS-24 with the pre-Golgi intermediate compartment. *Molecular Biology of the Cell.* 10:435-453.

Zhang, M., M. Jiang, and G-N. Tseng. 2001. MinK-related peptide 1 associates with Kv4.2 and modulates its gating function. *Circulation Research.* 88:1012-1019.

Zhang, T., and W. Hong. 2001. Ykt6 forms a SNARE complex with syntaxin 5, GS28, and Bet1 and participates in a late stage in endoplasmic reticulum-Golgi transport. *Journal of Biological Chemistry.* 276:27480-27487.

Zheng, H., J. McKay, and J.E. Buss. 2007. H-Ras does not need COP I- or COP II-dependent vesicular transport to reach the plasma membrane. *Journal of Biological Chemistry.* 282:25760-25768.

Zhou, W., Y. Qian, K. Kunjilwar, P.J. Pfaffinger, and S. Choe. 2004. Structural insights into the functional interaction of KChIP1 with Shal-type K^+ channels. *Neuron.* 41:573-586.

Zuber, C., J.H. Cormier, B. Guhl, R. Santimaria, D.N. Herbert, and J. Roth. 2007. EDEM1 reveals a quality control vesicular transport pathway out of the endoplasmic reticulum not involving the COPII exit sites. *PNAS.* 104:4407-4412.